PB-249 562

EVALUATION OF A PARTICULATE SCRUBBER ON A COAL-FIRED UTILITY BOILER

D. S. Ensor, et al

Meteorology Research Incorporated

Prepared for:

Industrial Environmental Research Laboratory

November 1975

DISTRIBUTED BY:

NTIS

National Technical Information Service
U. S. DEPARTMENT OF COMMERCE

051009

PB 249 562

EPA-600/2-75-074
November 1975

Environmental Protection Technology Series

UNITED STATES
ENVIRONMENTAL PROTECTION AGENCY

Reproduced by
NATIONAL TECHNICAL
INFORMATION SERVICE
U S Department of Commerce
Springfield VA 22151

RESEARCH REPORTING SERIES

Research reports of the Office of Research and Development, U.S. Environmental Protection Agency, have been grouped into five series. These five broad categories were established to facilitate further development and application of environmental technology. Elimination of traditional grouping was consciously planned to foster technology transfer and a maximum interface in related fields. The five series are:

1. Environmental Health Effects Research
2. Environmental Protection Technology
3. Ecological Research
4. Environmental Monitoring
5. Socioeconomic Environmental Studies

This report has been assigned to the ENVIRONMENTAL PROTECTION TECHNOLOGY series. This series describes research performed to develop and demonstrate instrumentation, equipment and methodology to repair or prevent environmental degradation from point and non-point sources of pollution. This work provides the new or improved technology required for the control and treatment of pollution sources to meet environmental quality standards.

EPA REVIEW NOTICE

This report has been reviewed by the U.S. Environmental Protection Agency, and approved for publication. Approval does not signify that the contents necessarily reflect the views and policies of the Agency, nor does mention of trade names or commercial products constitute endorsement or recommendation for use.

This document is available to the public through the National Technical Information Service, Springfield, Virginia 22161.

PB249562

TECHNICAL REPORT DATA
(Please read Instructions on the reverse before completing)

1. REPORT NO. EPA-600/2-75-074	2.	3. RECIPIENT'S ACCESSION NO.
4. TITLE AND SUBTITLE Evaluation of a Particulate Scrubber on a Coal-Fired Utility Boiler		5. REPORT DATE November 1975 6. PERFORMING ORGANIZATION CODE
7. AUTHOR(S) D. S. Ensor, B. S. Jackson, S. Calvert, C. Lake, D. V. Wallon, R. E. Nilan, K. S. Campbell, T. A. Cahill, and R. G. Flocchini		8. PERFORMING ORGANIZATION REPORT NO. MRI 75 FR-1352
9. PERFORMING ORGANIZATION NAME AND ADDRESS Meteorology Research, Inc. 464 West Woodbury Road Altadena, California 91001		10. PROGRAM ELEMENT NO. 1AB012; ROAP 21ADL-092 11. CONTRACT/GRANT NO. 68-02-1802
12. SPONSORING AGENCY NAME AND ADDRESS EPA, Office of Research and Development Industrial Environmental Research Laboratory Research Triangle Park, NC 27711		13. TYPE OF REPORT AND PERIOD COVERED Final; 6/74-6/75 14. SPONSORING AGENCY CODE

15. SUPPLEMENTARY NOTES

16. ABSTRACT

The report gives results of a performance test and engineering analysis of a mobile-bed scrubber on a full-scale coal-fired utility boiler. The scrubber nominally operated at the design particulate removal efficiency of 95%, but the concentration of submicron particles was greatly influenced by mist entrainment. The entrainment resulted in a difference of aerosol penetration through the scrubber as a function of elemental composition and outlet submicron particle concentration independent of pressure drop through the scrubber. The variable concentration of submicron entrained particles made the application of the penetration data as a function of particle size to development of performance models unfeasible. The engineering analysis showed that the 1972-installed cost was $29/kw and the annual operating cost is 0.5 mills/kwh (75% availability). An initial decline in scrubber availability after startup resulted from now-corrected minor design problems. Steadily improving reliability is attributed to the utility's providing maintenance and solving operating problems.

17. KEY WORDS AND DOCUMENT ANALYSIS

a. DESCRIPTORS		b. IDENTIFIERS/OPEN ENDED TERMS	c. COSATI Field/Group
Air Pollution	Utilities	Air Pollution Control	13B
Aerosols		Stationary Sources	07D
Scrubbers		Particulate	07A
Boilers			13A
Coal			21D
Combustion			21B

18. DISTRIBUTION STATEMENT Unlimited	19. SECURITY CLASS *(This Report)* Unclassified	21. NO. OF PAGES 213
	20. SECURITY CLASS *(This page)* Unclassified	22. PRICE $ 7 75

EVALUATION OF A
PARTICULATE SCRUBBER ON A
COAL-FIRED UTILITY BOILER

by

D.S. Ensor and B.S. Jackson, Meteorology Research, Inc.
S. Calvert and C. Lake, Air Pollution Technology, Inc.
D.V. Wallon, R.E. Nilan, and K.S. Campbell, Stearns-Roger, Inc.
T.A. Cahill and R.G. Flocchini, University of California--Davis

Meteorology Research, Inc.
464 West Woodbury Road
Altadena, California 91001

Contract No. 68-02-1802
ROAP No. 21ADL-092
Program Element No. 1AB012

EPA Project Officer: Leslie E. Sparks

Industrial Environmental Research Laboratory
Office of Energy, Minerals, and Industry
Research Triangle Park, NC 27711

Prepared for

U.S. ENVIRONMENTAL PROTECTION AGENCY
Office of Research and Development
Washington, DC 20460

November 1975

CONTENTS

Page

List of Figures v

List of Tables vii

Acknowledgement ix

Glossary of Terms xi

Sections

I Introduction 1

II Conclusions 3

III Performance Tests 7

IV Test Results 35

V Engineering Analysis 75

VI References 79

Appendices

FIGURES

No.		Page
1	Scrubber System	8
2	Sketch of Ducts Showing Sampling Ports (Not to Scale)	10
3	Assembly Drawing of Model 1502 Inertial Cascade Impactor	14
4	Schematic Diagram of Diffusion Battery System	18
5	University of California, Davis, Aerosol Analysis System	20
6	Collection Disc with Substrates	22
7	Diagram of the Plant Process Visiometer	26
8	Velocity Traverse Inlet Ducts, 11/18	38
9	Results of Inspection of Scrubber Packing Compartments	39
10	Combined Penetrations for Diffusion Battery and Cascade Impactor (December 10, 1974)	49
11	Combined Penetrations of Diffusion Battery and Cascade Impactor (December 11, 1974)	50
12	Combined Penetrations for Diffusion Battery and Cascade Impactor (December 12, 1974)	51
13	Scrubber Penetrations for Selected Elements	56
14	Scattering Coefficient as a Function of Mass Concentration	64
15	Scattering Coefficient Measured Upstream and Downstream	65
16	Effect of Particle Size Distribution on Particle Volume/b_{scat} [Ensor and Pilat, 1971]	68

Preceding page blank

FIGURES (continued)

No.		Page
17	Microphotograph of Stage G Particle Deposit Outlet Sample (d_{50} = 0.37 μm)	72
18	Microphotograph of Filter	73

TABLES

No.		Page
1	Nominal Cut Diameters for Impactor Tests	15
2	Cumulative Loss Fraction in Flow Piping (Percent)	33
3	Ratio of Daily Mass Concentration in Each Duct to the Average Mass Concentration	37
4	Scrubber Collection Efficiency	41
5	Data Pairs Used in Penetrations	43
6	CNC Data for Diffusion Battery Tests	44
7	Comparison of Count-Basis Versus Gravimetric-Basis Total Mass Loading	46
8	Ratio of Elemental Concentrations Relative to Si for Six Inlet Tests	53
9	Ratio of Elemental Concentrations Relative to Si for Ten Outlet Tests	54
10	Penetration of the Elements Through the Scrubber for December 10, 1974	57
11	Particle Penetration Summary	58
12	Comparison of Mobile Bed Studies	59
13	Plant Process Visiometer and Inertial Impactor Data	63
14	Correlation of Mass Concentration with Scattering Coefficient	66
15	Test Conditions	70

ACKNOWLEDGEMENT

The technical coordination and assistance of Dr. Leslie E. Sparks, Environmental Protection Agency project officer is greatly appreciated. The efforts of Public Service Company of Colorado personnel in providing assistance during the source test and the engineering evaluation were vital to the success of the project.

Preceding page blank

GLOSSARY OF TERMS

A = coefficient of regression equation

A_z = calibration constant

B = coefficient of regression equation

b_{ext} = extinction coefficient, m^{-1}

b_{scat} = extinction coefficient due to scattered light, m^{-1}

d_{pc} = particle diameter with 50 percent penetration through scrubber, micron

d_{pi} = particle diameter of size i, micron

d_{50} = particle diameter with 50 percent collection efficiency, micron

E = fractional efficiency

L = stack diameter, m

LF_s = loss fraction due to laminar diffusion and sedimentation

LF_c = cumulative loss fraction

LF_a = loss fraction due to impaction at bend

LF_T = loss fraction due to turbulent deposition

M_p = mass of particles in the infinitesimal size range (dp + ddp), g

M_{pi} = cumulative mass concentration of particles smaller than "d_{pi}", g/cm^3

N_a = number of characteristic X rays of element Z

Np = cumulative number concentration of particles smaller than "dp", no./cm^3

N_{pt} = total number concentration of particles, no./cm^3

Preceding page blank

$\overline{Pt}$ = penetration of aerosol through scrubber

Pt_i = penetration for each size fraction

Q = total charge

r_c = correlation coefficient for fit to log normal size distribution

W_t = total particle mass, mg

Z = atomic number

ΔP = pressure drop, cm H_2O

$\beta(\theta)$ = volume scattering function, m^2/m^3

$(\rho t)_z$ = area density, ng/cm^2

σ_g = geometric standard deviation

θ = scattering angle, radian

SECTION I

INTRODUCTION

OBJECTIVE

The objective of this study was to test and evaluate a full-scale scrubber system used to control fly ash emissions from a coal-fired utility boiler. The scrubber was not to be "tuned" for best performance, but simply to be operated in the normal manner.

The primary objective of the field study was to determine the efficiency of the scrubber as a function of particle size. The plant operating parameters, plume opacity, and chemical composition of the emissions were also measured to interpret the efficiency data.

The engineering evaluation was a complete study of the economics and operating history of the scrubber. The scrubber system was to be typical of the industry, with sufficient operating experience for a basis of evaluation.

SCOPE

The subject scrubber was a Turbulent Contact Absorber (TCA), manufactured by Universal Oil Products (UOP), installed on the Cherokee #3 Boiler, owned and operated by the Public Service Company of Colorado in Denver.

The field work extended over two test periods: November 3, to November 23, 1974, and December 9 to December 13, 1974. The first sampling period was terminated because of plant problems. The Meteorology Research, Inc., (MRI) team was responsible for the cascade impactors, opacity, and plant data, while the Air Pollution Technology, Inc., (APT) team was responsible for the operation of a diffusion battery.

The engineering analysis, conducted by Stearns-Roger, Inc., considered information from startup in October 1972 to November 1974.

SECTION II

CONCLUSIONS

The conclusions from this study are:

1. The scrubber was nominally operating at the design particulate removal efficiency of 95 percent of the mass of particulate matter entering the scrubber.

2. The penetration of submicron particles was much greater than that measured in previous studies of TCA scrubbers [Calvert et al, 1974]. Based on the present observations of random variation in efficiency at constant pressure drop, the inconsistent behavior of the three sections of the scrubber and the differences in the chemical composition of inlet and outlet aerosol, entrainment of mist appears to significantly influence the concentration of submicron aerosol at the outlet of the scrubber system. The dominent and poorly defined influence of mist entrainment observed in this scrubber may be unique for this particular scrubber during the particular time period of the test. Thus, the application of the data to developing general mobile bed scrubber models is not feasible.

3. The mass penetration as a function of particle diameter was a strong function of the elemental composition of the particles. The insoluble materials, such as Al and Si (presumed to be in an insoluble oxide form), have a much lower penetration than the total penetration based on mass, whereas the soluble elements such as Cu and Zn, have larger penetrations. The implication is that much of the submicron emission was due to entrainment of droplets. There was also an apparent generation of sulfur particulate matter in the scrubber.

4. The origin of the entrained mist may have been the scrubbing beds. The superficial gas velocity through the scrubber beds was calculated to be 4.5 m/sec. The recommended superficial gas velocity is 2.8 m/sec ± 20 percent. Superficial gas velocities greater than 3 m/sec forces the contactors to the top of the compartments with an increased pressure drop and scrubber liquid entrainment.

   The superficial gas velocity through the chevron type entrainment separators of 3.3 m/sec was within the recommended operating velocities. Thus, a heavy entrainment of mist from

Preceding page blank

the scrubber bed followed by a normally operating mist eliminator may have produced the observed variable concentration of submicron particles.

5. The opacity was measured at both the inlet and outlet of the scrubber with a Plant Process Visiometer. The scattering coefficient was correlated with mass (the correlation coefficient is 0.8) and the results were explained by Mie light scattering equations.

6. The installed cost of the scrubber was $4,400,000 or $29/kw (1972 dollars).

7. The annual operating costs in the year prior to November 1974 were approximately $495,000/year. Based on 75 percent availability, the cost was 0.5 mills/kwh.

8. The major maintenance problems are:

   - breakage of mobile bed contactors
   - plugging and corrosion of the air reheaters
   - operational problems with the quillotine dampers
   - migration of mobile bed contactors
   - failure of the recirculation pumps
   - failure of the rubber linings in the piping
   - buildup of solids in the presaturator
   - problems with mist eliminators
   - problems with stack damper interlock system
   - failure of recirculation system venturi flowmeters
   - problem with booster fan bearings
   - weather related problems such as freezing of process lines.

9. An analysis of scrubber reliability indicated that after a dramatic decline in availability of the unit after installation, the availability has been increasing with time. This has been attributed to the efforts of the Public Service Company of Colorado in providing maintenance and solutions to many of the persistent problems.

10. In a feasibility analysis of producing a "problem-free" scrubber system (no equipment is ever truly problem-free), it was found that many improvements have been devised since installation of the scrubber. These include an indirect flue gas reheater, an enclosure for the scrubber, and the use of improved components such as newer design recirculation pumps. Improvements which require more development are better mobile contactors and more reliable flue gas isolation gates.

SECTION III

PERFORMANCE TESTS

DESCRIPTION OF SYSTEM

Power Plant

The Cherokee Power Plant is located in north Denver, Colorado, near the South Platte River. The #3 unit has a nameplate rating of 150 mw. The Babcock and Wilcox Radiant Boiler (installed in 1961) has a steam capacity of 0.52×10^6 Kg/hr (1.14×10^6 lb/hr) at a design pressure of 1.48×10^7 Pa (2150 psi) and a steam temperature of 554.1°C (1,000.5°F). The gas cleaning equipment consists of mechanical collectors, an electrostatic precipitator, and a wet scrubber arranged in series.

The unit normally burns coal or natural gas. The coal is mined in western Colorado and has a sulfur content of about 0.5 percent, ash content of 9 percent, and a heating value of 2.492×10^7 J/Kg (10,712 BTU per pound).

Scrubber

The Model 6700 Turbulent Contact Absorber Scrubber, designed by UOP, Air Correction Division, was installed in 1972 to supplement control of particulate matter by the electrostatic precipitator and mechanical collectors. A diagram of the system is shown in Figure 1. The flue gas from the precipitator passes into two parallel induced draft fans. A bypass damper is used to direct the flue gas either into the stack or into the scrubber. The flue gas (under design conditions), 17,000 AM^3/min, at 137°C (610,000 ACFM at 280°F), enters the booster fans to offset the pressure drop through the scrubber. In the presaturator, 1440 ℓ/min (380 GPM) of makeup water is sprayed into the gas to reduce the temperature to approximately 52°C (125°F). From the presaturator, the gas enters the scrubber. The scrubber consists of three stages of fluidized beds packed with 3.8 cm (1.5 in.) diameter plastic balls arranged into three seperated parallel scrubber sections. The two outer sections each handle 20 percent of the flow, while the center section handles the remaining 60 percent. All three sections can operate independently to provide flexibility of operation.

Preceding page blank

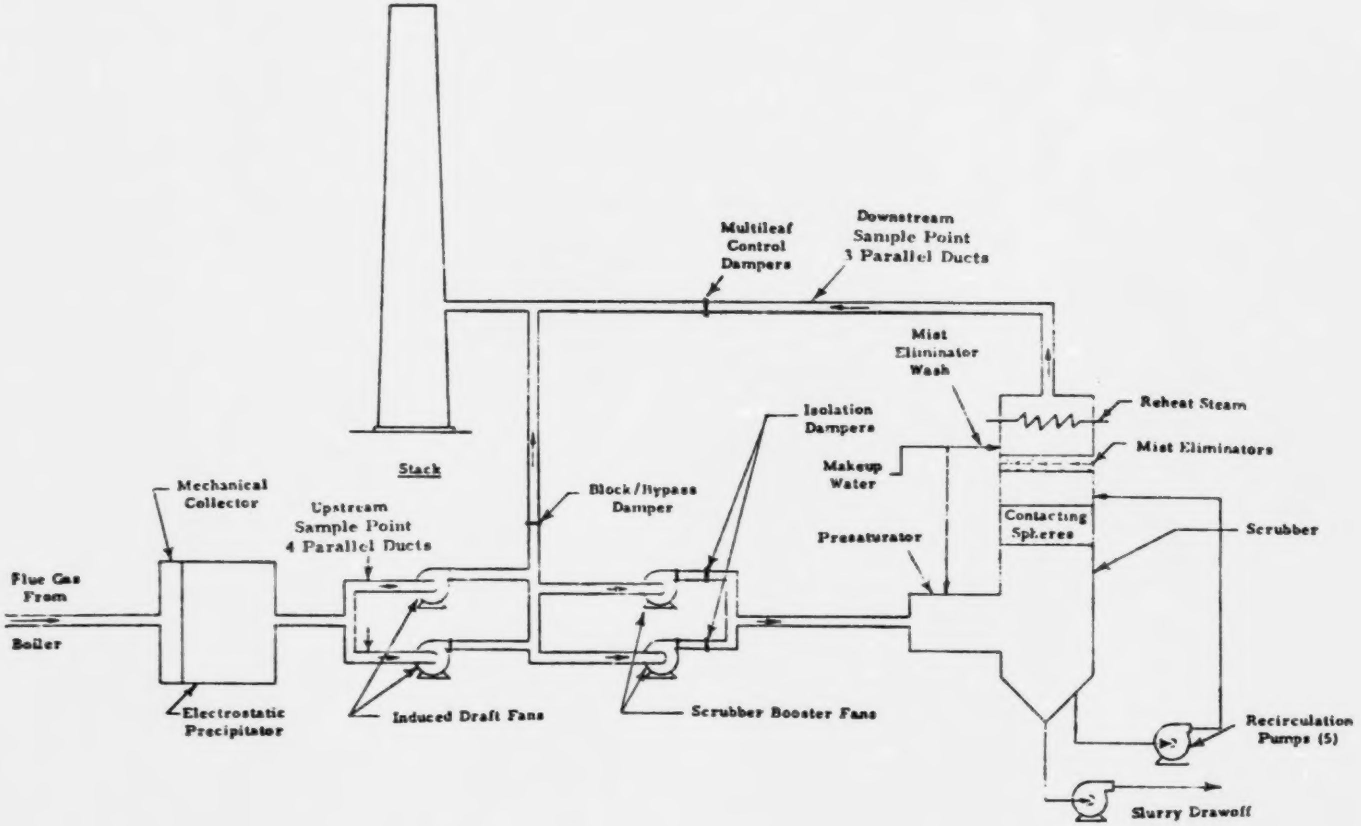
Flue Gas
From
Boiler
Mechanical Collector
Electrostatic Precipitator
Upstream Sample Point 4 Parallel Ducts
Induced Draft Fans
Stack
Block/Bypass Damper
Multileaf Control Dampers
Downstream Sample Point 3 Parallel Ducts
Isolation Dampers
Scrubber Booster Fans
Makeup Water
Presaturator
Mist Eliminator Wash
Reheat Steam
Mist Eliminators
Contacting Spheres
Scrubber
Recirculation Pumps (5)
Slurry Drawoff

Figure 1. Scrubber system

The scrubber liquor, 113,700 ℓ/min (30,000 GPM) is pumped with five pumps from the bottom of the scrubber to a header equipped with spray nozzles at the top of the packing. Under normal operation, 853 ℓ/min (225 GPM) of slurry is purged from the system to prevent buildup of solids in the recirculated liquor. The slurry from the scrubber is pumped to an ash pond for disposal.

The scrubbed gas passes through a chevron-type mist eliminator made of fiberglass reinforced plastic where entrained droplets are removed. The mist eliminators are sprayed once a shift from the top to prevent accumulation of solids.

The gas is then heated by steam coils to 85°C (185°F) before entering the stack to prevent corrosion of the stack and duct work and to provide plume buoyancy after discharge into the atmosphere. The steam coils are equipped with two sets of soot blowers to remove fly ash from the heat transfer surfaces.

The scrubber was designed to the following specifications [Raban, 1974]:

Gas Flow	1,036,000 AM^3 /hr, 610,000 ACFM 138°C (280°F)
Liquid to Gas Ratio	7.4 ℓ/m^3 (55 gal/1000 ft^3)
Δ P	30.5 cm H_2O (12 in. H_2O)
Inlet Concentration	0.92 gm/m^3 (0.40 grains/SCF)
Outlet Concentration	0.046 gm/m^3 (0.02 grains/SCF)
Efficiency of Removal	95 percent

Test Points

The scrubber inlet test points were located at the outlet of the electrostatic precipitator and at the inlet of the induced draft fan. The sample ports were about 4 m above grade. The ducts were about 30° from vertical and the cross sections are shown in Figure 2.

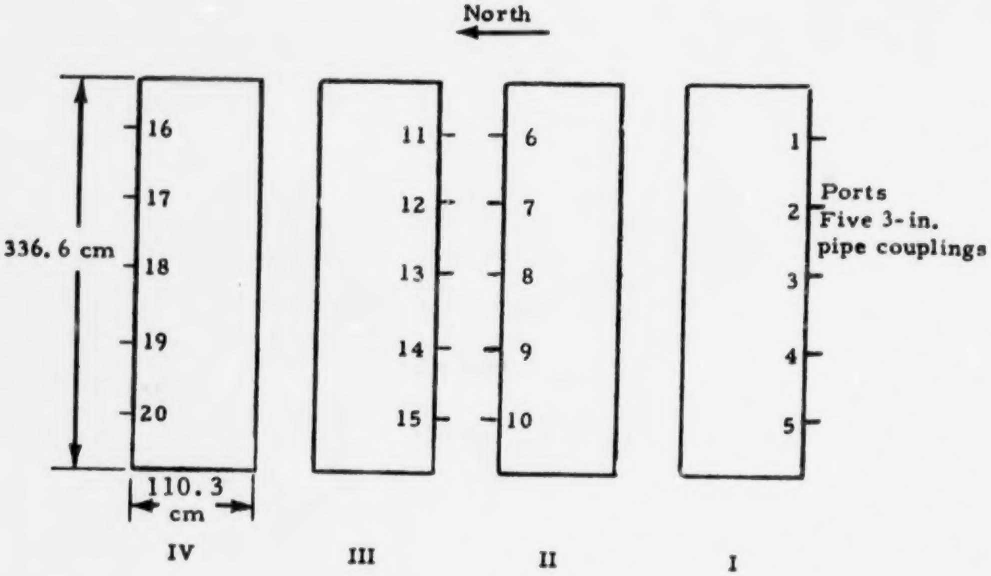
North
336.6 cm
110.3 cm
16
17
18
19
20
11
12
13
14
15
6
7
8
9
10
1
2
3
4
5
Ports
Five 3-in.
pipe couplings
IV
III
II
I

Inlet Ducts

Top

Outlet ports, 3 each side, 8 center, 10 cm ID, 62.9 cm-64.8 cm deep

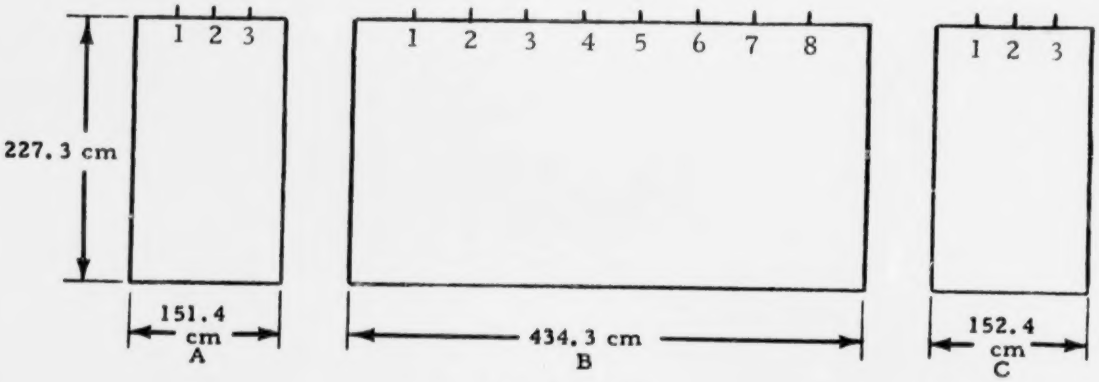
227.3 cm
1 2 3
1 2 3 4 5 6 7 8
1 2 3
151.4 cm
A
434.3 cm
B
152.4 cm
C

Outlet Ducts

Figure 2. Sketch of ducts showing sampling ports (not to scale)

The scrubber outlet ports were downstream of the air reheater. The ports in the top of the horizontal duct were accessible from a catwalk across the top of the scrubber. Immediately downstream of the sample point are multileaf control dampers.

TEST PROGRAM

Test Parameters

The tests were assigned primary and secondary priorities. The primary tests formed the major substance of the study. The secondary tests were scheduled around the primary tests.

1. Primary Tests

Impactors for Mass Distribution

The use of cascade impactors for mass size distribution from 0.3 to 20 μm formed the bulk of the data.

Diffusion Battery

The diffusion battery tests were essential to measure the size distribution less than 0.3 μm in diameter.

Plant Process Visiometer

Two Plant Process Visiometers (PPV) were installed in the duct work at the sample points. The instrument was used to provide a real time output of opacity to detect upsets in the boiler, precipitator, or scrubber.

2. Secondary Tests

EPA Method 5

The EPA Method 5 tests for total mass were assigned a low priority. One test was conducted.

Impactor Test for Count

The impactors were operated for short times to obtain light deposits. The deposits were examined with optical and electron microscopes at MRI. Mylar substrates and silver membrane filters were used.

Impactor Tests for Elemental Analysis

The tests for elemental analysis had similar test procedures as the normal mass size distribution sampling. The major differences were the use of a Mylar collection surface and a Whatman 41 backup filter.

Test Strategy

This included 3 phases:

- Phase 1 - Evaluation of the distribution of aerosol mass concentration at the inlet. With the limited resources in manpower and equipment, the evaluation of the source was attacked one aspect at a time. All four inlet ducts were sampled at the same time. The cascade impactor trains were supplemented with in-stack filter probes to establish the consistency of the concentration.
- Phase 2 - Evaluation of outlet distribution of aerosol mass concentration. Similar parallel tests were used on the outlet of the scrubber to indicate the variation in the ducts.
- Phase 3 - Simultaneous inlet-outlet tests for scrubber efficiency. The final phase of the field program was the simultaneous inlet-outlet tests with both primary and secondary tests.

TEST METHODS

Cascade Impactor

The impactor used in this study was designed at Meteorology Research, Inc., to facilitate sampling of particulate matter in stacks. A drawing of the sampler is shown in Figure 3. The design is based on a simple annular arrangements of jets and collectors reported by Cohen and Montan [1967]. The simple jet-collection plate geometry has been thoroughly studied by many investigators [for example, Marple and Liu, 1947]. The use of a collection disc allows flexibility in choice of substrates. For example, either a greased surface or a filter mat can be used to enhance particle collection. Also, inert materials can be used for special sampling conditions. The assembly has been constructed using quick disconnect rings to increase the flexibility of application. "O" rings are used under direct compression for a positive gas seal of the plates containing the jets. The nominal cut diameters are shown in Table 1.

Particle Collection Substrates

The performance of a cascade impactor is strongly dependent on the surface where the particles are collected. The two most popular substrates have been glass fiber filter mats and greased surfaces. A greased surface was used in preference to the filter mat because recent data reported by Smith et al [1975] indicate that glass fiber filter mats react with stack gases. Also, Rao [1975] reported that filter mats have poor collection efficiency. (These studies were in preliminary form at the beginning of this project.)

In preparation for the field work, a number of materials were screened as coatings to enhance particle collection. Apiezon L high-vacuum grease composed of high-molecular weight hydrocarbon had the best properties of the materials tested in terms of stability and particle adhesion. Thus it was selected for use in these tests.

Collection Substrates -

The collection discs were prepared by cleaning them in acetone and coating the upper area with a solution of Apiezon L high-vacuum grease in benzene. The collection discs were heated for 3 to 4 hours at 171°C (340°F) to drive off volatiles. After heating, the plates were allowed to cool in a dessiccation chamber

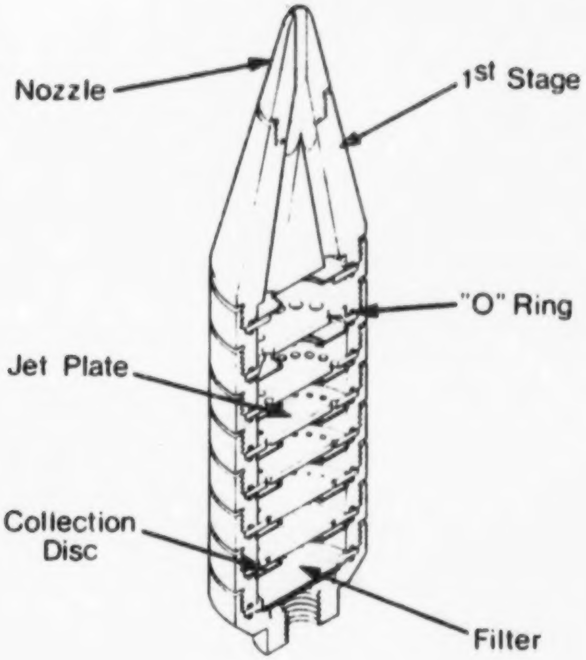
Nozzle
1st Stage
"O" Ring
Jet Plate
Collection Disc
Filter

75-113

Figure 3. Assembly drawing of Model 1502 Inertial Cascade Impactor

Table 1. NOMINAL CUT DIAMETERS FOR IMPACTOR TESTS

Stage	Particle Size at 50 Percent Efficiency (microns)
A	30
B	15
C	6.0
D	2.4
E	1.5
F	0.65
G	0.37
Filter	Less than 0.37

Flow rate 14 ℓ/m.

for 24 hours. The discs were then weighed on a Cahn 4100 analytical balance to 0.01 mg. The weights of the discs were approximately 2100 mg. Counterweights were used to improve the sensitivity of the weighing. The discs were stored in labeled 15 x 60 mm petri dishes.

Test Procedures -

The impactors were assembled with the collection discs and a Gelman Type A final filter. Care was taken to avoid contamination. The test was conducted as described by Pilat et al [1970]. The test train was a commercial EPA Method 5 (Joy Manufacturing Co.) modified to use an in-stack impactor. The probe and out-of-stack filter were replaced by the in-stack impactor, a stainless steel probe with a long radius bend near the impactor, and a vacuum hose connected to the first impinger.

A velocity traverse was taken with a Type S pitot tube as described by EPA Method 2 just before the impactor tests. The impactor sample was taken at one point in the duct without traversing. Care was taken to select an inlet nozzle and sample rate to allow isokinetic sampling.

The sample times were carefully selected to avoid overloading of the collection discs. The maximum weight per disc is about 10 mg to avoid particle losses from the stage as reported by Bird et al [1973].

The tests downstream of the scrubber were conducted with heated impactors. A rubber coated heating jacket, made by Electrofilm, Inc., with a temperature sensor, was slipped over the impactor and connected to the oven temperature controller of the Method 5 train. A temperature 17°C (30°F) above the duct temperature was selected for most tests.

After the test, the impactor was removed from the duct, detached from the probe, and allowed to cool. In a trailer, the sampler was carefully disassembled. The collection discs were placed into 60 x 15 mm petri dishes for protection and storage. The material lost to the walls of the impactor was brushed onto the appropriate substrate surface. The samples were desiccated and then weighed again on the Cahn 4100 balance. The petri dishes were sealed with tape.

Diffusion Battery

Description -

Inertial impaction devices (cascade impactors) are normally insufficient for measurement of particulates less than 0.3 μm (actual diameter). Fractionation of these particles is best accomplished by diffusional collection devices, or diffusion batteries, usually consisting of closely spaced parallel plates or long, thin tubes. Large quantites of pumps, dilution apparatus, and other battery related equipment are bulky and prove to be cumbersome in field use. For this and other reasons, Air Pollution Technology, Inc. developed a portable screen diffusion battery which is lighter and more mobile than previous devices.

The Portable Screen Diffusion Battery utilizes a series of layered screens intermittently separated for sampling purposes (Figure 4). Size fractionation by the diffusion battery is detected by measurement of overall particle concentrations of the gas stream into and out of a known number of screens using a condensation nuclei counter (CNC). Concentrated aerosol samples are diluted until compatible with the CNC ($\sim 10^4$ particles/cm^3). Screen penetration data are then analyzed to determine size distribution and cumulative mass loading of the particulates in the stream. If desired, cascade impactor and diffusion battery analyses can be combined and an overall characterization of the particulate size distribution (and scrubber penetration) obtained.

Test Procedures -

A minimum of two diffusion battery sample runs was taken per day; one inlet and one outlet. Each run consisted of a continuous series of CNC readings from the sample ports over a period of approximately 60 minutes. Normally, CNC counts were taken at each diffusion battery sampling point in order of increasing number of screens and then the process was repeated until three to four sets of readings were obtained. Continuous monitoring of flows, temperatures, and pressures enabled steady operation of the diffusion battery. Conditions in the duct (pressure, gas velocity, temperature, and water vapor content) were obtained during the impactor tests.

The size of particles entering the diffusion battery was limited using a cascade impactor precutter on the in-stack end of the probe. Isokinetic sampling was not maintained because the particles to be

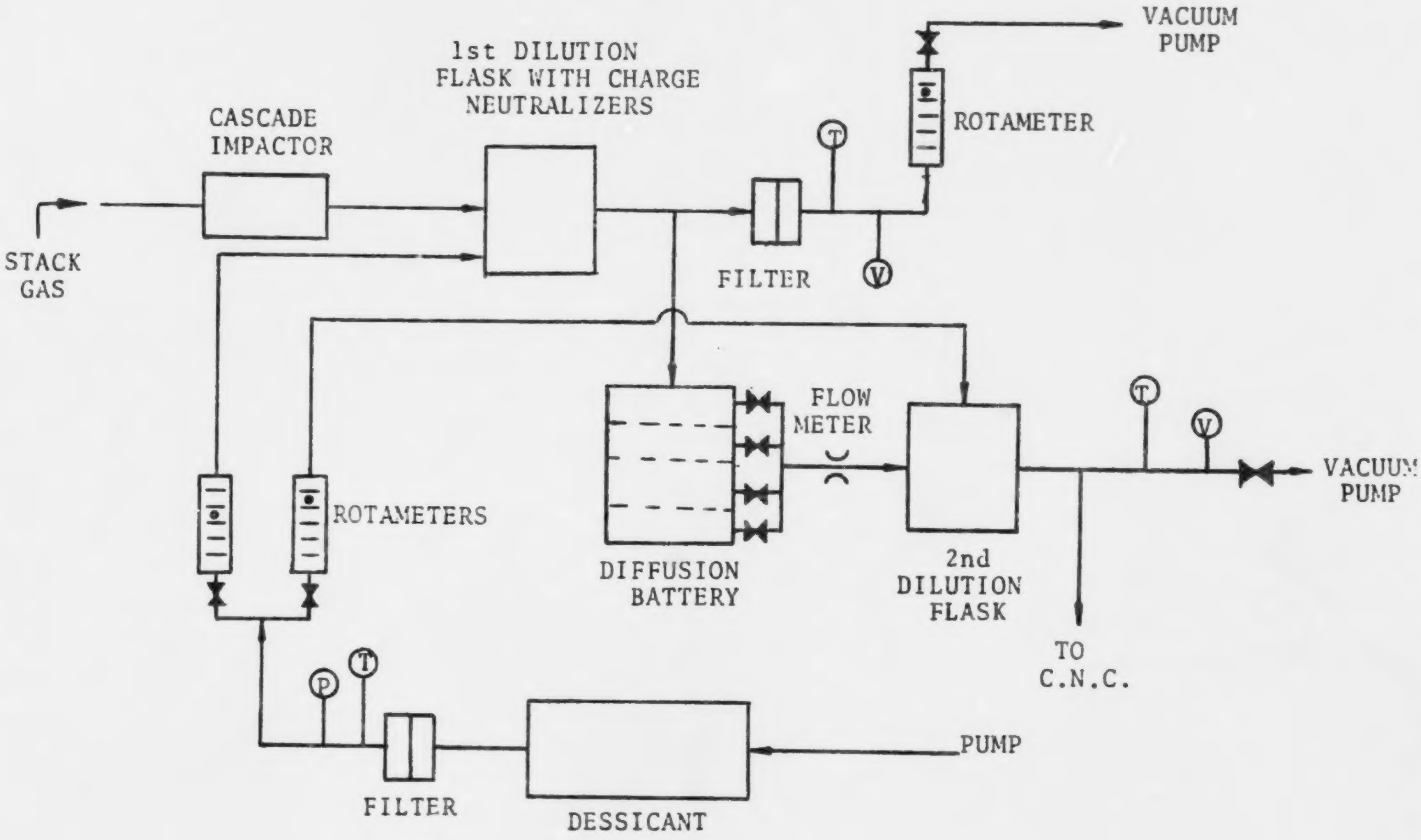
STACK GAS
CASCADE IMPACTOR
1st DILUTION FLASK WITH CHARGE NEUTRALIZERS
FILTER
T
V
ROTAMETER
VACUUM PUMP
DIFFUSION BATTERY
FLOW METER
2nd DILUTION FLASK
T
V
VACUUM PUMP
TO C.N.C.
ROTAMETERS
P
T
FILTER
DESSICANT
PUMP

Figure 4. Schematic diagram of diffusion battery system

measured were too small to be segregated by inertial effects from bends in the gas streams. The sample stream entering the diffusion battery was immediately diluted with heated, dried, filtered air to control condensation. Two Polonium 210 charge neutralizers were inserted into the flask to eliminate electrostatic effects.

A portion of the resultant aerosol was directed through the diffusion battery and the outlet diluted to a concentration measurable by the Gardner CNC. The aerosol from the second dilution flask was sampled with the Gardner CNC. The excess aerosol was exhausted through the vacuum pump. The excess aerosol from the first dilution was passed through an absolute filter and pumped to the atmosphere. The Gardner CNC was calibrated daily against a standard B. G. I. Pollak, Model P, CNC and found to read consistently 33 percent lower than the Pollak CNC for the concentration range used in the testing.

Elemental Analysis

Ion-Excited X-Ray Analysis Method (IXA) -

The elemental analyses of the samples were accomplished with ion-excited X-ray analysis (IXA) at the Crocker Nuclear Laboratory, University of California, Davis. This system described by Flocchini et al [1974] permits analysis sensitivity over a wide range of elements. The method has been primarily used for atmospheric aerosol and water trace analysis. One of the efforts in this study was to extend the capability to stack measurements.

The basic sensing system is shown in Figure 5. An 18 MeV alpha beam from the cyclotron passed through remotely readable graphite collimators and impinged on the thin target which was mounted at an angle of 45° to the incoming beam. The sample or target is mounted into a 35 mm slide. The target slide changer was operated under real time computer control. Beam spot uniformity was achieved by the use of a diffusion foil (6.4 μm Al) and different sized target collimators. The beam was then collected by a Faraday cup and integrated to a precision of about 2 percent to give the total charge, Q, that passed through each sample. X-rays that passed through an active filter and a 25 micron Be window were converted into electrical pulses by a 10 mm^2 x 3 mm liquid nitrogen-cooled Si (Li) detector and associated pulsed optical feedback circuitry. Data were accumulated in a Digital Equipment Corp. PDP-15/40 computer with Nuclear Data 2200 Analog-to-Digital Converter's integral to the system, giving a spectrum of characteristic X-rays and a smooth background.

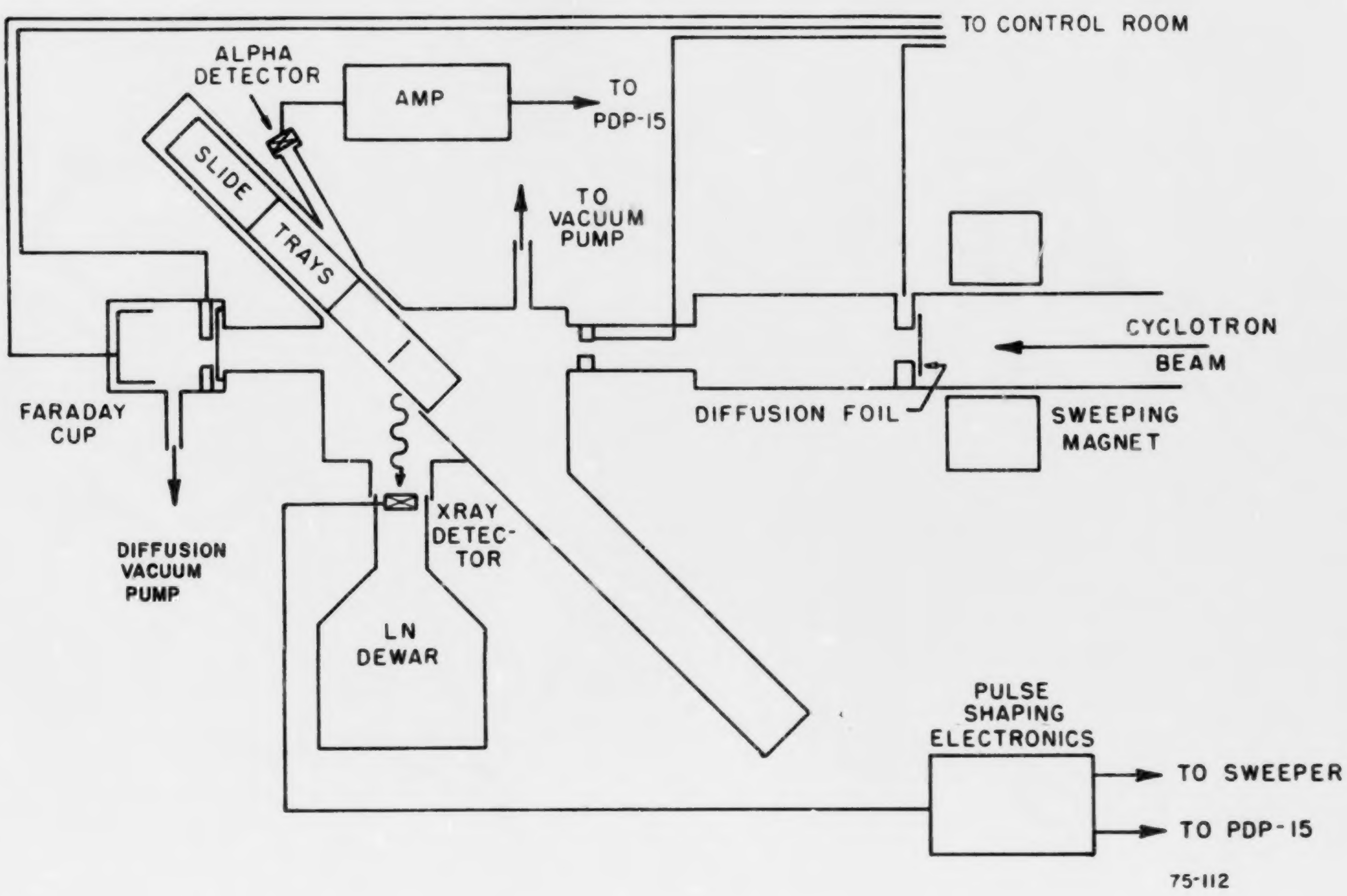
TO CONTROL ROOM
ALPHA DETECTOR
AMP
TO PDP-15
SLIDE
TRAYS
TO VACUUM PUMP
CYCLOTRON BEAM
DIFFUSION FOIL
SWEEPING MAGNET
FARADAY CUP
DIFFUSION VACUUM PUMP
XRAY DETECTOR
LN DEWAR
PULSE SHAPING ELECTRONICS
TO SWEEPER
TO PDP-15
75-112

Figure 5. University of California, Davis, Aerosol Analysis System

The number of characteristic X-rays, N_z, corresponding to some transition of element Z were correlated with the area density $(\rho t)_z$ of the element present in the sample by

$$N_z = A_z (\rho t)_z Q \tag{1}$$

where A_z is a constant determined with the use of elemental standards. Once A_z was known, N_z could be extracted from each spectrum quickly, accurately, and automatically, since analysis time was routinely less than two minutes per sample.

Substrates for Elemental Analysis -

The impactor jet design was found to be quite suitable for Ion-Excited X-Ray Analysis (IXA). The area of the ion beam is about 1 cm^2 or about 1/12 of the cross sectional inside area of the impactor. The holes are in multiples of 2, allowing an even number of deposits to be analyzed by the beam. An exception is the first stage where one deposit is analyzed. The first stage deposits have an area of 0.6 cm^2 each and can be easily covered by the beam. A jet too large would have a deposit of particulate matter larger than the beam and would result in a poor analysis.

A substrate was needed with a much lower density and atomic number than the particle deposit. The X-rays scattered from, or created by, a dense background would mask the spectra from the sample. The collection surface should have a low background of heavy metals to reduce the problems of background substraction. Also, it is not desirable to transfer the particle deposit to another surface because of contamination and loss of sample.

These problems were eliminated with the development of a new substrate-collection disc system. The collection disc with a substrate, shown in Figure 6, is a basic component of the impactor. The disc is a self-supporting aluminum stamping designed for low tare weight (2000 mg) and low cost. It is intended to be used only once for a permanent record of the test and to prevent the likelihood of contamination of the sample from previous tests. The collection substrate was a 92-gage Type S Mylar washer coated on both sides with grease (Apiezon L) to hold it in place and present a tacky surface for particle collection. The Mylar washer with the sample is peeled from the metal stamping and mounted in a 35 mm slide holder for analysis.

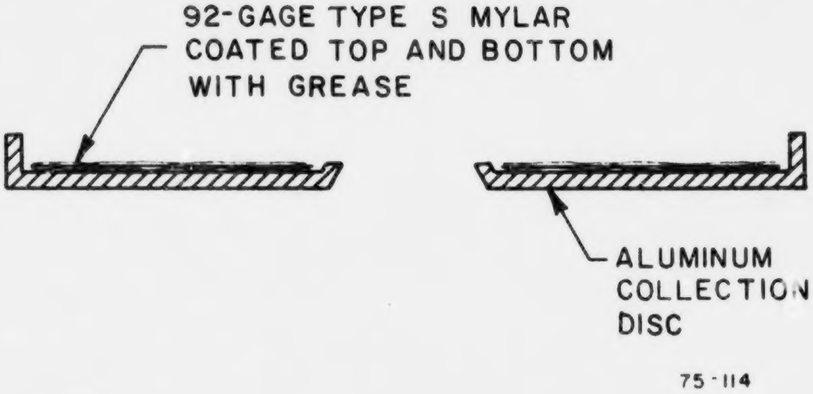
92-GAGE TYPE S MYLAR COATED TOP AND BOTTOM WITH GREASE
ALUMINUM COLLECTION DISC
75-114

Figure 6. Collection disc with substrates

Thus, both the requirements of a rigid mount for handling and a thin substrate for analysis were accomplished.

Washers of 92-gage Type S Mylar were punched to loosely fit into the collection disc. The washers were thoroughly washed in acetone and then ethanol to remove any contamination. The washers were then dipped into a dilute solution of Apiezon L high-vacuum grease dissolved in benzene. The excess solvent was allowed to drain, then the washer was placed into the collection disc and pressed flat with a rod.

The discs were then heated for 3-4 hours at 171 °C (340 °F) to drive off volatile material. The discs were then placed in a desiccation chamber for 24 hours and then weighed on a Cahn 4100 analytical balance to 0.01 mg. Improperly prepared substrates would often pull from the metal backing during heating. These were discarded and the concentration of grease in benzene increased. Care was taken not to overload the surfaces with grease. Whatman 41 filter paper was used in the backup filter because of its low trace contamination [Dams et al, 1972]. The Apiezon L high-vacuum grease was tested before the test for trace metals and none were detected. The Mylar was tested in a similar manner.

Blanks of both the Whatman 41 filter paper and a prepared collection disc were saved for every impactor test. In addition, only the filters from the same box and grease from the same tube were used during the test to avoid any problems which might have been introduced by the quality control of the manufacturer.

The source tests for the elemental analysis were conducted in a manner similar to that for mass size distribution. After the test, the desiccated samples were reweighed on the Cahn balance to obtain the mass collected.

The samples for elemental analysis were hand-carried to the Crocker Laboratory, Davis, California. At the Crocker Laboratory, the Mylar washer containing the sample was peeled from the disc and a section 1/2 of the total was sliced from the washer and mounted in a 35 mm slide plastic holder. The sample was then analyzed in the normal manner for 29 elements.

Data Analysis

The basic analysis data were in the form of nanograms-per centimeter for elements sodium and heavier. These data were printed out and stored on magnetic tape. The impactor flow rates, particle size cut points (d_{50}), and mass loadings were then used to convert the data to nanograms per cubic meter of gas and to make the necessary corrections. The ion beam analyzed only one impinged spot for Stages A, B, and G, while two spots were covered for the rest. Thus, since there are 8 holes in Stage A, 12 in B, 24 in C through F, and 12 in G, the total sampled volume in cubic feet was divided by 12 except for Stage A, which it was divided by 8. Since the ion beam area was known to be 1.1 cm^2, a factor could now be calculated for each run to form the product, $(X\ ng/cm^2)\ (Y\ cm^2/m^3) = XY\ ng/m^3$, the desired end product. The filter conversion factors were obtained by dividing the total active area by the total flow.

The particle size cut points for each stage (d_{50}) was used to make corrections for self-absorbtion of X-rays. The stage d_{50}'s are reported in Appendix C.

The stage d_{50}'s generally varied little from run to run (i.e., the Stage A d_{50} point was 29.0 ± 3.6 μm for all runs). With knowledge of the particle diameter and approximate chemical composition, particle size effects were calculated for each stage [see Harrison and Eldred, 1973, for details and references]. These techniques had previously been used in the 1974 international interlaboratory comparison [Camp et al, 1974] and proved able to accurately handle corrections for up to a 30 μm ground rock sample for elements Al and heavier.[a] In fact, this was precisely the correction factor used for Stage A. The other stage corrections were also derived from this formula.

	Stage A	B	C	D	E → G	Filter
Al	2.6	1.7	1.4	1.16	1	2.2
Si	2.3	1.5	1.3	1.12	1	1.8
S	1.9	1.26	1.17	1.07	1	1.4
Cl	1.8	1.20	1.12	1.05	1	1.26
K	1.5	1.12	1.07	1.03	1	1.14
Ca	1.4	1.09	1.05	1.02	1	1.10
Ti	1.3	1.07	1.03	1.02	1	1.06
V	1.25	1	1	1	1	1.05
Cr	1.2	1	1	1	1	1.04
Mn	1.15	1	1	1	1	1.03
Fe	1.1	1	1	1	1	1.02
Other	1	1	1	1	1	1

[a] Na and Mg were seen on may samples, but error and uncertainties associated with correction effects did not allow quantitative values to be calculated in most cases.

Corrections for layering were not applied, as the light loadings of the samples and the non-uniform distribution of the deposits made such corrections highly uncertain but, fortunately, small. Only for Al and Si on Stages E, F, and G for the downstream samples were the corrections larger than the particle size corrections, with a value of about 10 percent.

The filter correction, due to absorbtion of X-rays in the filter matrix, was very difficult to establish. Little previous work is available on penetration of fine aerosols from stack samples into Whatman 41 filter material. One sample, taken from a stack, was included in the 1974 interlaboratory comparison, however. Since this sample included sulfur, which was present only in fine particles in this present study, we assumed that the sulfur value for Whatman 41 should also be corrected by the factor of 1.4 that gave the correct result for the test sample. This value amounts to about twice the correction reported by Dzubay and Nelson [1974] for Gelman GA-1 filter, a filter about one-half as thick as Whatman 41. All other elements were then also scaled at similar scaling factors.

It should be stated that, despite previous successes in use of particle size correction codes, serious uncertainties due to composition and morphology exist, and no correction should be believed to be better than ±30 percent. The data, corrected for all above considerations, was then tabulated and provided in a printed format that minimized space and provided easy comparison of run to run, stage to stage, by element.

Plant Process Visiometer

Description -

The Plant Process Visiometer (PPV) is a light scattering instrument developed at Meteorology Research, Inc., for real-time monitoring of stack opacity. A diagram of the instrument is shown in Figure 7. The aerosol was removed from the stack with a stainless steel probe and was transported into the measurement chamber. The aerosol particles in the chamber were illuminated by a flash lamp with an opal glass filter. The scattered light was detected by a photomultiplier tube at approximately right angles to the flash lamp. The optics have been designed so that the output of the photomultiplier tube is proportional to the extinction coefficient due to scattered light. The instrument is a physical analog of the following equation:

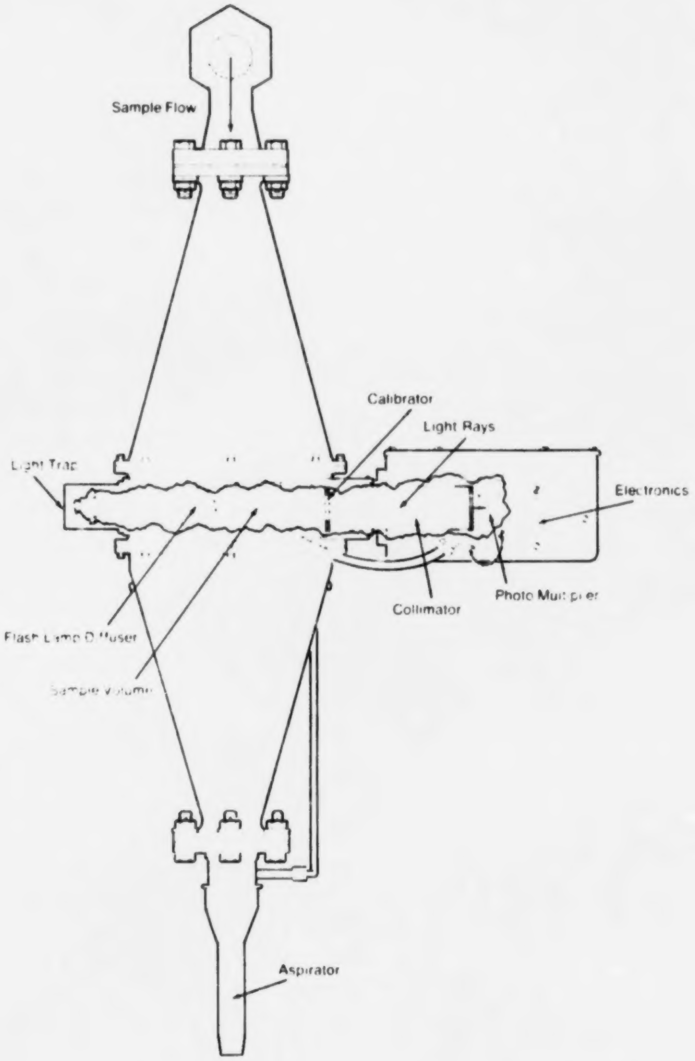
Sample Flow
Calibrator
Light Rays
Light Trap
Electronics
Collimator
Photo Multiplier
Flash Lamp Diffuser
Sample Volume
Aspirator

Figure 7. Diagram of the Plant Process Visiometer

$$b_{scat} = 2\pi \int_0^{\pi} \beta(\theta) \sin \theta d\theta \qquad (2)$$

where

b_{scat} = the scattering coefficient due to scattered light

$\beta(\theta)$ = volume scattering function

θ = scattering angle

If there is no light absorption, the scattering coefficient is identical to the extinction coefficient. The extinction coefficient is related to plume opacity with the Bouguer Law.

$$\text{Opacity (percent)} = \left(1 - \exp(-b_{ext} L)\right) 100 \qquad (3)$$

where

b_{ext} = extinction coefficient, m^{-1}
L = stack diameter, m

The instrument was spanned with an internal calibrator consisting of an opal glass lens of known scattering coefficient. The lens was mechanically placed in the view of the detector for calibration and was retracted into a sealed chamber between calibrations. the PPV calibrator was calibrated with oil smoke with reference instruments using both an Integrating Nephelometer and a transmissometer. The PPV was described in detail by Ensor et al [1974].

Installation -

The Plant Process Visiometer at the inlet of the scrubber was installed upright at port number 12. The 1.3 cm ID probe extended 60 cm into the duct with the nozzle aligned with the flow. The sample rate was 230 liters per minute. A high-efficiency aspirator at the exhaust of the optical chamber was supplied with compressed air from a Rotron blower. The exhaust from the aspirator was returned to the stack through an adjacent port.

The unit at the outlet of the scurbber was placed on the walkway above the test ports. The 152 cm stainless steel probe was placed vertically down into the duct in from section B of the scrubber. The probe was clad with extra electric strip heaters to increase the temperature of the stack gas to approximately 100 °C. The gas from the high-efficiency aspirator was exhausted to the atmosphere.

In both instruments, the probe and upper cone of the optical chamber were electrically heated. The stack, probe, and optical chamber contained temperature sensors. A remote control panel was rack-mounted in the work trailer. The light scattering coefficients were recorded on strip charts, and the temperatures were displayed with a panel meter and multipoint switch. The remote control panel had controls to allow remote operation of the instruments. The outlet instrument was equipped with an automatic zero and span system functioning on a two-hour cycle.

Test Procedures -

The Plant Process Visiometers were adjusted to provide a mid-scale reading. The full-scale reading of the inlet and outlet Plant Process Visiometers were 0.06 and 0.45 m^{-1}, respectively.

The internal opal glass calibrator was used as a field reference. After installation, the instruments were operated continuously. The zero and span was checked at least three times per day by back-flushing with clean air and activating the calibrator. Thus both a check of the electronics and drift and contamination of the optical surfaces was obtained. When required, the units were cleaned and adjusted.

ERROR ANALYSIS

An error analysis was conducted to aid in procedure development and interpretation of the results.

Cascade Impactors

Cascade impactors were used as the principal means of obtaining information about the inlet-outlet size distributions. It was important to understand the sources of error and how the error can be minimized.

The procedural errors include the accuracy of the weighing of the deposits, reading of the test data such as temperature, gas volume, time, and pressures. The errors from the impactor design and construction include wall losses, accuracy and precision in construction of critical components, and particle reentrainment from the collection surface.

Some of the design and construction limitations can be reduced by procedures such as recovering the wall losses and by sampling at certain flow rates and times to reduce reentrainment errors and by calibration of the impactor. The experimental data obtained with commercial impactors was reported by Smith et al [1974].

Smith et al [1974] reported that all impactors tested had appreciable wall losses for particle diameters above ten microns. This error can be reduced by brushing the material from the wall onto appropriate collection discs. The flow velocity through the impactor jets should not be above 65 m/sec to be absolutely certain of avoiding reentrainment of particles from the collection substrate. The extent of reentrainment will depend on the properties of the material and the amount of deposit. Lundgren [1967] reported that reentrainment increased as the collection surface became coated with particles. However, Rao [1975] reported that collection efficiency increased with increased particle load. When the particle weight is over 10 mg, part of the deposit may break away from the surface and migrate within the impactor. The light-weight deposit places importance on accurate weighing. The analysis of impactor errors was limited to the weighing error and in the calculation of collection efficiency error. The effects of weighing errors on the results of impactor tests have been analyzed by Sparks [1971]. An analysis of the weighing error using three different estimations was reported by Fegley et al [1975]. The results indicate that, when the weight of sample per stage is less than 1 mg when weighed with a balance with a precision of 0.05 mg, the error in the fractional mass will be greater than ten percent.

The error in the particle diameter was analyzed by the use of the Ranz and Wong [1952] solutions describing the impaction of particles from a round jet impinging on an infinite flat plate. The results reported by Fegley et al [1975] indicated that the tolerance of machining the jet holes is weighted nine times the other errors in determining particle diameter. Measured hole diameters for each impactor stage were used in the reduction of the data to minimize the effect of the hole tolerance on the calculated stage d_{50}. The error in the d_{50} will be less than five percent.

Diffusion Battery

The Screen Diffusion Battery was calibrated in Air Pollution Technology's (APT) small particle laboratory. An aerosol of known size distribution was generated and passed through the diffusion battery. The total number concentration was measured with a condensation nuclei counter at the battery inlet and at several locations along the battery corresponding to different solidity factors. Screen solidity factor is a semi-empirical quantity which is obtained by laboratory calibration and depends upon the cumulative number of screens. The penetration of particles (percent) was then calculated and plotted against solidity factors on semi-logarithmic paper. The experiment was repeated with the same aerosol until a smoothed average curve relating number penetration to solidity factor was obtained. From the smoothed curve, a correction factor for the theoretical diffusion battery performance was determined.

The scatter of data points about the smoothed (fitted) calibration curve represents the experimental error in the penetration measurement. This measurement error included meter reading error, accuracy of the CNC, etc. The measurement error was defined in terms of relative error, or the deviation from the averaged penetration value divided by the averaged value.

This procedure was repeated on other aerosols of known size distribution. The maximum relative error was then determined from these experiments for each solidity factor. The maximum relative error the the Screen Diffusion Battery determined by this method is 10.4 percent for solidity factors of 13, 26, and 40.

Elemental Analysis

The ion-induced X-ray analysis is subject to two sources of uncertainties: system errors and sample effects.

The system uncertainties include:

1. Statistical uncertainty in peak counts
2. Uncertainty in gravimetric standard
3. Integration of ion beam
4. Ion beam attenuation
5. Electronic correlations
6. Peak integration and background uncertainties

The total of the system errors are within ±15 percent.

The uncertainties introduced by the nature of the sample include:

1. The particle size effect corrections
2. Degredation of the samples by the beam and in preparation
3. Hetrogeneous distribution of mass across the substrate

The error in the lower stages, C through E, was within ±10 percent from these effects, while the errors on the first two stages (A and B) were within ±30 percent. The larger error band is due to the large particle sizes. The values of Si and Al concentration for the first stage (A) was ±40 percent. Larger errors are expected for the lighter elements because of greater self-attenuation of the X-rays.

The analysis was repeated for selected samples. It was found the results were within the stated system error of ±15 percent.

The Crocker Laboratory has also participated in intercomparison of trace element determinations of standard air pollution samples. In a recent intercomparison, the technique yielded a ratio to accepted concentrations of ten elements of 1.033 ± 0.08 [Camp et al, 1975]. Thus, the errors due to both the system and sample matrix are well within the stated limits.

Plant Process Visiometer

The two major sources of error thought to be important for the instrument were losses of particles in the sample probe and light losses in the optical chamber.

Wall Losses of Particles in the Sampling Probe -

Wall deposition of particles in the flow piping to the optical chamber was due to simple sedimentation and Brownian and eddy diffusion in turbulent flow regions. In addition, the bend in the sampling probe causes large particles to impact on the outside wall of the turn. In an effort to minimize these effects, the sample tube was selected to be of fairly large inner diameter (about 1.6 cm) which allowed a sample flow rate of 140 to 280 liters per minute.

Several theories describing these phenomena are available in the literature. Each is defined for the entire size range of interest (0.01 - 10 μm), but none is experimentally verified for the entire range. A combination of these theoretical approaches were used to generate an estimate of wall losses under the conditions encountered in the scrubber evaluation. The details of these calculations are described in Appendix A.

The sampling probe was operated for near-isokinetic sampling, which required a mean flow velocity of 15-21 m/sec (50-70 ft/sec). The pipe flow Reynold's Number for this entire velocity range is on the order of 10^4, indicating that turbulent flow occurred in all tests. However, the turbulent flow is not thoroughly developed until 25-40 pipe diameters downstream from the inlet [Schlichting, 1968]. Despite the fact that the right angle turn exists in the first 25 diameters of the PPV sampling probe, it was assumed for the purposes of the sedimentation, Brownian diffusion, and eddy diffusion calculations that the probe could be represented as a straight pipe with 40 diameters of laminar flow followed by a varying length of turbulent flow. The effects of the turn were analyzed separately and under the assumption of laminar flow.

To ensure that the calculations would be conservative for the entire flow velocity range, the upper velocity boundary was used for the turbulent deposition claculations (where deposition increases with increasing velocity), while the lower velocity boundary was used for sedimentation and laminar diffusion calculations (where deposition increases with decreasing velocity).

A cumulative loss fraction as a function of sampling probe length was computed assuming that the 40 diameters of laminar diffusion/sedimentation flow were followed by the 3.6 cm radius turn and then by varying lengths of fully developed turbulent flow. The cumulative loss fraction, referenced to the probe inlet concentration, can thus be defined as

$$LF_C = 1 - (1 - LF_B)(1 - LF_R)(1 - LF_T) \quad (4)$$

where LF_C = cumulative loss fraction

LF_B = loss fraction due to laminar diffusion and sedimentation

LF_R = loss fraction due to impaction at bend

LF_T = loss fraction due to turbulent deposition.

Table 2 is a summary of the results. The largest particle size for which $LF_R = 0$ (5.8 μm) and the particle size often referenced in the literature (3.0 μm) are included as special cases.

For all calculations, the ambient pressure was considered to be atmospheric, 1524 m (5000 ft), the ambient temperature to be 120°C (250°F), and the ambient density to be the atmospheric value corrected to the above temperature. The tube walls have been considered 100 percent effective in retaining the particles once deposited.

For 0.01 μm, the losses are due to Brownian diffusion in the laminar region with no losses in the bend or the turbulent region.

The 0.1 μm losses are due to Brownian diffusion in the turbulent region where the laminar sublayer is quite small.

The lack of losses for 1.0 μm is due to the inability of the relatively large particle to diffuse rapidly in the laminar range and its inability to penetrate the laminar sublayer rapidly in the turbulent case. The latter occurs because the low inertia of the 1.0 μm particles makes them subject to the random fluctuations of the turbulent buffer and core regions.

For particles larger than this, simple sedimentation occurs in the laminar flow regime and the increased particle inertia carries them to the walls in turbulent flow.

Table 2. CUMULATIVE LOSS FRACTION IN FLOW PIPING
(Percent)

Particle Diameter (μm)	Laminar Portion	Turn	Total Pipe Length (m)				
			1.2	1.8	2.4	3	3.6
0.01	0.3	0.3	0.3	0.3	0.3	0.3	0.3
0.1	0.0	0.0	0.1	0.1	0.2	0.2	0.3
1.0	0.0	0.0	0.0	0.0	0.0	0.0	0.0
3.0	0.1	0.1	1.0	1.9	2.7	3.6	4.4
5.8	0.3	0.3	15.6	28.5	39.5	48.8	56.6
10.0	0.8	70.2	83.8	91.2	95.2	97.4	98.6

These calculations are consistent with the wall deposition observed during the test. As long as the temperature was maintained above the dew point of the stack gas, little evidence of particle deposition on the walls was observed. Also, it is suspected that the large particles predicted to be lost to the walls are resuspended after deposition.

Light Losses -

The light loss errors in the PPV resulted from two sources: the angular integration truncation errors and the secondary attenuation error.

The angular integration truncation error results from the optical geometry. The instrument would be very long to measure the light scattered from 0 to 180°. In a practical instrument, the light scattered from 10 to 165° is measured. The error is also a function of the particle size distribution in addition to the instrumental geometry. Ensor et al [1974] reported that calculated errors for various size distributions are ±20 percent of scattering coefficient.

Secondary attenuation may occur in concentrated aerosol when the scattered light is attenuated from the scattering volume to the detector. The error is a function of the distance from the light source to the detector and the concentration of the aerosol. For the scattering coefficient of less than 0.2 m^{-1} measured during the test, the error was less than 5 percent.

SECTION IV

TEST RESULTS

TEST SUMMARY

The test began on November 3, with the setting up of the trailer, motel laboratory, and installation of the Plant Process Visiometers. The testing of the inlet ducts (Phase 1) was started with two impactor trains and two in-stack filter trains.

The sampling of the outlets (Phase 2) was started on November 14. It was found that striking differences in concentration existed between the three ducts. A Method 5 test was conducted on November 20 on duct B at the same time as an impactor test.

The simultaneous inlet-outlet tests (Phase 3) were started on November 20 with an APT crew operating the diffusion battery. On November 22, however, the fuel was switched from coal to gas to allow plant personnel to perform simple maintenance on the scrubber booster fan. The plant operating personnel decided to stay on natural gas as long as possible to perform other maintenance. It was decided at that time to remove the PPVs and complete the test work at a later time.

The Phase 3 activities were completed during December 9 to 13. The tests included the sampling for count, elemental composition, and mass tests.

All test phases were successful and provided a useful data base which was systematically accumulated during the test.

DISTRIBUTION OF MASS LOADING BETWEEN DUCTS

Sampling

Inlet tests typically consisted of two impactors and two in-stack filter holders run concurrently, one in each duct. Sampling times ran between 5 and 10 minutes and were varied somewhat, depending on measured mass loading, flue gas velocities, and the ratio of natural gas to coal being used as fuel by the power plant.

At the outlets, the filter holders were dispensed with in favor of impactors. Sample times ranged from 10-20 minutes. The impactors were placed in heating jackets and heated to 17-28° C (30-50° F) above the temperature of the flue gas to prevent condensation of water. Near the end of the outlet test period, the flue gas velocity in duct A dropped below 10 m/sec (30 ft/sec) and sampling in that duct was suspended.

Analysis

For the analysis, mass concentrations per unit volume were calculated for all ducts based on the above tests and an average mass loading was calculated for each duct. The ratio between the mean mass loading and the mass loading in each duct was calculated. The results are shown in Table 3.

At the inlets, at least one sample was taken in each available port. However, testing was not extensive enough to determine a mass distribution within each duct. At the outlets, sample positions were restricted due to the geometry of the ducts and the sampling ports.

The inlets were reasonable uniform in mass concentration. On the average, the variation was within 30 percent. Individual sample variation could be as large as 2:1. It was felt that this variation was random and would average out with consistent testing of a single inlet duct during the inlet-outlet tests.

The scrubber outlet ducts, however, had considerable reproducible differences. The primary cause of the variation between outlet ducts was the plugging of the air reheater in duct A. The imbalance in the flows is shown by the velocity profiles in Figure 8. The three scrubber sections are independent and it was felt that the "B" compartment had performance most representative of normal operation.

After the first test segment, the plant maintenance personnel inspected the scrubber on November 30. Figure 9 shows a summary of their findings.

During the inspection of the scrubber, it was found that 2 of 9 compartments in C and 3 of 36 compartments in B were empty which may also explain some of the variation in efficiency.

Table 3. RATIO OF DAILY MASS CONCENTRATION IN EACH DUCT TO THE AVERAGE MASS CONCENTRATION

Inlet Ducts

Date	Time	IV	III	II	I	Mass Conc. mg/DSM^3 [a]
11/7	1530	1.25	0.78	1.53	0.43	569
11/8	1040		0.94	1.06		512
	1430	1.17	0.94	0.89	1.00	558
11/9	1130	0.76	0.78	1.58	0.85	405
	1235		1.00			739
	1430	0.56			1.44	511
11/11	1000	1.13	1.69	0.67	0.51	976
	1300	0.75	1.95	0.93	0.37	814
11/12	1030	0.69	2.12	0.51	0.68	948
	1250	0.74	1.83	0.81	0.63	1791
11/13	0953	0.77	1.33	0.85	1.06	875
	1201	1.35	0.72	0.60	1.33	1268
	1428	0.90	0.71	0.48	1.91	1343
Average		0.92	1.23	0.90	0.93	
Standard Deviation		0.26	0.53	0.37	0.48	

Outlet Ducts

		A	B	C	
11/19	1021	1.14	0.72	1.55	133
	1133	1.53	0.69	1.21	136
	1351	1.63	0.70	1.10	205
11/18	1027	0.45	0.59	2.55	174
	1221	2.15	0.67	0.67	85
	1402	1.47	0.63	1.44	171
11/15	1025		1.24	0.41	158
	1208		0.37	2.53	128
	1429		1.15	0.63	87
Average		1.40	0.75	1.34	
Standard Deviation		0.57	0.27	0.78	

[a] Dry Standard Conditions 21.1° C, 760. mm Hg

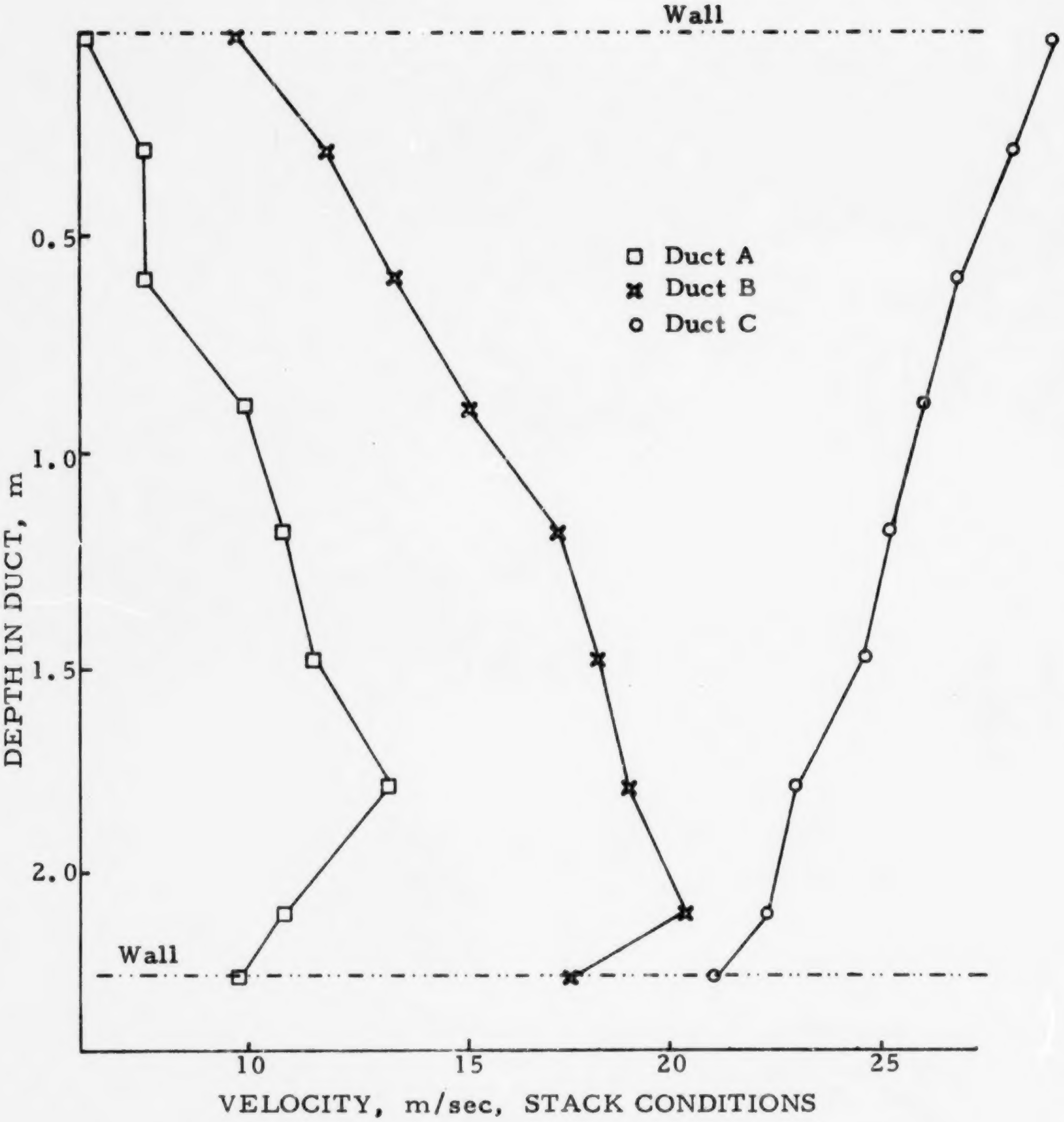

75-236

Fig. 8. Velocity traverse inlet ducts, 11/18

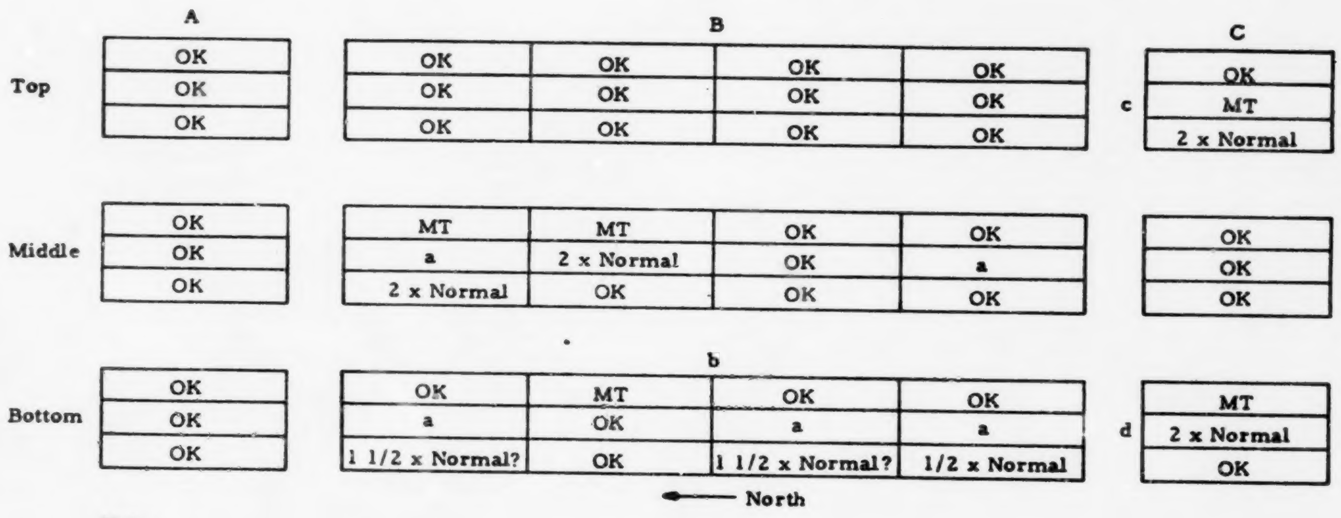

	A	B					C
Top	OK	OK	OK	OK	OK		OK
	OK	OK	OK	OK	OK	c	MT
	OK	OK	OK	OK	OK		2 x Normal
Middle	OK	MT	MT	OK	OK		OK
	OK	a	2 x Normal	OK	a		OK
	OK	2 x Normal	OK	OK	OK		OK
				b			
Bottom	OK	OK	MT	OK	OK		MT
	OK	a	OK	a	a	d	2 x Normal
	OK	1 1/2 x Normal?	OK	1 1/2 x Normal?	1/2 x Normal		OK

← North

Notes:

Section A - 1' x 2' hole through demister; demister spray nozzle had fallen off.
a. The compartments were not visible from inspection plate.
b. 4" wide plate by inspection door is loose.
c. Loose vertical grid.
d. Vertical grid open.
Section C - 2 bolts had fallen out of recirculation spray nozzles; no evidence of damage to lining.
MT - Indicates that compartment is empty of packing

Figure 9. Results of inspection of scrubber packing compartments

Before the final sampling segment in December, the plant personnel performed minor maintenance. The packing in section C was redistributed; however, B section was not repaired. Also, the clogged reheater was cleaned to some extent by drying the deposit and dislodging with the soot blowers. This was partially successful, as indicated with the December velocity transverses in Appendix B.

SCRUBBER EFFICIENCY

Introduction

The Phase 3 tests were used to compute the efficiency of the scrubber. Sufficient data were taken to allow selection of the runs taken during steady-state plant conditions. The data used in the efficiency determinations are summarized in Table 4. The diffusion battery tests were restricted to duct B at the outlet because of the relatively nominal behavior of that section of the scrubber.

Total Mass Collection Efficiency

The mass collection efficiency was computed using only the cascade impactor data. The results were summarized along with some control room data in Table 4. The pressure drop across the system was reported to indicate the magnitude of the effect of the existence of the air reheaters. The outlet gas flow was the total for the system as determined from the velocity traverses. One of the unexpected results was the lack of correlation of efficiency on the pressure drop.

The average efficiency of the December tests was 92 percent, slightly lower than the design efficiency of 95 percent.

Mass Penetration as a Function of Particle Diameter

The collection efficiency of the scrubber as a function of particle size is of interest because the particle effects (opacity, etc.) are a function of particle size. A convenient way of presenting the results is in the form of penetration defined by

$$\overline{Pt} = \frac{\text{mass concentration out}}{\text{mass concentration in}} . \qquad (5)$$

The fractional efficiency is simply

$$E = 1 - Pt. \qquad (6)$$

Table 4. SCRUBBER COLLECTION EFFICIENCY

DATE	LOAD	O_2	OUTLET GAS FLOW ACTUAL	SECTION A				SECTION B				SECTION C			
				Δ P SYSTEM	Δ P BED	Δ P MIST ELIMIN.	EFF.	Δ P SYSTEM	Δ P BED	Δ P MIST ELIMIN.	EFF.	Δ P SYSTEM	Δ P BED	Δ P MIST ELIMIN.	EFF.
	mw	Percent	m^3/hr	cmH_2O	cmH_2O	cmH_2O		cmH_2O	cmH_2O	cmH_2O		cmH_2O	cmH_2O	cmH_2O	
11/20	166	3.6	a	41	9.9	0.76	ND	45	25	2.5	84.7	46	24	8.3	ND
11/21	164	3.4	a	39	9.6	0.76	ND	43	18	1.8	89.9	44	20	5.1	ND
12/10[b]	157	3.4	9.47×10^6	36	15.2	1.7	96.3	41	20.8	2.5	92.6	41	18.5	3.8	86.9
12/11	160	3.0	10.2×10^6	38	14.7	1.5	96.4	42	22.1	3.2	93.2	44	22.4	2.5	96.7
12/12	160	2.6	8.78×10^6	38	14.7	1.8	79.6	44	22.9	2.5	93.1	46	24.1	3.8	92.1

[a] Full velocity traverses were not taken.

[b] The control room data were incomplete. Interviews, data from other days and the log book were used to supplement available information.

Methods of Calculation -

Scrubber penetration as a function of particle size is computed from data on the inlet and outlet particle size distributions and concentratiosn. The major steps involved in the computation are as follows:

1. Reduce cascade impactor data to the form of cumulative particle mass concentration for each impactor cut diameter.

2. Convert diffusion battery data from number distribution to mass distribution and then plot cumulative mass concentration against particle diameter as for the cascade impactor data.

3. Determine the slopes of the cumulative mass distribution curves at several values of particle diameter for scrubber inlet and outlet by a graphical technique and then compute penetration at each particle diameter.

Penetration analysis required that simultaneous inlet-outlet cascade impactor runs were selected. Table 5 is a list of runs used in calculating the penetrations.

Screen Diffusion Battery Data -

Tests were limited to the duct B and were performed as indicated in Table 6. As the cascade impactor runs were of shorter duration than the diffusion battery runs, simultaneous matching of results was difficult. Penetration comparison required averaging inlet and outlet data from the diffusion battery (nonsimultaneous) and averaging the cascade impactor runs (simultaneous) over the entire day.

Of 15 runs taken, six were found suitable for comparison with cascade impactor analyses. No test difficulties were encountered in these runs and operating conditions of the boiler were indicated to be steady by the plant instrumentation. Table 6 includes diffusion battery and cascade impactor comparable runs.

Data for the runs in Table 6 were averaged and converted to overall particle penetration versus screen solidarity factor by the ratio of outlet to inlet concentration for varying thickness of screen. Screen solidarity factor is a semi-emperical quantity which is developed by laboratory calibration and which is dependent upon the cumulative number of screens. A graphical stripping technique developed by Sinclair [1972] was used in conjunction with laboratory calibrations to reduce the penetration data to a count-basis size distribution.

Table 5. DATA PAIRS USED IN PENETRATIONS

	INLET			OUTLET			
DATE	TIME	RUN	LOCATION	TIME	RUN	LOCATION	COMMENTS
11/20	1030	56	8	1034	53	B	
	1343	55	8	1328	57	B	
11/21	1110	60	8	1107	61	B	
12/10	1207	113	8	1142	110	A	Elem. Sampling
	1116	114	8	1110	109	B	Elem. Sampling
	1530	119	8	1530	116	B	Elem. Sampling
	1617	120	13	1630	118	C	Elem. Sampling
	1224	8	13	1628	9	B	Diffusion Battery
12/11	1215	123	13	1215	122	C	Elem. Sampling
	1240	124	13	1445	125	B	
	1445	127	8	1446	126	A	
	1624	12	13	1108	10	B	Diffusion Battery
12/12	1140	133	8	1140	129	B	
	1300	135	8	1300	132	B	
	1110	134	8	1113	130	A	
	1320	136	8	1300	131	C	
	919	13	13	1529	15	B	Diffusion Battery

Table 6. CNC DATA FOR DIFFUSION BATTERY TESTS

RUN NO.	READING SET	CONCENTRATION AT INDICATED SCREEN SOLIDITY FACTOR, PARTICLES/cm^3 x 10^{-4}			
		Solidity Factor			
		0	13	26	40
8	1	4.0	3.3	2.13	1.33
	2	2.97	2.17	1.53	0.87
	3	2.80	1.87	1.23	0.77
	4	2.57	1.73	1.33	0.70
9	1	69.3	39.0	32.3	28.3
10	1	35.2	15.7	11.7	6.9
	2	31.7	12.7	8.2	6.1
	3	35.3	16.0	10.7	7.1
	4	31.0	14.0	7.9	5.8
12	1	5.27	4.30	3.66	2.87
	2	4.27	3.50	2.83	1.87
	3	3.30	2.63	1.97	1.30
13	1	4.80	3.40	2.87	1.97
	2	3.87	2.87	2.23	1.57
	3	2.97	2.03	1.70	1.17
	4	2.80	1.90	1.53	1.17
15	1	7.83	4.70	2.60	1.63
	2	7.30	4.43	2.37	1.70
	3	7.20	3.93	3.37	1.50
	4	7.37	4.07	2.47	1.60

Cumulative mass loading was determined by a combination of graphical integration, density, and overall count using a particle density of 1.0 g/cm^3. Table 7 contains the comparison of count-based total mass loading with the gravimetric analysis of the diffusion battery bypass filter. Effects of density on calculations are included and appear to agree optimally in the region of 2.0 g/cm^3.

The count bias distributions on the plots of cumulative mass loadings for both inlet and outlet runs for each day are in Appendix B. Overall penetration for the entire particle size distribution is defined as:

$$\overline{Pt} = \frac{1}{W_t} \int_0^W Pt_i \, dW \tag{7}$$

where W_t is the total particle mass and Pt_i is the penetration for particle diameter, d_{pi}, and it is given by:

$$Pt_i = \frac{f\,(d_{pi})\text{ outlet}}{f\,(d_{pi})\text{ inlet}} = \frac{\left[\frac{dW}{d\,(d_{pi})}\right]\text{ outlet}}{\left[\frac{dW}{d\,(d_{pi})}\right]\text{ inlet}} \tag{8}$$

where $\left[\frac{dW}{d\,(d_{pi})}\right]$ is the slope of the cumulative mass versus

particle diameter curve at d_{pi} and equals $f\,(d_{pi})$.

By measuring the slope at each given d_{pi} for both inlet and outlet, values for Pt_i were determined as a function of d_{pi}.

Table 7. COMPARISON OF COUNT-BASIS VERSUS GRAVIMETRIC-BASIS TOTAL MASS LOADING

RUN NO.	INLET/ OUTLET	PRE-CUTTER d_{50} μm	TOTAL MASS LOADING, Mg/DNm^3 [a]			
			VARIOUS PARTICLE DENSITIES			FINAL FILTER GRAVIMETRIC ANALYSIS
			1.0 g/cm^3	2.0 g/cm^3	3.0 g/cm^3	
8	Inlet	0.24	12.3	24.6	36.9	27.9
9	Outlet	0.26	1.84	3.68	5.52	3.23
10	Outlet	0.26	13.1	26.2	39.3	103.0
12	Inlet	0.24	28.3	56.6	84.9	43.3
13	Inlet	0.27	2.31	4.62	6.93	2.71
15	Outlet	0.28	0.28	0.56	0.84	0.85

[a] Normal conditions, 0° C, 760 mm Hg

Particle size distributions by number for the size range smaller than about 0.3 μm (the lowest cascade impactor cut diameter) were obtained from screen diffusion battery data by means of methods described in the previous nection. Conversion of number distribution to mass distribution is necessary in order to put the diffusion battery and cascade impactor data on the same basis. The method used to make this conversion is a graphical integration of the following equation:

$$M_{pi} = \frac{N_{pt}}{100} \int_{o}^{N_{pi}} \frac{dm_p}{dN_p} \, d\left(\frac{N_p \times 100}{N_{pt}}\right) \qquad (9)$$

where N_p = cumulative number concentration of particles smaller than "d_p", no./cm^3

N_{pt} = total number concentration of particles, no./cm^3

d_p = particle diameter, μm

d_{pi} = a specific particle diameter, μm

m_p = mass of particles in the infinitesimal size range (d_p + ddp), g

M_{pi} = cumulative mass concentration of particles smaller than "d_{pi}", g/cm^3.

The quantity (dm_p/dN_p) is simply the mass per particle of diameter "d_p". The quantity (N_p x $100/N_{pt}$) is the number percent of particles smaller than "d_p". Thus, equation (7) can be evaluated from a plot of mass per particle versus cumulative number percent of particles, both quantities being evaluated at the same particle diameter to provide a point on the plot. The total and cumulative number concentration data are obtained as described previously.

Penetration -

Equations (7) and (8) define overall penetration and techniques described previously and were used in calculation of penetration versus cut size. Penetrations for the cascade impactor and the diffusion battery were computed separately and then plotted together. The reason for this is that while the relationship between cumulative mass concentration and particle size obtained from diffusion battery data depends on particle density, the penetration does not. The slopes of the cumulative mass concentration plots for the inlet and the outlet are both proportional to particle density. Thus, the ratio of the slopes (i. e., the penetration is independent of density because it cancels out. In the comparison of cascade impactor and diffusion battery penetration data, however, there is still some dependency on the value taken for particle density because particle size must be computed from aerodynamic size. This introduces an influence of the square root of particle density.

Presentation of Results -

The results for each run are found in Appendix B. The combined cascade impactor and diffusion battery penetrations were determined using a daily average of all simultaneous runs (Figures 10, 11, and 12).

Generally, the size distributions and penetrations were consistent, though loadings fluctuated considerably. The maximum penetration (minimum efficiency) was achieved in the region of 0.2 μm actual diameter, similar to results for another scrubber as reported by Sparks et al [1974].

Elemental Chemical Analysis

Introduction -

The measurement of the concentrations of a number of elements was intended mainly to provide data to aid in the interpretation of the scrubber performance. It was not planned to perform elemental balances or determine emission factors. The samples were taken during December 10-11, 1974.

Results -

The analysis results for 29 elements are tabulated in $\mu g/m^3$ as a function of particle diameter in Appendix C. The data were interpreted

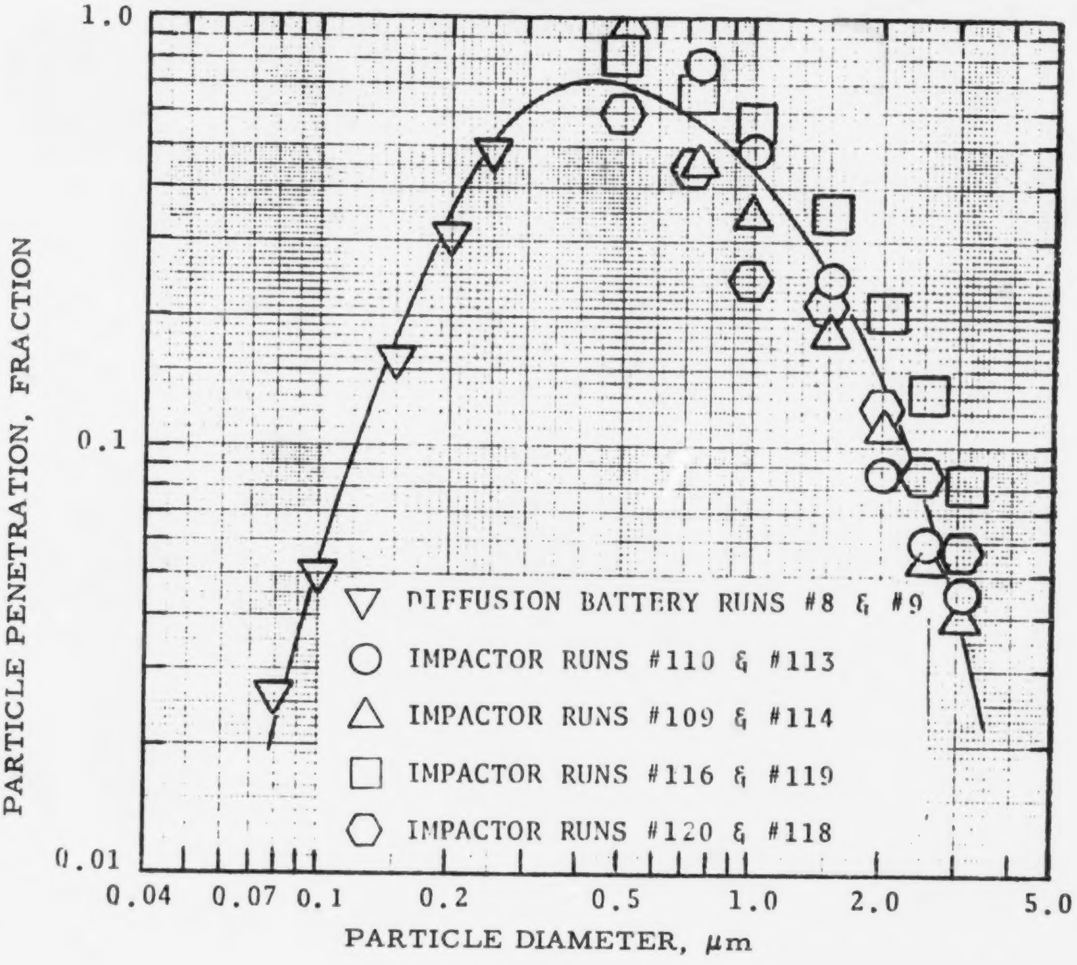

Figure 10. Combined penetrations for diffusion battery and cascade impactor (December 10, 1974)

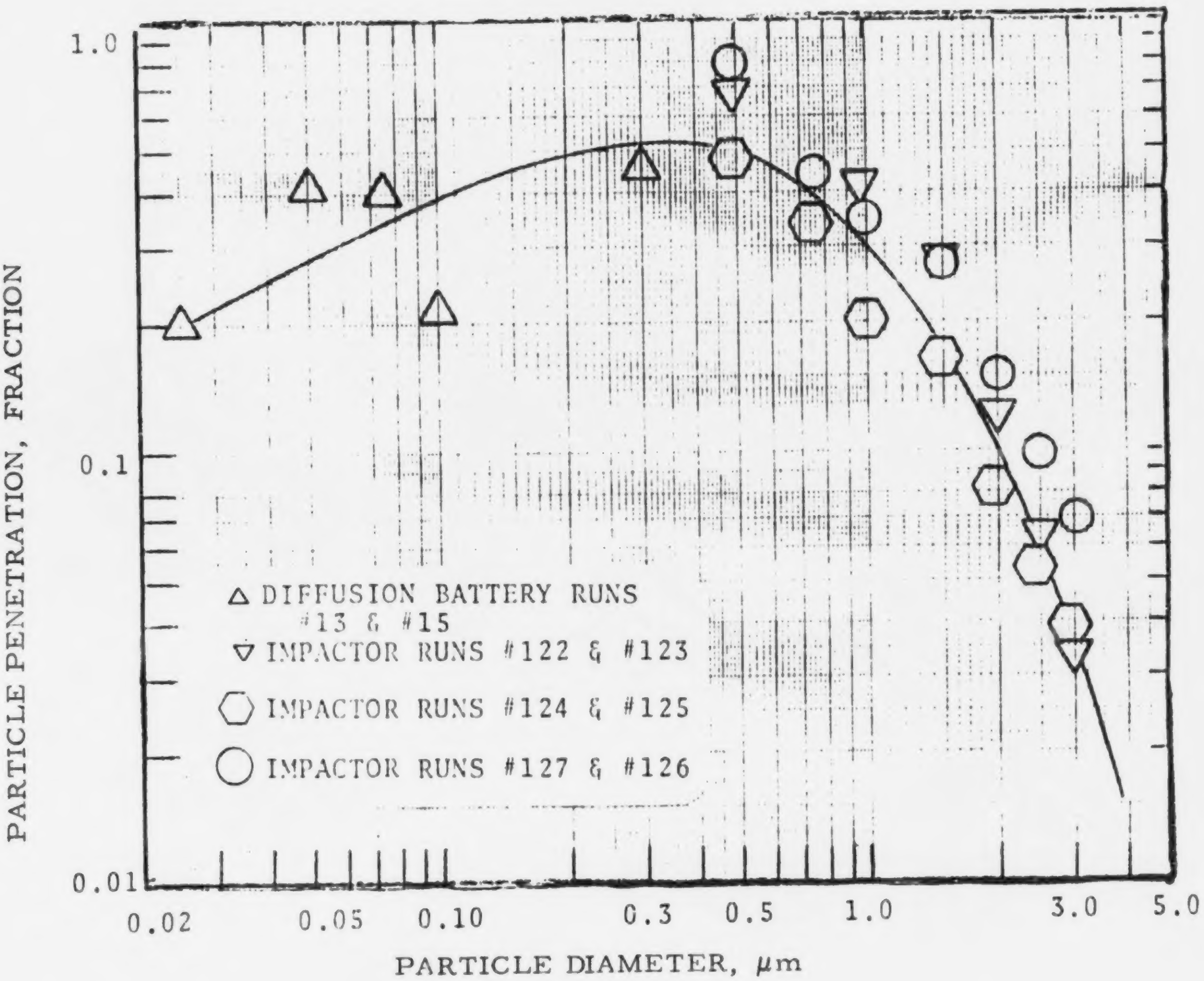

Figure 11. Combined penetrations of diffusion battery and cascade impactor (December 11, 1974)

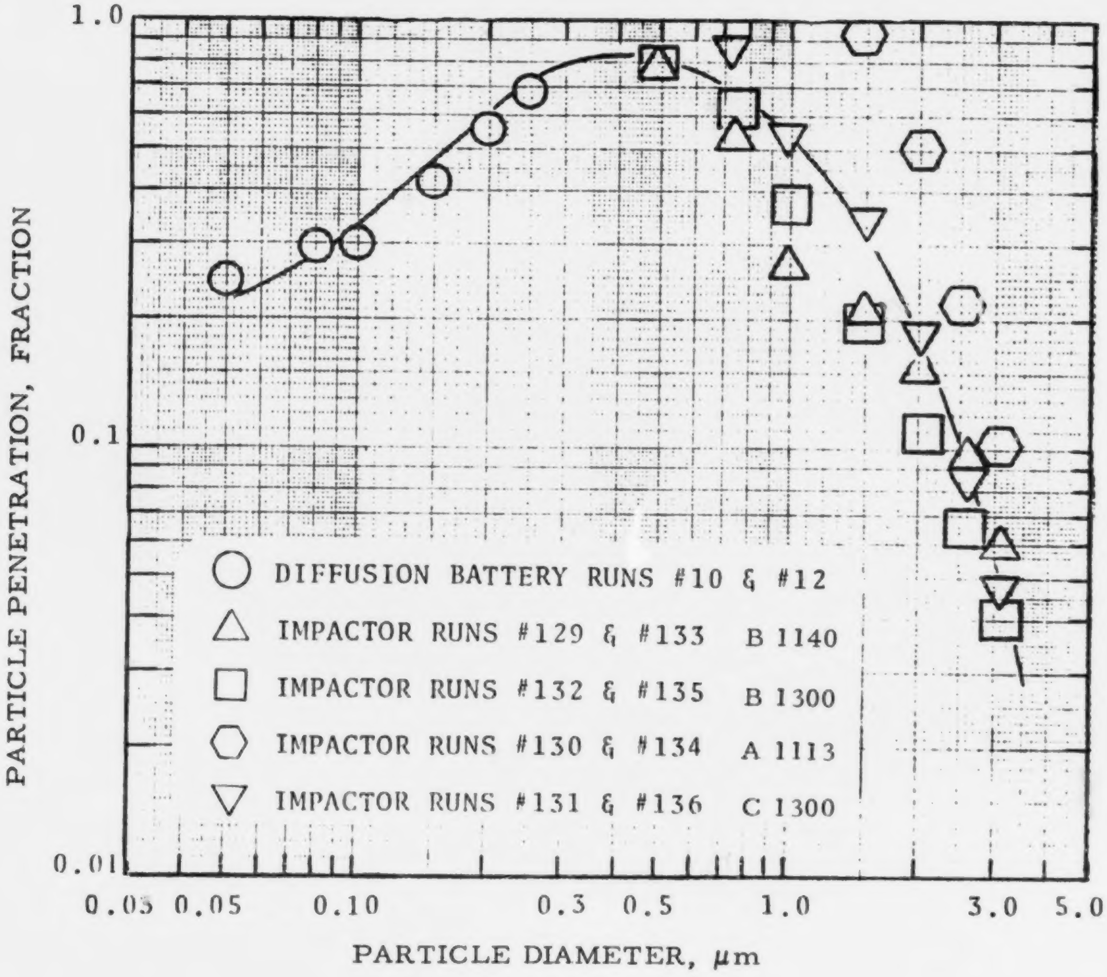

Figure 12. Combined penetrations for diffusion battery and cascade impactor (December 12, 1974)

by determining the relative changes in the chemical nature of the fly ash as a function of size and the elemental penetration through the scrubber.

The elemental concentration is ratioed to Si to indicate the relative changes in the character of the fly ash as a function of size. Si was used as the reference element for the following reasons:

1. It is the most abundant element in the Earth's crust and the major component of fly ash.

2. It is a relatively inert species in the fly ash and should be present as SiO_2. Thus, it can be used as a tracer.

The elemental ratios were computed by first calculating an average concentration (ng/m^3) for each element and then dividing by the average concentration of Si. In the tables, the elements below detectable concentrations are indicated by a dash. The changes in the ratio to Si indicate the variation in the chemical nature of the fly ash.

The elemental ratios for the inlet of the scrubber are shown in Table 8. The infrequent elements were omitted from the table for simplicity. There is enrichment for the elements S, Cu, and Zn similar to that reported by Davidson et al [1974] and Kaakinen et al [1974]. The explanation advanced for this enrichment is during combustion the volatile elements evaporate and then condense on the more inert materials when the stack gases cool. The heavier elements are present in small concentrations near the detectability limits of the technique and show indefinite trends.

In Table 9, the elemental ratios are shown for the exhaust of the scrubber. There is again enrichment for S, Cu, and Zn. The increase in S may have resulted in part from gas to particle conversion within the scrubber. There also appears an enrichment of the soluble elements such as K and Ca.

The enrichment of the exhaust of the scrubber as a function of particle size may be due to the entrainment of mist containing soluble elements. The entrainment of material through the mist eliminator has been reported by Statnick and Drehmel [1974] and Johnson and Statnick [1974].

The penetration of the elements through the scrubber was computed for December 10, 1974, with procedures similar to those used for the mass distributions. The following operations were performed:

Table 8. Ratio of elemental concentrations relative to Si for six inlet tests.

Mean Particle Size µm	30	15	6.0	2.4	1.5	0.65	0.37	Filter
Element								
Al	0.52	0.52	0.65	0.65	0.59	0.55	0.52	0.35
S	0.032	--	--	--	--	0.048	0.066	0.30
K	0.049	0.052	0.066	0.071	0.077	0.048	0.049	0.026
Ca	0.32	0.39	0.56	0.51	0.59	0.72	0.66	0.89
Ti	0.039	0.051	0.073	0.070	0.090	0.12	0.089	0.17
V	0.0049	0.0054	0.0086	0.0093	0.027	0.066	0.013	0.12
Mn	0.00004	0.00004	0.00005	0.00007	0.00014	0.0003	0.0002	--
Fe	0.22	0.29	0.50	0.52	0.67	0.73	0.52	0.54
Ni	0.0026	0.0071	--	--	0.011	0.036	0.012	--
Cu	0.0027	0.0061	0.011	0.0061	0.011	0.016	0.032	0.20
Zn	0.0007	0.0021	0.0024	0.0062	0.0083	0.020	0.12	0.48
Se	--	0.00005	0.00004	--	--	0.0002	--	--
Sr	0.00031	0.0013	0.0004	0.0004	0.0004	0.0005	0.0003	--
Pt	0.0004	0.0003	0.00001	0.0003	0.0003	0.0013	--	--
Au	0.00008	0.00005	0.00005	0.00004	--	--	--	--
Hg	0.0003	0.0003	0.0005	0.0004	0.0002	0.0006	0.0003	--
Pb	--	--	0.041	0.013	--	--	--	--

The elements Na, Mg, Cl, Cr, Co, As, Br, Rb, Zr, Ag, Ba were generally below the detection limits of the technique.

-- indicates the element was below the detection limit.

Table 9. Ratio of elemental concentrations relative to Si for **ten** outlet tests.

Mean Particle Size μm	30	15	6.0	2.4	1.5	0.65	0.37	Filter
Element								
Al	0.49	0.59	0.55	0.54	0.59	0.59	0.44	0.30
S	0.49	--	0.088	0.084	0.045	0.038	0.16	5.2
K	0.30	0.27	0.086	0.16	0.067	0.052	0.040	0.081
Ca	0.73	0.42	0.64	0.53	0.61	0.71	0.65	2.0
Ti	0.30	0.20	0.094	0.080	0.093	0.097	0.11	0.27
V	0.40	0.34	0.11	0.030	0.031	0.029	0.046	--
Mn	--	--	0.0018	0.0009	0.0006	0.0006	0.0006	0.0041
Fe	0.66	0.51	0.51	0.54	0.61	0.62	0.59	3.7
Ni	0.062	0.089	0.090	0.607	0.007	0.072	0.010	0.16
Cu	0.097	0.066	0.044	0.026	0.015	0.012	0.033	4.9
Zn	0.059	0.14	--	--	0.014	0.015	0.084	3.8
Se	--	--	--	--	0.0008	--	0.0005	0.002
Sr	--	--	--	0.002	0.002	0.002	0.002	0.005
Pt	--	--	0.007	0.601	0.001	--	0.0008	0.007
Au	--	--	--	0.002	--	0.0009	--	--
Hg	--	--	--	0.002	0.002	0.002	0.004	0.002
Pb	--	--	--	--	--	--	0.12	0.47

The elements Na, Mg, Cl, Cr, Co, As, Br, Rb, Zr, Ag, Ba were generally below the detection limits of the technique.

--indicates the element was below the detection limit.

1. The elemental data were averaged for the inlet and outlet using the same runs used for the mass penetration calculations.

2. The cumulative "smaller than" elemental concentration as a function of particle size was plotted for the inlets and outlets averaged runs.

3. The ratio of the slope of the cumulative curves for the inlet and outlet was used to compute the penetration for specific particle diameters.

The penetration of the elements is shown in Figure 13. The mass penetration has been plotted on the graph for reference. The striking implication of the elemental results is the large difference in penetration depending on chemical nature of the aerosol. Si and Al probably existing as insoluble oxides have a very low penetration through the scrubber, whereas the soluble elements have much higher penetration in the submicron region as well as a suggestion of a bimodal penetration, which may be due to entrainment through the scrubber mist eliminators.

The enrichment of the soluble elements such as K, Ca, Mn, Ni, Cu, and Zn relative to Si for both the large and small particles was unexpected. A possible explanation may be in consideration of collection mechanisms in the scrubber. The TCA scrubber contains a fluidized bed packed with plastic balls 3.8 cm in diameter. The scrubbing liquor is sprayed upon the packing. Calvert et al [1972] reported that the collection of particles in a TCA scrubber has been attributed to a bubble mechanism. The bubbles are generated as the stack gas moves up through the wetted packing. Junge [1963] summarized the process where a bubble upon breaking will form a bimodal distribution of droplets. The small particle fraction results from the fragments from the bubble film and the coarse particle fraction results from jetting produced during collapse of the bubble.

In Table 10, the elemental penetration is compared to the mass penetration. Again, the large difference between penetration of Al and Si and the other elements is apparent. It also appears that the scrubber is a source of sulfur-containing aerosols possibly in part from gas to solid phase reactions. The soluble elements, such as Cu, Zn, and Cr, appear to be generated from the evaporation of the scrubber liquor.

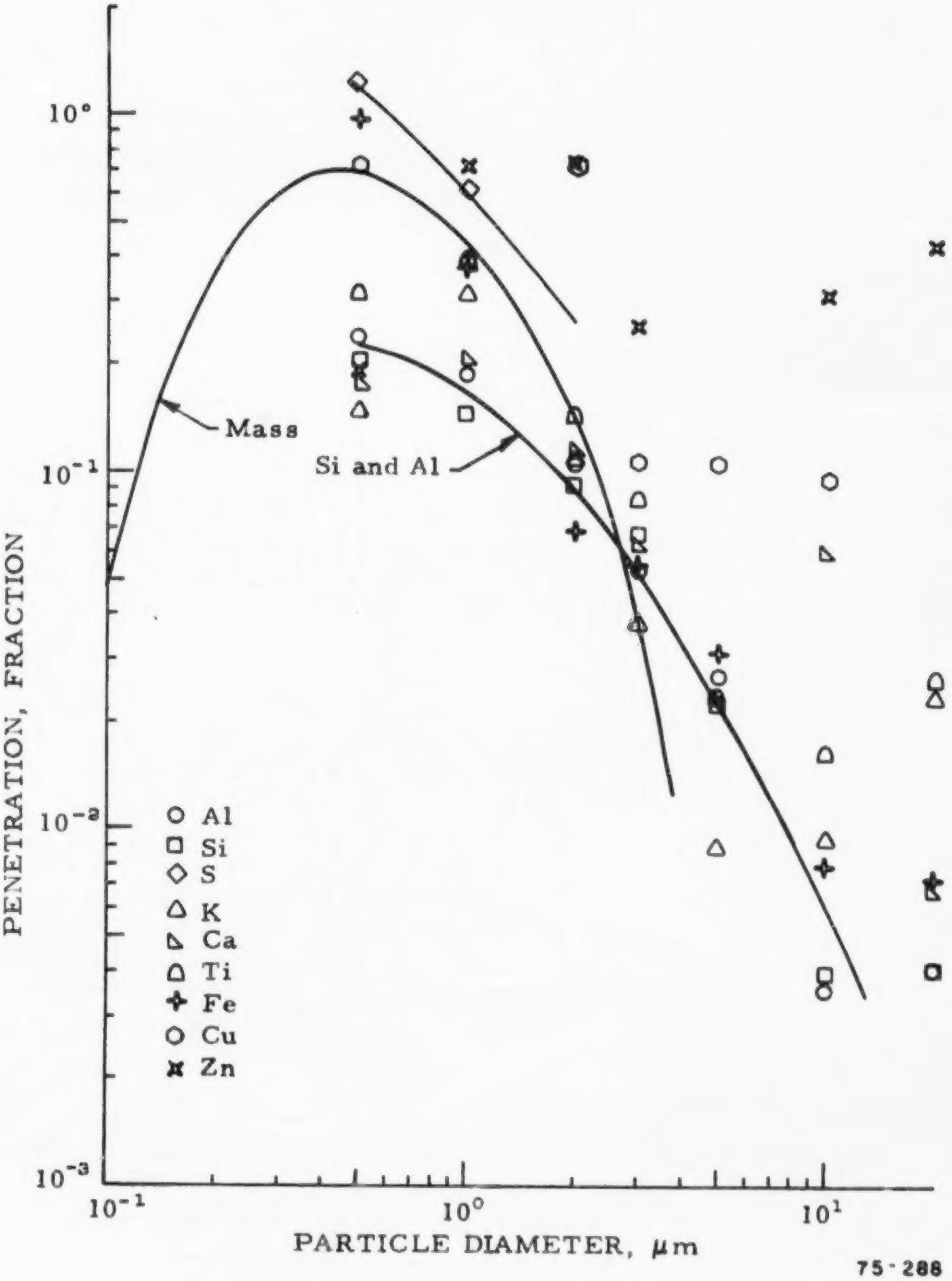

Figure 13. Scrubber penetrations for selected elements

Table 10. PENETRATION OF THE ELEMENTS THROUGH THE SCRUBBER FOR DECEMBER 10, 1974

Element	Penetration	Average Outlet Concentrations Micrograms/DSm^3 [b]
Al	0.029	326
Si	0.033	658
S	3.4 [a]	1030
K	0.043	50
Ca	0.059	508
Ti	0.073	96
V	0.14	27
Cr	1.10 [a]	57
Fe	0.18	1500
Ni	0.95	33
Cu	2.9 [a]	668
Zn	1.5 [a]	501
Br	0.28	5.7
Pb	0.64	120
For All Elements	0.108	
Total Mass	0.074	

---

[a] Penetrations greater than 1 indicate generation of particles.

[b] Dry Standard, 21.1 °C, 760 mm Hg

Discussion

Scrubber Performance -

The scrubber performance results were analyzed in depth for trends and to allow comparison to data in the literature.

Examination of the particle penetration data for each simultaneous pair of inlet and outlet runs shows a wide range of results, as summarized in the following table.

TABLE 11. PARTICLE PENETRATION SUMMARY

RUN NO. IN	RUN NO. OUT	DUCT	d_{pc},[a] μm	ΔP cm H_2O	F. out / F. in[b]
56	53	B	1.5	23.0	0.31
55	57	B	1.1	23.0	0.81
60	61	B	0.8	23.0	1.2
114	109	B	0.8	23.0	2.9
119	116	B	1.0	23.0	0.39
121	123	B	0.8	23.0	0.55
125	127	B	< 0.5	23.0	1.2
133	129	B	0.8	23.0	2.0
135	132	B	0.8	23.0	0.47
124	125	B	0.6	23.0	3.1
113	110	A	1.0	--	0.81
127	126	A	0.8	15.0	0.41
134	130	A	2.0	9.0	6.7
115	119	C	< 0.5	25.0	0.76
120	118	C	0.6	--	1.0
123	122	C	0.7	25.0	1.1
136	131	C	1.1	24.0	3.5

[a] Scrubber cut (50 percent penetration) diameter.

[b] Ratio of outlet filter to inlet filter particle concentrations $(mg/DSm^3)/(mg/DSm^3)$.

The scrubber performance cut diameter (i.e., particle diameter at 50 percent penetration), used to characterize efficiency, varied from less than 0.6 μm to 2.0 μm. No pattern of correlation between cut diameter and other parameters such as pressure drop was found. Thus, the variation was due to a combination of system fluctuations and measurement errors.

Penetrations found in this study are much higher than those reported in a previous study of the same scrubber [Calvert et al, 1974] and of other mobile bed scrubber on a coal-fired power plant [Statnick and Drehmel, 1974]. For example, Calvert et al reported a cut diameter of about 0.35 μm and a penetration at 1.0 μm of about 8 percent. Statnick and Drehmel reported that, for 25 cm of water scrubber pressure drop, penetration did not exceed 5 percent for any particle size and was about 2 for 1.0 μm particle diameter. These and some other points are compared in the following table with representative results from the present study.

TABLE 12. COMPARISON OF MOBILE BED STUDIES

INVESTIGATORS	d_{pc}, μm	PENETRATION AT PARTICLE DIAMETER SHOWN 0.5 μm	0.8 μm	1.0 μm	2.0 μm
Present[a]	0.8	0.8	0.5	0.4	0.15
Calvert et al [1974]	0.35	0.3	0.15	0.08	0.02
Statnick and Drehmel [1974]	--	0.07	0.03	0.02	0.002

[a] Approximate mean values for all runs, exclusive of 56/53 and 134/130.

The mean performance cut size found in this study is consistent with that predicted by means of Calvert's [1974] correlation of cut diameter with scrubber pressure drop. A venturi, or gas-atomizing, scrubber would have a 0.8 μm cut diameter at 23 cm of water pressure drop. This corresponds to about 0.7 μm for particle density of 1.0 g/cm^3. As discussed by Calvert et al [1974] a spray type of collection mechanism seems more appropriate than others, such as collection on packing spheres or in a packed bed.

Evidence of high outlet particle concentration due to entrainment from the scrubber weighs against one considering the agreement between predicted and experimental cut diameters to be anything more than coincidence. Facts which indicate the presence of outlet particles introduced by entrainment are as follows:

1. Outlet filter loadings are higher than inlets, based on the same gas sample volume, for many of the tests.
2. Penetrations in the present study are higher than those found by others.
3. Variations in penetration are not related to gas flow rate, pressure drop, or other known parameters, but can be attributed to variable entrainment.
4. Penetrations for scrubber section "A" are the same as for section "B" despite the gas pressure drop for "A" being about half that for "B".
5. Reheater and entrainment separator operating problems occurred during the test.
6. Elemental analyses of inlet and outlet particles show an apparent "generation" of particles containing soluble elements as described in the previous section.

The overall conclusion is that the scrubber performance data obtained in this study are specific for the operating factors and scrubber condition which existed during the test period. It is not possible to establish a general mobile bed scrubber performance model from these data because of the overshadowing and undefined influence of liquid entrainment.

Entrainment -

Both particle collection efficiency and entrainment are dependent on the gas velocity through the mobile bed and on the state of motion of the bed. Gas velocity is the parameter which has the greatest effect on the state of motion of the bed. Assuming that the flue gas is saturated with water vapor at 52° C (125° F), the partial pressure of water vapor is about 100 mm Hg and the water vapor concentration would be about 16 percent by volume at a total pressure of 635 mm Hg. The flue gas flow rate during the tests ranged about 1 x 10^6 Am^3/hr (6 x 10^5 ACFM) at 52° C (125° F) and 635 mm Hg.

Superficial gas velocity through the beds can be computed from the gas flow rate and bed area. Beds "A" and "C" have 4.58 m x 2.7 m rectangular cross sections (area = 12.7 m^2) and bed "B" has a 4.58 m x 8.37 m cross section (area = 38.3 m^2). Thus, the total superficial cross sectional area is 63 m^2 and the average superficial gas velocity is 4.5 m/sec (14.8 ft/sec).

A gas velocity of 4.5 m/sec is higher than recommended, for several reasons. To ensure proper fluidization, a velocity of 2.8 m/sec ± 20 percent is recommended. Research on pressure drop and state of motion of the bed has shown that at about 3.5 m/sec gas velocity there is a change in characteristics and at 4.5 m/sec it is quite pronounced. Pressure drop increases and bed expansion increases to the point where balls are held up against the top retainer rather than moving freely.

Recent studies (presently unpublished) by APT, Inc., have shown that entrainment from a mobile bed scrubber increases when the gas velocity exceeds about 3 m/sec, and it is severe when the velocity is 4 m/sec and higher. Extrapolation of the available data indicates that at a scrubbing liquid flow rate of 1.8 $m^3/min - m$ and a superficial gas velocity of 4.5 m/sec the entrainment flow rate might be roughly 1.5 to 2 percent of the scrubbing liquid flow rate. Thus, for a bed area of 63 m^2 the entrainment rate might be about 2 m^3/min.

The significance of 2 m^3/min of entrainment can be illustrated by assuming that the entrainment contains 15 percent solids and that the entrainment separator is 99 percent efficient. The rate of solids emission from the entrainment separator would be 3 Kg/min and the concentration in the flue gas would be 0.26 g/Nm^3. Outlet loadings in this test series ran about that magnitude and less.

It is not presently possible to predict the probable efficiency of the entrainment separator because there are insufficient data available on entrainment drop size from the mobile bed in the high flow rate range. However, the example given above illustrates the sensitivity of outlet emission rate to the bed operating conditions and the efficiency of the entrainment separator.

Reentrainment from the chevron type entrainment separator should not have been severe because the superficial gas velocity of 3.3 m/sec (based on total separator area of 86 m^2) is within the operating region for no or slight reentrainment. Irregularities such as plugging, broken or distorted baffles, etc., could cause local flooding and entrainment.

Particle collection can reasonably be expected to depend on gas velocity and bed conditions but it is not presently possible to predict the relationship. This is especially true when the fluidization of the bed may be impaired by the high gas rate and the maldistribution of balls among the bed sections.

ANALYSIS OF IN-STACK PLUME OPACITY

Data Reduction

The scattering coefficient was obtained from the strip charts and corrected for drift. A tabulation of scattering coefficient and data from impactor tests is shown in Table 13. The geometric mass mean diameter and geometric standard deviation were determined with a least square's fit to a log-normal size distrubution. The parameters of the log-normal sized distribution were also determined graphically as verification of the calculated results.

The analysis of these data consisted of comparing measured scattering coefficient (b_{scat}) with particle mass loadings and particle size distribution data obtained with the impactors. Figure 14 is a plot of b_{scat} vs particle mass for the data shown in Table 13.

The data in Figure 14 show the two groups of points, those of the inlet and those of the outlet. Averaged over the time period of the individual tests, there appears to be little real variation in b_{scat} indicating a small change in average mass loading during the test. It should be noted, however, that instantaneous b_{scat} fluctuations were monitored with the PPVs and were very prominent during apparent upset periods (see Figure 14). A Bailey meter installed on the duct work leading to the main stack exhibited similar peaks during upsets. However, the Bailey meter and PPV were not compared directly because the PPV monitored only duct B, while the Bailey measured a mixture of the three ducts.

Theresults of a linear regression analysis of the scattering coefficient data are in Table 14. The correlation of 0.766 for a linear fit indicated that 58.7 percent of the variation in the data is explained. Part of the unexplained variation in the regression was due to changes in particle size distribution.

Table 13. PLANT PROCESS VISIOMETER AND INERTIAL IMPACTOR DATA

TEST	DATE	TIME	b_{scat} m^{-1}	Mass[a] mg/Am^3	d_{50} micron	σ_g	r_c[b]	Vol. / b_{scat} cm^3/m^2
Inlet								
14	11/11	0945	0.088	118	11.3	3.51	0.991	1341
16	11/11	1240	0.077	190	15.0	3.00	0.994	2468
17	11/11	1250	0.077	158	29.3	4.00	0.987	2052
18	11/12	1015	0.100	165	9.9	3.72	0.990	1650
19	11/12	1015	0.100	171	12.0	3.77	0.992	1710
20	11/12	1245	0.120	281	14.3	3.66	0.996	2341
21	11/12	1245	0.120	340	33.1	5.22	0.993	2833
56	11.20	1030	0.116	110	3.1	3.28	0.961	948
55	11/20	1343	0.110	128	6.8	3.75	0.978	1163
62	11/21	0957	0.107	132	4.5	1.30	0.289	1233
60	11/21	1110	0.117	123	8.3	3.57	0.989	1051
68	11/21	1320	0.117	72.4	2.6	6.05	0.974	619
69	11/21	1405	0.128	64.6	15.1	3.94	0.981	505
73	11/22	1000	0.139	186	13.7	3.19	0.993	1338
		Avg	0.108					
Outlet								
37	11/18	1027	0.036	33.4	0.40	7.34	0.964	928
40	11/18	1221	0.036	18.0	1.71	6.3	0.975	500
41	11/18	1402	0.033	33.6	0.61	8.74	0.983	1018
46	11/19	1031	0.037	31.1	0.69	6.11	0.971	841
43	11/19	1133	0.035	29.4	0.62	4.04	0.966	840
51	11/19	1351	0.040	45.9	0.34	10.83	0.973	1148
63	11/20	1030	0.042	16.4				EPA Method 5
53	11/20	1034	0.042	23.0	1.22	4.11	0.936	548
57	11/20	1338	0.032	21.9	0.72	5.31	0.974	684
58	11/21	0955	0.031	13.8	0.71	6.00	0.941	445
61	11/21	1107	0.030	16.1	0.89	4.74	0.975	537
67	11/21	1317	0.032	15.7	0.67	10.0	-0.515	491
70	11/21	1402	0.032	19.1	0.68	3.24	0.988	597
74	11/22	0954	0.047	21.5	1.06	3.20	0.115	457
		Avg	0.0361					

A density of 2.0 g/cm^3 was assumed for the particles

a - Concentration at actual conditions.

b - coefficient of correlation for fit to log-normal size distribution.

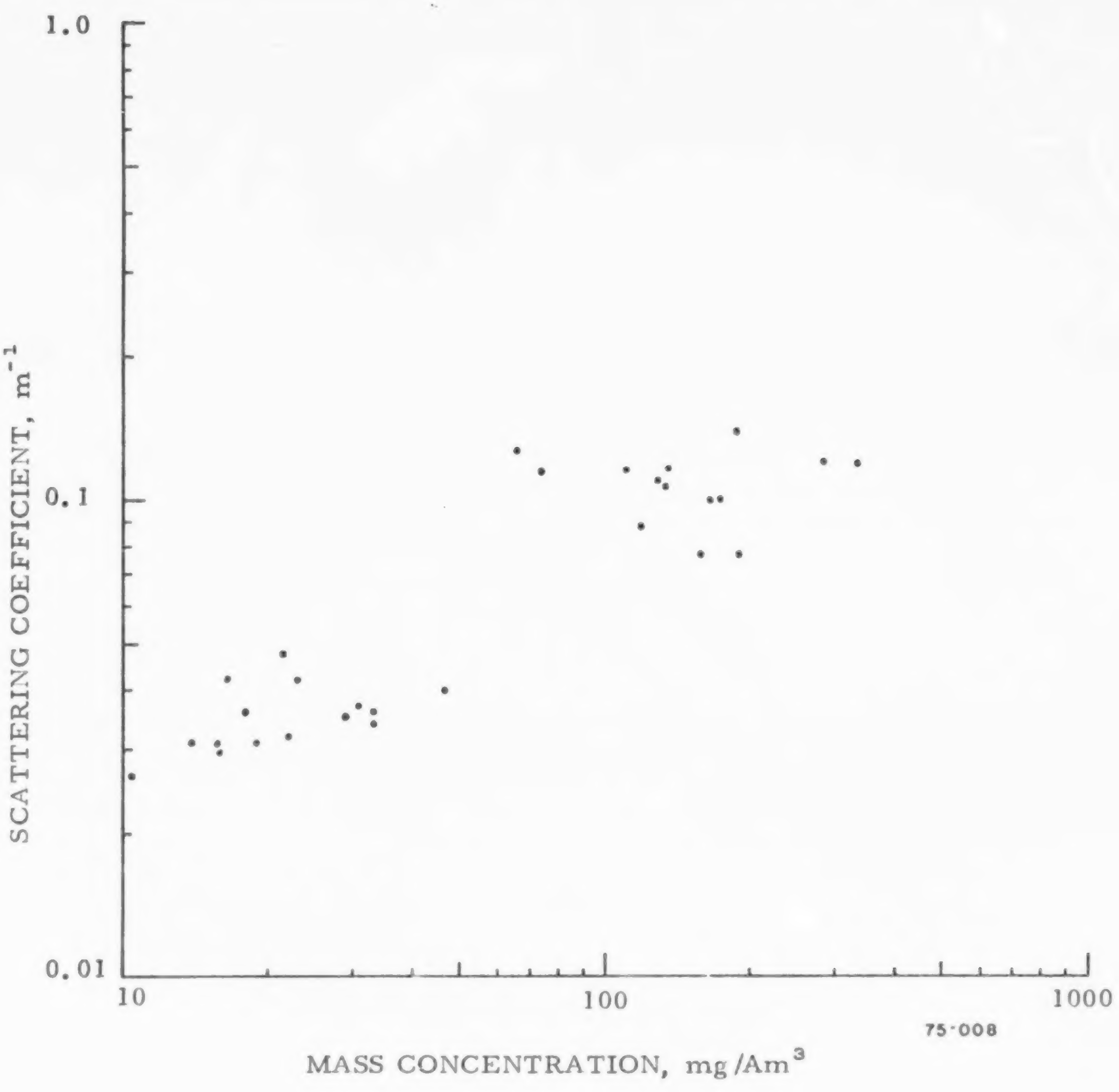

Figure 14. Scattering coefficient as a function of mass concentration

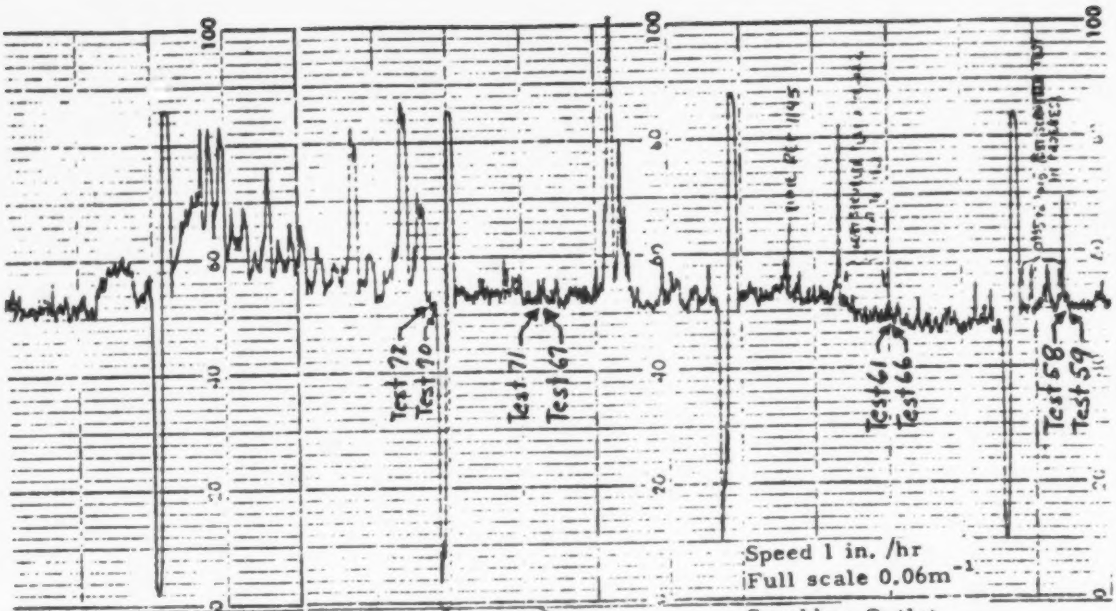

Scrubber Outlet

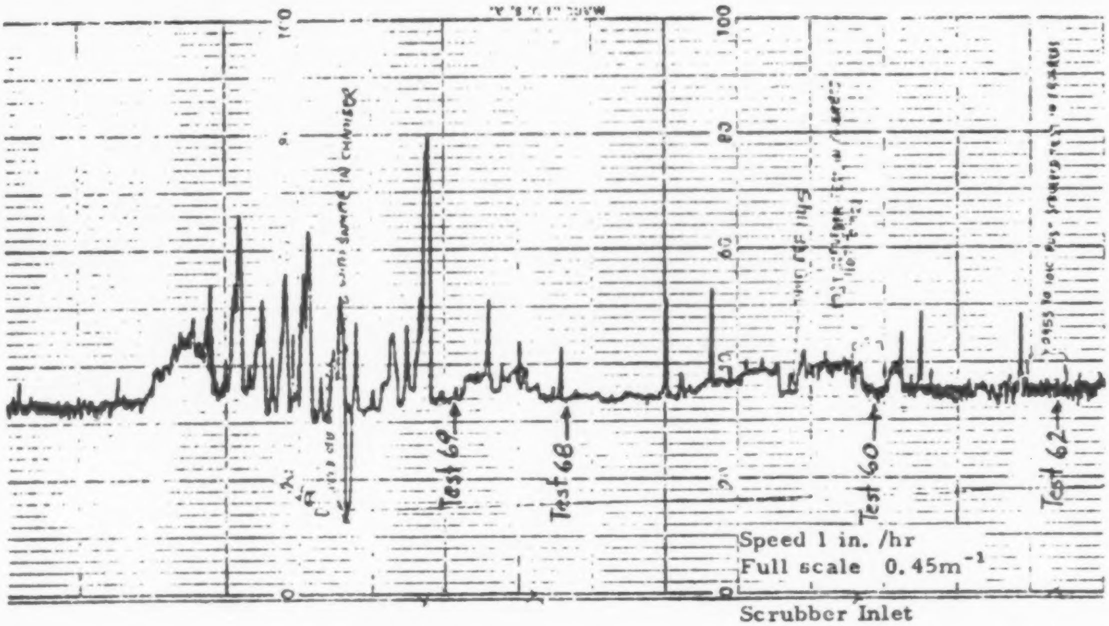

Scrubber Inlet

Figure 15. Scattering coefficient measured upstream and downstream

Table 14. CORRELATION OF MASS CONCENTRATION WITH SCATTERING COEFFICIENT

A	B	Correlation Coefficient	Std. Error of Estimate
	Mass concentration, mg/m^3 = A + B (scattering coefficient, m^{-1})		
-31.5	1683	0.766	56.2
	Log (mass concentration, mg/m^3) = A + B log (scattering coefficient, m^{-1})		
3.64	1.57	0.897	0.197
	Scattering coefficient, m^{-1} = A + B (mass concentration, mg/m^3)		
0.0408	3×10^{-4}	0.766	0.0256
	Log (scattering coefficient, m^{-1}) = A + B log (mass concentration, mg/m^3)		
- 2.11	0.514	0.897	0.113

Scattering coefficient for a given mass loading is dependent on the particle size distribution. Ensor and Pilat [1971] analytically related mass loading and size distribution to plume opacity. Assuming a log normal size distribution and using the Mie scattering equations, Ensor and Pilat calculated a curve similar to the one drawn in Figure 16 which relates the ratio of particle vol/b_{scat} to the geometric mass mean diameter. The curve shown is for a log normal size distribution and a geometric standard deviation of 4. Plotted on the same figure are data from the PPV output compared with the geometric mean diameter values derived from inertial impactor tests. The ratio of b_{scat} to mass concentration is proportional to an extinction size and is a measure of the effectiveness of a particle to obscure light. A minimum value indicates maximum light scattering effect.

Discussion -

The particulate size distributions obtained from the impactor data are not necessarily log normal. This probably accounts for the discrepancies that exist between the PPV measurements and the curve presented by Ensor and Pilat [1971]. The large difference between theory and the measurements for particles less than 0.4 microns radius may be an artifact introduced by the impactor. The smallest size resolved by the impactors was 0.4 microns diameter and, when submicron particles are sampled, most of the material falls on the filter. The size distributions are unreliable because they were determined by only one or two data points. However, the data do appear to behave in a manner similar to that which is predicted. There is a good consistency between both instruments.

In summary:

1. The PPV measures scattering coefficient and can be applied to a continuous indicator of mass loading.

2. The PPV is sensitive enough to monitor abrupt changes in scattering coefficient which can be related to boiler and scrubber upsets.

PARTICLE MORPHOLOGY

Introduction

Eight impactor tests were run with Mylar inserts for very short sample times. The purpose was to obtain light particle deposits, permitting particle count and sizing.

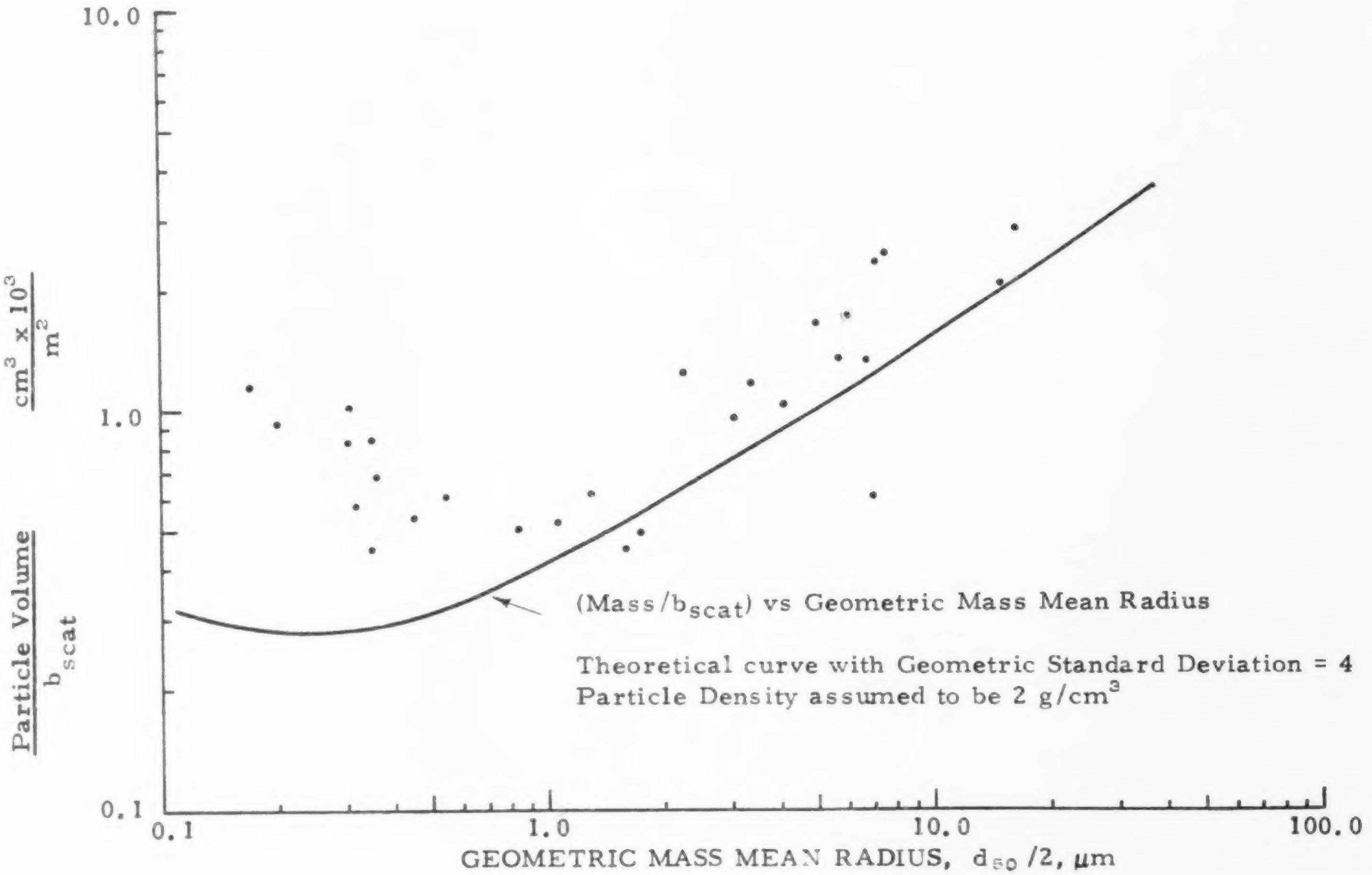

Figure 16. Effect of particle size distribution on particle volume/b_{scat} [Ensor and Pilat, 1971]

The Mylar inserts were dipped in an Apiezon L-benzene solution placed on a collection disc, and baked at 143°C (290°F) for two hours. Silver membrane filters of 0.47 and 0.8 μ pore size were used as impactor backup filters.

Impactors were inserted into the flue ducts pointing downstream and allowed to come to stack temperature. After a 20 minute warmup period, the impactors were turned into the flow and the samples were taken. Sampling time ranged from 2 to 30 seconds, summarized in Table 15. Four individual tests were run at the inlet and four at the outlet.

Analysis

In the laboratory, the samples were optically evaluated as sets. An inlet (Set 107) and an outlet (Set 103) sample set were chosen for analysis based on particle densities collected on all stages. Initial plans called for evaluation of the top three impactor stages, A, B, and C, with an optical microscope, and the lower stages, D through the filter, with a Scanning Electron Microscope (SEM). The nominal cut sizes are shown in Table 1.

For optical analysis, strips of the Mylar inserts were mounted on glass slides. Samples were then projected onto an image processor (Quantimet 720) screen through an optical transmission microscope. The Quantimet 720 automatically sizes particles and tallies them in preselected size categories. For a well-defined sample, an instantaneous documentation can be made. For a sparse sample, a special pointer can be used to document individual particles.

The SEM work was performed by Hi-Rel Laboratories of San Marino, California. A small section was cut from each sample and mounted on a holder. They were then placed in a Varian Ve-10 vacuum evaporator and 100-200 Å of gold-palladium alloy was deposited on the surface. They were documented with a Cambridge Model 54-10 SCM at magnifications of 500X to 5000X. Positive and negative photographs were taken.

Some unexpected problems affected the outcome of the data. The procedure for preparing the inserts (dipping in a grease solution, baking, and allowing to cool slowly) may have caused growth of grease crystals. These crystals were about 10 μm in size, the same size as particles expected on Stages B and C. Therefore, a severe background problem existed. Also, in the larger stages, particle deposition patterns were

Table 15. TEST CONDITIONS

Sample	Location	Duration (sec)
101	Outlet	30
102	Outlet	20
103[a]	Outlet	10
104	Inlet	2
105	Inlet	10
106	Inlet	5
107[a, b]	Inlet	3
108[b]	Outlet	5

[a] Samples evaluated.

[b] Silver membrane filters with 0.8 μ pore sizes were used.

ill defined and number counts were low. It was difficult to distinguish sampled aerosol from contaminants in background.

The particles collected on Stages E and D were embedded in the grease layer. Because a SEM can only detect surface features, particle identification and sizing were, in many cases, not possible. Eventually, measurement of Stage D was also done optically. However, the particle sizes detected on Stage D (~2 μm) border on the extreme limit of accurate measurement by the available optical microscope.

The particle deposits were found to have agglomerates as shown in Figures 17a and 17b. The agglomeration apparently takes place after capture of the particles, because the agglomerates appear to be resuspended.

The silver membrane filters selected for temperature stability as shown in Figures 18a and 18b did not have a smooth surface. Also, the particle capture appeared to take place within the pores of the matrix. Thus, qualitative evaluation was difficult.

Discussion

Inspection of the collected particles indicated that the first stages, A to D, were collecting particles about 2 times the diameter predicted by theory, while the last three stages performed as predicted. It is suspected that the short sampling times caused severe flow transients during the test which affected the collection efficiency. The significant result of the particle inspection was that no evidence for particle reentrainment was discovered.

The large particles exhibited the typical spherical shape of fly ash [McCrone et al, 1972], while the particles on the filter had more of an appearance of a floc. This may have been due to the agglomeration of very small particles or the soluble particles indicated by the trace element determinations.

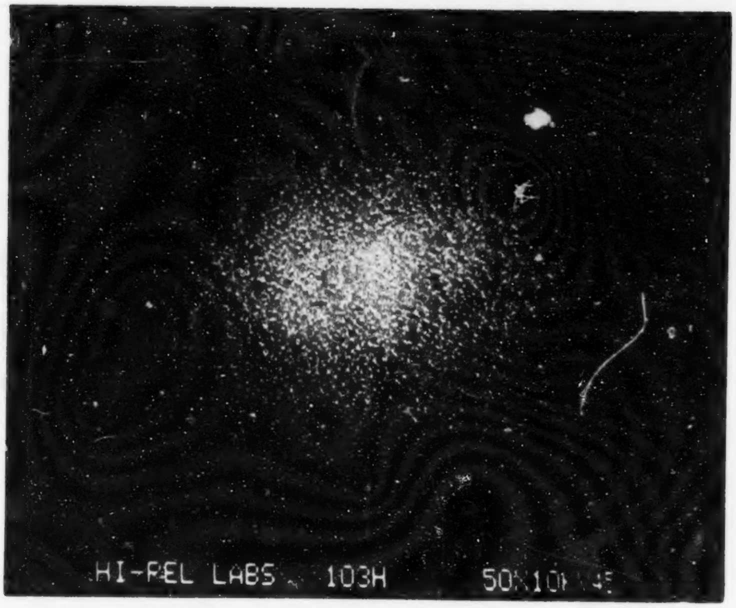
HI-REL LABS 103H 50X10K 45

a)

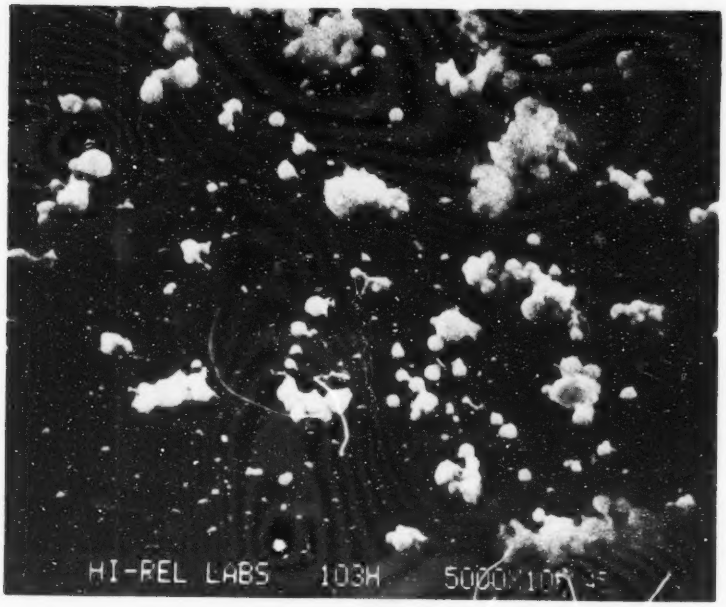
HI-REL LABS 103H 5000X10K 45

b)

75-285

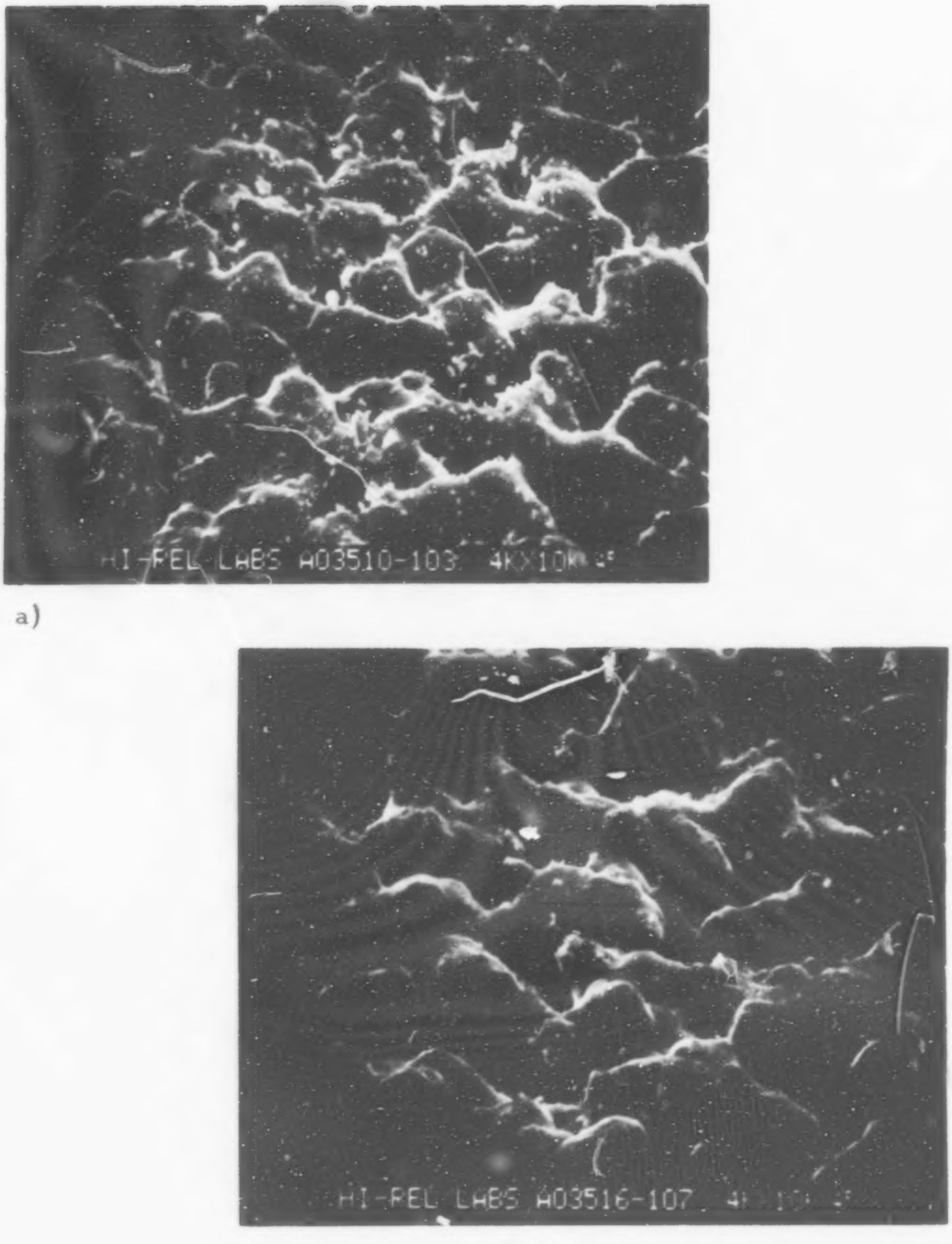
HI-REL LABS A03510-103 4KX10K
a)
HI-REL LABS A03516-107
b)

75-286

Figure 18. Microphotograph of filter.
a) Outlet 0.47 μm pore size
b) Inlet 0.8 μm pore size

SECTION V

ENGINEERING ANALYSIS

INTRODUCTION

The objective of the engineering analysis was to assemble the following information:

1. Capital costs
2. Operating costs
3. Major maintenance problems
4. Determine scrubber reliability
5. Estimate the cost required to minimize operating problems.

This section of the report will only be a summary of the findings reported by Stearns-Roger in Appendix D.

CAPITAL COSTS

The total installed cost in 1972 for the scrubber was $4,400,000. Based on the boiler nameplate rating of 150 mw, the cost is $29/kw or, based on the rated gas volume (see Section I), is $4.18/1000 m^3 hr ($7.10/1000 ACFM). The detailed cost itemization is given in Table 1, Appendix D.

In 1975 dollars, the scrubber would cost $5,800,000.

OPERATING COSTS

The total operating costs are approximately $495,000/year (fourth quarter 1973 and the first three quarters of 1974) based on 75 percent availability of the scrubber or 0.50 mills/kwh. The operating costs are summarized in Table 3, Appendix D.

MAINTENANCE PROBLEMS

The scrubber had a number of maintenance problems, many of which were solved during startup and operation. The problems mentioned here are the more persistent ones which have defied solution. The

Preceding page blank

maintenance problems are covered in detail in Appendix D. These include:

1. Breakage of Mobile Bed Contactors

   The plastic mobile bed contactors have been a chronic problem from breakage from wear. The desired lifetime of the spheres is one year, however, normally a lifetime of only 6000 hours was experienced.

   However, damage to the pump liners and plugging of the nozzles can result from the fragments entering the liquor recycle piping. Screens in the scrubber hopper have eliminated this problem with the penalty of adding screen cleaning to the required maintenance. Public Service Company of Colorado has tested a number of different packings and is currently using polyethylene spheres in the scrubber.

2. Migration of Mobile Bed Contactors

   The mobile bed contactors will also migrate from one section of the scrubber to another if an opening the width of a contactor exists in the partitions. Poor distribution of the contactors causes channeling of flue gas and a reduction in particle collection efficiency.

3. Guillotine Dampers

   The guillotine isolation dampers have caused problems due to breakage of the damper when closing against a buildup of fly ash and leakage.

4. Recirculation Pumps

   The recirculation pumps have been a source of problems in the past due to mechanical failure. A new pump has been tested by Public Service Company of Colorado and has been providing good service.

5. Reheater Section

   The scrubbed gases are heated by direct contact with three banks of steam coils. These coils are susceptible to pluggage and corrosion in the wet flue gas scrubber discharge. Addition of a second set of soot blowers and drying ash during periods of the scrubber shutdown with heavy soot blowing has had minimal effect. Corrosion problems have rendered the heaters inoperable. Both upper and lower layer reheat coils have been been removed.

6. Weather-related Problems

The freezing of lines has always been a problem during cold weather. All lines must be heat traced and drained when the scrubber is shut down.

Another solution is to enclose the scrubber in a weatherproof building. The major problem with this is the possibility of leakage of flue gas into the structure.

SCRUBBER RELIABILITY

The scrubber reliability followed a curve similar to other scrubber operations at Public Service Company of Colorado. After an initial drop in availability due to minor design problems, the availability has been steadily increasing due to solution of many of the problems.

As of November 30, 1974, the scrubber had operated at 100 percent of capacity 59.9 percent of the time and at 80 percent of capacity or greater 70.9 percent of the time. The availability of the scrubber is reported in T-15 and Figures 19 and 20 in Appendix D.

FEASIBILITY OF A "PROBLEM-FREE" SCRUBBER SYSTEM

The feasibility of using the design and operating experience to improve availability of the scrubber was investigated. The goal was to increase the availability of the scrubber, realizing that the maintenance required may slightly increase due to the extra equipment. The suggested modifications are summarized below:

		Estimated Availability (Percent)
Identical Scrubber	\$5,800,000[a]	60-70
Extra 33-1/3 Capacity Section	1,200,000	+ 10-15
Indirect Reheat, Incremental	200,000	
Scrubber Enclosure	90,000	+ 5-10
Miscellaneous Charges	80,000	
	\$7,370,000	85-95

---

[a] 1975 dollars

The capital cost of $7,370,000 is $49/kw for a 150 mw unit.

The important aspect of maintaining and improving the availability of the scrubber system is the attitude of the plant operating and maintenance people in keeping the unit on line.

The steadily increasing availability of the Cherokee scrubber is an indication that the Public Service of Colorado is committed to solving the operating and maintenance problems.

SECTION VI

REFERENCES

Bird, A. N., J. D. McCain, and D. B. Harris. Particulate Sizing Techniques for Control Device Evaluation. 66th Annual Meeting of the Air Pollution Control Assoc., Chicago, Illinois. Paper No. 73-282. June 1973.

Calvert, S. et al. Scrubber Handbook, Wet Scrubber System Study. Vol. 1, EPA PB-213-016, 1972.

Calvert, S., N. C. Jhaveri, C. Yung. Fine Particle Scrubber Performance. EPA-650/2-74-093. October 1974.

Calvert, S. Engineering Design of Fine Particle Scrubbers. Jounral Air Pollution Control Assoc., 24. p 929-934. 1974.

Camp, D. C., J. A. Cooper and J. R. Rhodes. Trace Element Determination in Aerosol Particulate Samples: Intercomparison II". X-Ray Spectrometry, 3, 47. 1974 .

Camp, D. C., A. L. VanLehn, J. R. Rhodes, and A. H. Pradzynski. Intercomparison of Trace Element Determinations in Simulated and Real Air Particulate Samples. X-Ray Spectrometry, 4. p. 123. 1975.

Cohen, J. J. and D. M. Montan. Theoretical Considerations, Design, and Evaluation of a Cascade Impactor. Am. Ind. Hyg. Ass. J., 28, pp. 95-104. 1967.

Dams, R., K. A. Rahn and I. W. Winchester. Evaluation of Filter Materials and Impaction Surfaces for Nondestructive Neutron Activation Analysis of Aerosols. Environ. Sci. Tech. 6. pp. 441-447. 1972.

Davidson, R. L., D. F. S. Natusch, and J. R. Wallace. Trace Elements in Fly Ash. Environ. Sci. Technol. 13, pp. 1107-1113. 1974.

Ensor, D. S., L. D. Bevan and G. Markowski. Application of Nephelometry to the Monitoring of Air Pollution Sources, 67th Annual Meeting of the Air Pollution Control Assoc. Denver, Colorado. Paper No. 74-110, June 1974.

Ensor, D. S. and M. J. Pilat. Calculation of Smoke Plume Opacity from Particulate Air Pollutant Properties. J. Air Poll. Control Assoc., 21, pp. 496-501. 1971.

REFERENCES (Continued)

Flocchini, R. G., T. A. Cahill, D. J. Shadoani, S. Lange, R. A. Eldred, P. J. Feeney, G. Wolfe, D. Simmeroth, and J. Suder. Monitoring California's Aerosols by Size and Elemental Composition, Part I: Analytical Techniques. Environ. Sci. Technol. In press.

Johnson, L. D. and R. M. Statnick. Measurement of Entrained Liquid Levels in Effluent Gases from Scrubber Demisters. EPA 650/2-74-050. 13 pp. June 1974.

Junge, C. E. Air Chemistry and Radioactivity. Academic Press, New York. pp. 157-159. 1963.

Lundgren, D. A. An Aerosol Sampler for Determination of Particle Concentration as a Function of Size and Time. J. Air Poll. Cont. Assoc. 17. 225 p. 1967.

Kaakinen, J. W., R. M. Jorden, R. E. West. Trace Element Study in a Pulverized-Coal-Fired Power Plant. University of Colorado, 67th Annual Meeting of the Air Pollution Control Assoc., Denver, Colorado. Paper No. 74-8. June 1974.

Marple, V. A. and B. Y. H. Liu. Characteristics of Laminar Jet Impactors. Environ. Sci. Technol. 8. pp. 648-654. 1974.

McCrone, W. C. and J. G. Delly. The Particle Atlas, 2nd Ed. Ann Arbor Science Pubs., Inc., Ann Arbor, Mich. 48106. 1973.

Pilat, M. J., D. S. Ensor, and J. C. Bosch. Source Test Cascade Impactor. Atmos. Environ., 4. pp. 671-679. 1970.

Raben, I. A. Use of Scrubbers for Control of Emissions from Power Boilers - U. S. Paper No. 13. Proceedings Symposium on Control of Fine Particulate Emissions from Industrial Sources. San Francisco, California. January 1974.

Ranz, W. E. and J. B. Wong. Impaction of Dust and Smoke Particles. Ind. and Eng. Chem., 44, 1371 p. 1952.

Rao, A. K. Sampling and Analysis of Atmospheric Aerosols. Particle Technology Laboratory, Mechanical Technology Laboratory, University of Minnesota. Publication 269. June 1975.

REFERENCES (Continued)

Schlichting, H. Boundary Layer Theory. McGraw-Hill, New York. 742 p. 1968.

Sinclair, D. A Portable Diffusion Battery. Am. Inst. Hygiene Assoc. J. pp. 729-734. 1972.

Smith, W. B., K. M. Cushing, and J. D. McCain. Particulate Sizing Techniques for Control Device Evaluation. Special Summary Report 21. 1974.

Smith, W. B., K. M. Cushing, and G. E. Lacey. Andersen Filter Substrate Weight Loss. EPA-650/2-75-022. 1975.

Sparks, L. E. Personal Communication. 1971.

Statnick, R. M. and D. C. Drehmel. Fine Particle Control Using Sulfur Oxide Scrubbers. 67th Meeting of the Air Pollution Control Assoc., Denver, Colorado. Paper No. 74-231. June 1974.

APPENDIX A

WALL LOSSES IN INLET PIPING OF THE PLANT PROCESS VISIOMETER

WALL LOSSES IN INLET PIPING OF THE PLANT PROCESS VISIOMETER

The most critical parameter affecting particle loss to flow piping walls is the Reynolds number, defined as

$$R_e = \frac{\rho_f \overline{U} D_P}{\mu_f}$$

where ρ_f = fluid density

$\overline{U}$ = mean flow velocity

D_P = pipe diameter

μ_f = fluid viscosity

If this dimensionless parameter exceeds 2300 (Schlichting, 1968), there exists a high probability that turbulent flow will develop if the pipe length is greater than 40 pipe diameters. This latter figure represents the nominal distance required for the turbulence to fully develop, and can be considered, for the purposes of this analysis, to be a laminar flow region.

The mechanism of particle loss in (horizontal) laminar flows is twofold: the particles will attain their terminal settling velocities rather quickly and be deposited on the walls by simple sedimentation, or be deposited on the walls by Brownian diffusion. The effects of the former mechanism are most observable on large particles with high inertia, while the latter mechanism is specific to small particles whose diameter is on the same order as the gas mean free path.

Turbulent losses occur because of the combined effects of Brownian and eddy diffusion. Eddy diffusion can be viewed as the deposition of particles that are small enough to nearly "follow" the random fluctuations of the turbulent flow, but if near the pipe wall and projected at it, are deposited due to their own inertia. Small particles (< 1 μm) have insufficient inertia, large ones (> 50 μm) will not respond to turbulent fluctuations.

The PPV sampling probe, which can be as long as 3.6 m (12 ft) maintains flow velocities in the range of 15-21 mps. Assuming a local altitude of 1.5 km above sea level, so that (U. S. Standard Atmosphere Tables, 1966)

ρ_{f_a} = ambient air density = 1.098 kg/m^3

λ_a = ambient mean free path = 7.68 x 10^{-6} m

C_a = ambient sound speed = 344.4 m/sec

T_a = ambient temperature = 15°C

and assuming T_f = gas temperature in the probe = 250°F, the sampling probe operates over a Reynold's number range of

$$8911 < R_e < 12,475$$

For the purposes of this calculation,

$$\rho_f = \rho_{f_a} \frac{T_a}{T_f}$$

and $$\mu_f = \frac{\beta T_f^{3/2}}{T_f + S}$$

where β = 1.458 x 10^{-6} kg/(m-sec-(°K)$^{1/2}$)

and S = Sutherland's correction = 110.4°K

Thus, the PPV probe will be a mixture of laminar and turbulent flow. In addition, the probe has a 3.6 cm radius right-angle bend This bend has the potential of generating pockets of turbulence (and the associated deposition) on the inside wall of the turn. Furthermore, the centrifugal force experienced by particles in the fluid stream will tend to deposit them on the outside wall of the turn by the mechanism of impaction. Although not consistent with the probe's actual geometry, the PPV flow piping was treated as a pipe of 40 diameters (0.66 meters) of laminar flow, followed by a 3.6 cm radius turn, followed by a straight pipe betveen 0.6 and 3 m in length, and in which fully developed turbulent flow had evolved. Presented below are the details of the theories appearing in the literature that were applied to this physical model.

A.1 Laminar Sedimentation

Fuchs [1964] cites the result of G. Natanson for particle loss due to simple sedimentation. The loss fraction due to sedimentation, LF_s, is given by

$$LF_s = 1 - \frac{2}{\pi}\left(2\,\epsilon\sqrt{1-\epsilon^{2/3}} + \arcsin(\epsilon^{1/3}) - \epsilon^{1/3}\sqrt{1-\epsilon^{2/3}}\right)$$

where $\epsilon = \dfrac{3\,V_s\,L}{8\,R\,\overline{U}}$

and where V_s = particle settling velocity

L = pipe length (0.66 meters)

R = pipe radius

The settling velocity is normally given by

$$V_s = BF$$

where B = particle mobility

F = force on particle

The force on the particle in this case is gravity, so that

$$V_s = B\,(\rho_p - \rho_f)\,g\,\frac{\pi}{6}\,d^3 \cong B\rho_p\,\frac{\pi}{6}\,g\,d^3$$

where ρ_p = particle density = 1.0 g/cc

g = acceleration of gravity

d = particle diameter

The particle mobility, as suggested by Fuchs (1964) is given by

$$B = \begin{cases} \dfrac{4.364\,\lambda_f}{6\pi\,\mu_f\,d^2} & \text{for} \quad \dfrac{2\,\lambda_f}{d} >> 1 \\[2em] \dfrac{1 + 0.864\left(\dfrac{2\,\lambda_f}{d}\right) + 0.29\left(\dfrac{2\,\lambda_f}{d}\right)\exp\left(\dfrac{-1.25\,d}{2\,\lambda_f}\right)}{3\pi\,\mu_f\,d} & \text{for} \quad \dfrac{2\,\lambda_f}{d} \sim 1 \\[2em] \dfrac{1 + 0.7\left(\dfrac{2\,\lambda_f}{d}\right)}{3\pi\,\mu_f\,d} & \text{for} \quad \dfrac{2\,\lambda_f}{d} << 1 \end{cases}$$

where λ_f = mean free path in the probe.

Since λ is given by

$$\lambda = 3\,\frac{\mu}{\rho}\sqrt{\frac{\pi}{8}\,\frac{M}{RT}}$$

where μ, M, and R are the viscosity, molecular weight, and gas constant, respectively, then

$$\frac{\lambda_f}{\lambda_a} = \frac{\mu_f}{\mu_a}\left(\frac{T_f}{T_a}\right)^{1/2}$$

A.2 Laminar Diffusion

Fuchs [1964] also specifies the losses to be expected from the action of Brownian diffusion. The loss fraction due to diffusion, LF_B, is a function of the dimensionless parameter

$$\eta = \frac{4\,D\,L}{D_P^2\,\bar{U}}$$

where D = particle diffusion coefficient.

The exact relation has been empirically determined to be

$$LF_B = \begin{cases} 1 - 0.819 \exp(-3.65\,\eta) - 0.097 \exp(-22.3\,\eta) \\ \qquad - 0.032 \exp(-57\,\eta) \text{ for } \eta > 0.01 \\ 2.56\,\eta^{2/3} - 1.2\,\eta - 0.177\,\eta^{4/3} \qquad \text{for } \eta > 0.01 \end{cases}$$

The diffusion coefficient is given by

$$D = K\,T_f\,B$$

where K = Boltzmann's constant

The particle mobility, B, is given by the equations listed in the previous section.

Diffusion is naturally expected to show its greatest effect for small particles. It should be noted that, because the denominator of η contains the product of $\bar{U}\,D_P^2$, as long as a constant flow rate and laminar flow conditions are maintained, changing the tube size will not vary the deposition rate.

A.3 Losses at Piping Bends

Particle deposition at abrupt turns in the flow direction has been studied in some detail due to its applicability in impactor work. The dimensionless inertia parameter, ψ, referred to as the Stokes' number, has been determined to govern inertial impaction, where

$$\psi = \frac{C\,\rho_P\,\bar{V}\,d^2}{18\,\mu\,R}$$

where C = Cunningham slip correction factor

$$= 1 + \frac{2\lambda_f}{d} [1.23 + 0.41 \exp(-0.44\, d/\lambda_f)]$$

According to Fuchs [1964], when the value of ψ is less than 0.05, particles will follow flow streamlines and not be deposited. Assuming the flow conditions described previously ($\overline{U}$ = 21 m/sec), the largest particle that meets the Fuchs criterion is 5.8 microns in diameter. Ten micron particles yield a Stokes number of 0.15. In impactor work, the impaction efficiency has been determined to be a function of $\sqrt{\psi}$. Stern et al [1960] performed experiments with impactors having circular jets and determined the impaction efficiency as a function of $\sqrt{\psi}$. Although not strictly applicable in this case, the Stern curve has been used to estimate the loss of 10 micron particles. The result indicates that roughly 70 percent of all 10 micron particles would be impacted on the pipe wall at the right angle turn. This figure has been for the loss fraction due to the probe bend of radius R, LF_R. Reiterating, LF_R for all particles of diameter $d < 5.8\ \mu m$ is equal to zero.

A.4 Turbulent Deposition

Turbulent losses are the result of a combination of Brownian and eddy diffusion, and are not completely understood. Several theories exist in the literature, however, and are compared to experimental results in a paper by Liu and Agarwal [1974]. They indicate that the theories of Friedlander and Johnstone [1957], Beal [1970] and Liu and Ilori [1973] describe the mechanism quite accurately in the larger particle ranges ($\geq 1\ \mu m$), but fail to varying degrees in the range where Brownian diffusion begins dominating deposition. The theory of Davies [1966], on the other hand, underestimates the rate of deposition in the large particle range, and overestimates slightly in the Brownian diffusion regime.

Parker [1968] relates the loss fraction equation common to all theories as

$$LF_T = 1 - \exp\left(- \frac{4\, v_t\, L}{\overline{U}\, D_P}\right)$$

where LF_T = loss fraction due to turbulent deposition

and v_t = transport or deposition velocity

The goal of all of the above mentioned theories is to evaluate v_t. All theories deal with the stopping distance of the particles of interest. It is assumed that the turbulent fluctuations hurl the particles at the wall boundary layers at a velocity proportional to the mean velocity, and only those particles brought to within one particle stopping distance will be deposited. The essential differences in the theories are to be found in the constant of proportionality between the "hurling" velocity and the mean velocity, and in the form of the empirical relations for the eddy diffusion coefficients that are required for the analysis.

The authors have selected a combination of the theories of Davies and Beal for deposition calculations. Specifically, the theory of Davies was used in the calculation of 0.01 and 0.1 μm deposition, while all other particle sizes were subjected to the Beal theory. The essentials of these theories are now presented.

A.4.1 Small Particle Turbulent Deposition [Davies, 1966]

All variables are first non-dimensionalized in the standard fluid mechanical fashion

$$y_+ = \frac{y\,U_*}{\nu}$$

$$V_+ = \frac{V_t}{U_*}$$

where y = distance from the pipe wall

U_* = friction velocity of turbulent flow

ν = kinematic viscosity

For the purposes of these calculations, the Blasius value of U_* is used:

$$U_* = \sqrt{\frac{1}{8} \cdot \frac{0.3164}{\sqrt[4]{R_e}}}\ \overline{U}$$

Y'_+ defines the non-dimensional thickness of the Brownian diffusion layer and is given by

$$Y'_+ = 20\,(D/\nu)^{1/3}$$

τ_+ is the non-dimensional relaxation time, given by

$$\tau_+ = \frac{\tau\, U_*^2}{\nu}$$

where τ is the relaxation time. Here,

$$\tau = Bm$$

where m is the particle mass.

If $a_+ = \frac{d_+}{2}$, where d_+ is the dimensionless particle diameter, the non-dimensional radial fluctuation velocity is given by

$$V'_+ = \frac{1}{2}\left(1 - \frac{a_+ + 10}{\tau_+}\right) + \sqrt{\frac{1}{4}\left(1 - \frac{a_+ + 10}{\tau_+}\right)^2 + \frac{a_+}{\tau_+}}$$

The non-dimensional particle stopping distance is given by

$$s_+ = V'_+\,\tau_+$$

The value of Φ is next calculated from

$$\Phi = \frac{s_+ + a_+}{10\,(D/\nu)^{1/3}}$$

The non-dimensional deposition velocity is then given by

$$\frac{1}{V_+} = \begin{cases} 10\left(\dfrac{\nu}{D}\right)^{2/3} f(\Phi) + [I]_{y'_+}^{R_+} \dfrac{1}{V_+}\ , & \text{for } s_+ + a_+ < y'_+ \\[2ex] [I]_{y'_+}^{R_+} + \dfrac{1}{V'_+}\ , & \text{for } s_+ + a_+ > y'_+ \end{cases}$$

In these equations,

$$f(\Phi) = 0.7877 - \frac{1}{6}\,\ell n \left\{\frac{(1+\Phi)^2}{1 - \Phi + \Phi^2}\right\} - \frac{1}{\sqrt{3}} \arctan \frac{2\Phi - 1}{\sqrt{3}}$$

and $$[I]_{y'_+}^{R_+} = \int_{y'_+}^{R_+} \frac{dy_+}{\epsilon/\nu}$$

where $$\epsilon/\nu = \frac{y_+^{(4 - 0.08\,y_+)}}{1000\left(\dfrac{2.5 \times 10^7}{R_e}\right)^{y_+/(400 + y_+)}}$$

and ϵ = eddy diffusion coefficient

R_+ = non-dimensional pipe radius

The above integral has been evaluated by computer and is tabulated in the paper by Davies.

A.4.2 Large Particle Turbulent Deposition [Beal, 1970]

Beal estimates the particle stopping distance, S, to be given by

$$S = \frac{\rho_P d^2 V}{18 \mu} + \frac{d}{2}$$

where $V = 0.9 U_*$

The average velocity, $\overline{V}$, of particles close to the pipe wall is considered to be composed of two components: that due to the fluid motion (V_f) and that due to Brownian diffusion (V_B). Hence,

$$\overline{V} = V_f + V_B$$

Beal defines a transport coefficient, K, and this parameter is related to the deposition velocity by the equation

$$V_t = \frac{K \overline{V} P}{K + P \overline{V}}$$

where P is the sticking probability, assumed to be 1.0 for this analysis.

The particle velocity due to fluid motion is taken from the data of Laufer (1951) and is given in non-dimensional form as

$$V_f^+ = \begin{cases} 0.05\, y_+, & 0 \leq y_+ \leq 10 \\ 0.5\, y_+ + 0.0125\,(y_+ - 10), & 10 \leq y_+ \leq 30 \end{cases}$$

Since the particles may be anywhere between $y_+ = S_+$ and $y_+ = d_+/2$, Beal averages the values of V_f^+ at these locations in a special fashion to obtain

$$V_f = \frac{U_*}{4} \left[V_{f_+}\left(\frac{d_+}{2}\right) + V_f^+ \left(S_+\right) \right]$$

V_B is given by the equipartition energy formula from the kinetic theory of gases

$$V_B = \left[\frac{K\,T_f}{2\pi m}\right]^{1/2}$$

The value of K depends upon the magnitude of S_+:

$$\frac{K}{U_*} = \begin{cases} \Bigg[\Bigg\{\frac{14.5}{3}\left(\frac{\nu}{D}\right)^{2/3} F - \frac{(14.5)^2}{1.5\,R_+}\left(\frac{\nu}{D}\right)^{1/3} G + \\ \qquad \left[5 + \frac{50}{\nu\,R_+}\,(D - 0.959\,\nu)\right] \ell n \left(\frac{D + 5.04\,\nu}{D + 0.04\,\nu}\right) \\ \qquad - \frac{250}{R_+} + \frac{\bar{U} - 13.73\,U_*}{\bar{U}}\Bigg\}^{-1}, & \text{for } 0 \le S_+ < 5 \\ \Bigg\{5\,\Bigg\{\left[1 + \frac{10}{\nu\,R_+}\,(D - 0.959\,\nu)\right] \ell n \left\{\frac{D + 5.04\,\nu}{D + \nu\left(\frac{S_+}{5} - 0.959\right)}\right\} \\ \qquad - \frac{10}{R_+}\left(6 - \frac{S_+}{5}\right)\Bigg\} + \frac{\bar{U} - 13.73\,U_*}{\bar{U}}\Bigg\}^{-1}, \\ \qquad \text{for } 5 \le S_+ < 30 \\ \frac{U_*}{\bar{U} - 13.73\,U_*}, & \text{for } S_+ > 30 \end{cases}$$

If A is defined as

$$A = \frac{\left[1 + \frac{5}{14.5}\left(\frac{\nu}{D}\right)^{1/3}\right]^2}{1 - \frac{5}{14.5}\left(\frac{\nu}{D}\right)^{1/3} + \left(\frac{5}{14.5}\right)^2\left(\frac{\nu}{D}\right)^{2/3}}$$

and

$$B = \frac{\left[1 + \frac{S_+}{14.5}\left(\frac{\nu}{D}\right)^{1/3}\right]^2}{1 - \frac{S_+}{14.5}\left(\frac{\nu}{D}\right)^{1/3} + \left(\frac{S_+}{14.5}\right)^2\left(\frac{\nu}{D}\right)^{2/3}}$$

$$C = \frac{\frac{10}{14.5}\left(\frac{\nu}{D}\right)^{1/3} - 1}{\sqrt{3}}$$

$$D = \frac{\frac{2S_+}{14.5}\left(\frac{\nu}{D}\right)^{1/3} - 1}{\sqrt{3}}$$

then

$$F = \frac{1}{2}\,\ell n\left(\frac{A}{B}\right) + \sqrt{3}\,\left[\tan^{-1} C - \tan^{-1} D\right]$$

and

$$G = \frac{1}{2}\,\ell n\left(\frac{B}{A}\right) + \sqrt{3}\,\left[\tan^{-1} C - \tan^{-1} D\right]$$

These equations were used for loss calculations for 1.0, 3.0, 5.8, and 10.0 microns, for pipe lengths of 2 to 10 feet using the values of flow parameters discussed in previous sections.

REFERENCES

Beal, S. K., 1970: Deposition of particles in turbulent flow on channel or pipe walls. Nucl. Sci. and Eng., 40, 1-11.

Davies, C. N., 1966: Deposition of aerosols from turbulent flow through pipes. Proc. Roy. Soc., A, 289, 235-246.

____________, 1966: Brownian deposition of aerosol particles from turbulent flow through pipes. Proc. Roy. Soc., A, 290, 557-562.

Friedlander, S. K., and H. F. Johnstone, 1957: Deposition of suspended particles from turbulent gas streams. Ind. Eng. Chem., 49, 1151-1156.

Fuchs, N. A., 1964: The Mechanics of Aerosols. New York, MacMillan Co., 408 pp.

Liu, B. Y. H., and T. A. Ilori, 1973: Inertial deposition of aerosol particles in turbulent pipe flow. American Society of Mechanical Engineers Symposium on Flow Studies in Air and Water Pollution, Atlanta, June 20-22, pp. 103-113.

Liu, B. Y. H., and J. K. Agarwal, 1974: Experimental observation of aerosol deposition in turbulent flow. Aerosol Sci., 5, 145-155.

Parker, G. J., 1968: Some factors governing the design of probes for sampling in particle - and drop - laden streams. Atmos. Envir., 2, 477-490.

Schlichting, H., 1968: Boundary Layer Theory. New York, McGraw-Hill, 742 pp.

Stern, S. C., H. W. Zeller, and A. I. Schekman, 1962: Collection efficiency of jet impactors at reduced pressures. I & EC Fundamentals, pp. 1, 1962.

U. S. Standard Atmosphere, 1962.

APPENDIX B

REDUCED DIFFUSION BATTERY AND IMPACTOR DATA

Table B-1 CASCADE IMPACTOR TESTS USED IN PENETRATION ANALYSIS

MONTH	DAY	RUN#	LOCATION
November	20	53	Outlet
		55	Inlet
		56	Inlet
		57	Outlet
	21	60	Inlet
		61	Outlet
December	10	109	Outlet
		110	Outlet
		113	Inlet
		114	Inlet
		116	Outlet
		118	Outlet
		119	Inlet
		120	Inlet
		122	Outlet
	11	123	Inlet
		124	Inlet
		125	Outlet
		126	Outlet
		127	Inlet
	12	129	Outlet
		130	Outlet
		131	Outlet
		132	Outlet
		133	Inlet
		134	Inlet
		135	Inlet
		136	Inlet

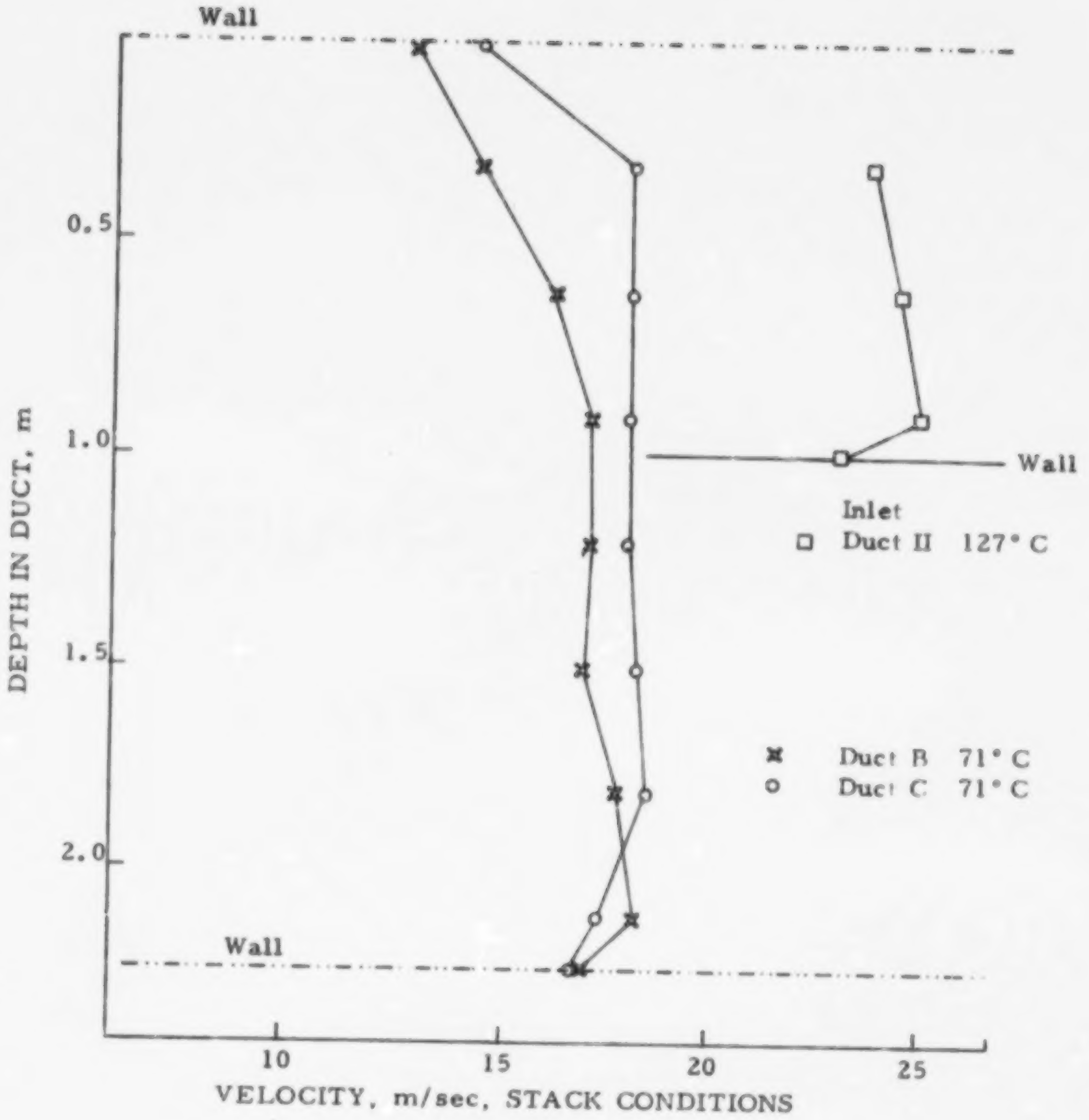

75-238

Fig. B-1. VELOCITY TRAVERSE INLET AND OUTLET DUCTS (NOVEMBER 20, 1974)

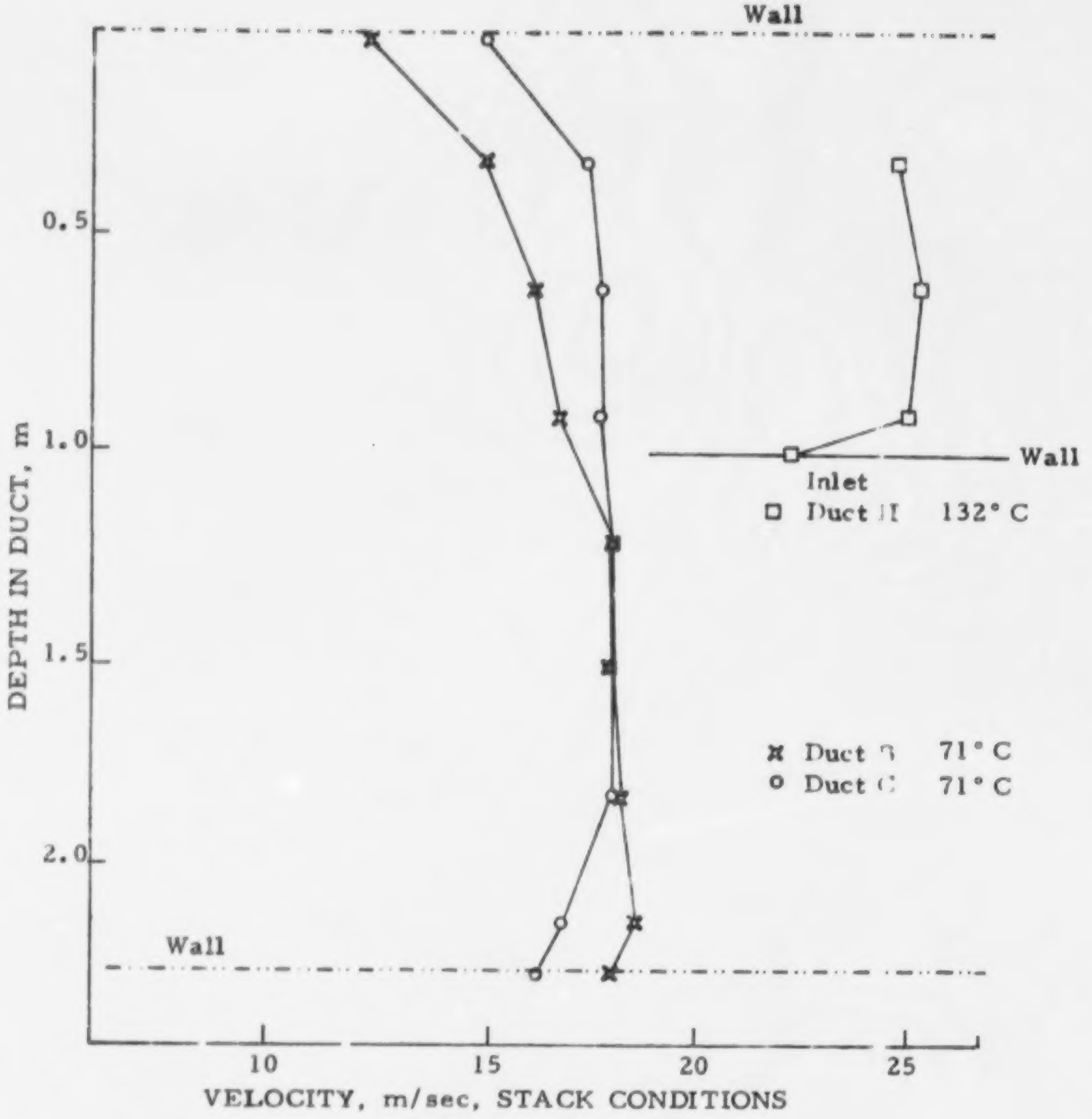

75-239

Fig. B-2. VELOCITY TRAVERSE INLET AND OUTLET DUCTS (NOVEMBER 21, 1974)

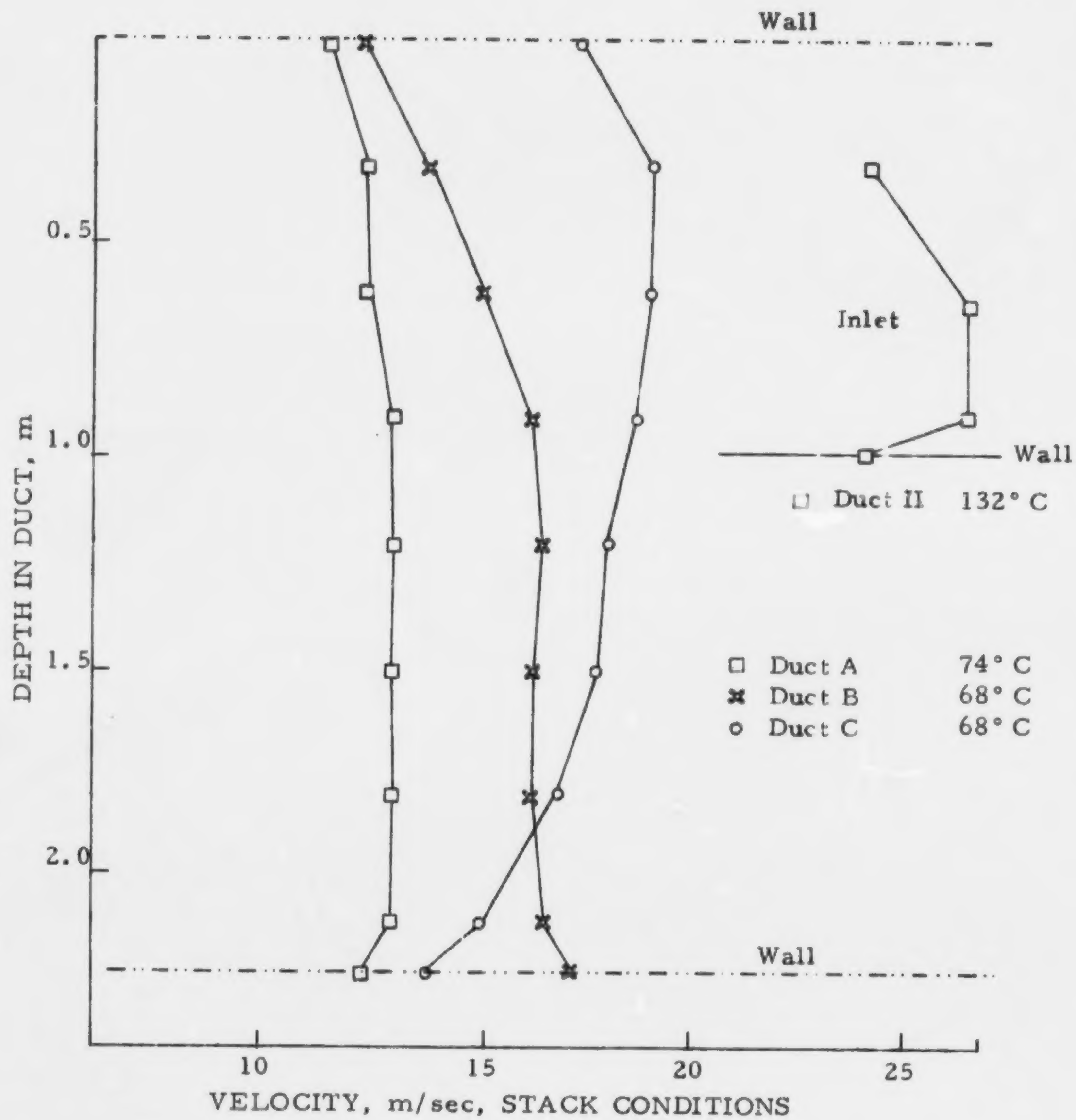

75-241

Fig. B-3. VELOCITY TRAVERSE INLET AND OUTLET DUCTS (DECEMBER 10, 1974)

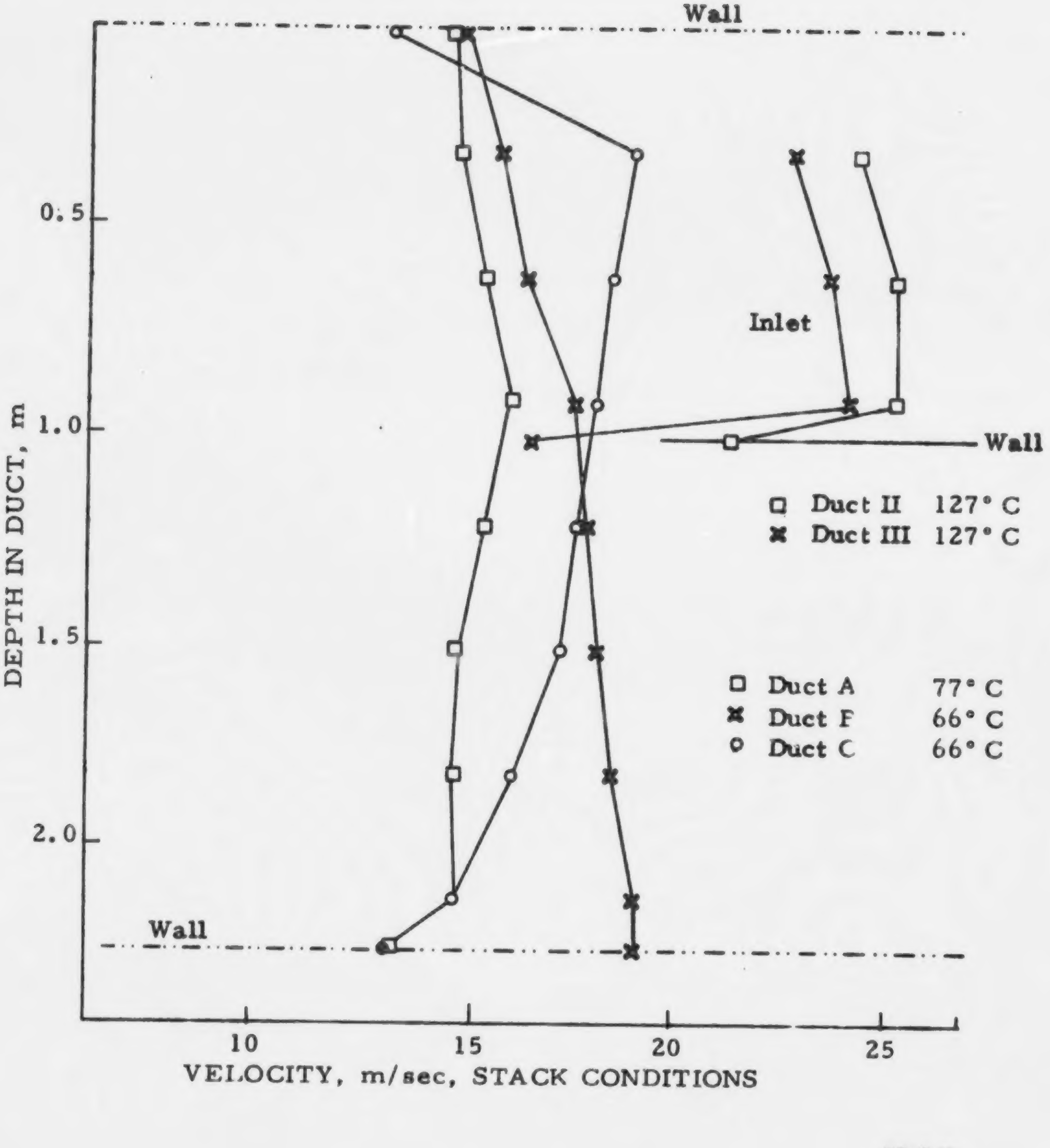

75-242

Fig. B-3. VELOCITY TRAVERSE INLET AND OUTLET DUCTS (DECEMBER 11, 1974)

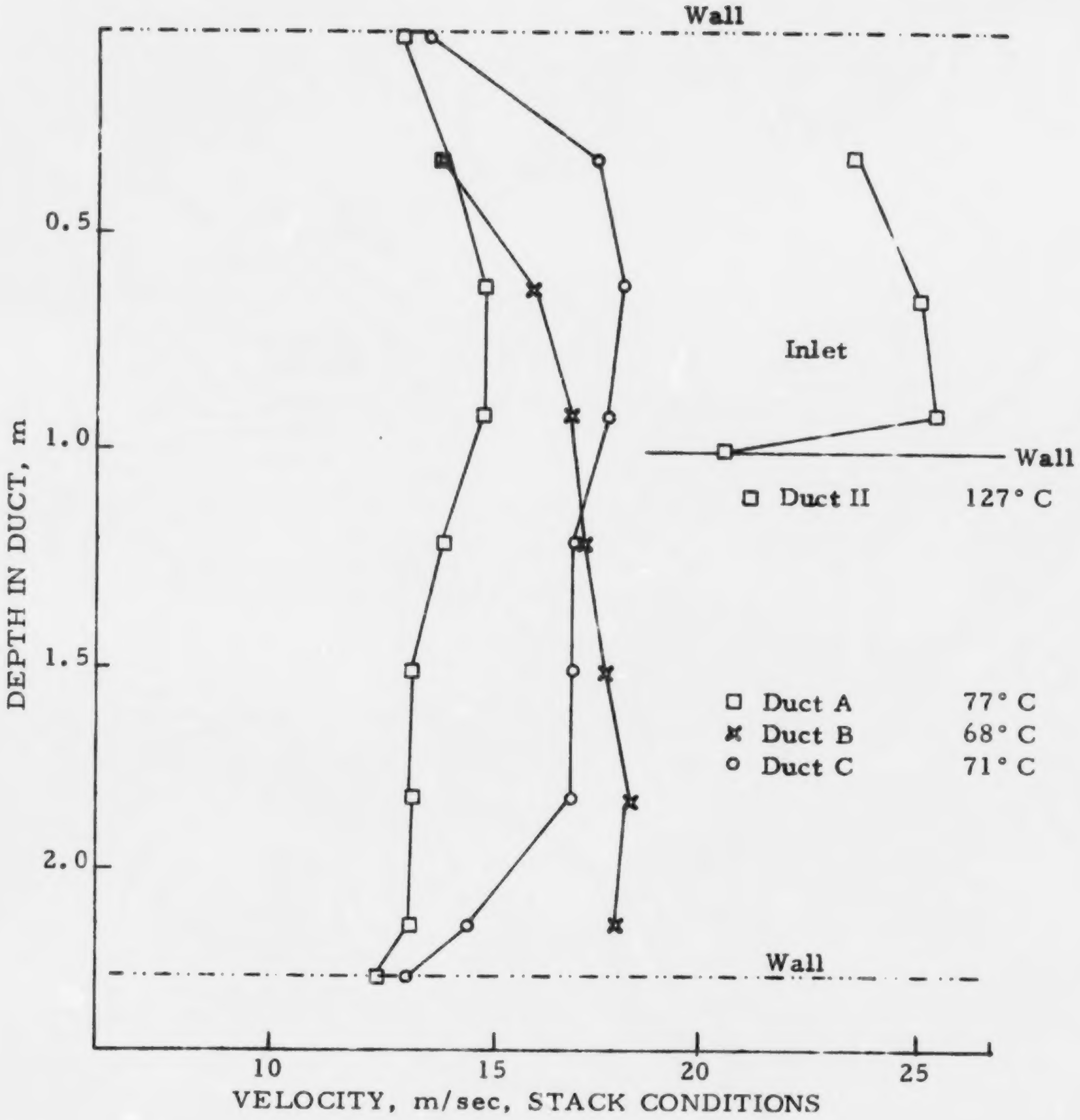

75-243

Fig. B-4. VELOCITY TRAVERSE INLET AND OUTLET DUCTS (DECEMBER 12, 1974)

Table B-2 DATA FOR RUN 56, INLET

STAGE NUMBER	CUT DIAMETER MICRONS	CUM. MASS CONC., MG/DSm^3 [a]	% WEIGHT < CUT DIAMETER
1	35	426	100
2	17	424	99
3	6.8	404	95
4	2.6	335	79
5	1.6	158	37
6	0.66	109	26
7	0.39	87.6	21
Filter		87.6	.21

Table B-3 DATA FOR RUN 53, OUTLET

STAGE NUMBER	CUT DIAMETER MICRONS	CUM. MASS CONC., MG/DSm^3	< % WEIGHT CUT DIAMETER
1	21	70.3	100
2	10	67.4	96
3	4.1	67.4	96
4	1.7	67.0	95
5	1.0	46.1	66
6	0.46	34.8	49
Filter		27.2	39

[a] Dry standard 21.1° C, 760 mm Hg

Table B-4 DATA FOR RUN 55, INLET

STAGE NUMBER	CUT DIAMETER MICRONS	CUM. MASS CONC., MG/DSm^3	% WEIGHT < CUT DIAMETER
1	35	493	100
2	18	456	92
3	6.5	434	88
4	3.2	291	59
5	1.6	132	27
6	0.64	61.5	12
7	0.54	49.0	10
Filter		42.1	8.5

Table B-5 DATA FOR RUN 57, OUTLET

STAGE NUMBER	CUT DIAMETER MICRONS	CUM. MASS CONC., MG/DSm^3	< % WEIGHT CUT DIAMETER
1	21	67.0	100
2	10	65.4	98
3	4.0	65.1	97
4	1.6	62.3	93
5	0.92	47.6	71
6	0.40	38.3	57
Filter		34.3	51

Table B-6 DATA FOR RUN 60, INLET

STAGE NUMBER	CUT DIAMETER MICRONS	CUM. MASS CONC., MG/DSm^3	% WEIGHT < CUT DIAMETER
1	33	489	100
2	16	435	88.9
3	6.1	410	83.9
4	3.0	265	54.2
5	1.5	113	23.0
6	0.59	45.0	9.2
7	0.50	24.6	5.0
Filter		17.3	3.6

Table B-7. DATA FOR RUN 61, OUTLET

STAGE NUMBER	CUT DIAMETER MICRONS	CUM. MASS CONC., MG/DSm^3	< % WEIGHT CUT DIAMETER
1	20	49.2	100
2	10	48.8	99.2
3	3.9	45.9	93.3
4	1.5	45.7	93.0
5	0.87	34.6	70.4
6	0.36	25.9	52.7
Filter		20.9	42.5

Table B-8 DATA FOR RUN 114, INLET

STAGE NUMBER	CUT DIAMETER MICRONS	CUM. MASS CONC., MG/DSm^3	% WEIGHT < CUT DIAMETER
1	29	1820	100
2	15	1010	55.5
3	5.3	745	40.9
4	2.5	384	21.1
5	1.6	129	7.1
6	0.69	43.7	2.4
7	0.27	25.9	1.4
Filter		16.2	0.89

Table B-9 DATA FOR RUN 109, OUTLET

STAGE NUMBER	CUT DIAMETER MICRONS	CUM. MASS CONC., MG/DSm^3	% WEIGHT < CUT DIAMETER
1	29	73.1	100
2	14	71.5	97.7
3	5.3	71.5	97.7
4	2.5	70.5	96.4
5	1.5	67.2	91.9
6	0.69	58.1	79.5
7	0.28	50.0	68.4
Filter		46.3	63.3

Table B-10. DATA FOR RUN 113, INLET

STAGE NUMBER	CUT DIAMETER MICRONS	CUM. MASS CONC., MG/DSm^3	% WEIGHT < CUT DIAMETER
1	32	4650	100
2	16	2330	50.2
3	6.2	1670	36.0
4	2.5	1010	21.8
5	1.5	380	8.2
6	0.66	111	2.4
7	0.28	63.1	1.4
Filter		54.2	1.2

Table B-11. DATA FOR RUN 110, OUTLET

STAGE NUMBER	CUT DIAMETER MICRONS	CUM. MASS CONC., MG/DSm^3	% WEIGHT < CUT DIAMETER
1	24	168	100
2	12	163	97.3
3	4.6	162	96.6
4	1.7	159	94.4
5	1.1	124	73.8
6	0.49	94.0	56.0
7	0.36	80.8	48.1
Filter		44.0	26.2

Table B-12. DATA FOR RUN 119, INLET

STAGE NUMBER	CUT DIAMETER MICRONS	CUM. MASS CONC., MG/DSm^3	% WEIGHT < CUT DIAMETER
1	33	541	100
2	17	429	77.2
3	6.4	417	77.1
4	2.5	344	63.5
5	1.5	164	30.3
6	0.68	116	21.5
7	0.29	84.0	15.5
Filter		73.3	13.6

Table B-13. DATA FOR RUN 116, OUTLET

STAGE NUMBER	CUT DIAMETER MICRONS	CUM. MASS CONC., MG/DSm^3	% WEIGHT < CUT DIAMETER
1	28	58.8	100
2	14	58.8	100
3	5.6	58.5	99.5
4	2.3	58.2	98.9
5	1.4	53.5	91.0
6	0.66	40.3	68.5
7	0.48	35.3	60.0
Filter		28.3	48.1

Table B-14. DATA FOR RUN 120, INLET

STAGE NUMBER	CUT DIAMETER MICRONS	CUM. MASS CONC., MG/DSm^3	% WEIGHT < CUT DIAMETER
1	31	414	100
2	16	392	94.6
3	5.8	378	91.3
4	2.7	300	72.3
5	1.7	125	30.3
6	0.76	63.7	15.4
7	0.31	41.2	10.0
Filter		31.8	7.7

Table B-15. DATA FOR RUN 118, OUTLET

STAGE NUMBER	CUT DIAMETER MICRONS	CUM. MASS CONC., MG/DSm^3	% WEIGHT < CUT DIAMETER
1	21	54.1	100
2	10	52.5	97.0
3	4.0	49.3	91.2
4	1.5	49.3	91.2
5	0.90	45.9	84.8
6	0.37	40.1	74.0
7	0.20	34.5	63.8
Filter		32.2	59.6

Table B-16. DATA FOR RUN 123, INLET

STAGE NUMBER	CUT DIAMETER MICRONS	CUM. MASS CONC., MG/DSm^3	% WEIGHT < CUT DIAMETER
1	35	1160	100
2	17	904	78.1
3	6.7	859	74.1
4	2.7	585	50.5
5	1.6	187	16.2
6	0.72	70.0	6.1
7	0.31	41.9	3.6
Filter		33.8	2.9

Table B-17. DATA FOR RUN 122, OUTLET

STAGE NUMBER	CUT DIAMETER MICRONS	CUM. MASS CONC., MG/DSm^3	% WEIGHT < CUT DIAMETER
1	28	64.7	100
2	14	63.0	98.4
3	5.3	63.0	97.5
4	1.9	62.5	96.5
5	1.3	60.0	92.8
6	0.56	50.8	78.5
7	0.42	41.9	64.8
Filter		37.0	57.1

Table B-18. DATA FOR RUN 124, INLET

STAGE NUMBER	CUT DIAMETER MICRONS	CUM. MASS CONC., MG/DSm^3	% WEIGHT < CUT DIAMETER
1	34	1300	100
2	17	1070	82.6
3	6.4	1010	77.7
4	3.0	556	42.7
5	1.8	185	14.2
6	0.84	62.7	4.8
7	0.34	35.2	2.7
Filter		20.4	1.5

Table B-19. DATA FOR RUN 125, OUTLET

STAGE NUMBER	CUT DIAMETER MICRONS	CUM. MASS CONC., MG/DSm^3	% WEIGHT < CUT DIAMETER
1	27	88.6	100
2	14	88.3	99.7
3	5.0	88.3	99.7
4	2.5	86.9	98.1
5	1.2	82.9	93.5
6	0.48	69.6	78.5
7	0.41	64.4	72.7
Filter		63.5	71.7

Table B-20. DATA FOR RUN 127, INLET

STAGE NUMBER	CUT DIAMETER MICRONS	CUM. MASS CONC., MG/DSm^3	% WEIGHT < CUT DIAMETER
1	36	2730	100
2	18	1500	54.9
3	7.1	1080	39.6
4	2.8	664	24.3
5	1.7	246	9.0
6	0.76	124	4.5
7	0.33	84.4	3.1
Filter		52.0	1.9

Table B-21. DATA FOR RUN 126, OUTLET

STAGE NUMBER	CUT DIAMETER MICRONS	CUM. MASS CONC., MG/DSm^3	% WEIGHT < CUT DIAMETER
1	30	89.7	100
2	15	89.5	99.7
3	5.9	88.6	98.7
4	2.3	86.6	96.5
5	1.4	74.6	83.1
6	0.57	40.6	45.2
7	0.33	28.5	31.8
Filter		21.3	23.8

Table B-22. DATA FOR RUN 133, INLET

STAGE NUMBER	CUT DIAMETER MICRONS	CUM. MASS CONC., MG/DSm^3	% WEIGHT < CUT DIAMETER
1	34	866	100
2	17	712	82.2
3	6.3	677	79.2
4	3.0	449	51.9
5	1.8	155	18.0
6	0.82	34.1	3.9
7	0.34	18.7	2.2
Filter		18.7	2.2

Table B-23. DATA FOR RUN 129, OUTLET

STAGE NUMBER	CUT DIAMETER MICRONS	CUM. MASS CONC., MG/DSm^3	% WEIGHT < CUT DIAMETER
1	27	81.9	100
2	14	78.9	96.4
3	5.4	78.1	95.3
4	2.2	75.2	91.8
5	1.4	64.2	79.3
6	0.62	46.4	56.6
7	0.44	41.6	50.7
Filter		38.3	46.7

Table B-24. DATA FOR RUN 134, INLET

STAGE NUMBER	CUT DIAMETER MICRONS	CUM. MASS CONC., MG/DSm^3	% WEIGHT < CUT DIAMETER
1	35	1070	100
2	18	850	79.8
3	6.8	775	72.8
4	2.7	467	43.8
5	1.6	126	11.8
6	0.73	22.5	2.1
7	0.32	16.8	1.6
Filter		16.4	1.5

Table B-25. DATA FOR RUN 130, OUTLET

STAGE NUMBER	CUT DIAMETER MICRONS	CUM. MASS CONC., MG/DSm^3	% WEIGHT < CUT DIAMETER
1	31	218	100
2	15	215	98.6
3	5.9	213	97.8
4	2.1	212	97.3
5	1.5	197	90.2
6	0.64	167	76.5
7	0.48	143	65.6
Filter		110	50.3

Table B-26. DATA FOR RUN 135, INLET

STAGE NUMBER	CUT DIAMETER MICRONS	CUM. MASS CONC., MG/DSm^3	% WEIGHT < CUT DIAMETER
1	35	1440	100
2	18	1070	74.4
3	6.8	956	66.6
4	2.7	526	36.6
5	1.6	173	12.0
6	0.74	58.1	4.0
7	0.32	30.1	2.1
Filter		25.4	1.8

Table B-27. DATA FOR RUN 132, OUTLET

STAGE NUMBER	CUT DIAMETER MICRONS	CUM. MASS CONC., MG/DSm^3	% WEIGHT < CUT DIAMETER
1	27	62.9	100
2	14	62.9	100
3	5.3	61.8	98.3
4	2.0	59.8	95.0
5	1.2	51.2	81.3
6	0.50	33.3	52.9
7	0.29	26.0	41.3
Filter		12.0	19.0

Table B-28. DATA FOR RUN 136, INLET

STAGE NUMBER	CUT DIAMETER MICRONS	CUM. MASS CONC., MG/DSm^3	% WEIGHT < CUT DIAMETER
1	34	1360	100
2	17	1010	74.1
3	6.4	901	66.4
4	3.0	543	40.0
5	1.8	175	12.9
6	0.84	51.6	3.8
7	0.34	22.8	1.7
Filter		18.7	1.4

Table B-29. DATA FOR RUN 131, OUTLET

STAGE NUMBER	CUT DIAMETER MICRONS	CUM. MASS CONC., MG/DSm^3	% WEIGHT < CUT DIAMETER
1	28	108	100
2	14	108	100
3	5.1	105	97.2
4	2.5	104	96.3
5	1.3	99.2	91.9
6	0.50	80.8	74.8
7	0.42	74.5	69.0
Filter		64.6	59.8

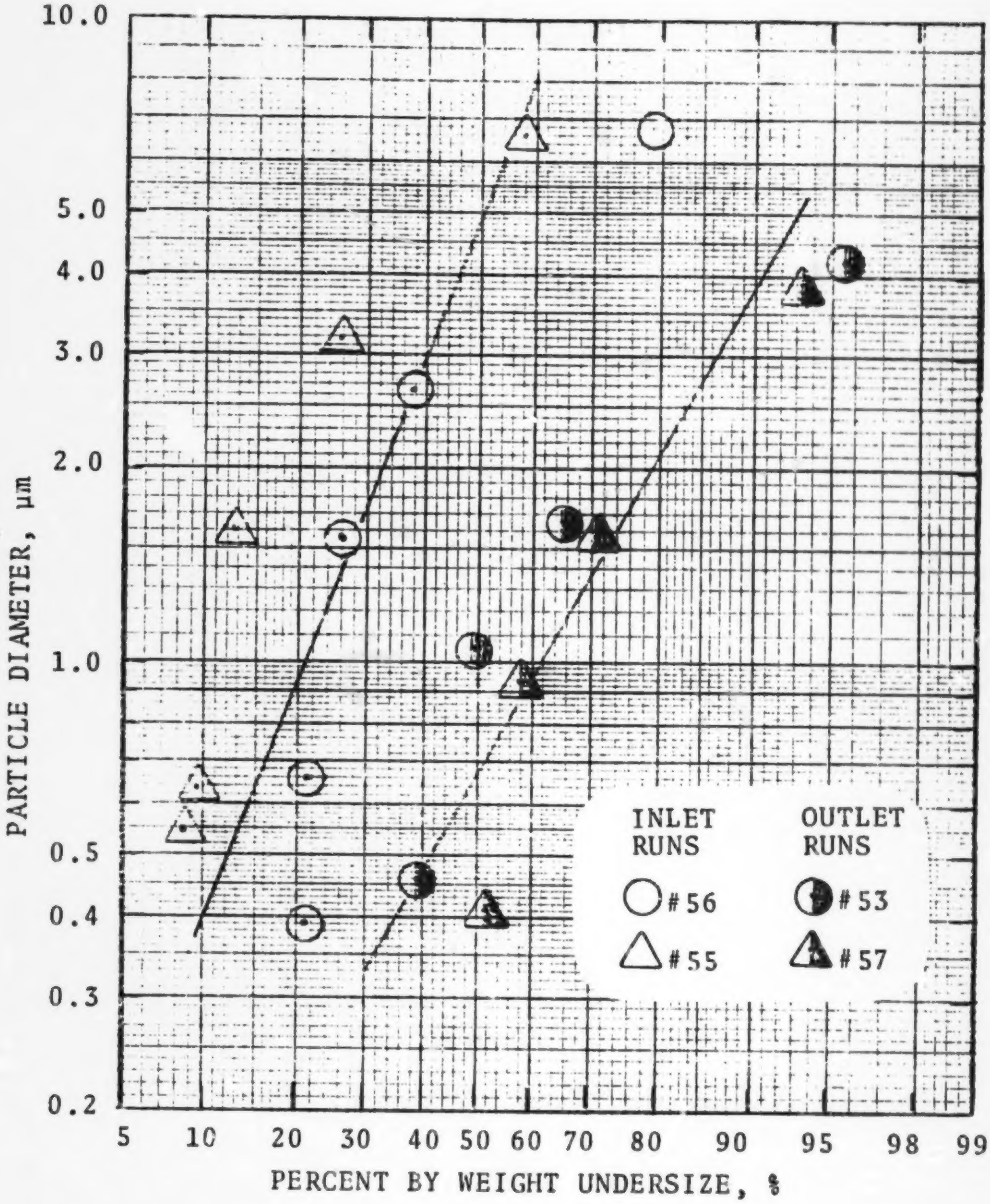

Figure B-5: Size distributions from cascade impactor tests

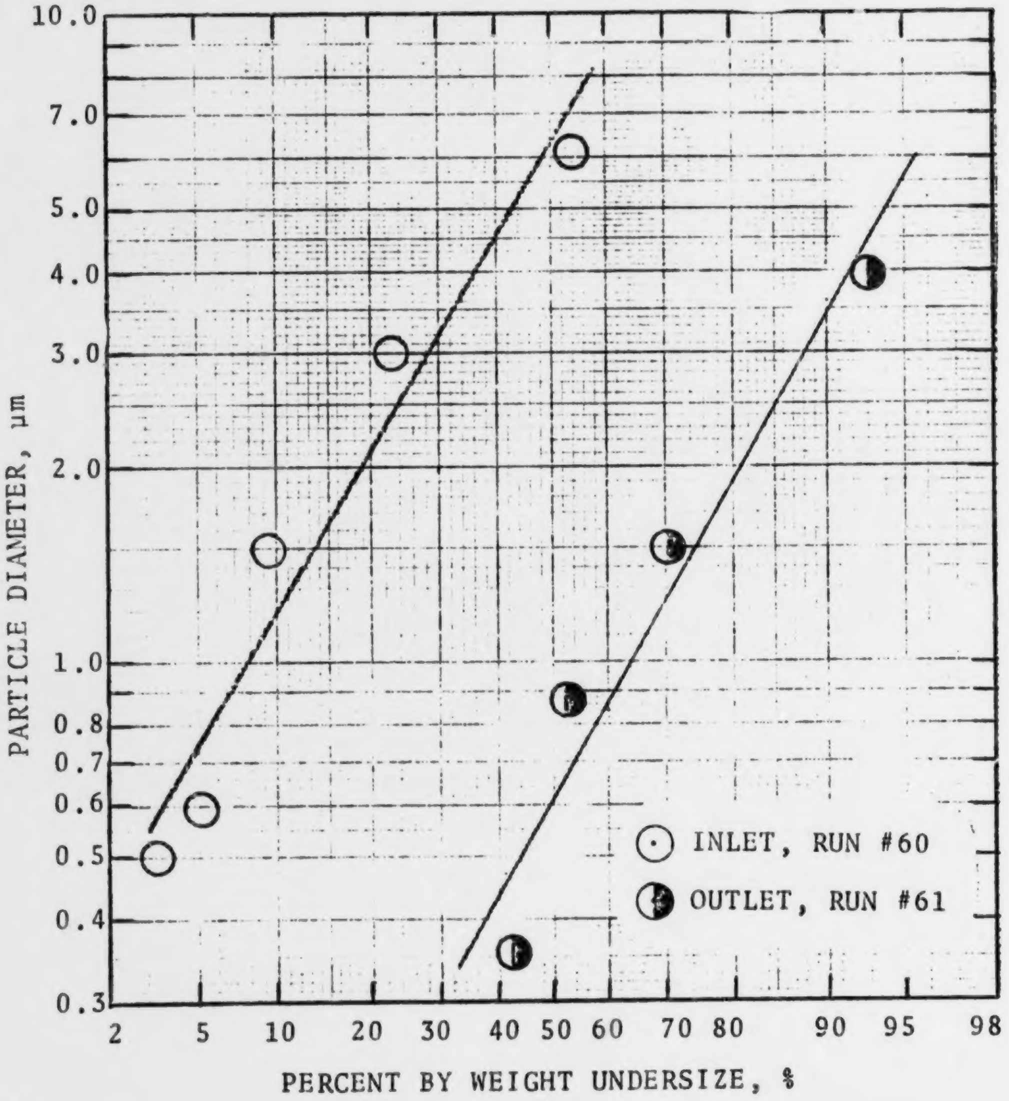

Figure B-6 Size distribution from cascade impactor tests

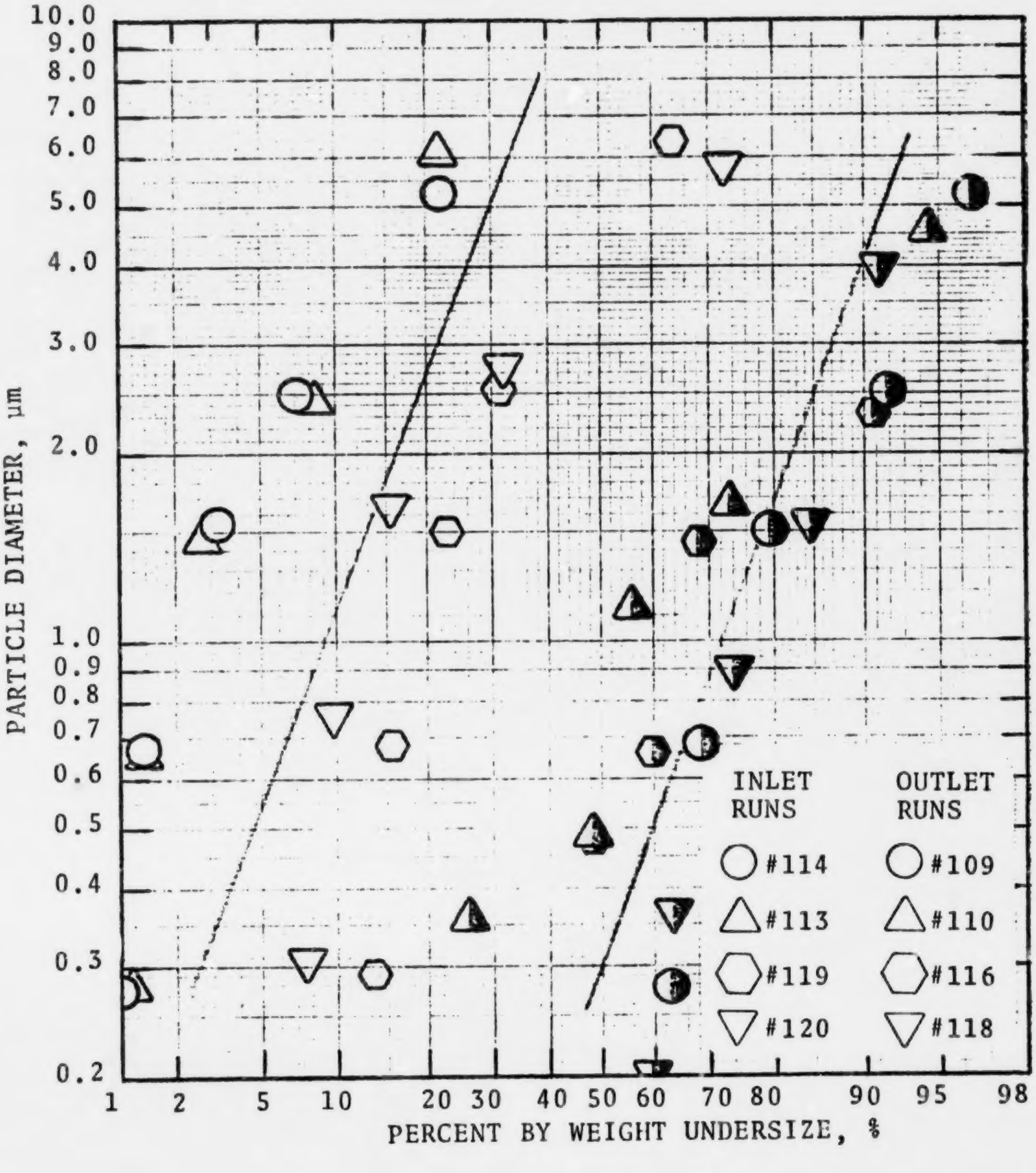

Figure B-7 Size distributions from cascade impactor tests

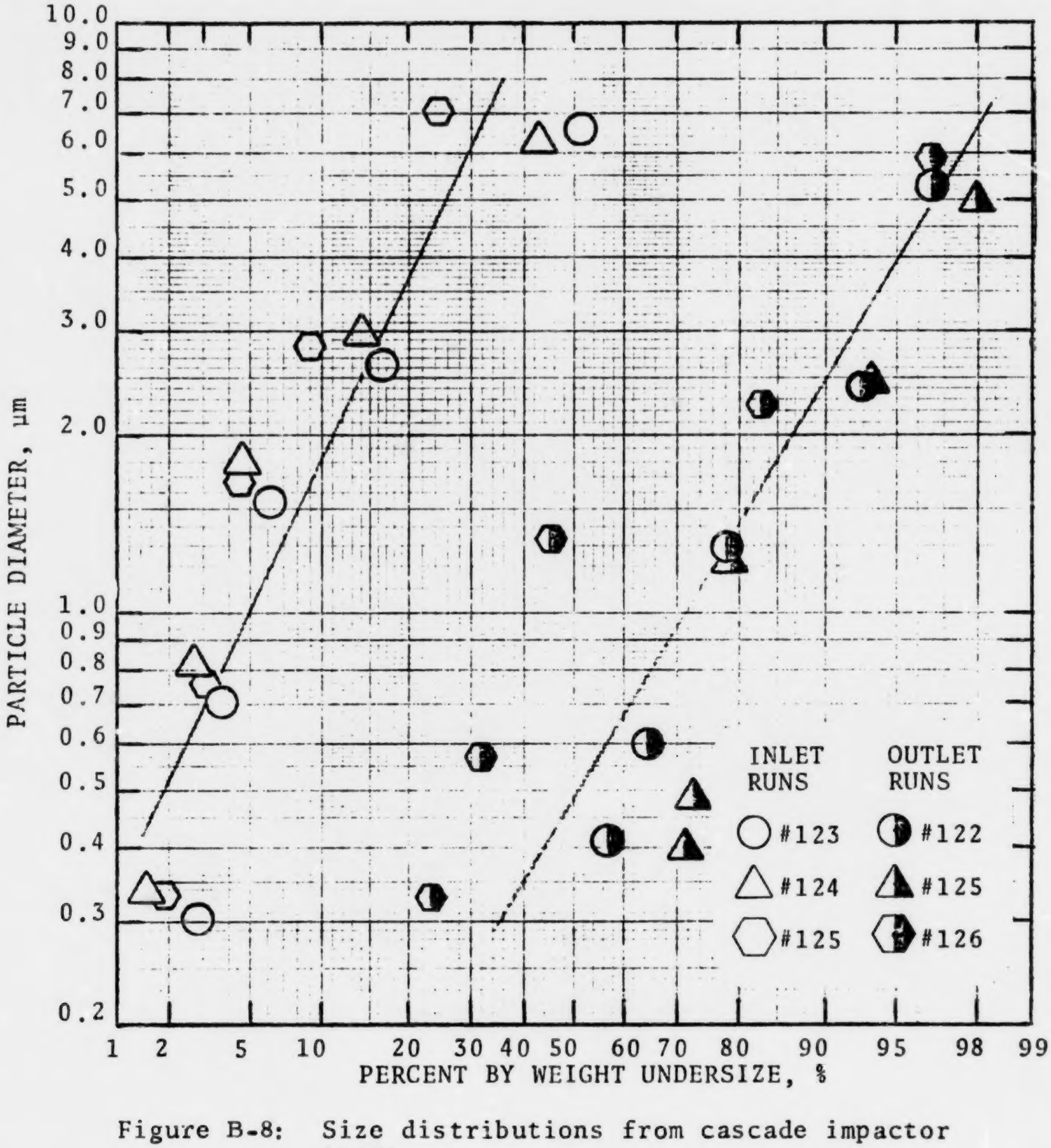

Figure B-8: Size distributions from cascade impactor tests

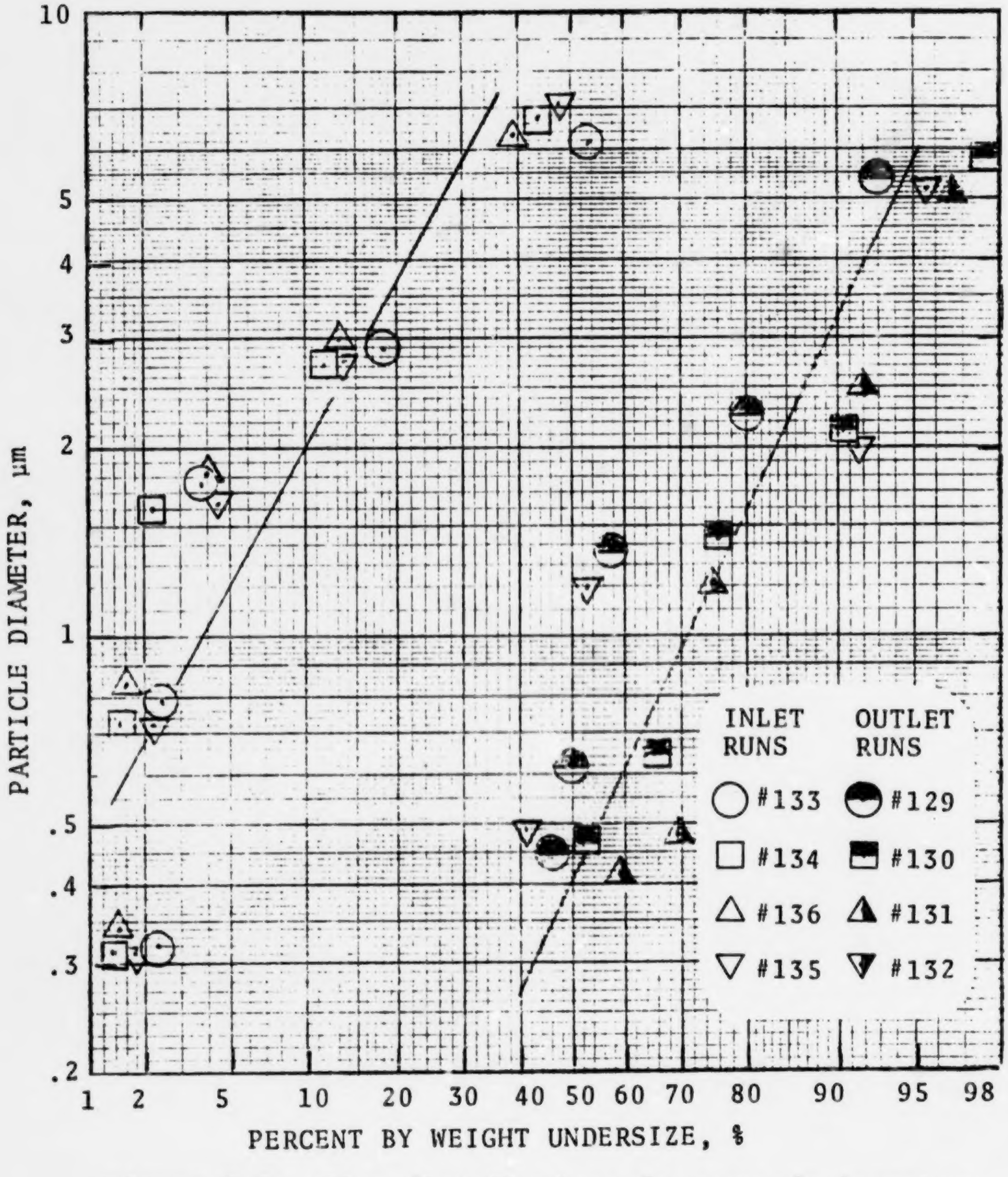

Figure B-9: Size distributions for cascade impactor tests

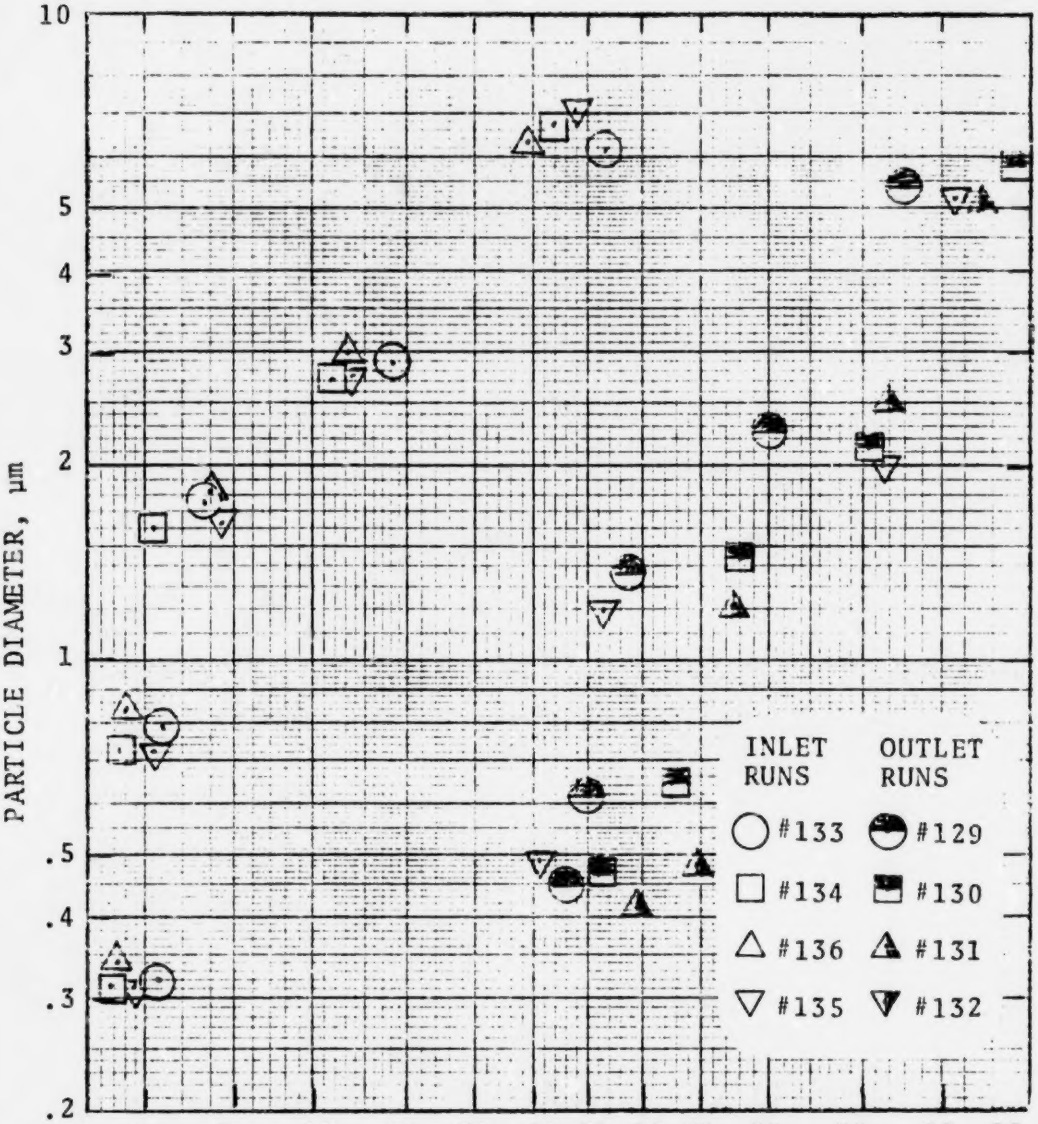

Figure B-10: Size distributions for cascade impactor tests

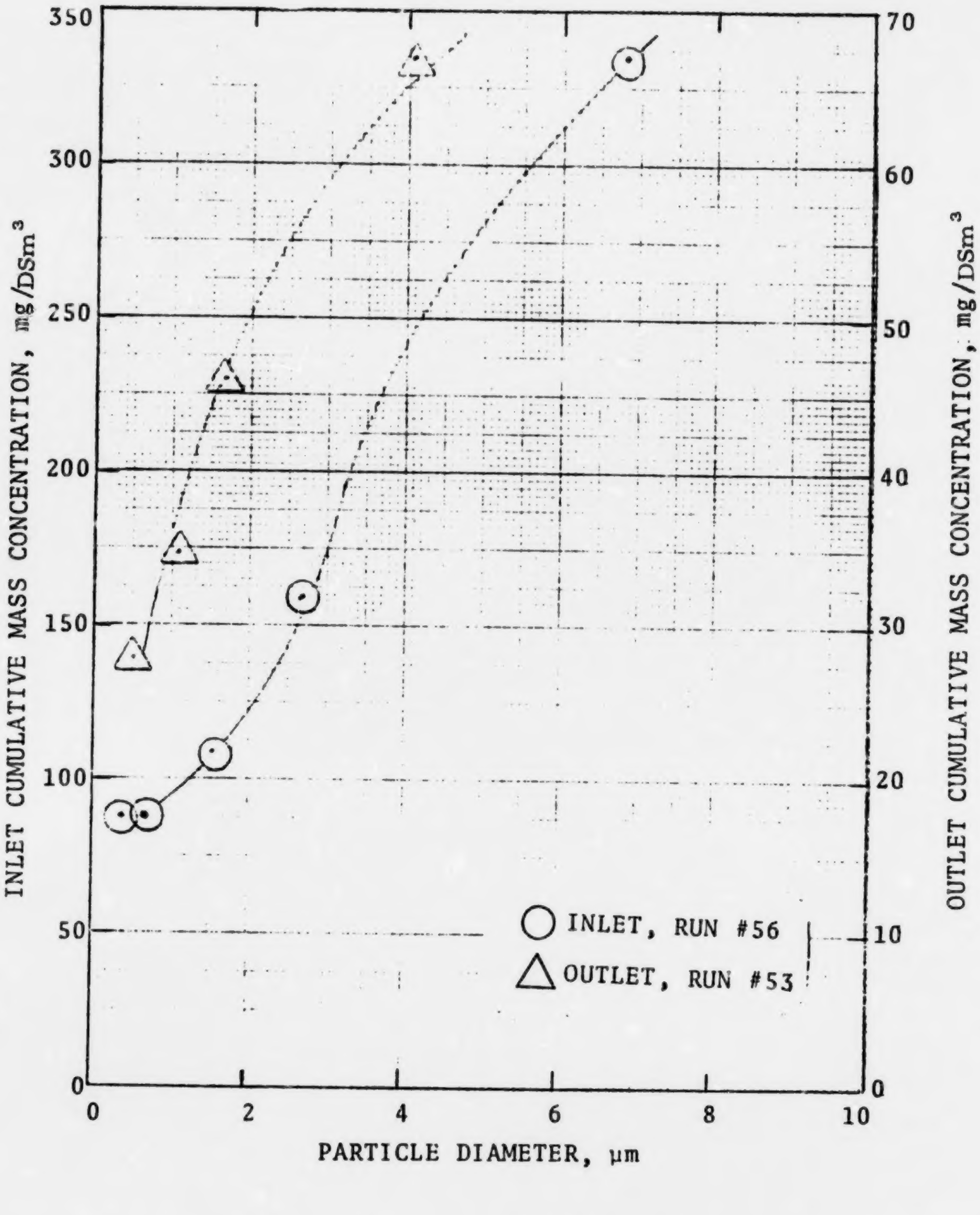

Figure B-11: Cumulative mass distribution from cascade impactor tests

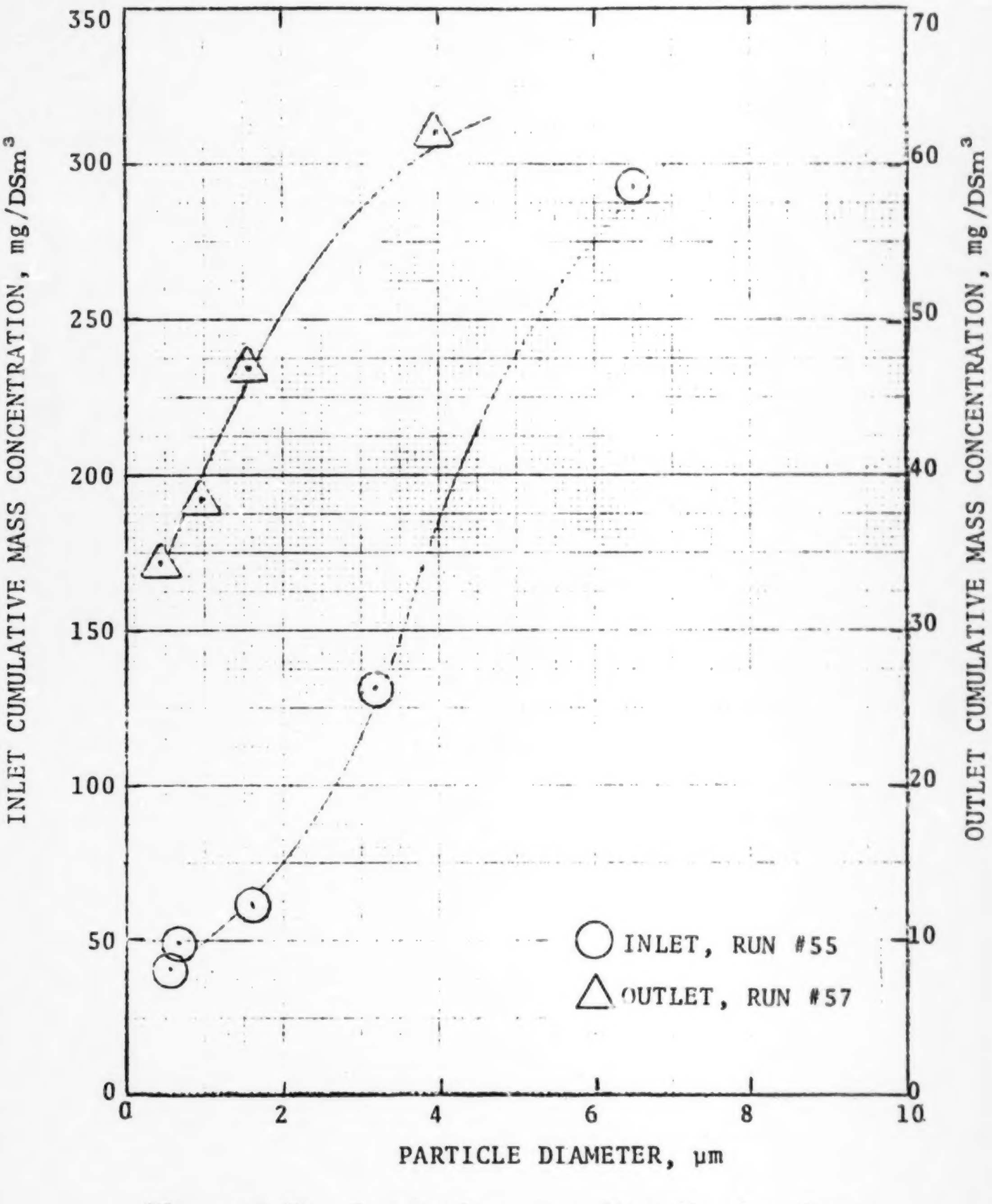

Figure B-12: Cumulative mass distribution from cascade impactor tests

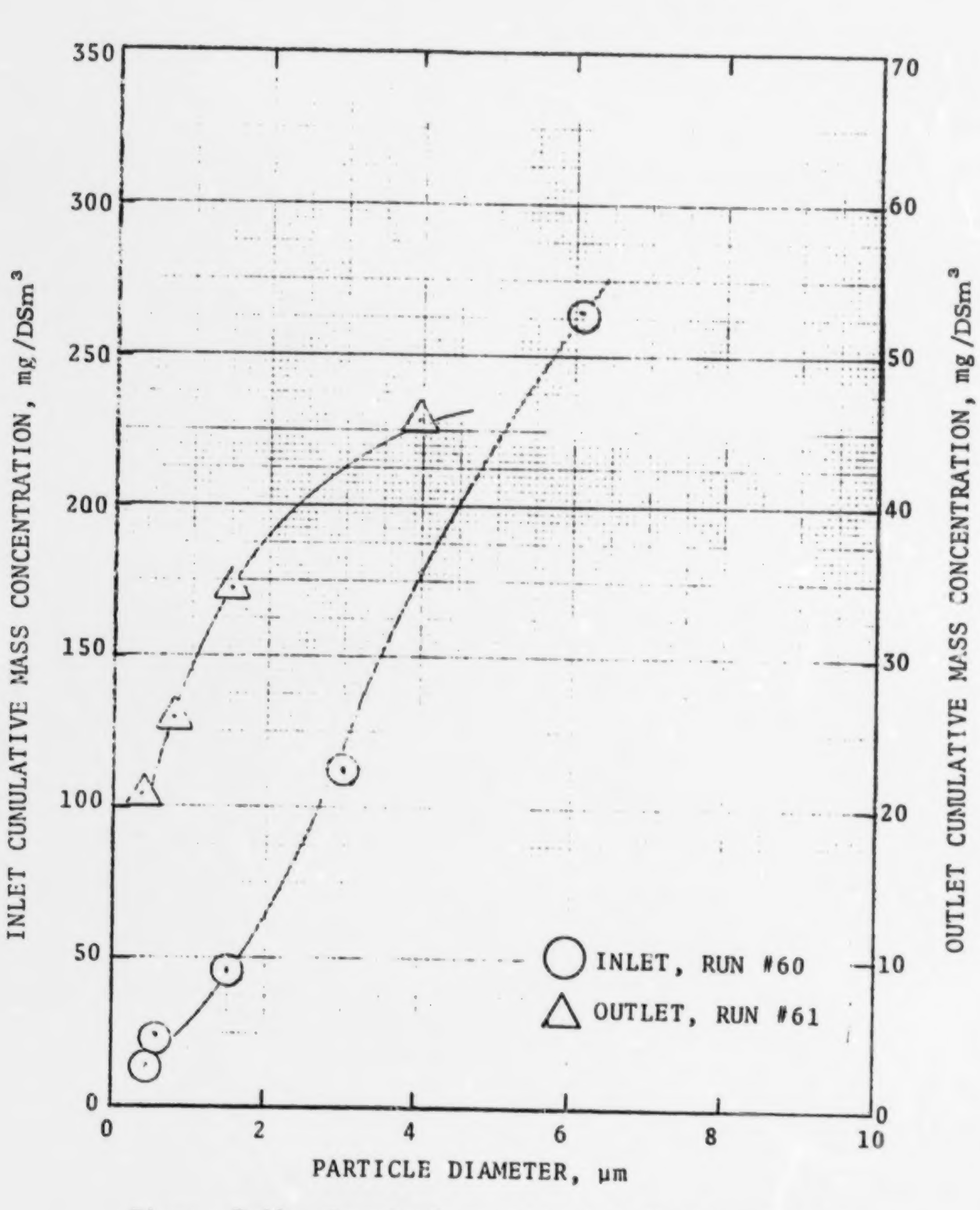

Figure B-13: Cumulative mass distribution from cascade impactor tests

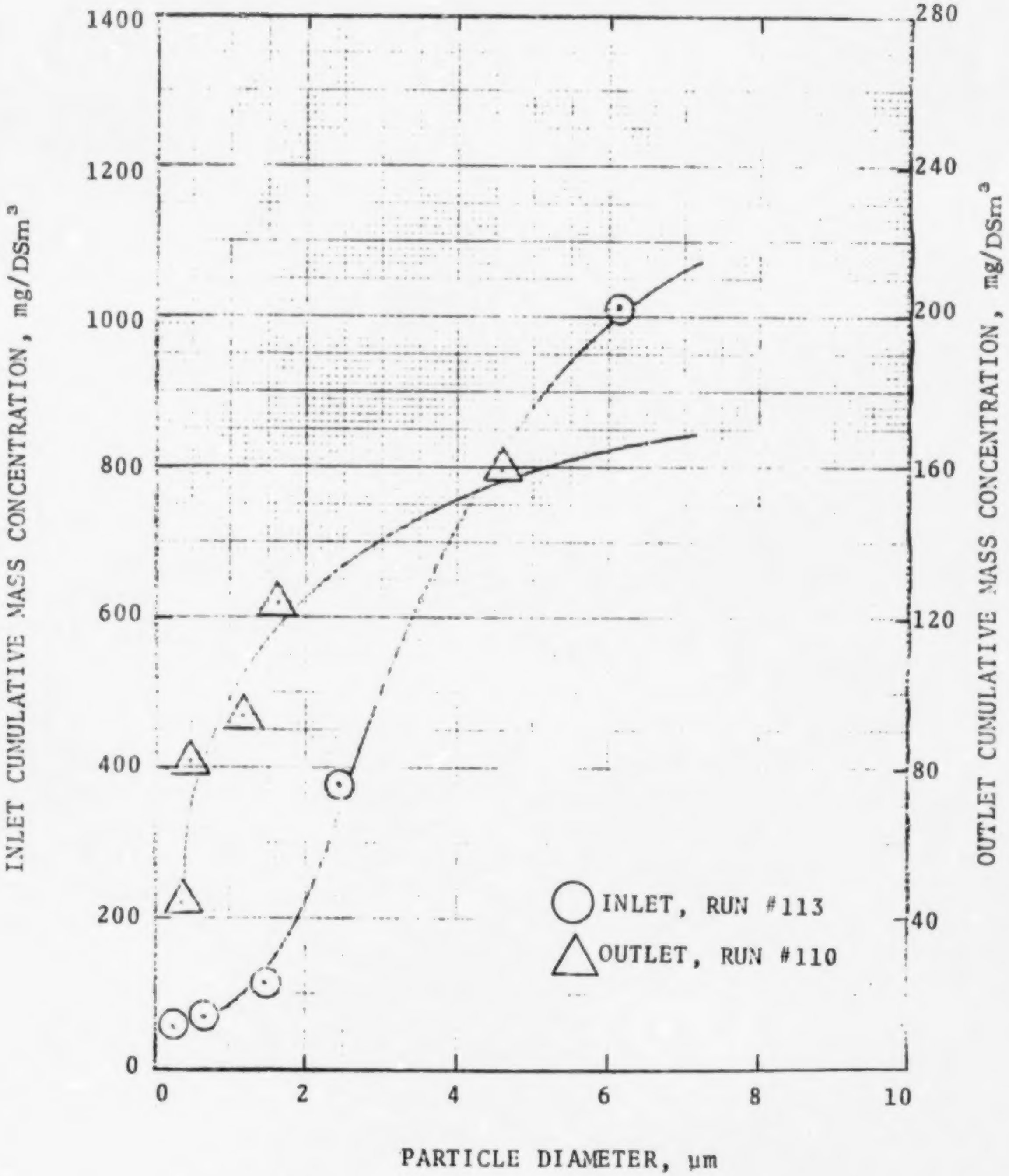

Figure B-14: Cumulative mass distribution from cascade impactor tests

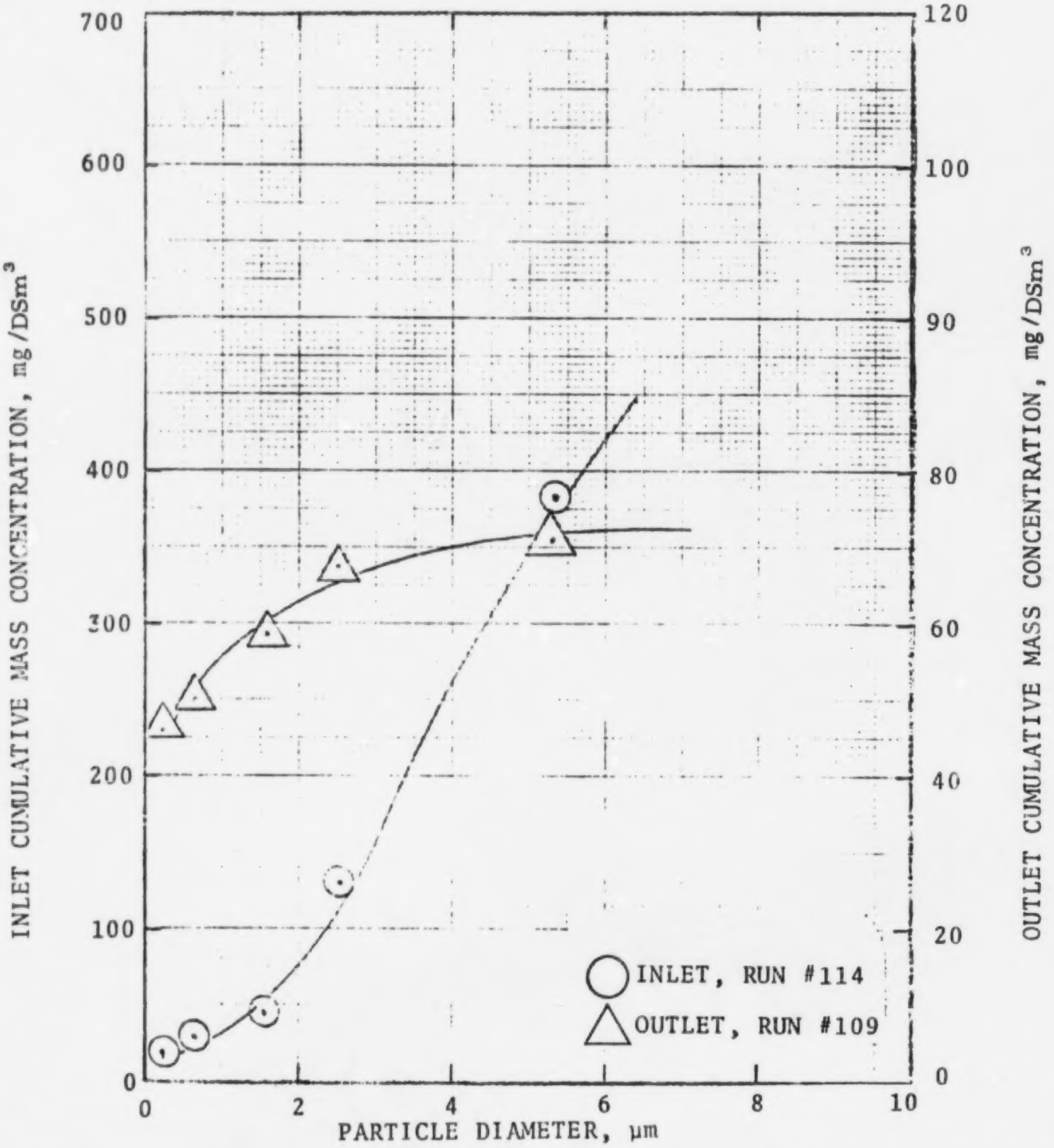

Figure B-15: Cumulative mass distribution from cascade impactor tests

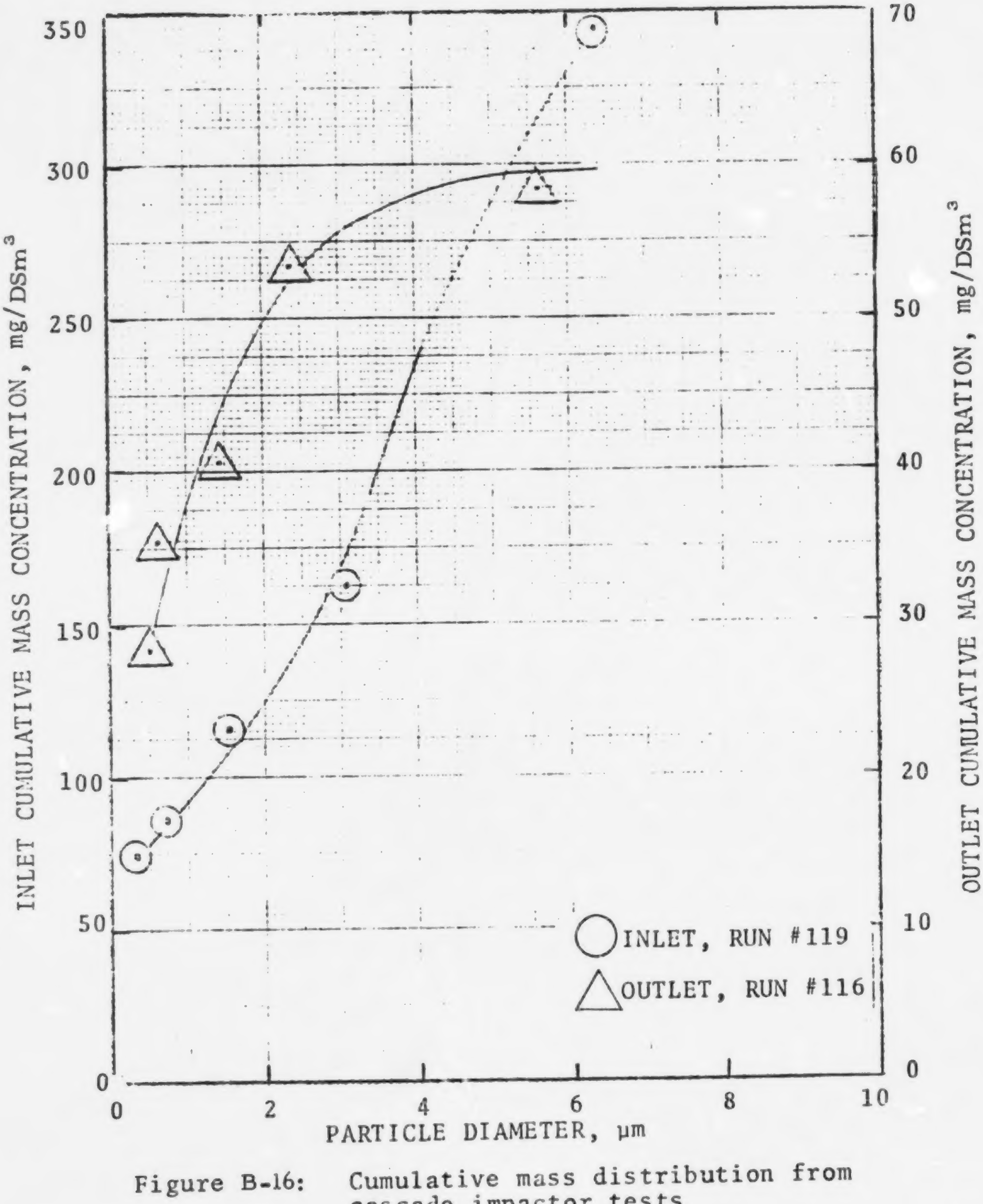

Figure B-16: Cumulative mass distribution from cascade impactor tests

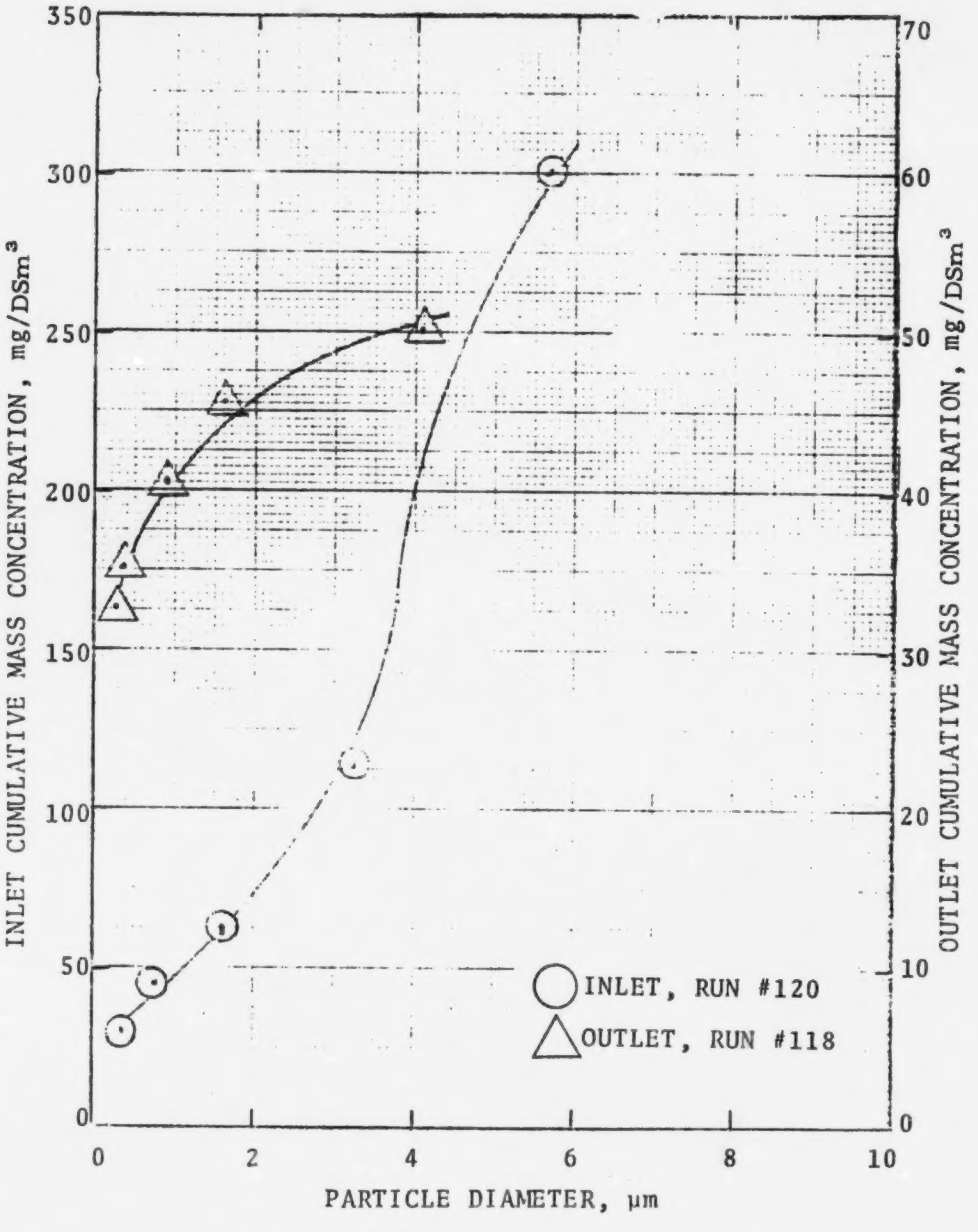

Figure B-17: Cumulative mass distribution from cascade impactor tests

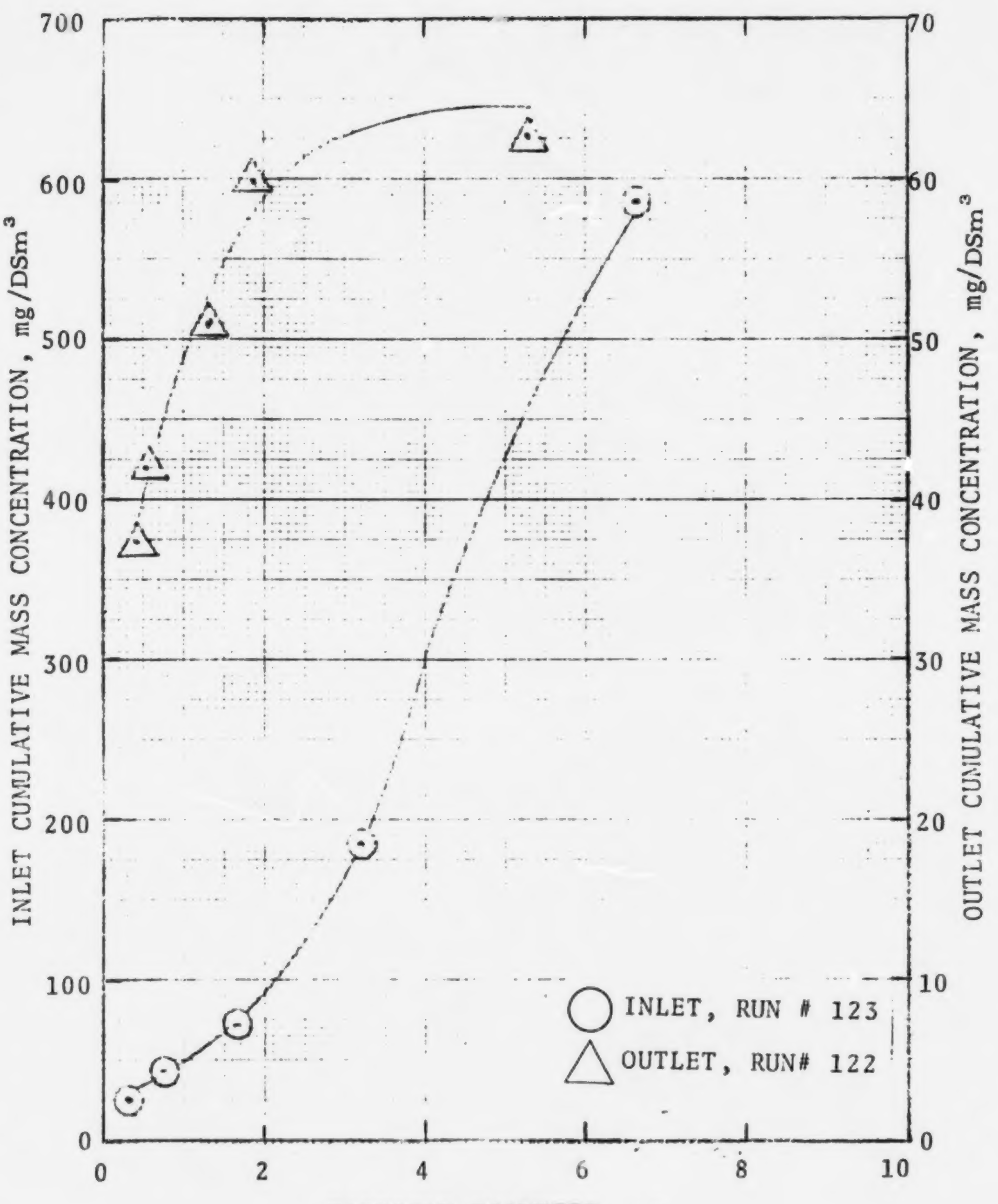

Figure B-18: Cumulative mass distribution from cascade impactor tests

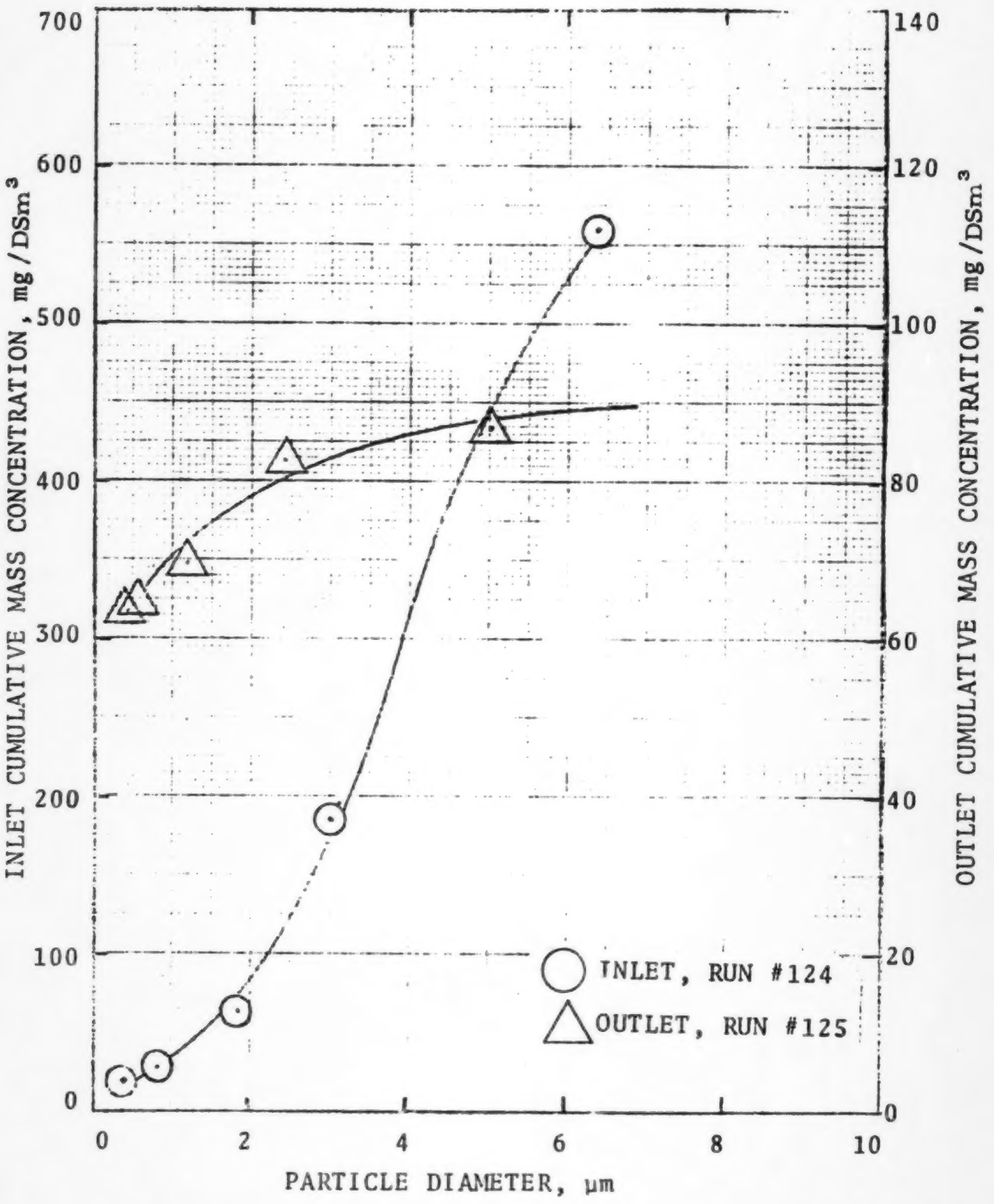

Figure B-20: Cumulative mass distribution from cascade impactor tests

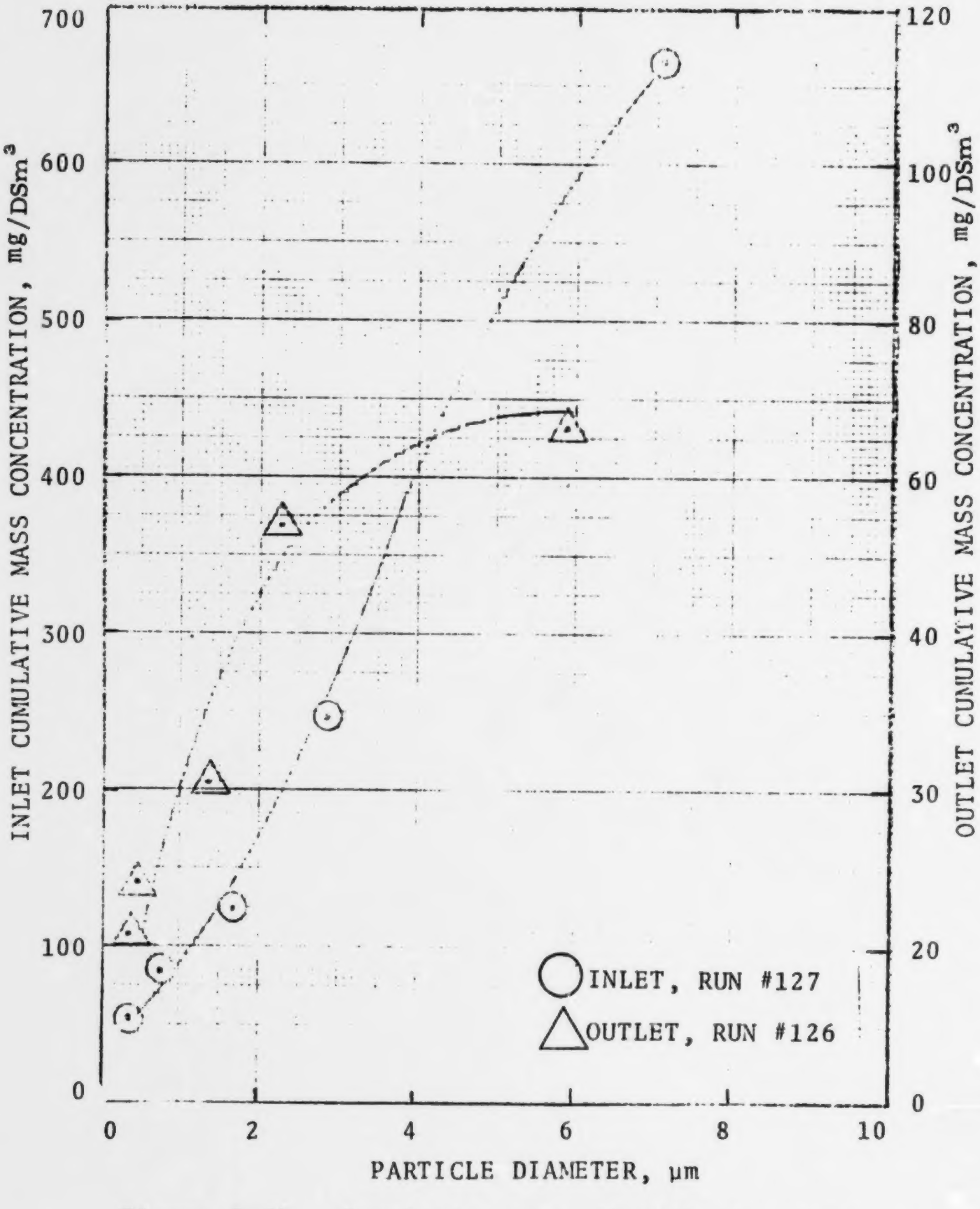

Figure B-21: Cumulative mass distribution from cascade impactor tests

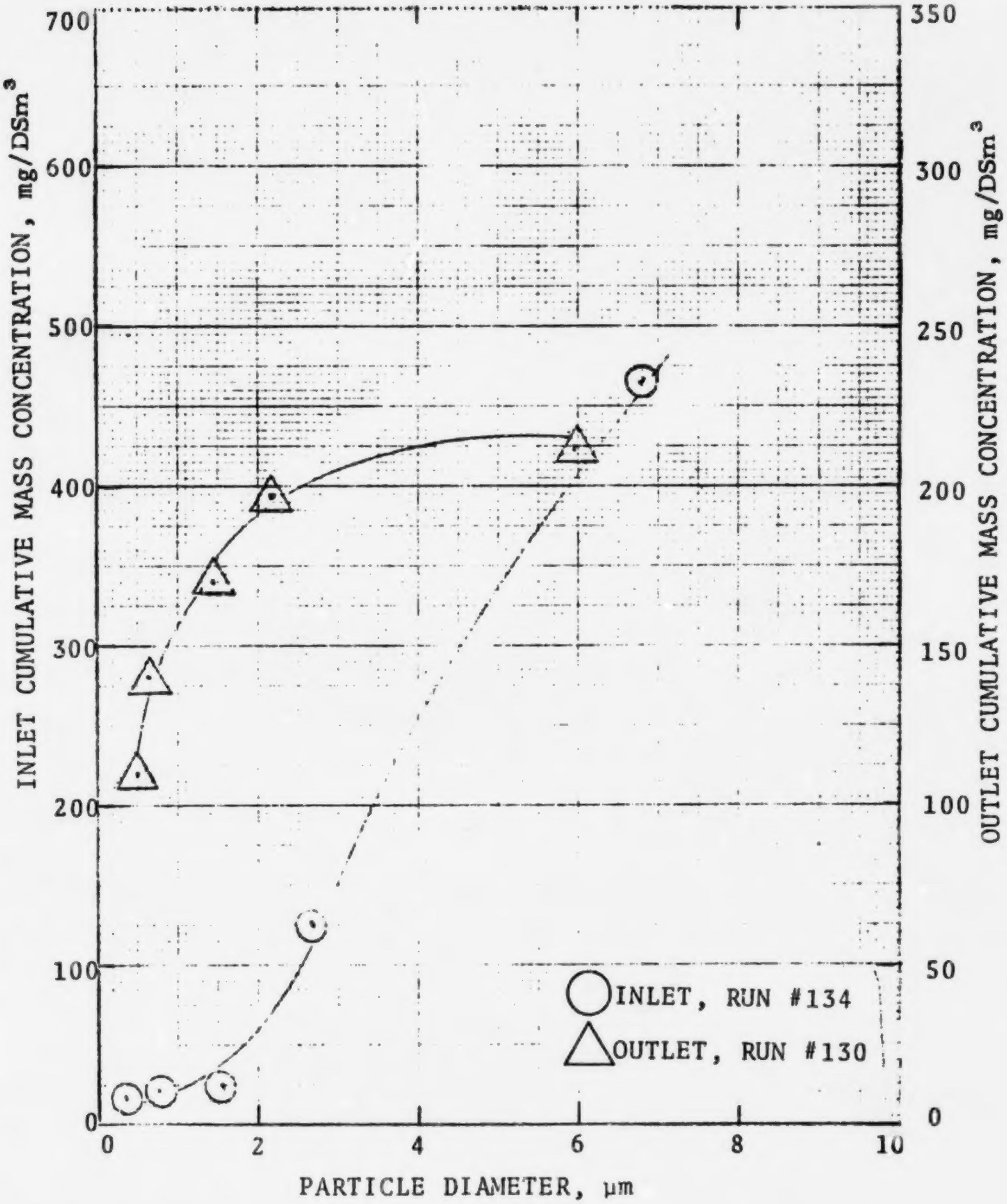

Figure B-22: Cumulative mass distribution from cascade impactor tests

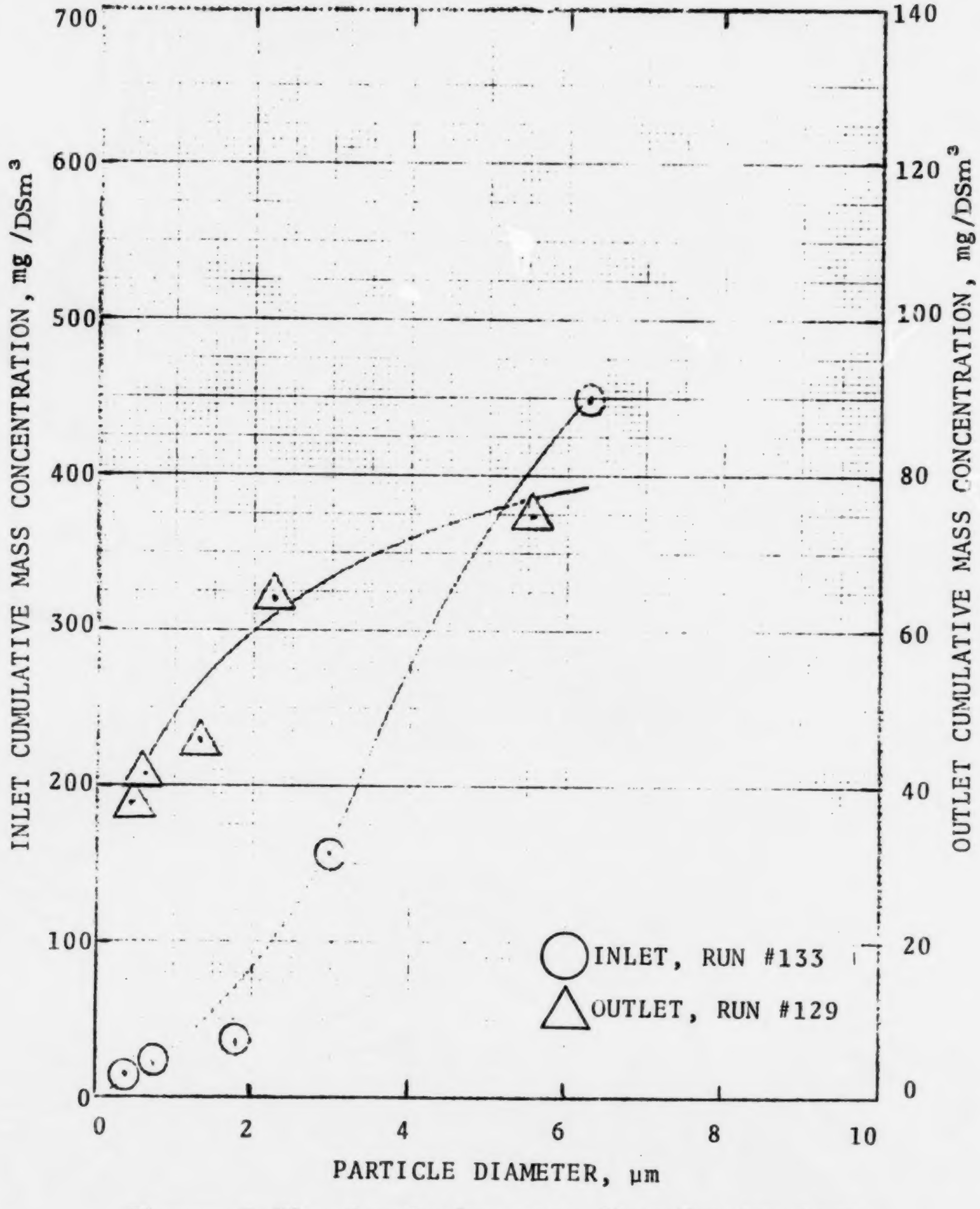

Figure B-23: Cumulative mass distribution from cascade impactor tests

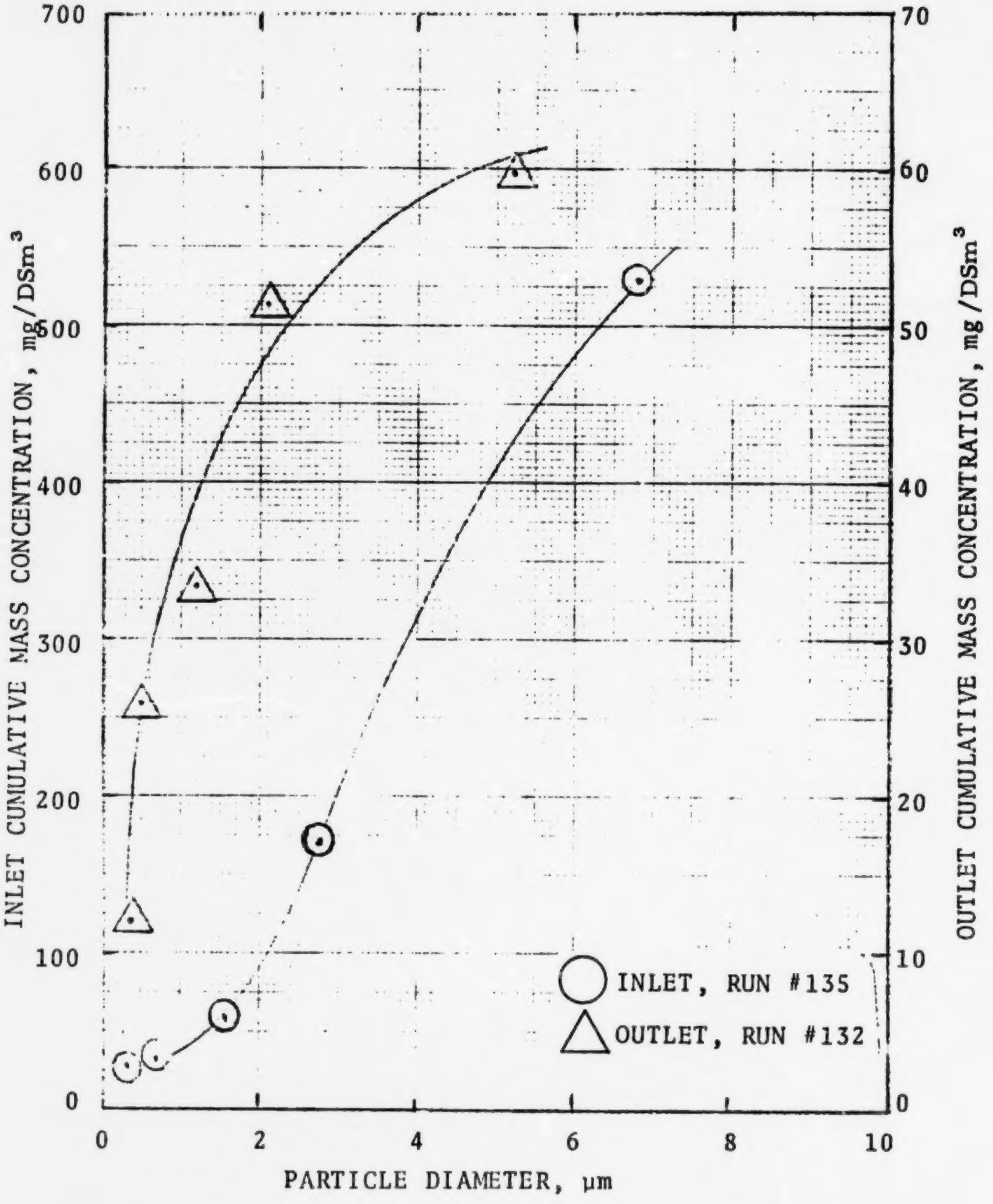

Figure B-24: Cumulative mass distribution from cascade impactor tests

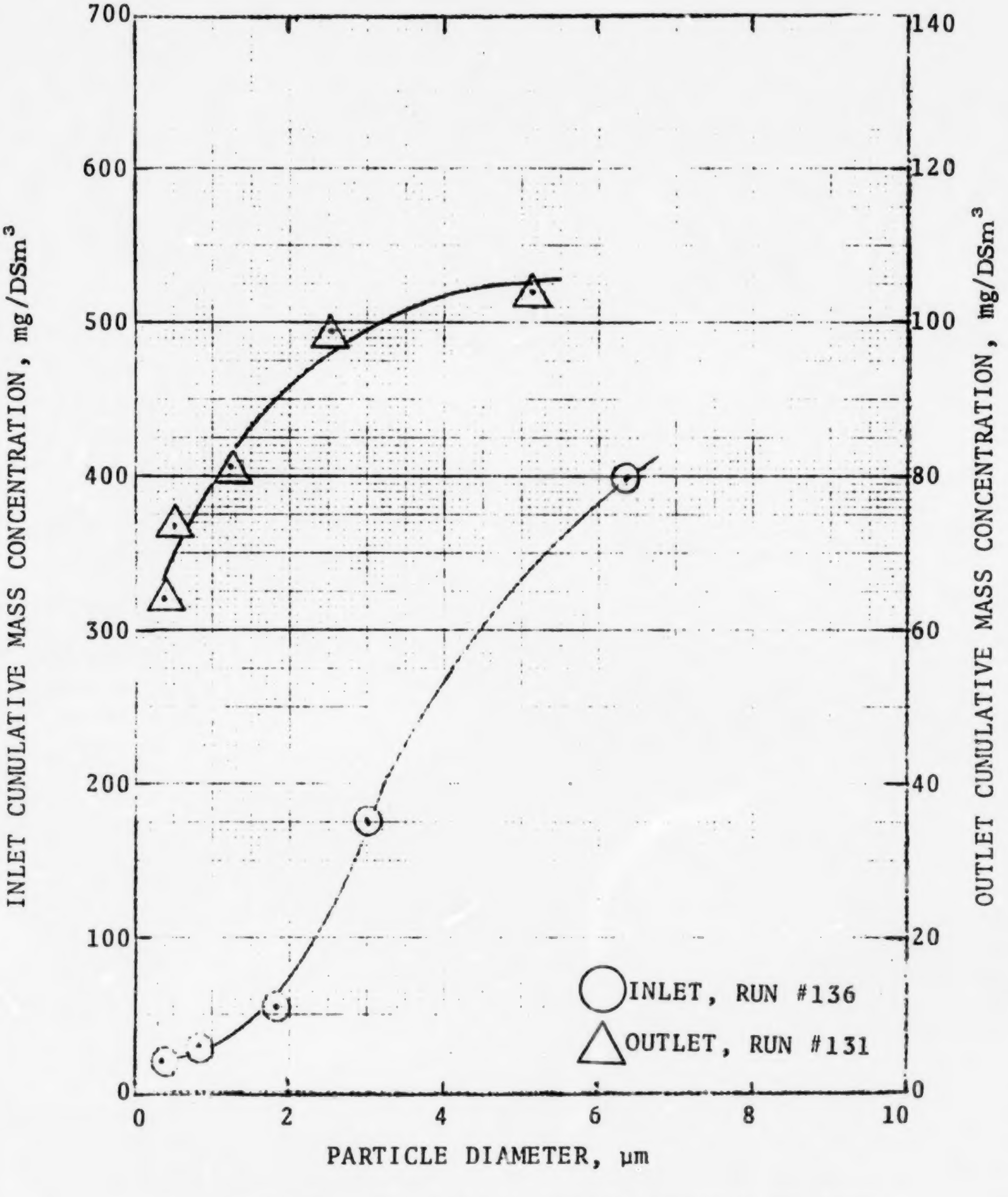

Figure B-25: Cumulative mass distribution from cascade impactor tests

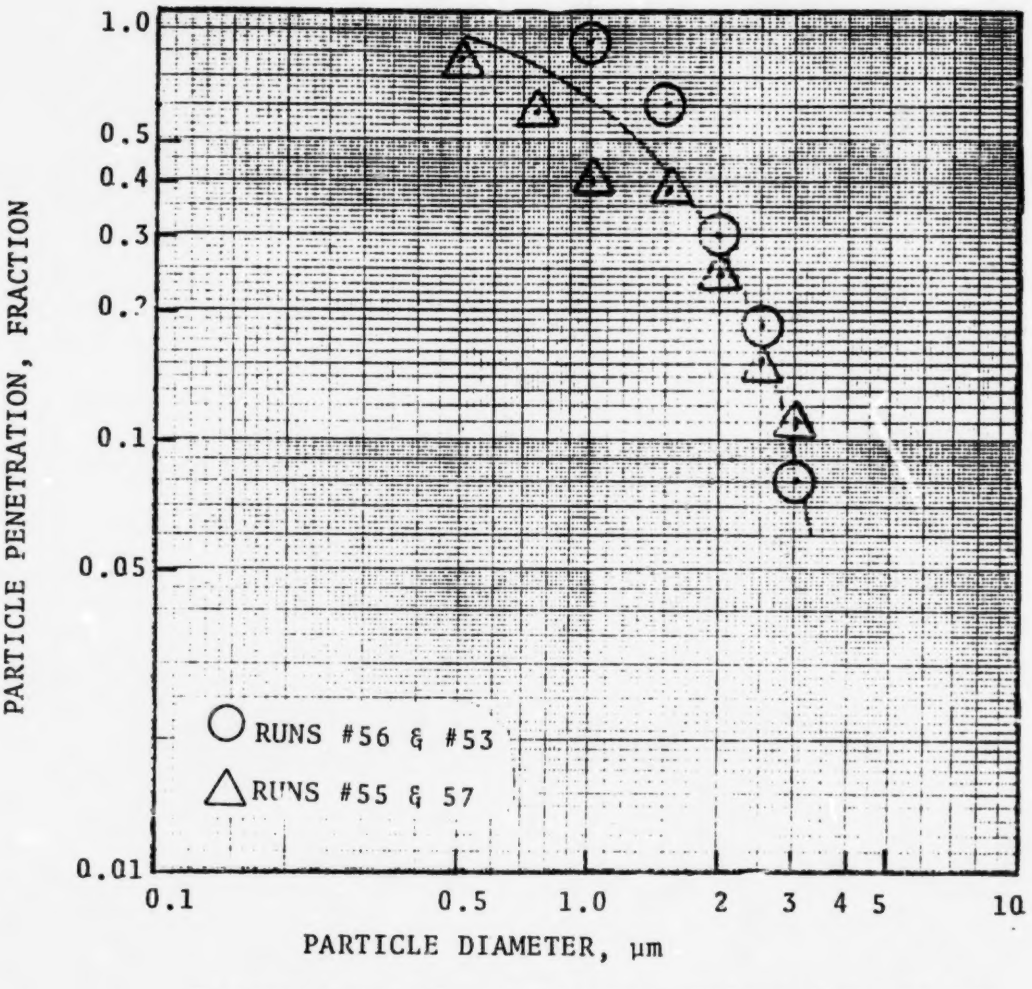

Figure B-26: Particle penetrations for cascade impactor tests

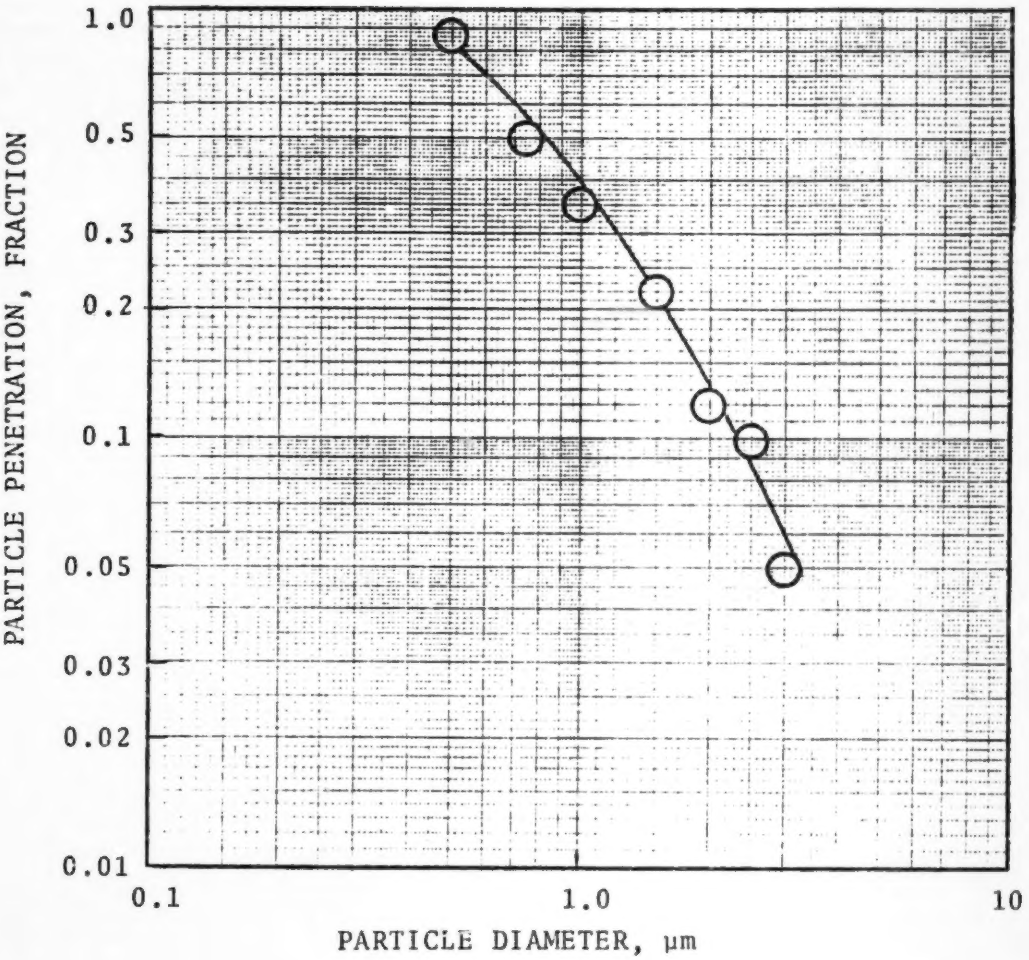

Figure B-27: Particle penetrations for cascade impactor tests #60 & #61.

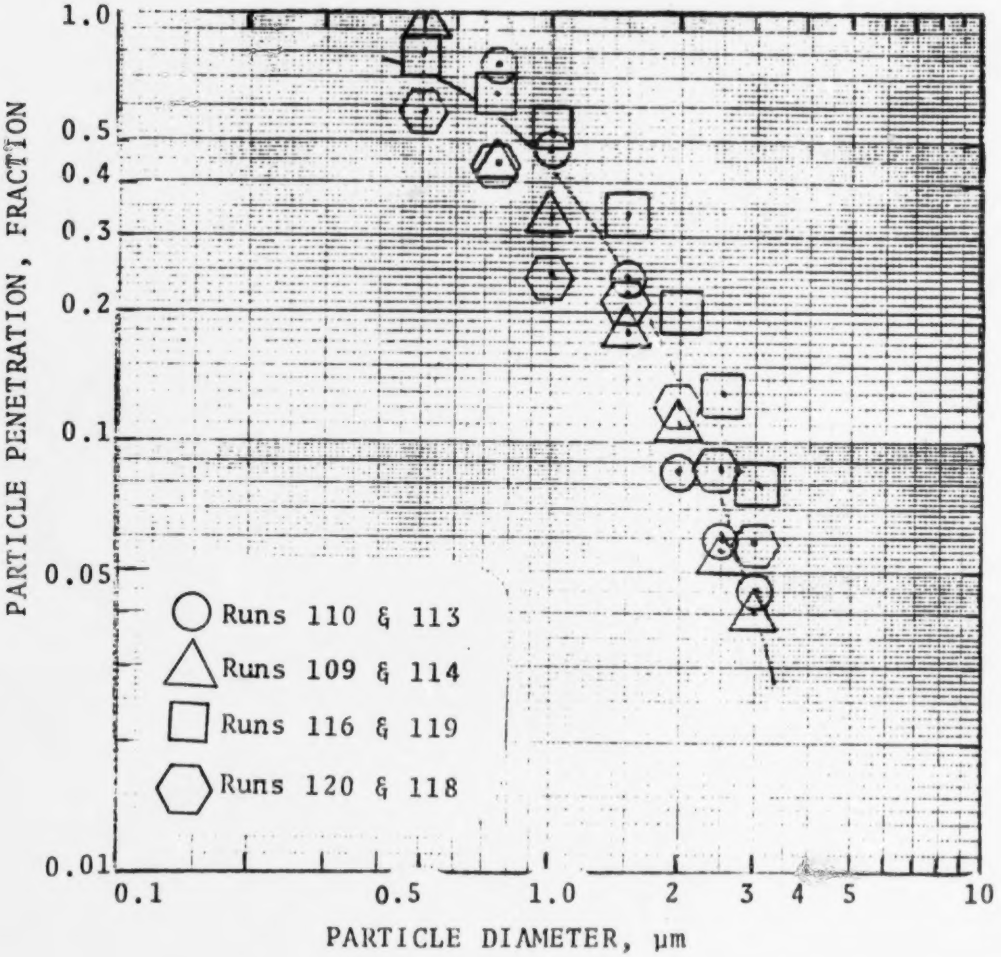

Figure B-28: Particle penetrations for cascade impactor tests

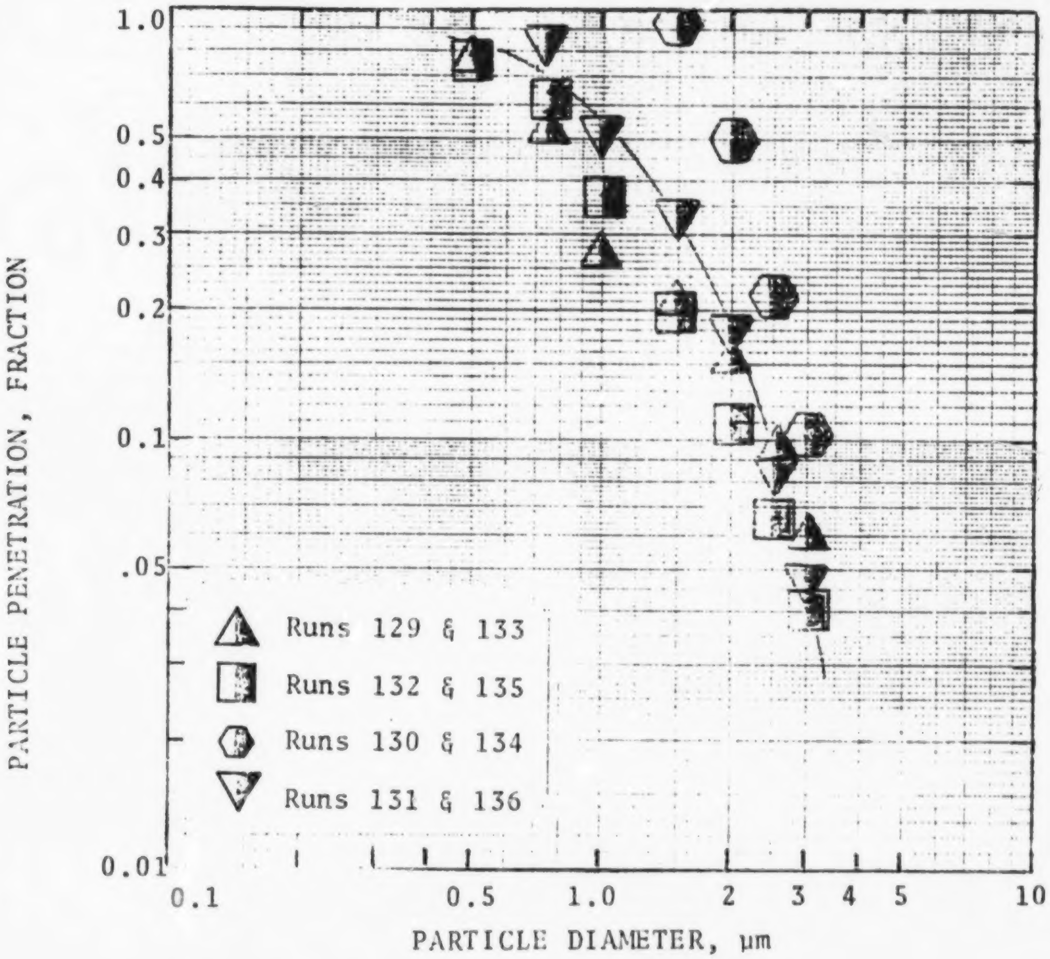

Figure B-29: Particle penetrations for cascade impactor tests

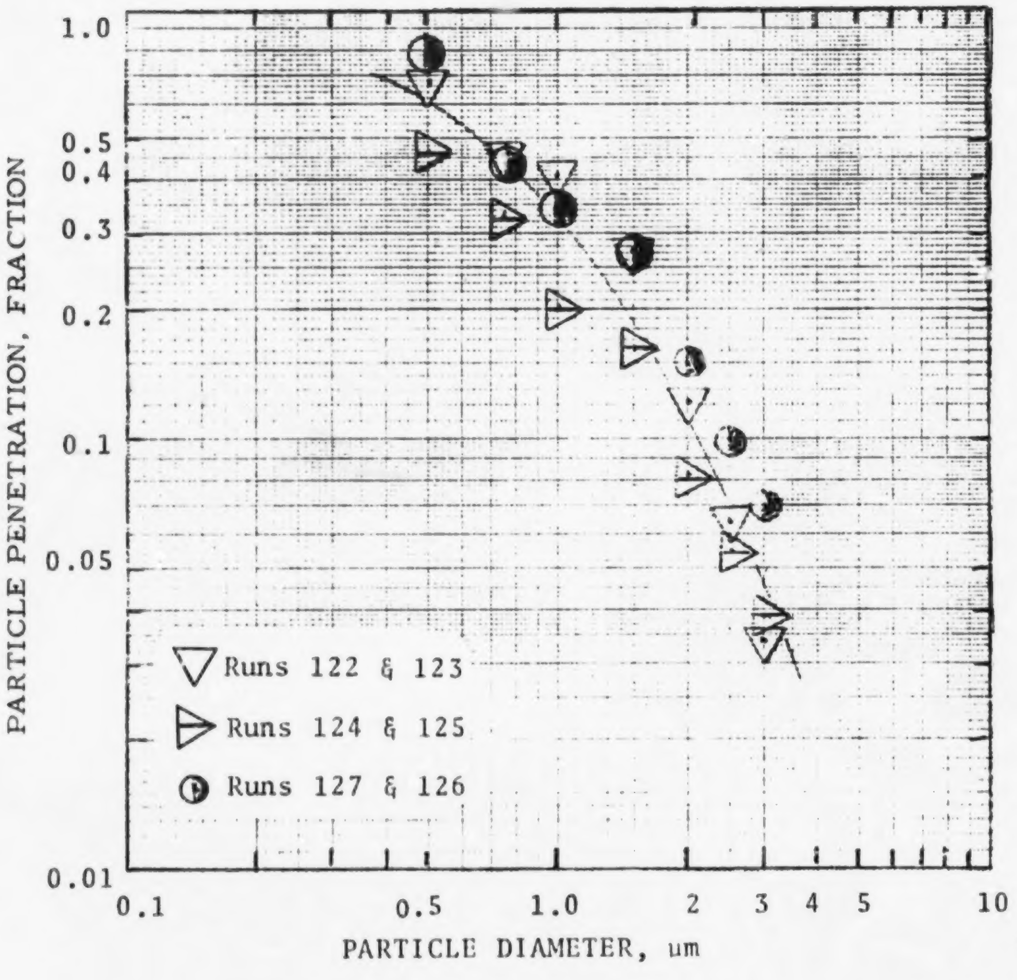

Figure B-30: Particle penetrations for cascade impactor tests

Table B-30. RUNS TAKEN WITH DIFFUSION BATTERY

DATE	RUN #	START TIME	FINISH TIME	LOCATION
11/21/74	1	09.40	10:45	Inlet
11/21/74	2	12:15	13:25	Inlet
11/21/74	3	14:10	15:00	Inlet
12/9/74	4	08:55	10:40	Inlet
12/9/74	5	13:05	14:10	Inlet
12/10/74	6	15:35	16:08	Inlet
12/10/74	7	10:00	10:20	Inlet
12/10/74	8	12:24	13:19	Inlet
12/10/74	9	16:28	16:58	Outlet
12/10/74	10	11:08	12:01	Outlet
12/10/74	11	12:51	13:39	Outlet
12/10/74	12	16:24	16:59	Inlet
12/10/74	13	09:19	10:27	Inlet
12/10/74	14	14:23	14:48	Outlet
12/10/74	15	15:29	16:09	Outlet

Table B-31. DIFFUSION BATTERY TESTS WITH COMPARABLE CASCADE IMPACTOR TESTS

INLET OR OUTLET	IMPACTOR RUN #	S.D.B. RUN #
Inlet	120	8
Outlet	118	9
Outlet	122	10
Inlet	123	12
Inlet	133	13
Outlet	129	15

Table B-32. DIFFUSION BATTERY NUMBER MEDIAN DIAMETERS AND STANDARD DEVIATIONS

D.B. RUNS	INLET		OUTLET	
	d_{pn},*μm	σ_g	d_{pn},*μm	σg
8&9	0.071	1.5	0.11	22.0
10&12	0.094	1.4	0.051	3.3
13&15	0.18	3.6	0.063	1.9

* d_{pn} refers to number median diameter

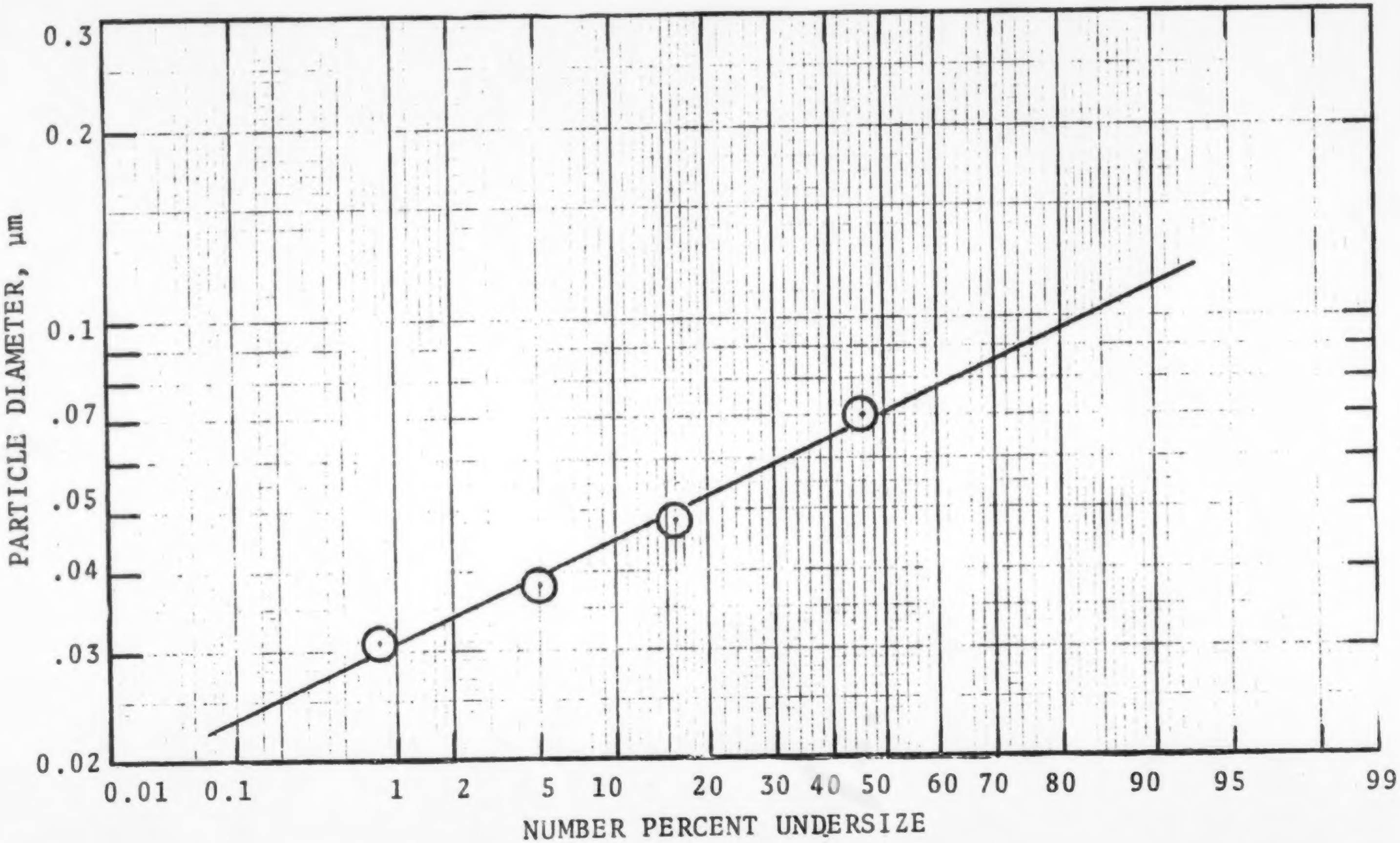

Figure B-31 Size distribution for Run #8 inlet by Screen Diffusion Battery

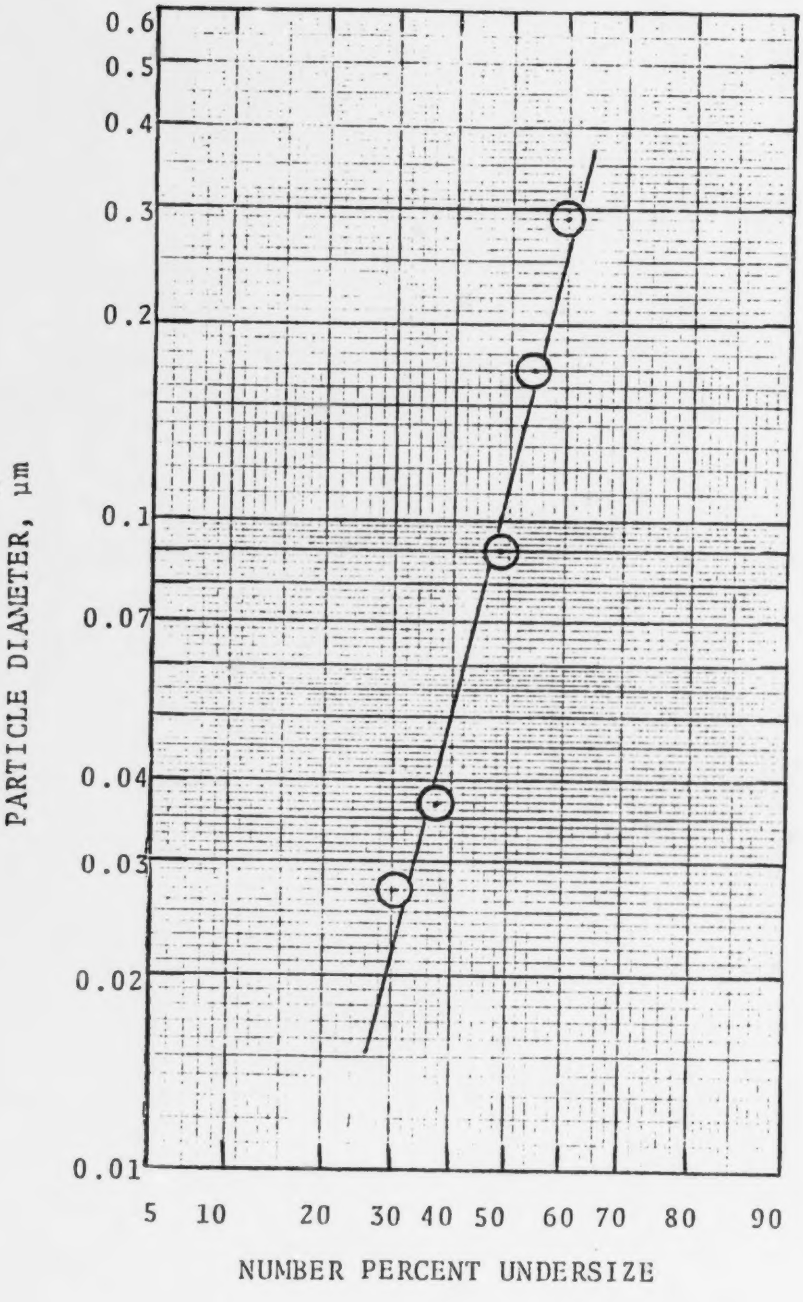

Figure B-32: Size distribution for Run #9 outlet by Screen Diffusion Battery

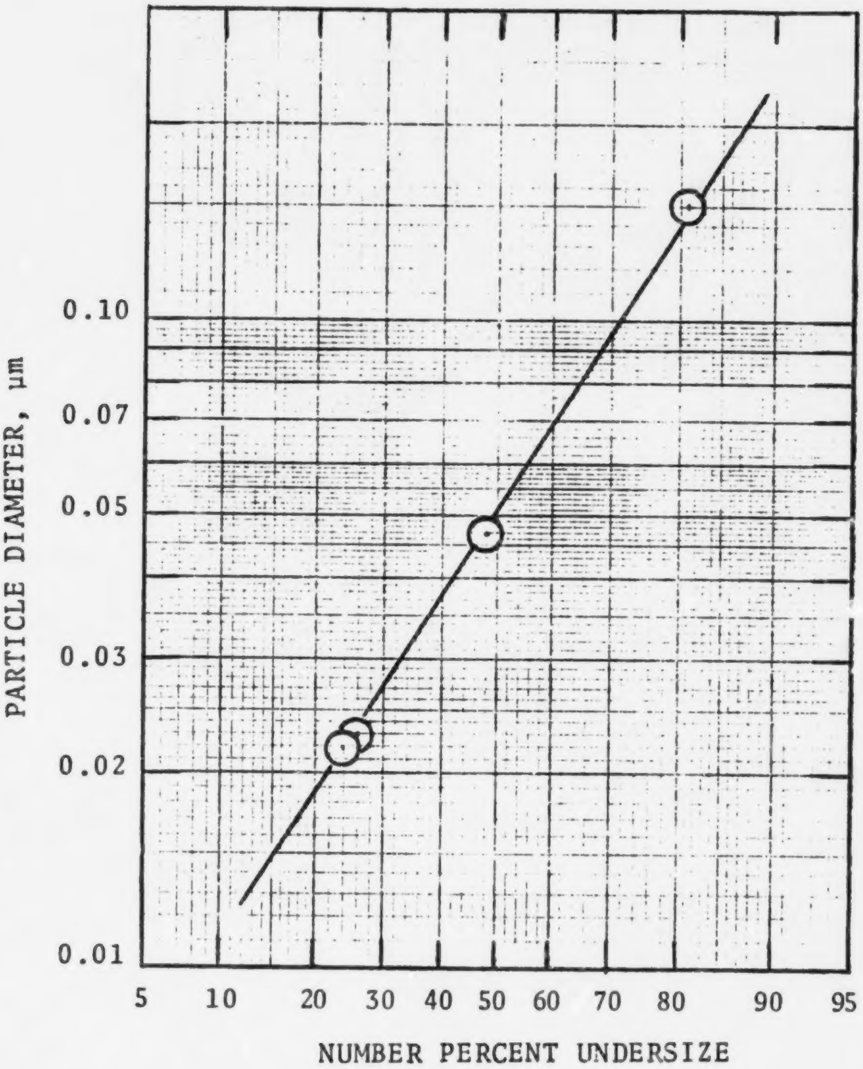

Figure B-33- Size distribution diffusion battery
Run #10, outlet

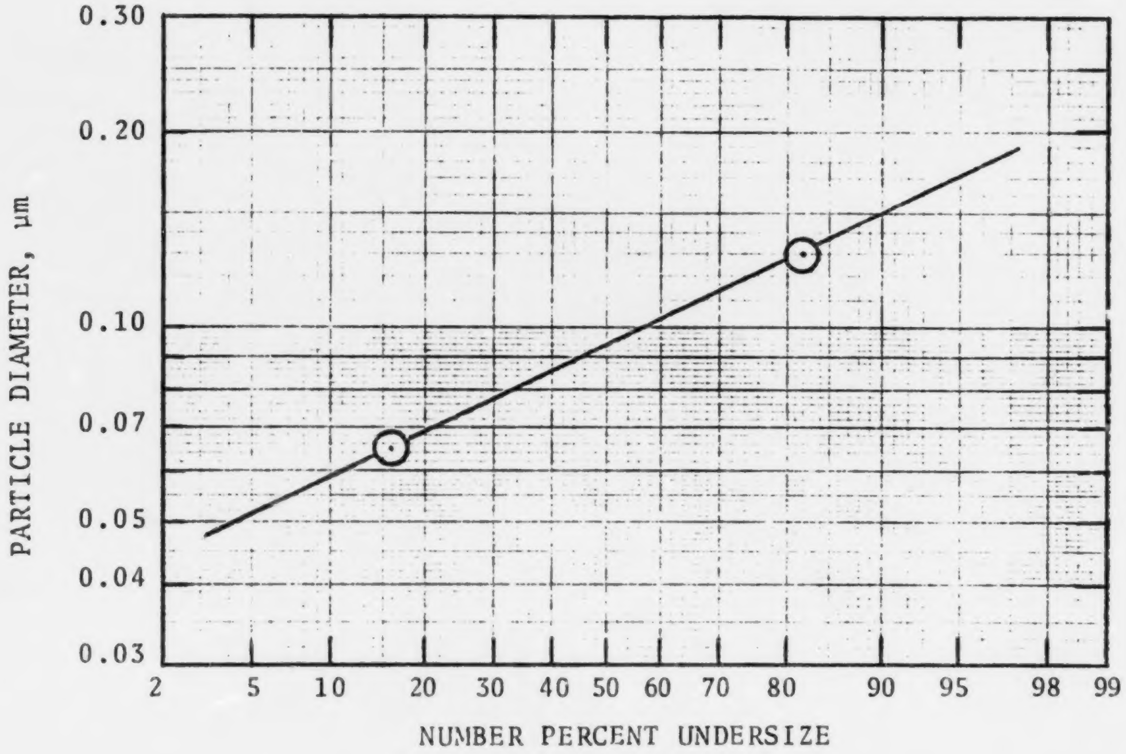

Figure B-34 - Size distribution diffusion battery
Run #12, inlet

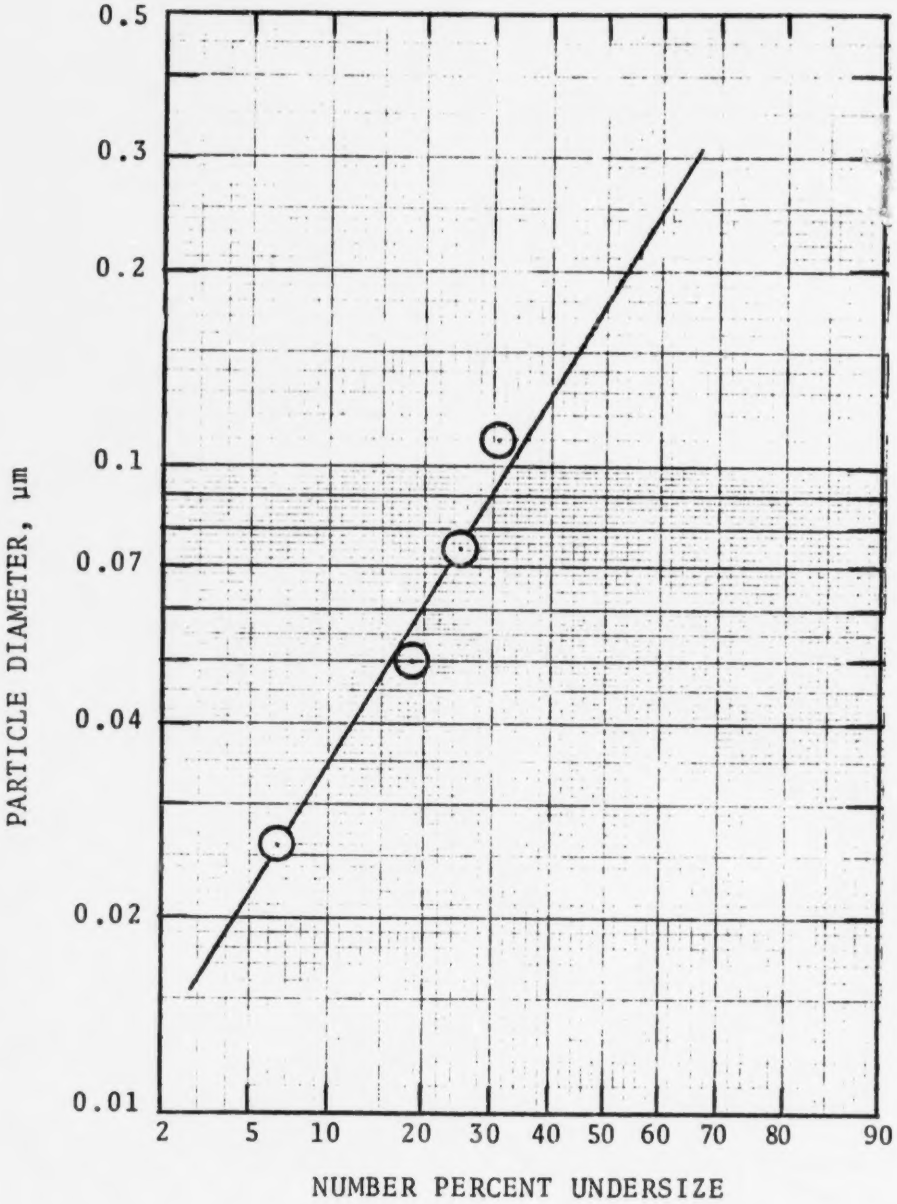

Figure B-35 - Size distribution, diffusion battery
Run #13 inlet

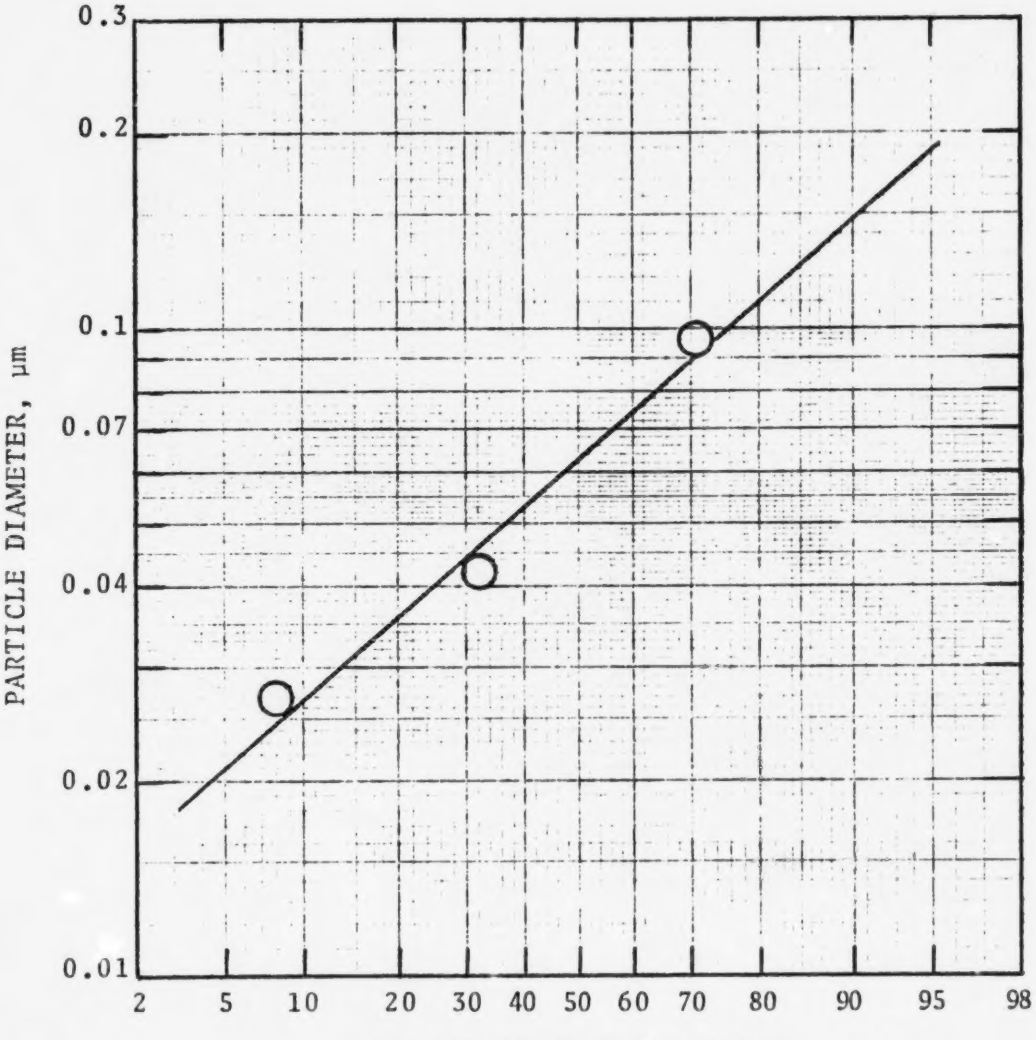

Figure B-36- Size distribution for diffusion battery Run #15, outlet

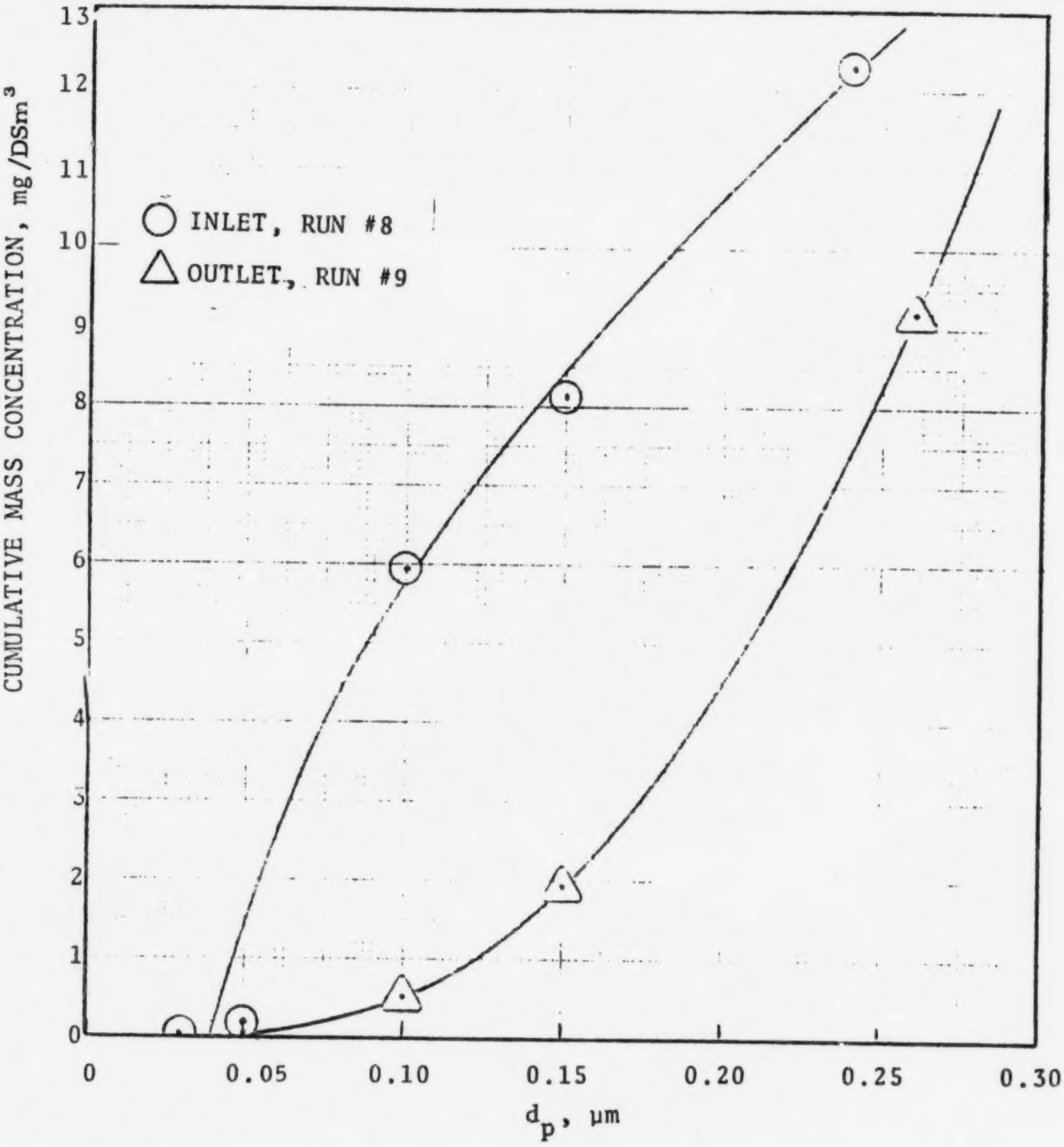

Figure B-37: Cumulative mass distribution, diffusion battery Runs #8 & #9

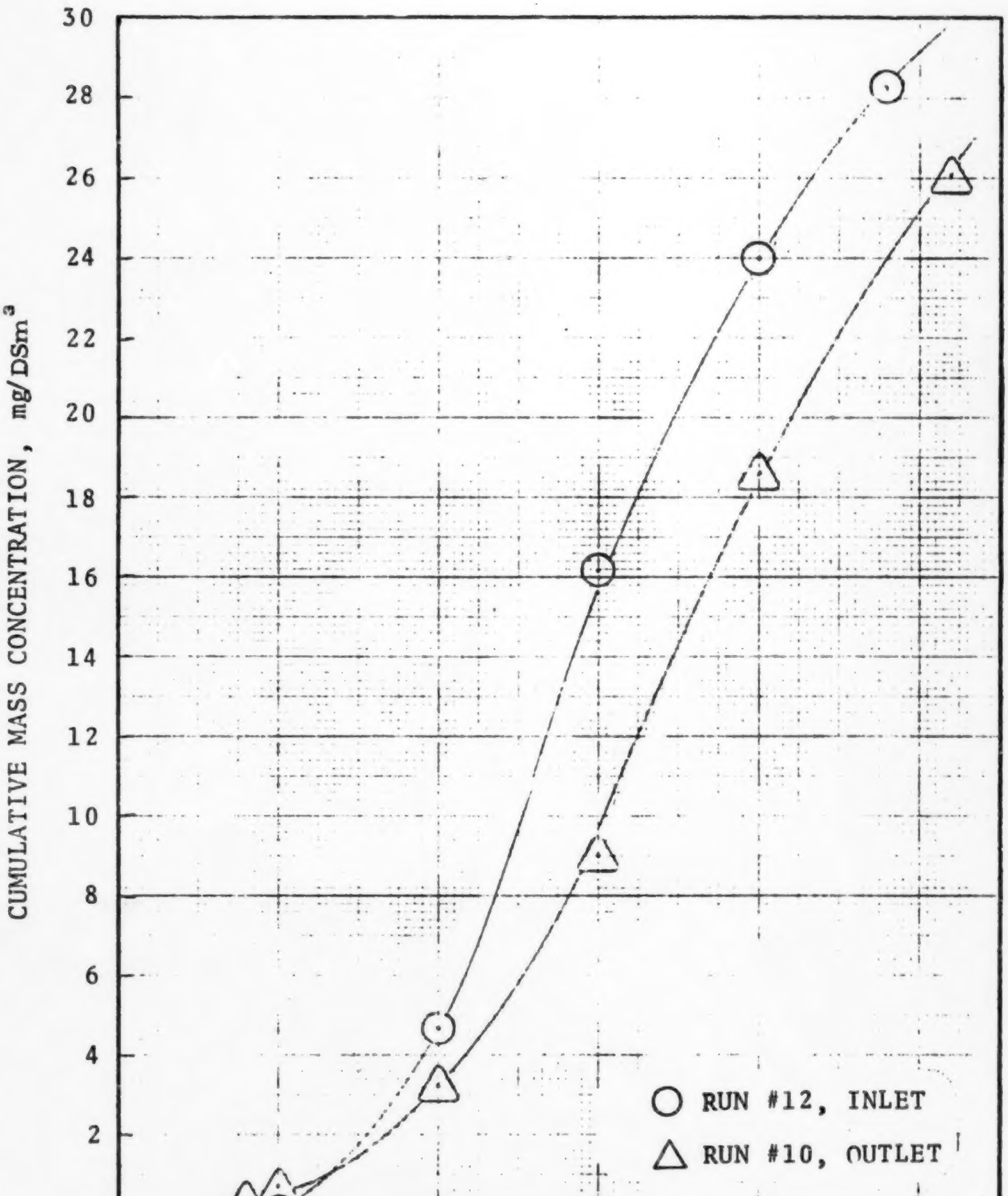

Figure B-38: Cumulative mass distribution, diffusion battery, runs #10 & #12

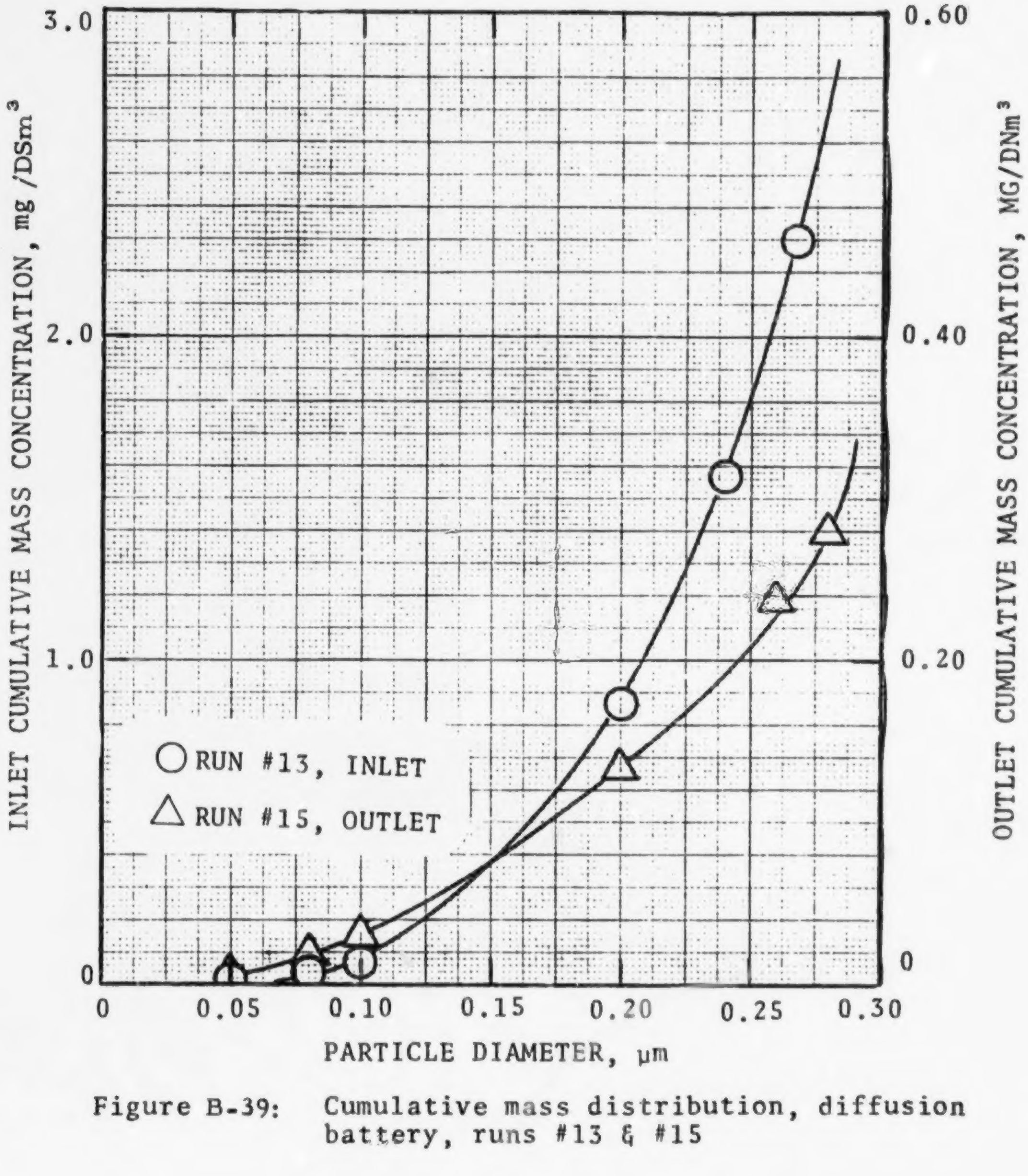

Figure B-39: Cumulative mass distribution, diffusion battery, runs #13 & #15

APPENDIX C

REDUCED ELEMENTAL CONCENTRATION DATA

Run No. 109 Location Outlet B

(Concentration, micrograms/DSm^3)[a] 12/10 1110 MST

Stage	A	B	C	D	E	F	G	H
D_{50}	28.6	14.4	5.28	2.49	1.51	0.69	0.28	
Elements								
Al	4.6*	5.6	24.4	12.8	37.2	37.0	8.8	22.6
Si	3.5	14.8	37.5	18.0	64.3	60.6	20.2	83.1
S	3.4*	3.6*	2.9*	2.7*	2.3	3.2*	2.8*	595.0
Cl	3.6*	3.9*	3.0*	2.9*	3.0*	3.2*	2.9*	9.0*
K	2.2	2.3*	2.4	2.5	5.2	3.6	1.1	7.0
Ca	4.4	5.1	16.9	10.6	36.4	33.7	15.5	345.4
Ti	1.4*	1.7*	2.4	1.5	5.6	5.9	2.6	36.4
V	3.7	1.7*	1.6*	1.5*	1.7*	1.9*	1.6*	5.7*
Cr	1.1*	1.5*	1.4*	1.3*	1.5*	1.6*	1.4*	22.4
Mn	-	-	-	-	-	-	-	0.4
Fe	1.0*	1.3	15.8	7.9	34.2	27.8	12.8	383.7
Co	-	-	-	-	-	-	-	-
Ni	0.9*	1.5*	1.4*	1.3*	1.5*	1.6*	1.4*	7.6
Cu	0.8	1.1*	1.0	0.7	1.4	1.2	0.7	672.4
Zn	1.1*	1.8*	1.7*	1.6*	1.8*	2.0*	1.8*	442.6
As	-	-	-	-	-	-	-	-
Se	-	-	-	-	-	-	-	0.3
Br	1.6*	2.7*	2.4*	2.3*	2.6*	2.6*	2.6*	5.7*
Rb	-	-	-	-	-	-	-	-
Sr	-	-	-	-	-	-	-	0.6
Zr	-	-	-	-	-	-	-	-
Ag	-	-	-	-	-	-	-	-
Ba	-	-	-	-	-	-	-	-
Pt	-	-	-	-	-	-	-	-
Au	-	-	-	-	-	-	-	-
Hg	-	-	-	-	-	-	-	-
Pb	3.2*	5.7*	4.7*	2.8	5.0*	5.1*	5.1*	90.2

---

* Concentration below reported detectable limit

- Not detected

[a] Dry standard 21.1° C, 760 mm Hg

Run No. 110 Location Outlet A
12/10 1142 MST

(Concentration, micrograms/DSm^3)^a

Stage	A	B	C	D	E	F	G	H
D_{50}	28.99	14.5	5.34	2.5	1.51	0.69	0.27	
Elements								
Al	8.4	10.7*	5.1	57.7	94.3	117.8	61.2	171.0
Si	17.2	17.1	10.4	100.6	173.0	212.4	135.0	333.2
S	7.2*	8.2*	5.2*	6.5*	7.1*	8.8	61.9	2302.1
Cl	7.8*	8.9*	5.5*	6.9*	7.2*	6.8*	7.5*	19.7*
K	4.3	3.7	2.4	7.7	6.9	10.2	3.3	27.5
Ca	8.2	9.4	8.9	58.0	101.7	142.2	43.1	279.9
Ti	2.9*	5.1	2.9*	7.7	14.8	21.9	19.5	12.3*
V	2.8*	3.8*	2.9*	3.6*	4.2*	4.0	8.6	12.5*
Cr	2.4*	3.4*	2.5*	3.2*	3.6*	3.4*	3.8*	145.9
Mn	-	-	-	-	-		0.1	0.6
Fe	16.3	7.8	2.5*	72.7	96.3	120.0	100.1	1736.6
Co	-	-	-	-	-	-	-	-
Ni	2.0*	3.3*	2.5*	3.2*	3.6*	3.4*	3.9*	87.2
Cu	1.4	2.5*	1.4	2.1	3.6	3.0	6.9	906.9
Zn	2.5*	4.1*	3.1*	3.8*	4.4*	4.1*	19.1	738.0
As	-	-	-	-	-	-	-	-
Se	-	-	-	-	-	-	-	0.2
Br	3.9*	6.0*	5.7*	6.2*	6.0*	5.5*	5.4*	9.8*
Rb	-	-	-	-	-	-	-	0.3
Sr	-	-	-	-	-	0.4	-	1.1
Zr	-	-	-	-	-	-	-	-
Ag	-	-	-	-	-	-	-	-
Ba	-	-	-	-	-	-	-	2.7
Pt	-	-	-	-	-	-	-	-
Au	-	-	-	-	-	-	-	-
Hg	-	-	-	-	0.2	0.3	-	-
Pb	7.8*	12.6*	11.3*	12.5*	11.8*	10.9*	10.7*	28.4

---

* Concentration below reported detectable limit

- Not detected

[a] Dry Standard 21.1° C, 760 mm Hg

Run No. 111 Location Outlet B
12/10 1232 MST
(Concentration, micrograms/DSm^3)[a]

Stage	A	B	C	D	E	F	G	H
D_{50}	29.0	14.5	5.37	2.64	1.32	0.525	0.443	
Elements								
Al	7.7	17.4	42.8	52.9	81.2	58.0	92.8	489.9
Si	12.6	29.9	73.5	95.3	128.6	100.9	167.0	1648.3
S	3.5*	3.8*	3.1	3.5*	3.5*	3.5	6.2	269.7
Cl	2.1	4.2*	3.8*	3.6*	3.6*	3.6*	4.0*	9.6*
K	2.0*	2.8	3.6	5.4	6.6	4.2	5.3	17.7
Ca	6.5	11.0	29.2	43.0	92.4	64.1	109.2	1231.3
Ti	1.4*	2.3	4.3	5.9	13.1	10.2	15.2	116.9
V	1.5	1.8*	2.0*	1.9*	2.1*	2.1*	2.3*	6.1*
Cr	1.1*	1.6*	0.8	1.7*	1.8*	1.8*	2.0*	5.4*
Mn	-	-	-	-	-	-	-	0.2
Fe	2.9	11.2	34.5	37.3	90.3	48.1	85.3	708.2
Co	-	-	-	-	-	-	-	-
Ni	1.0*	1.6*	1.7*	1.7*	1.9*	1.8*	2.0*	4.9*
Cu	0.5	1.0	1.9	1.3	2.4	1.4	1.7	3.8*
Zn	1.2*	1.9*	2.1*	2.0*	2.2*	2.2*	2.5*	20.7
As	-	-	-	-	-	-	-	-
Se	-	-	-	-	0.1	-	0.1	0.7
Br	1.7*	2.5*	3.0*	2.9*	2.9*	2.4*	2.6*	5.7
Rb	-	-	-	-	-	-	-	-
Sr	-	-	-	-	0.4	-	0.3	2.2
Zr	-	-	-	-	-	-	-	-
Ag	-	-	-	-	-	-	-	-
Ba	-	-	-	-	-	-	-	7.4
Pt	-	-	-	-	-	-	-	-
Au	-	-	-	-	-	-	-	-
Hg	-	-	-	-	0.4	-	-	1.4
Pb	3.3*	5.4*	5.9*	5.8*	5.7*	4.8*	5.1*	44.7

---

* Concentration below reported detectable limits
- Not detected

[a] Dry Standard 21.1° C, 760 mm Hg

Run No. 112 Location Outlet A

12/10 1314 MST

(Concentration, micrograms/DSm^3)[a]

Stage	A	B	C	D	E	F	G	H
D_{50}	30.2	15.1	5.91	2.30	1.35	0.580	0.338	
Elements								
Al	5.7*	5.1	42.0	26.1	62.5	100.5	85.9	60.0
Si	28.7	11.1	78.6	45.5	114.9	184.0	205.3	355.2
S	4.1*	3.8*	3.8*	3.8	1.6	8.2	27.0	1482.7
Cl	4.5*	4.2*	4.0*	3.3*	4.1*	4.2*	4.3*	8.8*
K	2.4	2.3	5.9	4.9	7.7	7.5	7.7	14.1
Ca	8.2	6.4	29.8	22.1	60.0	113.2	160.6	1126.5
Ti	1.6*	2.5	5.3	4.7	8.1	16.0	23.4	5.6*
V	0.9	1.8*	2.1*	2.0	2.4*	3.0	7.0	5.6*
Cr	1.3*	1.6*	1.9*	1.6*	2.1*	2.1*	2.2*	42.6
Mn	-	-	-	-	-	-	-	1.2
Fe	16.4	1.6*	25.8	19.9	53.1	99.8	122.8	787.2
Co	-	-	-	-	-	-	-	-
Ni	1.2*	1.6*	1.8*	1.5*	2.1*	2.1*	2.2*	39.3
Cu	3.6	1.1	1.2	0.6	2.3	2.8	1.6*	526.0
Zn	1.7	1.9*	2.2*	1.9*	1.3	2.5*	11.4	933.9
As	-	-	-	-	-	-	-	-
Se	-	-	-	-	-	-	0.1	0.2
Br	1.6*	2.5*	2.2*	2.5*	2.9*	3.0*	2.7*	4.3*
Rb	-	-	-	-	-	-	-	0.3
Sr	-	-	-	-	0.3	0.3	0.4	1.6
Zr	-	-	-	-	-	-	-	-
Ag	-	-	-	-	-	-	-	-
Ba	-	-	-	-	-	-	-	4.9
Pt	-	-	-	-	-	-	-	-
Au	-	-	-	-	-	-	0.2	-
Hg	-	-	-	-	-	0.5	-	1.4
Pb	3.1*	5.3*	4.4*	5.0*	5.8*	6.0*	5.1	10.0*

---

* Concentration below reported detectable limit

- Not detected

[a] Dry Standard, 21.1° C, 760 mm Hg

Run No. 113 Location Inlet 8

12/10 1207 MST

(Concentration, micrograms/DSm^3)[a]

Stage	A	B	C	D	E	F	G	H
D_{50}	32.0	16.0	6.17	2.45	1.45	0.657	0.28	
Elements								
Al	2621.5	5332.2	8507.4	3140.0	588.1	328.3	384.4	863.0
Si	4825.5	9630.8	11334.7	4580.7	941.8	551.0	654.4	2251.7
S	17.4*	19.8*	21.6*	15.7*	12.5*	22.7	6.7	248.4
Cl	18.7*	21.7*	21.3*	16.0*	12.6*	13.6*	12.5*	39.3*
K	236.8	575.0	696.5	265.5	69.8	39.0	33.1	60.1
Ca	1605.4	3987.3	5181.9	1801.9	440.5	293.6	355.1	1267.2
Ti	223.6	587.8	743.1	250.6	70.2	52.8	56.9	24.7*
V	19.0	43.0	63.7	24.8	15.0	10.1	8.4	25.0*
Cr	5.9*	9.5*	9.8*	7.4*	6.4*	6.9*	6.4*	22.1*
Mn	0.1	0.3	0.4	0.2	0.1	-	0.1	-
Fe	1111.4	3537.6	5139.3	1568.1	456.3	274.5	299.3	790.8
Co	-	-	-	-	-	-	-	-
Ni	5.3*	10.2*	11.2*	7.6*	6.4*	6.9*	6.3*	20.0*
Cu	12.1	40.2	8.8*	5.8*	9.3	6.5	2.3	15.4*
Zn	3.3	1 2*	13.4	8.8*	5.0	5.3	7.4*	29.8
As	-	-	-	-	-	-	-	-
Se	-	-	-	-	-	0.1	-	-
Br	5.7*	7.7*	8.7*	7.3*	8.4*	8.6*	8.4	30.2*
Rb	-	-	-	-	-	-	-	-
Sr	1.6	4.0	5.1	1.2	0.3	0.3	0.4	
Zr	-	-	-	-	-	-	-	-
Ag	-	-	-	-	-	-	-	-
Ba	-	-	-	-	-	-	-	6.7
Pt	-	-	-	-	-	-	-	-
Au	0.3	0.5	0.6	0.2	-	-	-	-
Hg	1.0	-	-	-	0.2	-	-	-
Pb	11.4*	21.7*	23.5*	24.1	16.6*	17.0*	16.6*	59.6*

---

* Concentration below reported detectable limit

- Not detected

[a] Dry Standard, 21.1° C, 760 mm Hg

Run No. 114 Location Inlet 8

12/10 1116 MST

(Concentration, micrograms/DSm^3)[a]

Stage	A	B	C	D	E	F	G	H
D_{50}	29.0	14.5	5.34	2.51	1.51	0.689	0.274	
Elements								
Al	5765.2	2334.6	1867.0	1258.4	336.0	161.6	295.8	436.6
Si	9439.7	4111.9	2787.4	1865.0	559.4	294.5	597.1	1439.0
S	17.2*	14.1*	13.7*	12.3*	16.3*	17.0*	41.2	238.7
Cl	18.4*	15.4*	14.0*	12.6*	16.5*	17.2*	18.0*	33.0*
K	570.4	236.3	168.3	129.3	41.6	18.5	31.0	26.5*
Ca	3648.2	1795.1	1299.0	820.1	307.8	181.6	532.9	1037.9
Ti	492.5	243.6	168.5	118.0	43.7	34.1	84.8	20.7
V	41.4	19.3	17.2	11.9	9.5*	9.9*	10.4*	21.0*
Cr	17.4	6.4*	6.4*	5.9*	8.5*	8.9*	9.2*	18.5*
Mn	0.3	0.2	0.2	0.2	0.1	-	0.2	-
Fe	2898.0	1387.2	1049.3	792.1	311.8	156.6	419.6	524.8
Co	-	-	-	-	-	-	-	-
Ni	6.8*	6.7*	6.6*	6.0*	8.2*	8.6*	8.9*	16.8*
Cu	5.6*	5.3*	14.8	9.5	3.5	6.9*	7.0*	13.0*
Zn	7.4*	8.5	10.1	6.9*	4.0	9.9*	7.7	28.0
As	-	-	-	-	-	-	-	-
Se	-	0.2	0.1	-	-	-	-	-
Br	12.2	6.4*	7.3*	7.0*	16.5*	17.0*	20.1*	24.8*
Rb	0.5	-	-	-	-	-	-	-
Sr	4.7	2.1	1.3	0.8	-	-	-	-
Zr	-	-	-	0.3	-	-	-	-
Ag	-	-	-	-	-	-	-	-
Ba	-	-	-	-	-	-	-	5.7
Pt	-	-	-	-	-	-	-	-
Au	0.7	-	-	-	-	-	-	-
Hg	4.2	1.4	1.3	0.8	-	-	-	-
Pb	13.9*	14.3*	14.6*	39.5	32.6*	33.6*	39.6*	49.0*

---

* Concentration below reported detectable limit

- Not detected

[a] Dry Standard, 21.1° C, 760 mm Hg

Run No. 115 Location Outlet C

12/10 1505 MST

(Concentration, micrograms/DSm^3)[a]

Stage	A	B	C	D	E	F	G	H
D_{50}	27.3	13.7	5.26	1.89	1.29	0.555	0.414	
Elements								
Al	8.0*	4.7	4.5	59.3	43.5	57.4	63.1	16.5
Si	8.0	6.8*	24.0	90.0	69.2	117.9	123.1	123.1
S	5.8*	6.1	5.9*	6.1*	4.8*	6.3*	5.0	600.7
Cl	4.5	6.4*	6.2*	6.4*	4.9*	6.4*	7.1*	10.5*
K	3.3	3.6	2.8	7.8	10.8	10.2	5.4	8.6*
Ca	2.9	2.6	8.4	42.6	46.9	65.0	83.7	207.5
Ti	2.3*	3.1	3.3*	7.2	10.2	8.7	13.7	36.7
V	2.3*	3.6	2.7	3.4*	2.8*	5.8	4.1*	6.7*
Cr	1.9*	2.5*	2.9*	3.0*	2.5*	3.3*	3.6*	19.3
Mn	-	-	-	-	-	-	-	0.3
Fe	9.8	3.8	11.0	40.8	54.7	59.7	81.4	419.7
Co	-	-	-	-	-	-	-	-
Ni	1.6*	2.4*	2.8*	2.9*	2.4*	3.2*	3.5*	16.6
Cu	1.3*	1.9*	2.3*	2.4*	2.0*	2.6*	2.8*	1476.5
Zn	1.8*	2.7*	3.3*	3.4*	2.8*	3.7*	4.1*	678.4
As	-	-	-	-	-	-	-	-
Se	-	-	-	-	-	-	-	-
Br	3.7*	5.7*	5.6*	5.0*	4.7*	6.4*	7.2*	7.8*
Rb	-	-	-	-	-	-	-	-
Sr	-	-	-	-	-	-	-	-
Zr	-	-	-	-	-	-	-	-
Ag	-	-	-	-	-	-	-	-
Ba	-	-	-	-	-	-	-	
Pt	-	-	-	-	-	-	-	-
Au	-	-	-	-	-	-	-	-
Hg	-	-	-	-	-	-	-	-
Pb	7.2*	12.0*	11.1*	10.1*	9.2*	12.6*	14.3	40.3
P	-	0.4	-	-	-	-	-	-

---

* Concentration below reported detectable limit

- Not detected

[a] Dry Standard, 21.1 °C, 760 mm Hg

Run No. 116 Location Outlet B

(Concentration, micrograms/DSm^3)[a] 12/10 1530 MST

Stage	A	B	C	D	E	F	G	H
D_{50}	28.4	14.2	5.58	2.32	1.44	0.662	0.467	
Elements								
Al	12.0*	10.9*	39.3	104.0	85.2	123.0	15.5	15.6
Si	10.5*	20.0	69.2	186.3	152.4	219.6	59.8	73.7
S	8.6*	8.2*	9.2	10.3*	8.8*	8.7	19.2	307.7
Cl	9.2*	15.8	8.8*	10.7*	8.9*	8.2*	7.0*	11.1*
K	6.5	5.3	6.0*	12.1	7.4	12.9	5.1*	7.4
Ca	5.9	10.4	31.7	88.2	75.0	136.4	12.2	106.4
Ti	4.2	4.0*	7.3	12.9	10.8	23.0	8.2	6.9*
V	3.3*	4.3	4.7*	5.9	5.2*	5.1	4.1*	7.0*
Cr	2.9*	3.5*	4.2*	5.0*	4.6*	4.2*	3.6*	24.6
Mn	-	-	-	0.2	-	-	-	0.4
Fe	4.1	5.7	27.2	111.2	89.4	118.9	37.8	287.4
Co	-	-	-	-	-	-	-	-
Ni	2.4*	3.4*	4.1*	4.8*	4.4*	4.0*	3.5*	11.1
Cu	1.9*	2.7*	3.3*	3.8*	1.3	2.7	2.8	179.9
Zn	2.7*	3.8*	4.6*	5.5*	5.0*	4.5	7.1	243.8
As	-	-	-	-	-	-	-	-
Se	-	-	-	-	-	-	-	-
Br	4.9*	7.3*	8.5*	11.5*	10.9*	9.6*	7.1*	8.0*
Rb	-	-	-	-	-	-	-	-
Sr	-	-	-	-	-	-	-	-
Zr	-	-	-	-	-	-	-	-
Ag	-	-	-	-	-	-	-	-
Ba	-	-	-	-	-	-	-	2.5
Pt	-	-	-	-	-	-	-	-
Au	-	-	-	-	-	-	-	-
Hg	-	-	-	-	-	-	-	-
Pb	9.6*	15.3*	17.0*	22.9*	21.5*	19.0*	14.1*	17.9

---

* Concentration below reported detectable limit

- Not detected

[a] Dry Standard, 21.1° C, 760 mm Hg

Run No. 117 Location Outlet B

(Concentration, micrograms / DSm^3)[a] 12/10 1431 MST

Stage	A	B	C	D	E	F	G	H
D_{50}	28.2	14.2	5.23	2.57	1.29	0.513	0.434	
Elements								
Al	15.2*	10.5*	68.2	206.0	157.7	122.5	41.8	34.5
Si	18.9	34.3	143.5	338.5	252.9	223.7	116.1	68.0
S	10.9*	7.8*	7.2*	9.0*	2.9	10.1	22.1	810.1
Cl	11.7*	5.7	7.5*	9.3*	6.8*	7.2*	6.6*	15.3*
K	5.7	3.3	9.2	27.0	15.2	14.1	8.5	9.0
Ca	11.1	9.4	52.3	192.6	163.5	171.4	74.1	225.6
Ti	5.6	3.8*	11.7	31.8	25.9	24.9	13.0	9.6*
V	4.2*	3.7*	4.0*	5.0*	4.0*	9.8	4.8	9.7*
Cr	3.6*	3.3*	3.6*	4.4*	3.5*	3.7*	3.4*	47.5
Mn	-	-	0.1	0.1	0.2	0.2	-	0.6
Fe	9.8	17.2	56.9	238.5	189.2	145.6	59.4	519.2
Co	-	-	-	-	-	-	-	-
Ni	3.1*	3.2*	3.5*	4.4*	3.4*	3.6*	3.4*	22.6
Cu	2.4*	2.6*	2.8*	3.5*	2.8*	1.2	3.8	902.2
Zn	3.5*	2.4	4.0*	5.0*	4.0	4.2*	10.4	703.5
As	-	-	-	-	-	-	-	-
Se	-	-	-	-	-	-	-	-
Br	6.0*	4.3*	4.9*	6.7*	4.9*	4.9*	4.4*	17.1
Rb	-	-	-	-	-	-	-	-
Sr	-	-	-	0.7	0.5	0.4	-	-
Zr	-	-	-	-	-	-	-	-
Ag	-	-	-	-	-	-	-	-
Ba	-	-	-	-	-	-	-	2.0
Pt	-	-	-	-	-	-	-	-
Au	-	-	-	0.5	-	0.2	-	-
Hg	-	-	-	0.5	0.4	-	-	-
Pb	11.7*	9.1*	9.9*	13.4*	9.6*	9.6*	8.7*	54.1

---

* Concentration below reported detectable limit

- Not detected

[a] Dry Standard, 21.1° C, 760 mm Hg

Run No. 118 Location Outlet C

(Concentration, micrograms/DSm^3)[a] 12/10 1630 MST

Stage	A	B	C	D	E	F	G	H
D_{50}	20.7	10.3	4.02	1.54	0.897	0.367	0.202	
Elements								
Al	8.9*	8.9	9.7	7.9	-	9.5	81.7	29.9
Si	7.8*	9.6	19.8	5.8*	-	12.5	156.5	96.3
S	6.4*	6.8*	6.0*	5.4*	-	6.1*	6.8	710.0
Cl	6.8*	7.4*	6.3*	5.7*	-	6.2*	6.5*	14.1*
K	3.8*	4.3	4.3*	4.4	-	4.5*	7.7	8.7
Ca	2.7	7.1	10.5	4.5	-	15.4	96.8	235.1
Ti	2.6*	3.3*	3.7	3.0*	-	3.6*	13.9	8.8*
V	2.5*	4.5	3.4*	3.0*	-	3.6*	3.8*	8.9*
Cr	2.1*	2.9*	3.0*	2.7*	-	3.2*	3.3*	37.2
Mn	0.1	-	-	0.1	-	-	-	0.6
Fe	8.2	11.3	8.0	3.2	-	15.7	75.1	429.0
Co	0.1	-	-	-	-	-	-	-
Ni	0.6	2.8*	3.0*	2.6*	-	1.7	2.0	9.7
Cu	1.4*	2.2*	2.4*	2.1*	-	2.4*	3.2	867.5
Zn	2.1*	2.1	3.4*	3.1*	-	3.6*	3.7*	443.9
As	-	-	-	-	-	-	-	-
Se	-	-	-	-	-	-	-	-
Br	2.6*	4.0*	4.2*	4.3*	-	4.7*	4.9*	8.1*
Rb	-	-	-	-	-	-	-	-
Sr	-	-	-	-	-	-	-	0.6
Zr	-	-	-	-	-	-	-	-
Ag	-	-	-	-	-	-	-	-
Ba	-	-	-	0.5	-	-	-	2.8
Pt	-	-	-	-	-	-	-	-
Au	-	-	-	-	-	-	-	-
Hg	-	-	-	-	-	-	-	-
Pb	5.1*	8.4*	8.4*	8.5*	-	9.4*	9.6*	89.3
P	0.1	-	-	-	-	-	-	-

---

* Concentration below reported detectable limit

- Not detected

[a] Dry Standard, 21.1° C, 760 mm Hg

Run No. 119 Location Inlet 8

(Concentration, micrograms/DSm^3) [a] 12/10 1530 MST

Stage	A	B	C	D	E	F	G	H
D_{50}	33.0	16.6	6.38	2.54	1.50	0.682	0.292	
Elements								
Al	939.4	575.1	1757.8	1355.9	529.3	85.9	207.4	182.2
Si	2577.1	1283.2	3244.8	2511.4	972.6	154.0	394.6	375.8
S	36.5*	38.3*	45.2*	38.7*	26.2*	22.4*	23.8	252.9
Cl	39.4*	42.3*	46.9*	40.3*	26.7*	23.0*	25.2*	58.4*
K	102.8	64.9	188.2	182.5	81.8	16.7*	36.1	46.3*
Ca	612.4	488.7	1690.6	1153.6	577.2	115.6	201.5	550.2
Ti	71.1	50.6	204.3	154.6	86.0	17.5	31.7	68.2
V	14.5*	18.3*	24.8*	30.4	19.8	13.3*	14.4*	43.2
Cr	12.0*	16.1*	22.5	18.6*	13.4*	11.6*	12.6*	32.6*
Mn	-	-	-	0.2	0.2	-	-	-
Fe	463.5	375.7	1495.4	1189.4	823.6	114.2	176.2	394.7
Co	-	-	-	-	-	-	-	-
Ni	10.3*	8.6	22.0*	18.8*	8.5	11.2*	6.2	29.6*
Cu	6.6	12.2*	17.9*	15.0*	19.0	3.5	23.6	148.6
Zn	11.7*	18.1*	25.8*	21.4*	15.4*	13.4*	132.0	702.2
As	-	-	-	-	-	-	-	-
Se	-	-	-	-	-	-	-	-
Br	15.7*	23.2*	36.5*	30.6*	17.7*	16.2*	17.1*	48.0*
Rb	-	-	-	-	-	-	-	-
Sr	-	-	0.9	0.6	0.4	-	-	-
Zr	-	-	-	-	-	-	-	-
Ag	-	-	-	-	-	-	-	-
Ba	-	-	-	-	-	-	-	-
Pt	-	0.4	-	0.8	0.3	0.2	-	-
Au	-	-	-	-	-	-	-	-
Hg	-	-	2.8	-	-	-	-	-
Pb	31.0*	48.8*	126.2	61.1*	35.1*	32.0*	33.7*	94.8*

---

* Concentration below reported detectable limit

- Not detected

[a] Dry Standard, 21.1° C, 760 mm Hg

Run No. 120 Location Inlet 13

12/10 1617 MST

(Concentration, micrograms/DSm^3)[a]

Stage	A	B	C	D	E	F	G	H
D_{50}	31.4	15.7	5.79	2.73	1.65	0.755	0.305	
Elements								
Al	223.5	293.9	1529.4	1810.7	487.0	218.1	305.1	46.2
Si	467.3	683.9	2407.8	2807.6	821.7	398.8	613.8	75.9*
S	14.9	31.5*	24.2*	26.1*	24.0*	24.1*	24.2*	51.1*
Cl	31.5*	34.7*	25.2*	27.0*	24.5*	24.6*	24.7*	50.9*
K	26.1	27.0	185.3	227.7	71.5	24.3	20.8	57.3
Ca	138.4	244.0	1558.7	1651.0	513.2	285.9	315.2	37.9
Ti	13.7	36.1	207.5	229.5	82.6	34.2	34.7	72.6
V	11.4*	15.0*	14.3	31.8	14.2*	14.2*	14.2*	32.3*
Cr	9.6*	13.2*	11.6*	12.7*	12.4*	12.5*	12.4*	28.5*
Mn	-	-	0.1	0.2	0.1	-	-	-
Fe	98.1	185.3	1469.6	1910.9	631.5	331.9	308.1	24.7*
Co	-	-	-	-	-	-	-	-
Ni	8.0*	5.1	11.6*	12.6*	7.2	14.3	5.7	25.9*
Cu	6.3*	7.3	9.3*	9.9*	7.7	5.8	9.6*	19.9*
Zn	9.3*	14.9*	13.3*	14.4*	14.2	11.8	14.3*	25.4*
As	-	-	-	-	-	-	-	-
Se	-	-	-	-	-	-	-	-
Br	11.5*	19.1*	14.9*	15.4*	16.6*	16.5*	17.4*	42.0*
Rb	-	-	-	-	-	-	-	-
Sr	-	-	1.2	1.5	0.6	-	-	-
Zr	-	-	-	-	-	-	-	-
Ag	-	-	-	-	-	-	-	-
Ba	-	-	-	-	-	-	-	-
Pt	0.2	-	-	-	0.2	-	-	-
Au	-	-	-	-	-	-	-	-
Hg	-	-	1.3	1.0	-	-	-	-
Pb	22.8*	40.3*	29.7*	30.6*	32.8*	32.7*	34.4*	83.0*

---

* Concentration below reported detectable limit

- Not detected

[a] Dry Standard, 21.1° C, 760 mm Hg

Run No. 121 Location Outlet B

(Concentration, micrograms/DSm^3)[a] 12/11 1216 MST

Stage	A	B	C	D	E	F	G	H
D_{50}	27.137	13.6	5.34	2.22	1.376	0.630	0.444	
Elements								
Al	7.2	7.4*	45.4	185.6	146.5	200.2	100.0	20.4*
Si	20.3	6.5*	98.9	283.8	230.4	303.9	242.7	243.9
S	2.2	3.7	6.7*	5.4*	3.5	13.9	36.5	357.2
Cl	5.5*	13.0	7.1*	5.6*	4.8*	4.6*	4.7*	11.7*
K	2.4	3.1	4.9*	17.0	8.5	10.2	5.0	9.4*
Ca	10.8	10.8	74.7	174.8	142.6	239.2	265.5	177.1
Ti	2.1*	2.6*	3.9*	22.3	18.4	30.7	2.7*	47.2
V	2.0*	2.9	3.9*	3.8	2.8*	7.5	2.7*	7.4*
Cr	1.7*	2.3*	3.4*	2.6*	2.4*	2.3*	2.3*	24.9
Mn	-	-	0.3	0.2	0.1	0.1	0.1	0.3
Fe	9.2	8.3	55.7	163.7	112.6	173.4	155.1	568.1
Co	-	0.1		-	0.2	-	-	-
Ni	0.7	2.2*	3.2*	2.5*	1.8	2.2*	1.6	5.9*
Cu	2.7	1.1	1.7	2.0*	1.8	1.8	1.8*	152.9
Zn	1.7*	2.5*	3.7*	2.9*	2.8*	3.1	4.0	164.1
As	-	-	-	-	-	-	-	-
Se	-	-	-	-	-	-	-	-
Br	2.0*	3.3*	4.9*	3.6*	3.2*	2.8*	2.9*	9.5*
Rb	-	-	-	-	-	-	-	-
Sr	-	-	-	0.5	0.4	0.8	0.9	-
Zr	-	-	-	-	-	-	-	-
Ag	-	-	-	-	-	-	-	-
Ba	-	-	2.1	-	-	-	5.0	7.1
Pt	-	-	0.7	-	0.3	-	0.2	-
Au	-	-	-	-	-	-	-	-
Hg	-	-	-	0.5	-	0.5	-	-
Pb	3.9*	6.9*	9.7*	6.0	6.4*	5.5*	5.7*	45.2

---

* Concentration below reported detectable limit

- Not detected

[a] Dry Standard, 21.1° C, 760 mm Hg

Run No. 122 Location Outlet C

(Concentration, micrograms/DSm^3)[a] 12/11 1215 MST

Stage	A	B	C	D	E	F	G	H
D_{50}	27.7	13.9	5.33	1.91	1.30	0.559	0.417	
Elements								
Al	4.0	6.5*	6.4	93.2	82.3	88.7	32.3	5 .0
Si	7.8	5.6*	6.3	141.8	136.9	155.4	64.1	177.0
S	6.8	2.6	4.8*	5.1*	4.8*	2.3	2.2	725.0
Cl	5.8*	3.4	5.0*	5.3*	4.9*	5.0*	4.5*	11.4*
K	2.5	2.7	3.4*	8.4	8.1	6.1	1.8	18.5
Ca	14.2	5.4	11.8	81.5	91.9	109.4	50.5	236.9
Ti	2.2*	2.3*	2.7*	10.0	13.1	14.5	5.7	64.5
V	3.0	2.3*	2.7*	2.8*	4.2	4.4	2.6*	7.2*
Cr	1.8*	2.0*	2.3*	2.5*	2.5*	2.5*	2.3*	79.8
Mn	-	-	-	0.2	-	-	-	1.1
Fe	5.3	8.6	6.6	73.3	81.0	78.9	32.4	518.8
Co	-	-	-	-	-	-	-	-
Ni	0.7	1.9*	2.3*	1.0	2.4*	1.4	2.2*	18.7
Cu	1.2*	1.3	1.8*	1.8	1.9*	1.9*	1.7*	1108.6
Zn	1.7*	2.2*	2.7*	2.8*	2.8*	2.9*	2.6*	651.3
As	-	-	-	-	-	-	-	-
Se	-	-	-	-	-	-	-	0.4
Br	2.1*	3.0*	3.3*	3.5*	3.4*	3.5*	3.2*	8.2*
Rb	-	-	-	-	-	-	-	-
Sr	-	-	-	-	-	-	-	1.6
Zr	-	-	-	-	-	-	-	-
Ag	-	-	-	-	-	-	-	-
Ba	-	-	-	-	-	-	-	0.9
Pt	-	-	-	0.2	-	-	-	-
Au	-	-	-	-	-	-	-	-
Hg	-	-	-	-	-	-	-	-
Pb	4.2*	6.4*	6.6*	6.9*	6.7*	6.9*	6.3*	105.7

---

* Concentration below reported detectable limit

- Not detected

[a] Dry Standard, 21.1° C, 760 mm Hg

Run No. 123 Location Inlet 13

(Concentration, micrograms/DSm^3)[a] 12/11 1215 MST

Stage	A	B	C	D	E	F	G	H
D_{50}	34.5	17.3	6.66	2.66	1.57	0.716	0.308	
Elements								
Al	5775.5	1737.3	4064.2	3735.3	781.0	227.7	686.3	400.2
Si	9746.9	3227.0	5972.3	5301.8	1309.1	435.7	1505.8	1643.7
S	35.9*	30.7*	33.1*	32.7*	25.7*	19.7	156.7	459.1
Cl	38.8*	33.9*	33.5*	33.4*	26.1*	24.1*	31.0*	59.8*
K	491.0	161.5	432.6	420.9	101.1	35.6	49.1	29.5
Ca	3440.1	1167.1	3893.6	3474.6	846.0	327.9	1124.8	1412.9
Ti	415.7	146.9	507.8	464.0	130.0	58.1	110.0	50.0
V	27.9	15.1*	54.7	62.2	34.6	41.5	17.4*	37.8*
Cr	12.5*	13.2*	15.5*	15.6*	13.2*	12.2*	15.5*	33.5*
Mn	0.2	-	0.3	-	0.1	-	0.1	-
Fe	2035.1	780.7	3826.8	3736.0	869.2	313.4	808.5	810.0
Co	-	-	-	-	-	-	-	-
Ni	11.1*	13.3	16.6*	16.5*	19.0	11.9*	15.2*	30.3*
Cu	30.4	14.1	39.6	37.3	10.6*	9.5*	12.1*	23.6*
Zn	12.2*	14.5*	18.2*	33.1	14.8*	13.6*	17.4*	20.3*
As	-	-	-	-	-	-	-	-
Se	-	-	-	-	-	-	-	-
Br	13.4*	17.3*	17.0*	18.0*	17.1*	15.8*	20.8*	46.2*
Rb	-	-	-	-	-	-	-	-
Sr	2.5	0.6	-	-	0.5	-	0.4	-
Zr	0.6	-	-	-	-	-	-	-
Ag	-	-	-	-	-	-	-	-
Ba	-	-	-	-	-	-	1.6	3.4
Pt	-	0.2	0.6	-	-	-	-	-
Au	-	-	-	-	-	-	-	-
Hg	1.9	-	-	-	-	-	0.6	-
Pb	26.7*	36.7*	262.0	36.1*	33.8*	31.1*	41.0*	91.2*

---

* Concentration below reported detectable limit

- Not detected

[a] Dry Standard, 21.1° C, 760 mm Hg

Run No. 124 Location Inlet 13

(Concentration, micrograms/DSm^3)[a] 11/12 1240 MST

Stage	A	B	C	D	E	F	G	H
D_{50}	34.4	17.2	6.34	2.99	1.81	0.835	0.342	
Elements								
Al	2341.8	2228.0	1441.7	3111.2	409.9	174.1	616.9	96.6*
Si	4555.4	3954.3	2321.9	4442.3	712.9	349.8	1115.6	1706.8
S	28.4*	28.9*	23.2*	31.4*	23.5*	19.9	97.9	497.2
Cl	30.6*	31.8*	24.0*	32.2*	23.8*	24.8*	24.8*	55.2*
K	186.9	206.3	152.0	289.8	47.8	48.9	38.8	55.7
Ca	1373.2	1497.6	1384.2	2439.5	469.2	331.8	846.4	1470.7
Ti	154.0	195.7	175.7	324.6	69.8	70.4	105.4	34.3*
V	38.6	27.8	37.5	38.9	34.0	29.1	14.0*	35.0*
Cr	9.7*	12.8*	11.2*	14.7*	12.1*	9.4	10.2	30.8*
Mn	0.1	0.1	0.1	0.2	-	0.1	-	-
Fe	762.1	997.3	1060.1	2075.8	486.4	374.8	537.2	773.2
Co	-	-	-	-	-	-	-	-
Ni	11.8	12.6*	11.5*	15.5*	11.8*	12.3*	12.2*	28.1*
Cu	6.8*	22.0	9.3*	12.5*	9.5*	9.8*	9.8*	16.0
Zn	9.3*	13.8*	12.7*	17.3*	13.5*	14.1*	12.6	25.3
As	-	-	-	-	-	-	-	-
Se	-	-	-	-	-	-	0.0	-
Br	12.5*	15.9*	15.7*	19.7*	17.3*	17.6*	16.0*	42.5*
Rb	-	-	-	-	-	-	-	-
Sr	0.7	0.8	0.8	1.2	-	-	0.3	-
Zr	-	-	-	-	-	-	-	-
Ag	-	-	-	-	-	-	-	-
Ba	-	-	-	-	-	-	-	4.9
Pt	-	0.2	-	-	-	-	-	-
Au	0.4	-	-	-	-	-	-	-
Hg	-	0.7	0.7	1.4	-	0.2	0.3	-
Pb	24.6*	33.5*	31.5*	39.3*	34.2*	34.7*	31.7*	84.2*

---

* Concentration below reported detectable limit

- Not detected

[a] Dry Standard, 21.1° C, 760 mm Hg

TABLE C17. COAL ANALYSIS

Date	12/10/74	12/11/74
Moisture, Percent	8.92 ± 0.08	13.4 ± 0.1
Volatile Matter, Percent	41.0 ± 0.1	43.5 ± 0.1
Fixed Carbon, Percent	40.4 ± 0.1	35.7 ± 0.1
C, Percent	63.4 ± 0.7	63.4 ± 2.0
H, Percent	4.69 ± 0.02	5.2 ± 0.3
N, Percent	1.61 ± 0.09	1.62 ± 0.06
P, Percent	0.23	0.23
S, Percent	0.43 ± 0.02	0.45 ± 0.02
Heat of Combustion BTU/lb	11,187	10,636

APPENDIX D

ENGINEERING ANALYSIS OF THE CHEROKEE #3 SCRUBBER

ENGINEERING ANALYSIS
OF
THE CHEROKEE #3
SCRUBBER

MAY 1975

PREPARED FOR METEOROLOGY RESEARCH, INC.

BY STEARNS-ROGER INC.

TABLE OF CONTENTS

SECTION 1 - INTRODUCTION

SECTION 2 - CAPITAL COSTS

SECTION 3 - OPERATING COSTS

SECTION 4 - MAJOR MAINTENANCE AND OPERATING PROBLEMS

SECTION 5 - SCRUBBER RELIABILITY

SECTION 6 - ESTIMATE OF A PROBLEM FREE SCRUBBER

SECTION 1

INTRODUCTION

In October of 1972, construction was completed on a scrubber to remove particulate matter from the flue gas emitting from the #3 boiler at Public Service Company of Colorado's Cherokee Station located in northeast Denver. This scrubber is part of a series of scrubbers and other pollution control devices that PSCC has installed in their efforts to provide an environmentally acceptable flue gas discharge from this station.

The purpose of this report is to provide an engineering analysis of the design and operation of the scrubber. This analysis includes:

1. Operating and capital costs
2. Review of operating and maintenance problems
3. Determination of scrubber reliability
4. Estimate of the cost to produce a "problem-free" scrubber

This report complements the testing program performed on the scrubber to aid in the total evaluation of its overall effectiveness.

1.1 Description of the Cherokee #3 Scrubber

A scrubber is a device to remove a pollutant from a gas stream by bringing a liquor in contact with the flowing gas. The Cherokee #3 Scrubber is a vessel that contains many plastic spheres held in place between a series of grids. With the proper balance of downward liquid flow and upward gas flow, these spheres remain in a constant state of motion. These spheres provide surface area for the liquid and gas phases to come into contact.

A flow diagram of the Cherokee #3 scrubber system is shown in Figure 1. The flue gas from the #3 boiler passes through a mechanical collector, an electrostatic precipitator, and into the two parallel operating induced draft fans. The gas can either go directly to the stack through the bypass damper or enter the scrubber system. This bypass arrangement allows the scrubber operation to be independent of the boiler operation.

The scrubber body consists of three separate sections labeled A, B, and C. A and C are designed to handle 20% each of the normal gas flow and B is designed to handle 60%. All three sections can operate independently of each other. This provides flexibility of operation at lower gas flows.

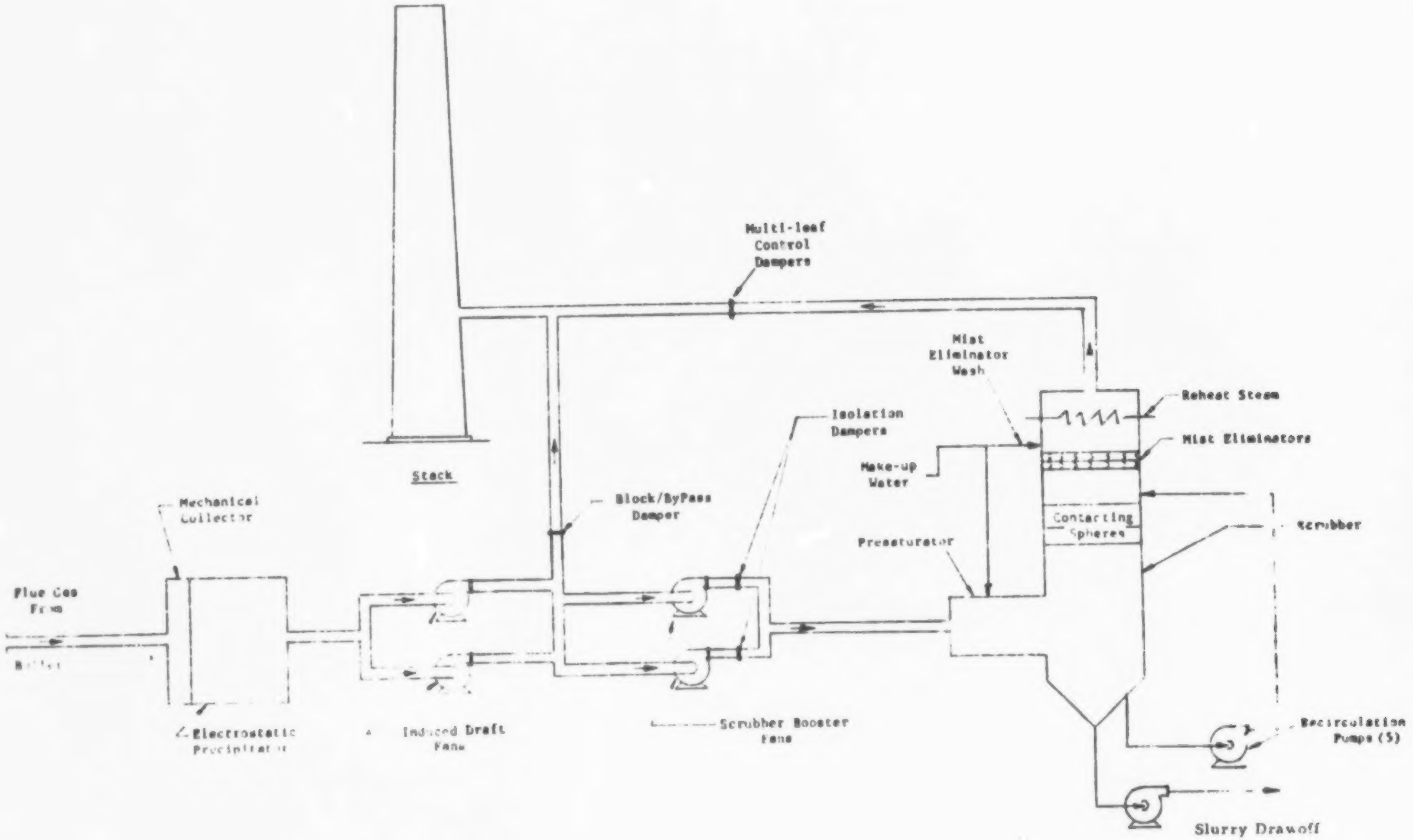
Multi-leaf
Control
Dampers
Mist
Eliminator
Wash
Reheat Steam
Mist Eliminators
Isolation
Dampers
Make-up
Water
Stack
Mechanical
Collector
Block/ByPass
Damper
Contacting
Spheres
Scrubber
Pressurator
Flue Gas
From
Boiler
Electrostatic
Precipitator
Induced Draft
Fans
Scrubber Booster
Fans
Recirculation
Pumps (5)
Slurry Drawoff

Figure 1

Cherokee #3 Scrubber System Flow Diagram

Under design conditions, 610,000 ACFM of flue gas enters the scrubber booster fans. After exiting the booster fans, the gas enters the presaturator and is sprayed with 380 GPM of make-up water. This water cools the gas from 280° F down to its saturation temperature which is approximately 125° F. This is done to prevent heat damage to the rubber lining in the scrubber and to saturate the flue gas prior to the scrubbing phase.

The gas then enters the scrubber body and is contacted with the recirculating liquor which enters the top of the scrubber through a header equipped with a set of spray nozzles. As the gas is contacted with the liquor, most of the fine particulate matter still remaining in the gas is wetted and removed by the liquor. Some amount of SO_2 is also absorbed and a low pH slurry is produced. This liquid slurry flows out the bottom of the scrubber where it is returned to the header by the recirculation pumps. Under normal operation, 225 GPM of slurry is continually purged from the system to prevent a buildup of scrubbed particles in the recirculated liquor. The slurry that is removed from the scrubber is pumped to an ash pond for disposal.

The scrubbed gas travels through a set of mist eliminators where entrained moisture is mechanically removed. The mist eliminators are periodically washed by water sprays to prevent any accumulation of solids on their blades.

The gas enters the reheater section and is heated by use of steam coils before entering the stack. The gas is reheated for two reasons; (1) to raise the temperature sufficiently above the dew point of the flue gas to prevent corrosion of the ductwork and stack lining due to condensation and (2) to raise the temperature of the flue gas to give it thermal drive to discharge from the stack. The steam coils are equipped with two sets of sootblowers to help maintain a clean surface on the coils. The heated, scrubbed gas then exits through the stack after entering the stack ductwork downstream of the bypass damper.

SECTION 2

CAPITAL COSTS

This section gives a breakdown of the capital costs required for the design, engineering and construction of the Cherokee #3 scrubber. This data is presented in Table 1. The total cost for the scrubber was $4,400,000 which amounts to an installed cost based on a nameplate rating of 150 MW of $29/KW. Based on the rated gas flow of 610,000 ACFM (280° F, 24.7" Hg) or 360,000 SCFM (70° F, 30" Hg), the cost is equal to $7.10/1000 ACFM or $12.00/1000 SCFM. This figure is the total installed cost of the scrubber which was completed in 1972. Since prices have escalated since then, the cost of a similar scrubber would be higher today. The 1975 cost of a similar scrubber installation, with some changes, is presented in Section 6.

The source of data for the capital costs was both PSCC's and Stearns-Roger's accounting records. Both cost sources were necessary because all of the major items were purchased directly by PSCC. These accounting records contain a separate charge for labor and material for some items. However, items that were done by subcontractors have labor and material charges combined. Because it was impossible to separate labor and material for all items, Table 1 gives just an installed cost for each account.

TABLE NO. 1

CHEROKEE #3 SCRUBBER
CAPITAL COST BREAKDOWN
1972 DOLLARS

ACCOUNT		INSTALLED COST	%
Excavation and Earthwork		$ 19,100	0.4
Concrete		100,800	2.3
Structural Steel and Buildings		324,300	7.4
Process Equipment			
Scrubber Vessel	$463,900		
Ductwork	224,600		
Presaturator	65,600		
Scrubber Fans and Motors	194,900		
Sootblowers	50,700		
Sootblowing Air Compressors	56,100		
Reheater	42,200		
Dampers and Isolation Gates	53,400		
Recirculation Pumps and Motors	48,900		
Miscellaneous Pumps and Motors	6,500		
Stack Lining	86,900		
Instrument Air Compressors	10,700		
Monitoring Equipment	16,400		
Miscellaneous Equipment	16,500	1,337,300	30.6
Piping		235,000	5.4
Electrical		444,300	0.2
Painting		28,000	0.6
Instrumentation		263,900	6.0
Insulation		110,700	2.5
Indirect Field Costs (includes: Field Supervision and Payroll Expenses; Construction Supplies; Temporary Facilities; Demolition; Construction Equipment)		385,000	8.8
PSCC Overhead Costs		74,600	1.7
Engineering		406,400	9.2
Pre Start-up and Revisions		67,800	1.6
Post Start-up and Maintenance		143,800	3.3
Contractor Fee		368,000	8.4
Interest During Construction		69,300	1.6
TOTAL		$4,377,300	100.0

SECTION 3

OPERATING COSTS

This section gives a breakdown of the costs involved in operating the #3 scrubber at PSCC's Cherokee Plant. A summary of these costs is presented in Table 2. These costs are direct costs only and do not include any indirect costs, such as general plant overhead or charges against capital (i.e., depreciation, interest, taxes, etc.). There are also no charges for general engineering work done by PSCC's Environmental Engineering and Planning Department. The total direct operating costs are approximately $495,000/year. Based on 75% availability of the scrubber, this amounts to a cost of 0.50 mills/KWH.

3.1 List of operating cost items

- 3.1.1 Operating labor and operating supervision
- 3.1.2 Utilities
- 3.1.3 Maintenance costs
- 3.1.4 Operating supplies
- 3.1.5 Miscellaneous

3.2 Operating labor and operating supervision

Operating labor consists of two functions, an inside control operator and an outside auxiliary tender. Both men have responsibility for operating other boiler equipment and the other two scrubbers at Cherokee. Therefore, it was necessary to have PSCC estimate how much of their time was spent on the #3 scrubber. They estimated that the control operator spends approximately 20% of his time on all three scrubbers. They also estimated that 50% of the auxiliary tender's time was spent on all three scrubbers. Using this as a basis, the yearly man-hour requirements for the Cherokee #3 scrubber only are 585 for the control operator and 1,460 for the auxiliary tender. The wage rates given in Table 3 are the current wage scale for PSCC operating personnel with 26% added for overhead. The 26% is the figure used by PSCC for payroll benefits such as vacations, insurance programs, etc.

The operating supervision costs are also based on PSCC's estimates. They estimate that about 5 hours per week of the shift supervisor's time is spent on the #3 scrubber. Wage rates and overhead costs are from the same source as that for operating labor.

3.3 Utilities

As can be seen from Table 3, utilities make up over 60% of the total operating costs. The usage rates were obtained from PSCC on an hourly basis. These rates were based on the scrubber system running at 100%

TABLE NO. 2

MAINTENANCE COSTS FOR CHEROKEE #3 SCRUBBER

SECTION	4TH QUARTER 1973		1ST QUARTER 1974		2ND QUARTER 1974		3RD QUARTER 1974		TOTAL	
	LABOR	SUPPLIES AND EXPENSE	LABOR	SUPPLIES AND EXPENSE	LABOR	SUPPLIES AND EXPENSE	LABOR	SUPPLIES AND EXPENSE	LABOR	SUPPLIES AND EXPENSE
Scrubber Tower & Reheat	1,092.00	9.14	489.00	*7,218.76	.00	29.79	3,481.00		5,062.00	7,257.69
Booster Fan 3A	.00	9.40	1,036.00	258.27	.00	.00	.00	112.00	1,036.00	379.67
Booster Fan 3B	.00	.00	1,351.00	9.81	68.00	17.38	.00	212.00	1,419.00	239.19
Duct and Breeching	1,987.00	45.48	3,495.00	474.81	111.00	111.08	673.00	4.25	6,266.00	635.62
Recirculation Pump 3A	1,327.00	29.25	94.00	63.28	.00	.00	.00	.00	1,421.00	92.53
Recirculation 3B1	48.00	.34	.00	.00	.00	.28	.00	.00	48.00	.62
Recirculation Pump 3B2	763.00	20.12	416.00	10.94	.00	.00	.00	.00	1,179.00	31.06
Recirculation Pump 3B3	229.00	5.26	174.00	.69	1,388.00	1,064.93	320.00	2.27	2,111.00	1,073.17
Recirculation Pump 3C	.00	.00	703.00	9.88	627.00	7.03	.00	.00	1,330.00	16.91
Make-up Pump 3A	.00	.00	.00	.00	110.00	.53	.00	.00	110.00	.53
Make-up Pump 3B	116.00	.63	.00	.00	85.00	.41	78.00	6.71	279.00	7.75
Slurry Pump 3A	.00	21.14	.00	.00	511.00	36.56	634.00	231.38	1,145.00	289.08
Slurry Pump 3B	.00	.00	248.00	63.43	520.00	296.12	365.00	164.55	1,133.00	524.10
Piping Valves	4,040.00	314.01	2,729.00	373.21	2,137.00	282.15	2,733.00	227.00	11,639.00	1,196.37
Soot Blowers	.00	171.95	.00	8.43	458.00	111.42	106.00	(9.09)	564.00	282.71
Instruments & Controls **	53.00	.33	215.00	85.81	.00	149.95	.00	.00	268.00	236.09
High Pressure Steam ***	47.00	.26	236.00	28.12	74.00	26.82	29.00	4.70	386.00	59.90
	$9,702.00	$627.31	$11,186.00	$8,605.04	$6,089.00	$2,134.45	$8,399.00	$955.77	$35,376.00	$12,322.99

* Includes $7,162.50 of contract maintenance for cleaning the reheater section

** 50% of total account

*** 10% of total account

TABLE NO. 3

CHEROKEE #3 SCRUBBER
OPERATING COSTS

	ANNUAL QUANTITY	UNIT COST $	TOTAL ANNUAL COST $	% OF TOTAL ANNUAL OPERATING COST
Operating Labor				
Control Operator	585 Man-Hr	8.23/Man-Hr*	4,800	1.0
Auxiliary Tender	1,460 Man-Hr	6.31/Man-Hr*	9,200	1.9
Operating Supervision	260 Man-Hr	8.82/Man-Hr*	2,300	0.5
Utilities**				
Electricity	23,000,000 KWH	0.006/KWH	138,000	27.9
Steam	98,600 metric ton (217,000 M lb)	1.[illegible]/metric ton (0.70/M lb)	151,900	30.7
Water	566,000 metric ton (1,248,000 M lb)	.0066/metric ton (0.003/M lb)	3,700	0.7
Air	2,650 x 10^3 m^3 (98,800 MSCF)	[illegible].83/10^3 m^3 (0.165/MSCF)	15,500	3.1
Maintenance				
Labor	See Table 2		35,400	7.1
Instrument Repair Labor	585 Man-Hr	[illegible].56/Man-Hr*	4,400	0.9
Material	See Table 2		12,300	2.5
Operating Supplies				
Lime		***	54,300	[illegible]
Polyethylene Balls	1,17[illegible] M	37.0/M	43,500	[illegible]
Miscellaneous				
Increase in Ash Handling		***	20,000	4.[illegible]
TOTAL			495,000	100.[illegible]

* Includes 65% [illegible] overhead

** Based on [illegible]

*** [illegible] Estimate (See [illegible] Section) capacity. Since the scrubber does not operate all the time, either because the unit is out of service, the unit is being fired on 100% gas, or the scrubber itself is out of service for maintenance, a total yearly on-line efficiency of 75% was used in computing the annual costs for utilities. An increase in on-line efficiency of 5% would increase the yearly utilities costs by approximately $19,000.

All unit costs for utilities were supplied by PSCC with the exception of air costs. This value was obtained from Stearns-Roger estimators as a good approximation of air costs. Air usage includes sootblowing, instrument, and service air.

If the scrubber is running at its full rated electrical load, the electric power consumption is 6.39 MW which represents 4.26% of the total #3 unit nameplate output.

3.4 Maintenance costs

All major pieces of equipment at the Cherokee station are unit coded. Any maintenance labor or material costs which are charged against any piece of equipment are entered on computer cards. Computer printouts of these charges are printed on a quarterly basis. Table 2 was assembled from these records for the last four quarters of scrubber operation ending with the third quarter of 1974. The four quarters were totalled and averaged to get a yearly cost which was entered in Table 2. For some areas which are common to all scrubbers, such as "Piping and Valves," an estimation was made as to what percentage should be charged to the #3 scrubber. Since the #1 scrubber was the only other scrubber operating during this period (the #4 scrubber came on line during the third quarter of 1974), the #3 scrubber was charged 50% of general scrubber accounts. The maintenance charges include payroll overhead charges.

The maintenance records do not include labor charges for instrument repair. The results engineers at Cherokee estimate that they spend an average of 48 hours/month on the #3 scrubber. Overhead charges of 26% were added to the base wage rate, as was done for operating labor.

3.5 Operating supplies

There are two major items that are included in operating supplies, lime and polyethylene spheres.

A slurry stream is continually purged from the scrubber to keep the slurry concentration at a specified level. This slurry stream is pumped to the ash disposal pond. Since the slurry has a low pH, lime is added to the ash pond to neutralize the water overflow and make it acceptable for release into the Platte River.

Lime charges for all three scrubbers are currently running about $18,000/month. Since #3 scrubber contributes 31% of the total scrubber slurry blowdown from the three scrubbers involved, 31% of the $18,000/month was charged to it. This amounts to $5,580/month or $67,000/year.

Since start-up, the spheres which provide the contact surface area have been replaced several times. Sometimes only individual sections would be replaced as needed. The use of spheres of different materials has provided different wear characteristics. The original polypropylene spheres lasted approximately 6,000 hours of operation with a very high breakage rate. Since the scrubber was down a little over 40% of the time the first year, 6,000 hours was not reached until the second year of operation. A total replacement rate of once a year was selected as a desirable goal. This replacement rate could be achieved if the ball wear continues to decrease.

The replacement costs are based on replacing the spheres with polyethylene spheres at the current cost of $37/1000. If Thermal Plastic Rubber spheres were used, the cost would be $65/1000 (see Section 4.2).

3.6 Miscellaneous

The only major miscellaneous cost item is the increased cost of ash handling. This increased ash handling is a result of the removal of particulate matter in the scrubber and the lime added to neutralize the slurry. PSCC estimates that ash handling has increased approximately 10% because of the #3 scrubber. The current total ash disposal costs are about $200,000/year. The #3 scrubber is therefore assessed $20,000 of this cost.

SECTION 4

MAJOR MAINTENANCE AND OPERATING PROBLEMS

This section discusses the major maintenance problems associated with operating the #3 scrubber at PSCC's Cherokee plant. The source and nature of these problems come from discussions with personnel from PSCC. Many of the maintenance problems have been solved or minimized, as is shown by the increase in reliability of the scrubber since the first year. PSCC feels that this scrubber exhibited a typical operational availability curve. Initially the scrubber operated well because of the "newness" of the equipment. Then a 8 to 9 month period of system debugging occurred followed by a steady increase in availability. PSCC points out, however, that each scrubber seems to have its own unique problems.

4.1 List of major maintenance problems

- 4.1.1 Breakage of mobile bed contactors (plastic spheres)
- 4.1.2 Migration of mobile bed contactors
- 4.1.3 Guillotine dampers
- 4.1.4 Recirculation pumps
- 4.1.5 Reheater section
- 4.1.6 Rubber lined piping
- 4.1.7 Presaturator build-up
- 4.1.8 Mist eliminators
- 4.1.9 Stack damper interlock system
- 4.1.10 Recirculation system venturi flowmeters
- 4.1.11 Booster fan bearings
- 4.1.12 Weather related problems

4.2 Breakage of mobile bed contactors (plastic spheres)

PSCC considers this to be their major maintenance problem. The scrubber is packed with 1,177,000 plastic spheres having a diameter of 3.8 cm (1.5 inch) and weighing 5 grams each. These spheres are held in place in the scrubber by a series of grids. The basic problem is that because of the turbulent nature of the system, the spheres wear out or break apart. The replacement of these spheres is a major expense item and also causes loss of operating time. In October and November of 1973 the scrubber was down for about 11 days to replace the spheres.

In addition to replacement costs, the sphere fragments were falling through the grids and into the recirculation pumps severly cutting the pump rubber lining. These fragments would also pass through the pump and plug up the nozzles in the recirculating system. This problem has been satisfactorily resolved by placing screens in the scrubber hoppers to keep the spheres from getting into the pump suctions. However, this creates another problem, that of screen plugging. Eventually enough of these sphere fragments collect on the screens, plugging the pump suctions to the point where the scrubber must be shut down to clean the screens.

In an effort to come up with a better packing, PSCC has tested and is still continuing to test spheres of different materials. To date the major types of spheres they have tested are:

1. Polypropylene
2. Polyethylene
3. High density polyethylene
4. Thermal plastic rubber (TPR)

Their experiences with the four above-mentioned materials are as follows:

1. Polypropylene - The scrubber was originally packed with spheres of this material, however, this type of sphere is no longer manufactured. The original cost was $32/1000 for orders of a million or more. Spheres of this material were weak at the poles and would wear out in this area first. The original packing lasted for approximately 6000 hours of operation with a very high breakage rate.

2. Polyethylene and High Density Polyethylene - These spheres are the major type currently being used in the scrubber. They currently cost $37/1000 for orders of a million or more. They have better wear characteristics, but they are manufactured by joining two halves together and they have a very high breakage rate at the seams. The half spheres are small enough to fall through the grids and cause plugging problems.

3. Thermal Plastic Rubber (TPR) - The TPR spheres are currently being tested in the scrubber. They have a higher initial cost of $65/1000 for orders of a million or more. Some earlier TPR spheres that were tested would tend to dimple at the poles, allowing them to pass through the grids, but the newer ones being tested now are better in this respect. The TPR spheres are to date showing good wear characteristics.

The development of spheres with better wear and breakage characteristics or the use of slightly heavier balls, would do a lot towards increasing reliability and decreasing operating costs.

4.3 Migration of mobile bed contactors

A second problem with the contacting spheres is the migration of the spheres from one section of the scrubber to another. This will occur even if there is only room enough for one sphere at a time to pass through one of the partitions. Special care must be taken if one of the vertical partitions should come up against a vessel entrance manway. The partition must extend into the portal area or the spheres will migrate around it.

Migration of the spheres allows the gas to channel through the empty sections and reduces contacting efficiency. If the pressure drop across the scrubber drops below 8" W.G., it is an indication that channeling of the gas is occurring. The scrubber is then shut down to repair any damaged partitions, redistribute the spheres, and replace any damaged spheres.

4.4 Guillotine dampers

The #3 Cherokee scrubber uses guillotine isolation dampers. There are two major problems associated with these dampers. The first problem occurs when the dampers are operated. The dampers are stopped by limit switches. When closing, an ash build up in the duct prevents the gate from closing completely and the lower limit switch is not contacted. Consequently, the gate continues to try to close against the ash and overtravels the jackscrews and shears the motor couplings. PSCC suggests that the closing of the dampers should be controlled by both a torque limiting coupling and a zero speed switch control scheme. That way, if the limit switch is not reached before resistance is encountered, the torque limiting control would prevent damage to the drive train.

The second problem is that they leak. Ash laden flue gas exits through various seams in the gate bonnets. This ash collects in the surrounding areas, covering the drive train motors, gear boxes, and couplings. This coating hinders all operational aspects of the gates and provides an unworkable atmosphere for maintenance and operation personnel.

4.5 Recirculation pumps

There have been several problems associated with the recirculation pumps. Originally five all rubber-lined pumps were installed. The original pumps had problems with shaft shearing. The shafts were milled wrong and had one stress concentration point where the shaft breakage occurred. A new milling procedure was used on the replacement shafts and there have been no problems with shaft breakage since.

Secondly, the recirculation pumps have overhead motors with V-belt drives. The original motor inboard bearings would fail if the belts were tensioned too tight. These bearings have been replaced with a better bearing design and there has been little problem with them since.

Besides the above modifications to the original pumps, two other types of pumps have been tried. One of the original pumps was removed and two test pumps were installed. The first pump initially performed satisfactorily. The second pump, however, performed exceptionally well and has been in service to date with only minor maintenance work. Its performance has been so good that PSCC is using these pumps on its latest scrubber installation on their #4 unit.

4.6 Reheater section

The exit gases from the scrubber are directly reheated by three banks of steam coils located just above the scrubber vessel outlet. Auxiliary steam from the boiler is reduced in pressure and injected into the upper two sets of finned-tube coils. The condensate from the two upper coils is then sub-cooled 10° F by injection through the lower plain-tube coils. The steam coils are designed to reheat the flue gas to 225° F.

The service life of these carbon steel reheater coils is a direct function of the performance of the mist eliminators. If droplets of low pH high TDS slurry get through the mist eliminator or are re-entrained off the mist eliminator blades, corrosion and plugging of the carbon steel tubes occur. When low pH droplets of slurry hit the smooth carbon steel subcooling tubes (wall temperature less than 200° F), rapid corrosion of the tubes results. When droplets of the low pH, high TDS slurry hit the finned carbon steel condensing coils, the water evaporates leaving an inorganic scale crystalized around fly ash particles; this eventually plugs the fins.

Because collected droplets have to drain off the blades countercurrent to the gas flow, some re-entrainment of slurry droplets is probably a fact of life for horizontal mounted mist eliminator blades. If the duct section that expands into the mist eliminator section expands at too great an angle, there is flue gas separation at the expansion point and backflow at the edges of the mist eliminators; as a consequence, there is a higher than design flue gas velocity at the center of the mist eliminator bundle. These high velocities can increase the rate of re-entrainment in the mist eliminator.

The initial installation provided a set of sootblowers below the middle finned-tube section of coils to blow the ash off the tubes periodically. Whereas these blowers did keep the ash blown off the leading edges of the middle finned-tube section, they were ineffective with the remainder of finned-tubes. In April and May of 1973 the scrubber was taken out of service in order to completely remove the coils and clean them with high pressure jets. The pluggage problem continued and two steps were taken to more efficiently clean the tubes. First, a second set of sootblowers was added just below the upper layer of finned-tubes, and second, an operational change was instituted. Whenever the unit was being fired on 100% gas, the gas flow to the scrubber was shut off and the reheater was left on. This tended to bake the ash onto the coils and dry the scale. This dryer scale could then be blown off by the sootblowers more easily. These changes appeared very promising; however, just recently major tube failure and excessive corrosion has rendered this reheater virtually inoperative. PSCC is now planning to install a protective coating in the outlet ductwork to the stack to prevent corrosive attack of the outlet breeching. PSCC is also investigating the installation of an indirect reheat system similar to that now installed on the Cherokee #4 scrubber. PSCC feels that the indirect reheat system will be the only acceptable long range solution.

4.7 Rubber lined piping

Since there is some absorption of SO_2 from the flue gas, the recirculating liquid streams are low in pH and are therefore corrosive to most types of metals. This necessitates the use of rubber lined pipe and 316L stainless steel valves. However, the collection of the fly ash produces a slurry which is also erosive when pumped. If care is not taken when the rubber lining is applied, it will be eroded away and the pipe will then be exposed to failure by corrosion.

The recirculation line splits on the discharge of the recirculation pumps prior to entering the scrubber. The section where the pipe Y's is particularly vulnerable to problems with rubber linings. The original piping was lapped wrong in this area and the pipe failed and had to be replaced.

In January and February of 1973 just a few months after initial start-up, the scrubber was down for 32 days to inspect and repair piping.

4.8 Presaturator build-up

The presaturator section cools the hot flue gas to near the saturation temperature of the gas (approximately 125° F) by use of water sprays. Originally the spray nozzles were oriented vertically. There was a build-up of soft solids in the area of the wet-dry interface. This accumulation of solids would eventually slough off and fall into the scrubber hoppers and plug the screens. There were also times when the water would spray back into the fans. This problem was corrected by repositioning the nozzles so that they pointed 45° into the scrubber. This moved the wet-dry interface further downstream and has prevented water from entering into the fans.

4.9 Mist eliminators

The mist eliminators are constructed of fiberglass reinforced plastic (FRP) blades. As the scrubber comes up on load, it is thought that these blades may shudder to some extent, thereby increasing the pressure drop across them restricting the gas flow. The scrubber has experienced as high as 4-5" W.G. drop across the mist eliminators. In other scrubber installations PSCC uses stainless steel blades in their mist eliminators, and the pressure drops are not as great. Although they have not replaced the FRP blades in the #3 scrubber as of yet, they do feel that stainless steel blades are better.

4.10 Stack damper interlock system

The flue gas from the #3 unit passes through a mechanical collector, an electrostatic precipitator, the boiler I.D. fans and into the scrubber booster fans. There is also a bypass duct which goes directly from the I.D. fans into the stack. There are guillotine isolation dampers at the discharge of each booster fan and a stack damper in the bypass duct. This allows for the following conditions:

1. If the scrubber is off-line it can be isolated from the boiler and the flue gas bypassed to the stack. Therefore, the scrubber can be taken off-line for repairs without causing a boiler outage.
2. If the flue gas flow is too high to the scrubber, some of it can be bypassed to the stack.
3. If the flue gas flow is too low to the scrubber, the stack damper will open and allow some recirculation of flue gas back to the scrubber to assure the necessary gas velocity in the scrubber.

Originally the stack damper interlock system did not respond quickly enough. When an upset condition occurred which would trip the scrubber, the guillotine dampers which isolate the scrubber would close and the stack damper would start to open. However, since the stack damper was slow to respond, the flue gas would back pressure the boiler and cause it to trip.

In order to get the stack damper to respond faster to a scrubber upset, a manual push button control was installed in the control room. The control operator is now able to activate the stack damper immediately whenever necessary.

Also, the source of instrument air was changed for the stack damper control system. Originally the stack damper control air came from the same point that the scrubber control air was tied into the main air supply. If instrument air was lost to the scrubber, the damper would be shut. The stack damper control air was changed so that it is tied into the boiler I.D. instrument air supply. This insures that the stack damper cannot be inoperable due to loss of instrument air while the boiler is still on line.

PSCC also had problems with dampers mechanically freezing up. This problem can be eliminated by frequent exercising and by complete cold testing prior to the initial scrubber startup.

4.11 Recirculation system venturi flowmeter

The recirculation lines were originally equipped with venturi flowmeters. The venturi flow section was made of fiberglass, the throat was made of alloy 20 S.S., and the flanges were made of carbon steel. Low pH recirculated slurry accumulated on the high pressure leg sample port in the area between the throat and the pipe. This corroded through the carbon steel flanges. The meters have been taken out and PSCC has plotted a curve of the recirculation pump motor current versus recirculation flow. This gives them a fairly accurate estimation of the recirculating flow without actual flow measurement.

Two other possible solutions would be to replace the carbon steel flanges with flanges of more acid resistant material, or to use magnetic flow meters for flow measurement.

4.12 Booster fan bearings

The bearings on the booster fans are a minor maintenance item. It is impossible to prevent some small build-up of ash on the fan blades even though the blades are cleaned with soot blowing air. This build-up causes the fan to be slightly imbalanced and wears the bearing out faster than normal. This problem is minimized if care is taken to insure continuous operation of the fan soot blowers.

4.13 Weather related problems

Freezing lines have always been a problem with the scrubber operation during extreme cold weather because of the large number of water and slurry streams. Special care must be taken to make sure all lines (including control air lines) are insulated and heat traced. Also, lines should be drained whenever possible when the scrubber is shut down for extended periods of time during cold weather. Most of the down time during the first two months of operation can be attributed to freezing of control lines and process lines. In December of 1972, a malfunction of the booster fan controls caused a quick shutdown during unseasonably cold weather. There was not time for proper drainage of all lines and half of the month was lost while repairs were made to piping, valves, and the Bailey control system components which were damaged by the freezing weather.

An alternate solution to protect against cold weather problems is to enclose the entire scrubber installation in a weather-proof building. This was done when the Cherokee #4 scrubber was installed. However, there is one major problem associated with doing this; that is the possibility of filling the enclosure with raw flue gas.

SECTION 5

SCRUBBER RELIABILITY

This section reviews the operating reliability of the #3 scrubber from start-up in October, 1972 to the end of November, 1974. The data was obtained from the availability log summary sheets which are kept each month by PSCC. These sheets keep a record of when each section of the scrubber is on or off line. They also record whenever the boiler is out of service or burning 100% gas.

5.1 Areas covered in the reliability study

5.1.1 Breakdown of hours at different % capacity
5.1.2 Accumulative % available to date
5.1.3 Accumulative % available previous 12 months

5.2 Breakdown of hours at different % capacity

The #3 scrubber is designed with three separate sections which are labeled A, B and C. Sections A and C have one recirculation pump each and are each designed to each handle 20% of the total capacity of the scrubber. Section B has three recirculation pumps and is designed to handle 60% of the total capacity. It is possible for any combination of the three sections to be running at any time. Therefore, it is possible to run at every increment of 20% of full capacity with the following combination.

SECTIONS ON LINE	SECTIONS OFF LINE	% OF CAPACITY
A + B + C	-	100
A + B	C	80
B + C	A	80
B	A + C	60
A + C	B	40
A	B + C	20
C	A + B	20
-	A + B + C	0

PSCC's reliability log gives a record of down time for each section along with the reason the section was down. By using the above combinations, it was possible to show how many hours each month the scrubber ran at various capacities. This breakdown is presented in Table 4. Also included in the table is a record of the hours the boiler operated each month, and the hours that the boiler was burning 100% gas. Table 5 gives a brief description of the major maintenance items which caused the scrubber to be down each month. An explanation of these maintenance problems is given in Section 4.

TABLE NO. 4

CHEROKEE #3 SCRUBBER
BREAKDOWN OF HOURS AT DIFFERENT % CAPACITIES

MONTH/YEAR	0%	20%	40%	60%	80%	100%	BOILER	BOILER (100% GAS)
Oct. - 72	52	2	107	0	21	136	318	
Nov. - 72	625	0	0	0	42	53	720	
Dec. - 72	438	0	42	4	0	209	693	
Jan. - 73	298	0	0	2	4	440	744	
Feb. - 73	547	0	0	0	53	72	672	
Mar. - 73	360	0	0	0	110	274	744	
Apr. - 73	235	0	11	0	0	410	656	
May - 73	744	0	0	0	0	0	744	
Jun. - 73	112	0	1	0	4	518	635	
Jul. - 73	1	0	0	0	35	708	744	
Aug. - 73	3	0	0	0	5	736	744	
Sep. - 73	57	0	0	37	356	270	720	
Oct. - 73	78	0	0	0	2	664	744	
Nov. - 73	178	0	0	32	110	400	720	
Dec. - 73	0	0	1	0	5	676	682	
Jan. - 74	0	17	0	0	547	175	739	
Feb. - 74	0	0	0	0	0	35	35	
Mar. - 74	70	0	0	5	21	65	161	
Apr. - 74	0	0	0	0	184	514	698	
May - 74	0	0	0	0	0	235	235	458
Jun. - 74	0	0	0	0	0	48	48	672
Jul. - 74	0	0	0	2	34	527	563	181
Aug. - 74	10	0	0	0	0	8	18	726
Sep. - 74	27	0	0	0	1	0	28	692
Oct. - 74	6	0	1	0	22	669	698	
Nov. - 74	5	6	3	0	10	645	669	
TOTAL	3,846	25	166	82	1,566	8,487	14,172	2,729
%	27.1	0.2	1.2	0.6	11.0	59.9	100.0	

TABLE NO. 5

CHEROKEE #3 SCRUBBER
LIST OF MAJOR MAINTENANCE ITEMS WHICH RESULTED IN SCRUBBER DOWN TIME

Month/Year	Maintenance Items
Oct-72	Recirculation pump (B-section), booster fan trip
Nov-72	Freeze problems, control failures
Dec-72	Major freeze damage to process and control lines, plugging (B-section)
Jan-73	Victaulic coupling and pipe failures
Feb-73	Victaulic coupling and pipe inspection and repair, reheater tube leak (C-section)
Mar-73	Slurry drawoff line failed, demister holddowns replaced, recirculation pump and inlet gate drive mechanism (C-section)
Apr-73	Reheater steam leak
May-73	Remove, repair and clean reheaters
Jun-73	Steam and air leaks, booster fan control linkage, demister repair
Jul-73	Recirculation line and flow nozzle (A-section)
Aug-73	Tie in of power for #4 scrubber, piping repair (A-section)
Sept-73	Recirculation pump (A-section), repair B3"Y" piping
Oct-73	Ball maintenance
Nov-73	Ball maintenance, plugged reheater (C-section)
Dec-73	Minor steam leaks
Jan-74	Recirculation elbow leak (A-section), recirculation pump (C-section), control failures (B-section)
Feb-74	Boiler off stream
Mar-74	Recirculation block valve, booster fan bearings
Apr-74	Recirculation pump liner (C-section)
May-74	No down time
Jun-74	No down time
Jul-74	Recirculation pump (A-section), "Y" piping leak (C-section)
Aug-74	Start-up problems
Sept-74	Vertical grid replacement
Oct-74	Booster fan vibration
Nov-74	"Y" piping (A-section), control failures, booster fan bearing (A-section), discharge block valve (B-section), reheater blowdown (C-section)

5.3 Accumulative % available to date

For this study, availability of the scrubber was defined as:

$$\text{Availability} = \frac{\text{hours of scrubber operation}^{*} - \text{hours boiler was burning 100\% gas}}{\text{hours of boiler operation} - \text{hours boiler was burning 100\% gas}}$$

The reason that the hours the boiler was burning 100% gas was subtracted from the total hours of scrubber and boiler operation is because the scrubber is normally either left running with water systems operating only or completely shut down during periods of 100% gas burning operation.

It is interesting to note that the scrubber is out of service a majority of the time during August and September of 1974 when the unit returned to mixed fuel burning. The reason for this is that after long periods of idleness, due to either maintenance or 100% gas burning, the scrubber usually experiences minor start-up problems. When start-up troubles with the scrubber were encountered, every effort was made to use any available gas on the unit. Consequently the scrubber had a poor percentage availability for the months involved, but the overall availability was not effected very much.

Table 6 was constructed from the data in Table 4. In Table 6 the % available each month, accumulative % available to date and accumulative % available for the previous 12 months are calculated.

These values are given for two capacity levels; 100% of capacity and 80% of capacity or greater. The reason that both capacity levels are calculated can be best seen from Table 4. There is a significant amount of time that the scrubber operates at 80% of capacity. For example, in January of 1974, although the scrubber only operated at 100% of capacity for 175 hours, it did operate at 80% of capacity for 547 hours. Although the scrubber is not treating all of the boiler flue gas, it is felt that some credit should be given the scrubber for handling most of the flue gas. In most cases running at 80% of capacity will probably allow PSCC to meet particulate emission standards.

The accumulative % availability to date reflects the total hours of scrubber operation since start-up. This value is plotted by month in Figure 2. This figure shows that after an initial drop, the availability of the scrubber has been increasing steadily. This is typical of other PSCC scrubber operations. The initial drop is attributed to the many minor design problems which arise soon after start-up. The

---

*Hours of scrubber operation is related directly to the time the boiler was operating.

TABLE NO. 6

CHEROKEE #3 SCRUBBER
AVAILABILITY SUMMARY

MONTH/YEAR	TOTAL HOURS BOILER ON*	100% CAPACITY				80% CAPACITY			
		TOTAL HOURS	% AVAILABLE	ACCUMULATIVE % AVAILABLE TO DATE	ACCUMULATIVE % AVAILABLE PREVIOUS 12 MONTHS	TOTAL HOURS	% AVAILABLE	ACCUMULATIVE % AVAILABLE TO DATE	ACCUMULATIVE % AVAILABLE PREVIOUS 12 MONTHS
Oct. - 72	318	136	42.8	42.8	42.8	157	49.4	49.4	49.4
Nov. - 72	720	53	7.4	18.2	18.2	95	13.2	24.3	24.3
Dec. - 72	693	209	30.2	23.0	23.0	209	30.2	26.6	26.6
Jan. - 73	744	440	59.1	33.9	33.9	444	59.7	36.6	36.6
Feb. - 73	672	72	10.7	28.9	28.9	125	18.6	32.7	32.7
Mar. - 73	744	274	36.8	30.4	30.4	384	51.6	36.3	36.3
Apr. - 73	656	410	62.5	35.1	35.1	410	62.5	40.1	40.1
May - 73	744	0	0.0	30.1	30.1	0	0.0	34.5	34.5
Jun. - 73	635	518	81.6	35.6	35.6	522	82.2	39.6	39.6
Jul. - 73	744	708	95.2	42.3	42.3	743	99.9	46.3	46.3
Aug. - 73	744	736	98.9	48.0	48.0	741	99.6	51.7	51.7
Sep. - 73	720	270	37.5	47.0	47.0	626	86.9	54.8	54.8
Oct. - 73	744	664	89.2	50.6	50.9	666	89.5	57.7	58.0
Nov. - 73	720	400	55.6	50.9	54.9	510	70.8	58.7	62.9
Dec. - 73	682	676	99.1	54.1	60.5	681	99.9	61.4	68.5
Jan. - 74	739	175	23.7	52.1	57.4	722	97.7	63.8	71.7
Feb. - 74	35	35	100.0	52.3	61.5	35	100.0	64.0	76.4
Mar. - 74	161	65	40.4	52.1	63.6	86	53.4	63.8	78.4
Apr. - 74	698	514	73.6	53.3	64.6	698	100.0	65.9	81.9
May - 74	235	235	100.0	54.2	72.9	235	100.0	66.6	91.4
Jun. - 74	48	48	100.0	54.4	72.2	48	100.0	66.7	92.4
Jul. - 74	563	527	93.6	56.2	71.4	561	99.6	68.2	92.1
Aug. - 74	18	8	44.4	56.1	67.4	8	44.4	68.1	90.9
Sep. - 74	28	0	0.0	56.0	71.7	1	3.5	68.0	91.0
Oct. - 74	698	669	95.8	58.1	72.5	691	99.0	69.6	92.5
Nov. - 74	669	645	96.4	59.9	78.6	655	97.9	70.9	96.7

* Excludes Time Unit Was On 100% Gas.

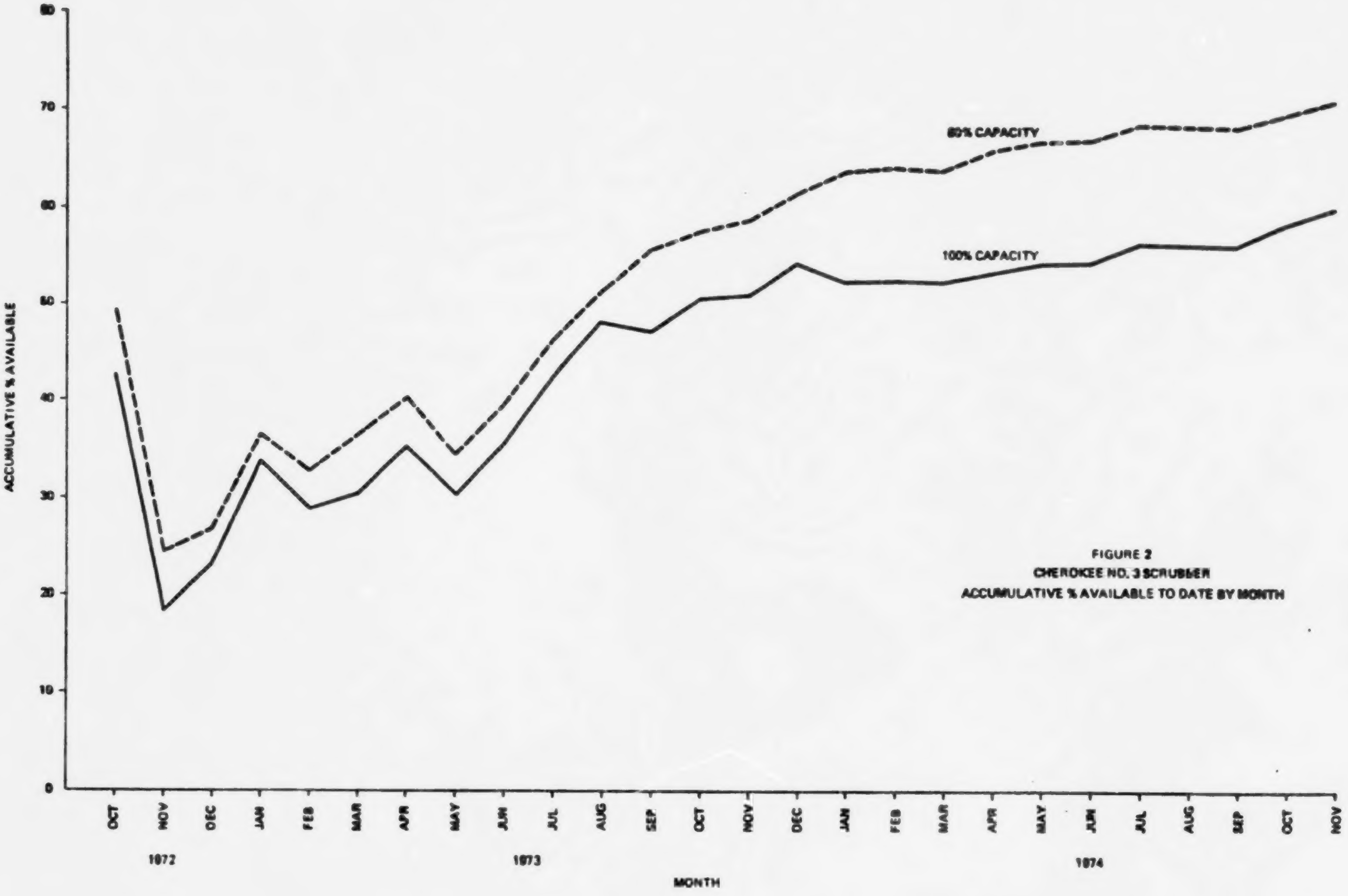

FIGURE 2
CHEROKEE NO. 3 SCRUBBER
ACCUMULATIVE % AVAILABLE TO DATE BY MONTH

following increase in availability is attributed to the solving of these problems and the increased operating knowledge which is gained through operating experience.

As of November 30, 1974, the scrubber had operated at 100% of capacity 59.9% of the time and at 80% of capacity or greater 70.9% of the time.

5.4 Accumulative % available previous 12 months

In order to more clearly see the increase in availability with time, after the first year when each new month is added to the log, only the previous 12 months availability is calculated. This value is tabulated by month in Table 6 and plotted in Figure 3. Looking at the last month tabulated (November, 1974), reveals that the scrubber operated at 100% of capacity 78.6% of time and at 80% of capacity or greater 96.7% of the time during the previous year. The figure also shows that the scrubber has been operating at 80% of capacity or greater with over 90% availability since May of 1973.

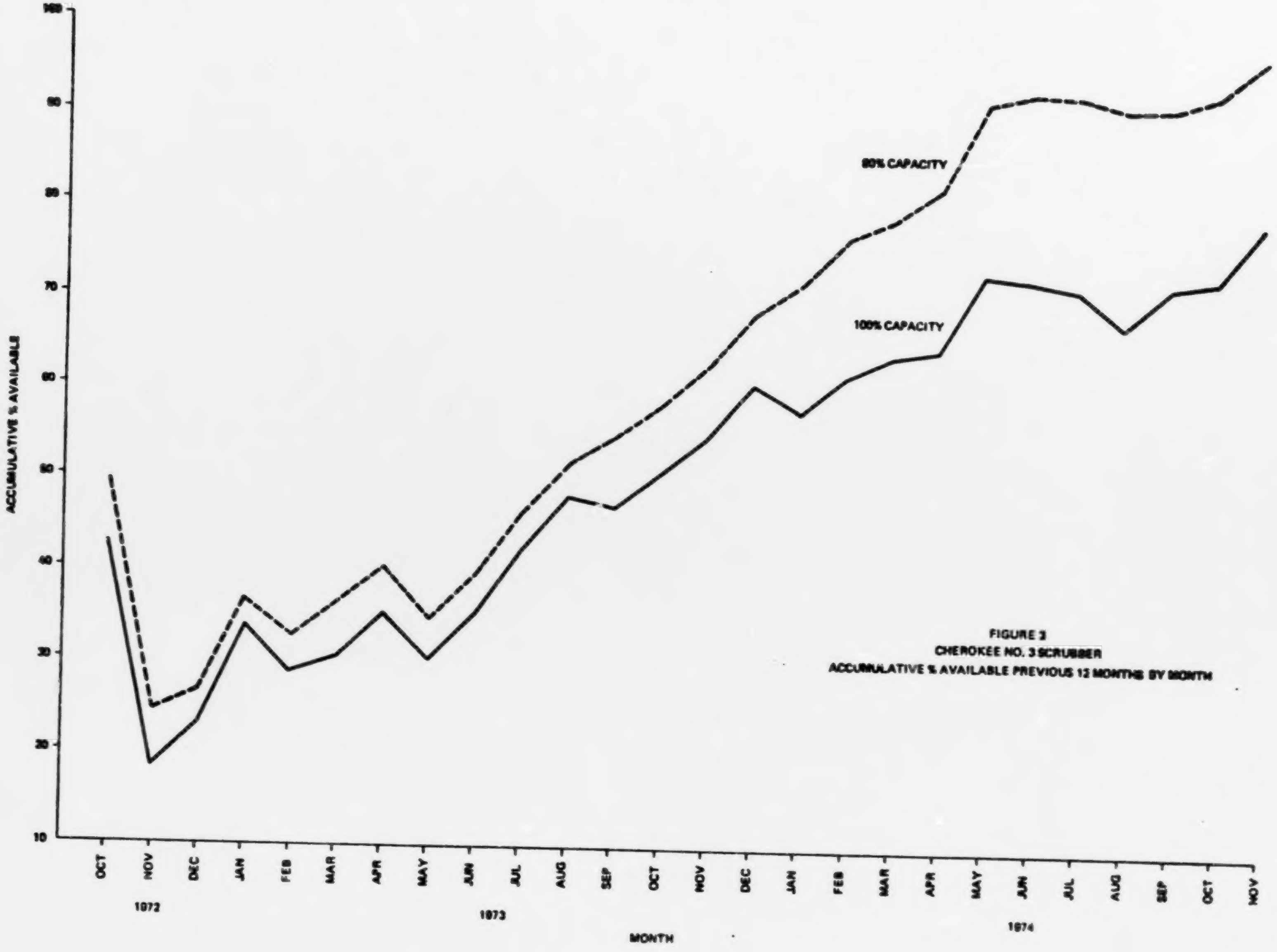

FIGURE 3
CHEROKEE NO. 3 SCRUBBER
ACCUMULATIVE % AVAILABLE PREVIOUS 12 MONTHS BY MONTH

SECTION 6

FEASIBILITY AND COST OF A "PROBLEM FREE" SCRUBBER SYSTEM

The original objective for this part of this study was to prepare a conceptual design of and a feasibility-level cost estimate for a "problem free" scrubber system. As the work progressed, it became obvious that "problem free" is difficult to define. From a strict definition standpoint there is not and probably never will be a totally "problem free" scrubber system. In any system made up of a variety of operating mechanical components (pumps, fans, valves, scrubbers, etc.) there are--over the life of the system--failures, breakdowns, overhauls, replacements, etc., of the mechanical components; such things frequently cause shutdowns and such things, although routine, are considered by many to be "problems."

If a less restrictive definition is allowed, "problem free" still means different things to different people: to a maintenance superintendent it means minimum maintenance attention and cost; to an enforcement officer it means maximum on-line time; to a corporate executive it probably means minimum capital cost; and to an operating superintendent it means minimum operating attention.

From the broad definition standpoint, "problem free" becomes some optimum balance between availability, capital cost and operating/maintenance attention. This optimum balance is not constant; it will change from plant location to location depending on such things as space availability, regulations, cost of capital, availability of trained personnel, etc.

Many ways of improving scrubber system availability and reducing operating/maintenance attention were studied. The problems that were investigated fall into several different categories.

1. Problems which require further research and development. An example is the development of a mobile contactor with better breakage/abrasion characteristics. The development of a better contactor would result in less downtime and lower operating costs by increasing the interval between contactor replacement, and increasing the interval between recirculation pump suction screen cleanings.

   Another item which still requires more development work is the manufacture of a better isolation gate. The large size of the ducts needed to handle the amount of flue gas from a typical power plant, necessitates the use of large isolation gates. Their large size makes the gates subject to mechanical failures such as jacking mechanism problems associated with proper monitoring of full open and close limits, ash buildup, and corrosion.

2. As experience is gained from operations, improvements are made in the design of various individual scrubber system components. Recirculation pumps are an example. Many pump vendors are producing pumps which can handle the low pH scrubber slurry with better performance than earlier designs. Knowledge of this experience with various pumps is needed to select the right pump for scrubber application. The same holds true for lining materials and other materials of construction for valves, piping, nozzles, etc.

Since "problem free" is a subjective term and, as such, difficult to precisely define, it was decided that the objectives of this part of the study would be limited to investigating ways of shifting the reliability-capital cost-operating/maintenance attention balance to improve reliability and reduce operating/maintenance attention at the expense of greater capital cost. Before discussing specific items, there are two other points that should be made.

1. If there is sufficient space, availability can be improved by spending additional money to provide redundant stand-by modules. Thus, if one module is down for repairs or maintenance, the remaining modules can carry the full flue gas load. The expenditure of additional money does not diminish the operating/maintenance "problems," it just provides spare equipment to be put in service to maintain system availability when an operating module is shut down for repairs or maintenance.

2. In the real world, engineered solutions to "problems" do not always necessarily diminish or solve a "problem." For instance, a recirculation pump that looks good in other similar services, may not perform up to expectations in the scrubber system. A spherical contactor material that looks good in laboratory tests may not look as good in actual full-scale plant tests. This is to say that the engineered improvements discussed in this section should increase availability and decrease operating/maintenance attention but that the success of these fixes cannot really be evaluated until the modifications have been made and tested.

3. There are some specific, definable changes to the basic scrubber design which would significantly improve availability. These changes are discussed and priced out in the following text.

a. Addition of a Spare Section

As mentioned before, availability can be improved by adding an extra scrubber section which acts as a spare whenever another section is out of service. As can be seen from Table 6 and Figure 2 in Section 5, the difference in availability between operating at 100% capacity and 80% capacity varies by 10-20% for the last year or so of operation. If a spare section had been available, much of that difference might have been eliminated. The addition of a redundant section would not solve any maintenance problems; in fact, it would increase maintenance costs because there would be more equipment to maintain.

If an extra scrubber section were designed into the original scrubber system, the optimum design would probably be based on four independent 33 1/3% capacity sections. This approach to increasing availability is very costly. The addition of an extra section would require duplication of all related equipment. It is estimated that a scrubber system with 4 x 33 1/3% sections would cost about $1,200,000 more than the 1975 capital cost for the existing Cherokee #3 scrubber system.

b. Indirect Reheat

The major possible change in design for the present system concerns the reheat system. In the present direct reheat system, the reheat coils are located in the flue gas duct and as a result the coils are subject to plugging and corrosion. The use of an indirect reheat system is considered more reliable although more expensive. With an indirect reheat system outside air is heated and mixed with the flue gas as it leaves the scrubber.

This requires extra reheat fans, an extra damper, and extra ductwork for each scrubber section. Although the unit cost of reheat transfer surface is lower for indirect reheat, more surface is required because of the extra volume of air introduced. Similarly, the direct reheat system has sootblowers to clean the coils which would not be necessary with an indirect system. Taking all the above things into consideration, it is estimated that an indirect reheat system--designed into the original scrubber system--would cost approximately $200,000 more than a direct reheat system and would thus add $200,000 to the total 1975 scrubber system cost. It should be noted that the actual cost of a retrofit indirect reheat system has been estimated at almost $600,000.

The use of an indirect reheat system also results in slightly higher operating costs. There would be additional steam requirements because of the increased volume to be heated brought about by the introduction of the reheat air and additional electrical requirements for the reheat air fans. It is estimated that this would add about $35,000/year in utility costs.

Indirect reheat is in use on the Cherokee #4 scrubber. Some problems are being experienced with condensation of the flue gas in the stack, however, this is a result of the reheat fans not being able to supply enough reheat air to maintain a sufficient temperature in the stack. It appears that if the fan capacity is increased, the indirect reheat system will perform satisfactorily.

c. Scrubber Enclosure

Housing the scrubber in a heated, ventilated enclosure would eliminate many of the problems of freeze-ups during cold weather. The cost of adding such an enclosure including metal sidings, fans, heating and cooling systems, and electrical work would be approximately $90,000.

d. Miscellaneous Changes

There are many smaller changes which could add to the reliability of the scrubber operation. The last type of recirculation pump tested by PSCC is showing superior performance as far as maintenance problems are concerned. These pumps are more expensive and if used would add approximately $45,000 to the pump costs.

The use of magnetic flow meters instead of venturi flow meters would give better recirculation flow measurements and would add another $15,000.

It is also recommended that the outlet duct be coated to reduce the chance of corrosion if there is a loss of the reheat system. This would add another $20,000 to the scrubber costs.

In order to more fully understand the economic effect on any changes to the design of the present scrubber, it is necessary to update the cost of the scrubber. Using the latest Chemical Engineering Plant Cost Index values ("Chemical Engineering," April 14, 1975) of 137.2 for 1972 and 179.9 for February, 1975, an estimated 1975 cost for an identical scrubber would be approximately $5,800,000. This represents an increase of $1,400,000 over the original cost of $4,400,000 reported in Section 2.

If all the above changes were made in the redesign of the existing scrubber, it is quite conceivable that 90 + % scrubber availability could be obtained. The system would still have the normal maintenance requirements, possibly even greater than with regular power plant equipment.

The list below summarizes the changes mentioned and costs involved.

		Estimated Availability
Identical Scrubber (1975)	$5,800,000	60-70%
Extra 33 1/3 Capacity Section	1,200,000	+10-15%
Indirect Reheat, incremental	200,000	
Scrubber Enclosure	90,000	+ 5-10%
Miscellaneous Changes	80,000	
	$7,370,000	85-95%

This capital cost of $7,370,000 figures out to be $49/KW for a 150 MW unit as compared to the original $29/KW.

In closing, it should be pointed out that one of the most important aspects of increasing the reliability of the scrubber operation is the willingness of the operating and maintenance personnel to deal with the many scrubber system problems that arise. The attitude at PSCC is that they are committed to the existing scrubbers at Cherokee, and they will try to do everything necessary to keep them on line. This attitude is reflected in the increased reliability of the system since the scrubbers have started to operate.